DEVELOPMENTS IN WATER SCIENCE

4

ADVISORY EDITOR V.T. CHOW

JEAN J. FRIED

GROUNDWATER POLLUTION

ELSEVIER

GROUNDWATER POLLUTION
Theory, Methodology, Modelling and Practical Rules

DEVELOPMENTS IN WATER SCIENCE, 4

advisory editor

FURTHER TITLES IN THIS SERIES

1 G. BUGLIARELLO AND F. GUNTHER
COMPUTER SYSTEMS AND WATER RESOURCES

2 H.L. GOLTERMAN
PHYSIOLOGICAL LIMNOLOGY

3 Y.Y. HAIMES, W.A. HALL AND H.T. FREEDMAN
MULTIOBJECTIVE OPTIMIZATION IN WATER RESOURCES SYSTEMS:
THE SURROGATE WORTH TRADE-OFF METHOD

GROUNDWATER POLLUTION

Theory, Methodology, Modelling and Practical Rules

JEAN J. FRIED

Professor of Fluid Mechanics
at the University of Strasbourg
Scientific Adviser at the
Ecole Nationale Supérieure des Mines de Paris

ELSEVIER SCIENTIFIC PUBLISHING COMPANY
AMSTERDAM — OXFORD — NEW YORK 1975

ELSEVIER SCIENTIFIC PUBLISHING COMPANY
335 Jan van Galenstraat
P.O. Box 211, Amsterdam, The Netherlands

AMERICAN ELSEVIER PUBLISHING COMPANY, INC.
52 Vanderbilt Avenue
New York, New York 10017

Library of Congress Cataloging in Publication Data

Fried, Jean J
Groundwater pollution.

(Developments in water science ; 4)
Bibliography: p.
Includes index.
1. Water, Underground--Pollution. I. Title.
II. Series.
TD423.F74 333.9'104 74-29680
ISBN 0-444-41316-2

With 172 illustrations and 5 tables

Printed in The Netherlands

To my Parents
for their unlimited patience

This Page Intentionally Left Blank

ACKNOWLEDGMENTS

The idea of writing this book occurred during my visit in 1973 as Gledden Senior Visiting Fellow at the University of Western Australia in Perth, where I gave two courses on groundwater pollution and groundwater numerical analysis. I take this opportunity to thank the staff of the University for the excellent working facilities which were provided.

Most of my investigations were performed during my stay at the Ecole Nationale Supérieure des Mines de Paris and I am indebted to Mr. Y. Emsellem, former Head of the Centre d'Informatique Géologique, now President General Director of Arlab, for many stimulating ideas and fruitful discussions.

NEDLANDS (Western Australia)
STRASBOURG (France) 1974

This Page Intentionally Left Blank

KEYS TO THIS BOOK

We hope that this book will be of interest for engineers, students and applied mathematicians and we wish to give a few reading directions for an optimal use of it.

Chapter 1 presents the main pollutants and their characters of miscibility which justify the foundations of groundwater-pollution studies on miscible-displacement theories.

Chapter 2 outlines the basic elements of dispersion theory, otherwise detailed by Fried and Combarnous (1971), and stresses the derivation of the mathematical representations from laboratory experiments and their limits.

Chapter 3 gives the methodological rules for studying a case of groundwater pollution quantitatively. It shows how to handle such a problem and it defines the sequence of operations. To illustrate this methodology, two type-projects are presented that could be used as models of propositions for groundwater-pollution studies (especially in the case of pollution from sanitary landfills). Chapter 6 describes some typical case histories which explain how to apply the methodology, while Chapter 4 gives the main field experiments and formulas necessary to collect the various pollution parameters and Chapter 5 presents some useful numerical models with their finite-difference discretization.

With Chapter 7, we have tried to widen the subject, showing that groundwater pollution is part of larger economical problems linked to the management of water resources. We show that the methodology specific to groundwater pollution described in Chapter 3 is an application of more general methods, supported by mathematical tools and refined mathematical data-processing methods, which we describe briefly. We then give the basic concepts of an economical and political approach to water resources and groundwater-pollution problems.

Although Chapter 8 is a consequence of experimental considerations, it is highly mathematical and theoretical and has been written to show applied mathematicians that even ground-to-ground pollution problems offer very good opportunities of developing their own mathematical research and to induce them to come into this very applied branch of physics and help it with their mathematical knowledge.

Chapter 9 develops the numerical-analysis methods and procedures necessary to set a pollution problem numerically and to solve it on a computer. It stresses the close interrelationships between the physics of the phenomena and the modelling.

Four Appendices have been added to provide specific information. Appendix I provides basic information on groundwater hydrology, sufficient for a correct understanding of groundwater and pollution flow. Appendix II explains the basis of geophysical electrical soundings, which are much-used field techniques to detect pollution without disturbing the medium and with a restricted number of boreholes.

Appendix III is a summary of basic algebraic notions, necessary to understand the techniques of Chapter 9: a non-specialist, such as a geologist, should be able to build a mathematical model with Appendix III and Chapters 5 and 9.

Appendix IV is a description of the international norms for drinking water and provides the concentration thresholds used in pollution studies.

An engineer will mostly use Chapters 3, 4, 5, 6 and 9 to obtain a practical knowledge of and practical solutions for his pollution problems. If this practical man is responsible for a whole project, Chapter 7 will be of great help for him.

An applied mathematician, or a research scientist will find interest in Chapters 2 and 8 which are theoretical or close to the laboratory. Of course they should read all the other chapters which bring them into the physics of the phenomena.

This book can be used as a textbook on the understanding and the quantification of groundwater-pollution problems; we feel that Chapter 8 should then be skipped, except for § 8.4.1, which is an introduction to the philosophy of modelling. At the undergraduate level, Chapter 2 on dispersion is a basis for laboratory and mathematical work; at the graduate level, the chapters on methodology (3 and 7) and on field experiments should be studied.

INTRODUCTION

Pollution has become the ever-increasing monster that threatens our civilization (what is left of it, at least), the Moloch that will eat us. This is what the information media say, and perhaps they are right; now again perhaps they are wrong, or at least too pessimistic. We feel that the real danger is not pollution but the ignorance of pollution problems. This book built around the example of groundwater pollution, is an attempt to rationalize and to quantify the problem and to show that the danger of pollution should not be despised, of course, but conversely, it should not be exaggerated. It emphasizes that pollution problems can be framed in good physico-mathematical theories and that they have technical and mathematical solutions. It stresses the fact that usual techniques, mathematical and experimental, developed in other fields, can be successfully applied in most pollution cases, once the correct sequence of their intervention can be defined. Moreover, it shows that the treatment of pollution falls well within the usual financial and technical possibilities of any country: it is a question of will, organization and technical skill much more than a question of money.

This book stresses the importance of mathematical modelling as the necessary and practical backbone of the proposed methodologies, but also warns the reader that a model, by definition, is an approximation of reality: as the efficient use of a tool depends on the worker, so the efficient use of a model will depend on its user, and probably more on his physical sense than on his mathematical capabilities. A good mathematician without physical sense is a very bad modeller, a good physicist or engineer, with a basic knowledge of mathematics, can be a very good modeller.

In brief, we hope to prove that the solutions to groundwater-pollution problems can be reached and we provide some means to reach these solutions. These means are based upon laboratory and field experimental methods, and mathematical modelling and characterized by constant comparisons between the mathematical frames and the physics of the phenomena.

This Page Intentionally Left Blank

CONTENTS

CHAPTER 1

GENERAL DESCRIPTION OF GROUNDWATER POLLUTION

1.1. DEFINITION OF GROUNDWATER POLLUTION

The theory says that a man can survive with five liters of water per day only and sometimes less. Yet an average of 40 to 50 liters per day is necessary for domestic and personal hygiene; more water is required for farming: a villager needs 100 liters at least; and in industrialized areas 400 to 500 liters per inhabitant are common requirements. To match this drastic increase in the demand for water, existing water resources have to be constantly developed and new sources have to be found; all available sources must be mobilized and especially groundwater.

Groundwater is generally a very good source of drinking water, because of the purification properties of the soils; it is also used for irrigation and spraying, and, where surface water is scarce, for industrial purposes. In many arid and semi-arid zones, it is the main source of water. An aquifer constitutes a natural reservoir of usually high-quality water. But although it is more protected than surface waters, groundwater appears to be subject to pollution, a phenomenon that can be defined as follows:

Pollution is a modification of the physical, chemical and biological properties of water, restricting or preventing its use in the various applications where it normally plays a part.

1.2. ORIGINS OF GROUNDWATER POLLUTION

Groundwater pollution is usually traced back to four main origins: industrial, domestic, agricultural and environmental pollution, each family being divided up into continuous and accidental types.

(1) Industrial pollution is carried to the aquifer by:

— used waters which contain chemical compounds and trace elements (such as metals, for instance) or which are at a rather high temperature. Radioactive pollution from atomic plants can also be brought in in this way

— rain infiltrating through waste disposals

— accidents like the breaking of a pipe line

(2) Domestic pollution is carried to the aquifer by:

— rain infiltrating through sanitary landfills

— accidents, like the breaking of septic tanks

(3) Agricultural pollution is due to irrigation water or rain carrying away fertilizers, minerals, salts, herbicides and pesticides.

(4) Environmental pollution is mainly due to seawater intrusion in coastal aquifers.

Remark. Bacteriological pollution mainly originates in domestic wastes such as fecal excretions and is not the object of a separate study. The factors that are usually studied in groundwater pollution are listed in Table I. The occurrence of these elements and compounds in the water does not necessarily mean that it is polluted, and, actually, pollution criteria will depend on the type of use made of the water: e.g., drinking purposes are a possibility, but also personal hygiene or recreation (swimming pools, for instance) or irrigation; in these last cases the hazards are less well known than the hazards to drinking water and there are no norms or international regulations for their control. International norms have been recommended by the World Health Organization (1972) for drinking-water quality only and these are presented in Appendix IV.

TABLE I

List of main possible groundwater pollutants and pollution indicators

Total dissolved solids
C O D (Chemical Oxygen Demand)
B O D (Biological Oxygen Demand)
Carbon (organically linked)
Hydrogen (organically linked)
Nitrogen
Detergents
Phenols
Oxygen
Sulfates (SO_4^{2-})
H_2S
Nitrates (NO_3^-)
Nitrites (NO_2^-)
Ammonium (NH_4^+)
Free CO_2
Bicarbonates (HCO_3)
Iron (Fe^{2+})
Total iron (Fe^{2+} and Fe^{3+})
Manganese
Sodium
Potassium
Calcium
Magnesium
Total hardness
Chloride
Fluoride
Phosphate (HPO_4^{2-})
Zinc
Lead
Copper
Arsenic
SiO_2
Temperature
pH
Conductibility
Redox potential

1.3. *PHYSICAL CHARACTERISTICS OF GROUNDWATER POLLUTION*

Careful observation of Table I and of the tables of admissible pollution levels and critical masses (Appendix IV) shows that most frequent and most dangerous forms of groundwater pollution are miscible with the water of the aquifer; and if they are not miscible, their critical masses are small enough that they could be considered as tracers of the water and the movement of traced water in water is certainly the best example of a miscible displacement. Of course, oil pollution is certainly not miscible, but it has been shown (Dracos and Schiegg, 1971) that oil reaching an aquifer after some accident does not move much and that the pollution of wells by hydrocarbons will be due to soluble parts or light elements behaving like tracers, the movement of which can be described by a miscible-displacement theory.

These considerations, which are confirmed by most field experiments, have led us to base this book on the theory of miscible displacements of two fluids, characterized by dispersion phenomena. Yet, we take into account the fact that the behaviour of miscible fluids is sometimes well described by neglecting mixing effects: it is the case of some large-scale studies and also of pollution movements through preferential paths, for instance, especially when pollution amounts are very small but their toxicity rather high.

In brief, groundwater pollution is mostly governed by dispersion (dispersive case), except when its movement, due to the velocity of the water, is much more important than its mixing with the water of the aquifer (convective case). Both cases and their links are described.

This Page Intentionally Left Blank

CHAPTER 2

THE THEORY OF DISPERSION IN POROUS MEDIA

The theory of dispersion in porous media is the qualitative description and the quantitative estimate of the behaviour of miscible fluids displacing one another in a porous medium.

When two miscible fluids are brought into contact, there is a sharp interface at the beginning which vanishes into a transition zone, as the differences between physical properties (concentrations, for instance) tend to be leveled with time. This global effect results from the simultaneous action of several physico-chemical phenomena, such as molecular diffusion and permeability contrasts of the porous medium.

The historical development of the theory of dispersion takes place in three steps:

(1) Laboratory experiments, investigating the displacement of miscible fluids in porous media.

(2) The derivation of mathematical processes, equations and formulas describing the laboratory experiments, providing synthetic explanations of their results and general equations of dispersion phenomena.

(3) The application of dispersion formulas and equations to field problems and real pollutions.

Laboratory experiments and mathematical interpretations and theory were conducted together and are strongly interdependent. The field application of dispersion theory is rather recent but is quickly gaining momentum as the urgent needs for pollution behaviour prediction and control increase. The application of dispersion theory to field studies shows the holes in the theory when confronted with reality. Thus a fourth step of development now takes place: the return to laboratory experiments and systematic field testing to improve the theory. (Fried and Combarnous, 1971.)

2.1. DESCRIPTION OF DISPERSION

2.1.1. A simple example

Let us consider a porous medium saturated with pure water contained in a cylindrical tube. At time zero, a chemical liquid compound mixed with water at concentration C_0, is injected in the tube. The concentration profile is a step function at time zero (Fig. 2.1.1). The movement is unidirectional, the injection rate is constant and we assume that there is no physico-chemical interaction, like adsorption for instance, between fluids and solid matrix. The concentration of the injected chemical compound varies with time; the concentration profile has the typical aspect of an S-curve (Fig. 2.1.1).

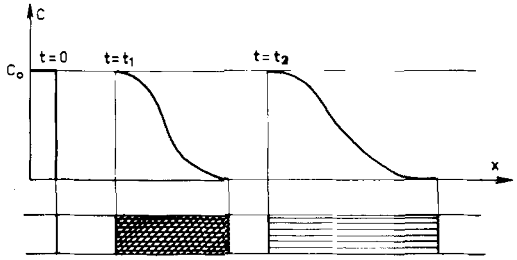

Fig. 2.1.1. Evolution of the transition zone with time.

The *transition zone* is defined as the zone where the concentration of injected liquid varies from 0 to C_0. The width of the transition zone increases with time. It is a typical effect of dispersion, the quantification of which leads to the various equations of dispersion.

2.1.2. Definition of dispersion

Dispersion in fluid flow in porous media is the occurrence and evolution of a transition zone between two domains of the fluid phase with different compositions.

The occurrence and evolution of a transition zone between two moving miscible fluids may be interpreted as a tendency towards a uniform chemical composition of the mixture, although we shall see that the mechanisms of dispersion are rather complex and cannot be described in one sentence.

2.1.3. Mechanisms of dispersion

Dispersion results from the simultaneous action of both a purely mechanical phenomenon and a physicochemical phenomenon.

(a) Mechanical action: the velocity distribution of a fluid flowing through a porous medium is not uniform. This is due to boundary effects of the solid matrix, which can be divided up into three types:

(1) the fact that the fluids are viscous usually implies a zero velocity on the solid surface, thus creating a velocity gradient in the fluid phase as in capillary tubes (Fig. 2.1.2a);

(2) the variations of pore dimensions create discrepancies between the maximum velocities along the pore axes (Fig. 2.1.2b);

(3) the streamlines fluctuate with respect to the mean direction of flow (Fig. 2.1.2c)*.

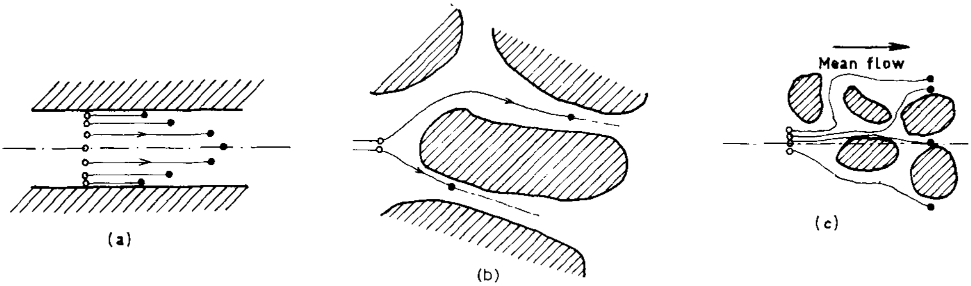

Fig. 2.1.2. The components of dispersion. Fluid particles: o at time t; • at time $t + dt$

These three types of mechanical action take place simultaneously and yield the "mechanical dispersion" (Fig. 2.1.3).

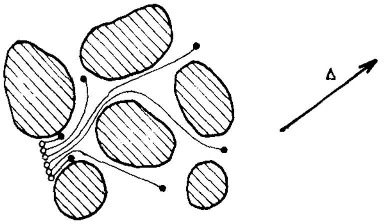

Fig. 2.1.3. General aspect of dispersion.

The observation of these elementary phenomena suggests a geometrical aspect of dispersion: the existence of two basic effects, the first one in the direction Δ of the mean velocity and due to differences between the velocity components along Δ, the second one in the plane orthogonal to Δ due to differences between the velocity components in that plane. These effects are respectively called "longitudinal dispersion" and "lateral dispersion". We shall see that these effects are fundamental in the theory of dispersion as well as in its application to pollution problems.

(b) Physicochemical action: the physicochemical dispersion is molecular diffusion, which results from the chemical potential gradient. Chemical potential is correlated to the concentration. Molecular diffusion takes place even in a fluid at rest.

As in the case of mechanical dispersion, the action of molecular diffusion may be classified into types. Dividing the fluid into streamtubes, for the sake of simplicity, we observe two types:

---

[*] Fig. 2.1.2c is bidimensional for obvious reasons of draughting problems. It should be understood as a 3-D representation, of course.

(1) inside a streamtube, the differences of concentration in the tube mean direction tend to disappear. It is a longitudinal effect (Fig. 2.1.4a);

(2) between two adjacent streamtubes, there is a transfer of mass, in order also to smooth out the differences in concentrations. It is a lateral effect (Fig. 2.1.4b and c).

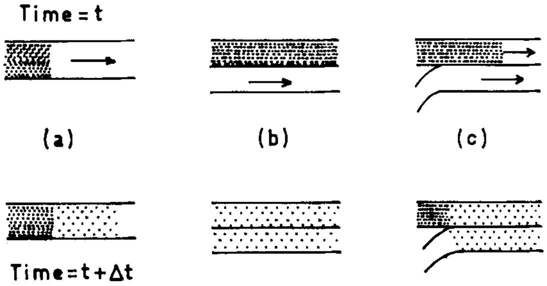

Fig. 2.1.4. Diffusion effects in dispersion.

Actually, molecular diffusion is always present in dispersion and is a most important factor in regularizing mechanical dispersion. It accounts to a great extent for lateral dispersion and for the analogies between the mathematical representations of dispersion and heat transfer.

2.1.4. Characteristic parameters of dispersion

The characteristic parameters of dispersion are divided up into two sets: parameters the numerical values of which measure dispersion; and parameters influencing the process of dispersion.

Parameters measuring dispersion

The quantitative approach to dispersion requires a definition of the *scale* or *level* at which the measurements are made. This concept of scale is most important in physics and especially in the context of flow through porous media: it will dominate our course as a fundamental concept of the methodologies governing groundwater-pollution studies.

The theory of dispersion is usually based upon the use of three main levels: a local level; a fluid-volume or pore-volume level; and a macroscopic level.

Local level. At this level the parameters describe a physical quantity at a point, i.e. in an "infinitely small" volume element, consistent with molecular-physics data. It is the usual level of fluid mechanics where, for instance, the movement equations of Navier-Stokes hold.

Fluid-volume level. At this level, the parameters are defined as "means", with respect to some averaging process, of the corresponding local parameters over a finite volume of fluid. In a porous medium, the concept of "pore quantities" (such as pore velocity) is based upon this definition and the average is taken over a set of pores. The definition of an average is described in each case, especially when non-additive quantities are involved.

Macroscopic level. This level is introduced in the theory of flow through porous media to help define a continuum equivalent to the set fluid and solid matrix. The parameters are the "means", with respect to some averaging process, of the corresponding local parameters over a finite volume of porous medium.

Dispersion is measured through three physical quantities (i.e. quantities which have a direct physical meaning and the numerical values of which can be obtained directly, at least in theory) and a set of mathematical quantities (i.e. quantities resulting from a mathematical interpretation of the theory of dispersion). The physical quantities are: densities, concentrations, and velocities. The mathematical quantities are called the "dispersion coefficients".*

Densities. The notation ρ used alone represents the classical density at the pore-volume or macroscopic levels. At these levels ρ_i is the specific density of constituent i and ρ is the specific density of the mixture. We may sometimes use ρ at a local level, but then this symbol is always coupled to a symbol of velocity or concentration which defines its scale: for instance ρu is a local motion quantity. We have:

$$\rho = \sum_i c_i$$

where c_i is the concentration defined below.

Concentrations. Several definitions of the *microscopic concentration* of a substance A in a mixture M may be used.

The *mass concentration* c is the mass m_a of the substance A in a small volume v of mixture, divided by the volume v or:

$$c = m_a/v$$

It is a useful definition when mixing occurs without volume changes, i.e. the total volume v of a mixture of two chemical substances with initial volumes

---

[*] Notations. Lower-case italic letters are used to describe the microscopic level and capital italic letters to describe the macroscopic and fluid-volume levels.

v_1 and v_2 is:

$$v = v_1 + v_2$$

The *mass fraction* c^* is the mass m_a of A divided by the mass m_m of M contained in the same volume, or:

$$c^* = m_a/m_m$$

c^* is an intrinsic quantity which does not depend upon the physicochemical ways of mixing. c and c^* are related:

$$c = \rho c^*$$

where ρ represents the density of the mixture.

The *molecular concentration* c_M is the number n_a of molecules of A divided by the volume of mixture v which contains the molecules or:

$$c_M = n_a/v$$

The *molecular fraction* c_M^* is the number n_a of molecules of A in a volume of mixture divided by the total number n_m of mixture molecules in the same volume:

$$c_M^* = n_a/n_m$$

At the fluid-volume level, the same definitions may be used, the reference fluid volume being large. Hence the mass concentration is C, the mass fraction C^*, the molecular concentration C_M, and the molecular fraction C_M^*.

Local velocities. The various compounds (i) of the mixture move with different velocities u_i. Two definitions of the average local velocity of the mixture are mainly used. The mass average velocity u:

$$u = (\sum_i c_i u_i)/(\sum_i c_i) = (\sum_i c_i u_i)/\rho$$

where c_i is the mass concentration of compound (i). The molecular average velocity u_M:

$$u_M = (\sum_i C_{Mi} u_i)/(\sum_i C_{Mi})$$

c_{Mi} being the molecular concentration of compound (i).

These velocities are referred to stationary coordinate axes. But diffusion and dispersion are mainly relative phenomena and it may be interesting to introduce relative-velocity concepts, indicating the motion of one compound relative to the motion of the mixture: $u_i - u$ is the diffusion or dispersion velocity of compound (i) with respect to u, and $u_i - u_M$ is the diffusion or dispersion velocity of compound (i) with respect to u_M. These velocities u_i, u, and u_M are the usual local or microscopic velocities in fluid mechanics.

Mean velocities in the fluid phase and at the macroscopic level. In a fluid volume B of any kind (for instance, the volume of a streamtube or the volume of several pores), the mean velocities are defined as follows:

The mass average velocity U of the mixture is defined by:

$$U = \left(\int_B \rho u \, \mathrm{d}x\right) \Big/ \left(\int_B \rho \, \mathrm{d}x\right)$$

The mass average velocity U_i of one compound is defined by:

$$U_i = \left(\int_B c_i u_i \, \mathrm{d}x\right) \Big/ \left(\int_B c_i \, \mathrm{d}x\right)$$

U may also be defined by:

$$U = (\sum_i CU_i)/\rho$$

At the macroscopic level, the velocity is the usual Darcy velocity V. When U is defined for a large number of pores, it is linked to V by the relationship:

$$U = V/\phi$$

where ϕ is the porosity of the medium.

Dispersion and diffusion coefficients. The mathematical model of diffusion and dispersion phenomena is a partial differential equation, the coefficients of which (called diffusion or dispersion coefficients) are useful measure parameters; for instance, they appear in formulas showing the width of the transition zone.

These coefficients have the physical dimensions L^2T^{-1}. It can be shown that these coefficients are usually tensors. We shall use the notations D for the diffusion tensor (D_i^j for a component of the tensor); and K for the dispersion tensor (K_i^j for the component of the tensor).

Parameters influencing dispersion

The parameters influencing dispersion may be classified into three groups: (1) parameters describing the porous medium; (2) characteristics of the fluid; and (3) characteristics of the displacements.

The porous medium. It influences dispersion by its geometrical structure. Generally, it is possible to define this structure by theoretical considerations of differential geometry, introducing the coordinates and the curvature at each point of the interface solid pore. Such complete knowledge cannot be reached by experiments, and this implies the introduction of mean parameters. Two sets of geometrical characteristics are commonly used (Scheidegger, 1963).

The first set is made up of the void fraction or porosity ϕ and of permeability k given by Darcy's law. The medium is taken as a continuum.

The second set is made up of parameters which are an attempt to measure the following pore characteristics: (1) the specific area which is the ratio of the interface solid pore in a sample to the volume of the sample; (2) the grain-size distribution for an unconsolidated medium; (3) the pore-size distribution, which may be defined in different ways; and (4) the degree of consolidation.

If chemical actions take place on the interface solid pore, such as adsorption, it is necessary to take the chemical constituents in the solid matrix into account.

The fluid phase. As a whole it is characterized by its velocity and its density, both defined as functions of its chemical composition. It may happen that the fluids are not quite miscible; then it is necessary to use the miscibility curve to define whether dispersion takes place or not (Stephen et al., 1964). In Fig. 2.1.5 two types of miscibility curves are presented for mixtures of two or three compounds, respectively Fig. 2.1.5a and b.

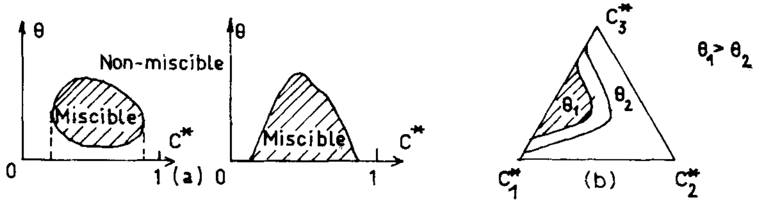

Fig. 2.1.5. Miscibility curves for two (a) and three compounds (b), θ is the temperature.

As molecular diffusion is an important component of dispersion, as previously mentioned, the diffusion coefficient D (for a binary mixture) is one of the parameters of dispersion formulas.

Characteristics of the displacement. Two aspects of displacement influence dispersion: the velocity distribution and the distance traveled by the transition zone.

2.2. CONCEPTUAL REPRESENTATIONS OF DISPERSION

In order to represent mathematically the dispersion of two miscible fluids in a porous medium, several models have been derived that can be classified into three categories: geometrical models, statistical geometric models, and probabilistic models. These various models have been thoroughly described in Fried and Combarnous (1971) and Bear (1972).

The geometric models were the first, very simple approach of dispersion problems, and they are not representative. They consist of fixed capillaries (either one capillary (Taylor, 1953, 1954) or a set of capillaries) which are connected or independent, where the asymptotic behaviour of two miscible displacing fluids is studied with molecular diffusion and velocity contrasts on the cross-section of the capillary. Such models represent specific porous media and cannot be generalized; they do not display transverse dispersion.

The next step has been the introduction of random capillaries models (Saffman, 1959, 1960; De Josselin de Jong, 1958): they consist of a network of straight pores, distributed and oriented at random and connected together. Their dimensions are of the order of real pore dimensions. One computes the distribution function of a particle displacement after a given time period, which yields the values of dispersion.

Straight pores do not represent a general porous medium. Yet, it has been possible with such models to display the transverse dispersion and compute its value relatively to longitudinal dispersion.

Statistical geometric models have been considerably improved by Bear and Bachmat (1967), who very completely describe the dispersion equation currently used in all practical applications of pollution studies nowadays. For that reason, we detail their approach (Bear, 1972).

They use the concept of the three regularization levels (§ 2.1.4). Their model is an assembly of randomly connected channels, of various lengths, cross-sections and orientations. Each channel, bounded by a solid surface, defines a streamtube the axis of which is an analytical curve. The total volume of the junctions is much smaller than the volume of the channels and, at a junction, the functional relationships between the flow parameters, such as velocities and pressures, and the parameters of the channel just left are no longer valid. The liquid is incompressible, Newtonian, with variable density and viscosity. The flow regime is laminar, convective acceleration is neglected and energy losses in the junctions can be neglected with respect to the energy losses in the channels.

Computations are conducted in three steps, corresponding to the three regularization levels: (1) derivation of the equations of mass conservation and movement for the fluid particles of the channel; (2) averaging of the equations on a channel section to obtain local equations; and (3) averaging of the local equations in a representative elementary volume of medium to obtain the macroscopic equations.

The representative elementary volume (R.E.V.) at a point is defined with respect to porosity: it is the smallest volume element containing the point, such that when several channels are added or subtracted, the global variation of volume leaves the porosity invariant.

The average $\bar{a}$ of a quantity a in the representative element volume Δv_0, centered at P, is defined by the integral:

$$\bar{a}(P) = \frac{1}{\phi \Delta v_0(P)} \int_{\phi \Delta v_0(P)} a \, dv$$

where dv is the element of pore volume, ϕ the porosity; $\bar{a}$ is assumed to be twice differentiable almost everywhere. The following equations are then obtained:

(1) the mass conservation equation:

$$\frac{\partial \bar{c}}{\partial t} = \frac{\partial}{\partial x^i}\left(D\overline{T}^{ij}\frac{\partial \bar{c}}{\partial x^j} - \overline{cu^i}\right) - \overline{cu^i}\,\frac{\partial(\phi \Delta v_0)/\partial x^j}{\phi \Delta v_0} \qquad [2.2.1]$$

$$\text{where } T^{ij} = \frac{d\xi^i}{d\sigma}\frac{d\xi^j}{d\sigma}\left(\frac{d\sigma}{ds}\right)^2$$

while Δv_0 is the volume of the R.E.V., ξ^j is the Cartesian coordinate of a point in a channel, σ and s respectively are the curvilinear abscissas of a flowline in a channel and of the channel axis measured from one end of the channel. D is the molecular diffusion coefficient.

The microscopic mass flux of dispersing fluid due to convection, cu^i, is made up of two parts, cU^i due to convection at the mean velocity in the R.E.V. and $c\tilde{u}^i$ due to convection with the local velocity fluctuations with respect to the mean velocity:

$$cu^i = cU^i + c\tilde{u}^i \qquad [2.2.2]$$

one sets:

$$\overline{\tilde{c}\tilde{u}^i} = -K^{ij}\frac{\partial \overline{c}}{\partial x^j} \qquad [2.2.3]$$

and the computation yields:

$$K^{ij} \simeq \overline{u^i u^j}\,\overline{\frac{L}{U}\left[1 + 2\frac{D}{LU} + 4\frac{D}{LU}\left(\frac{L}{a}\right)^2\right]^{-1}} \qquad [2.2.4]$$

where L is the mean channel length, a is a characteristic section dimension, U is the mean-mass pore velocity and D the molecular diffusion coefficient. The liquid is incompressible. Equations [2.2.1], [2.2.2] and [2.2.3] then yield:

$$\frac{\partial \bar{c}}{\partial t} = \frac{\partial}{\partial x^i}\left[(DT^{ij} + K^{ij})\frac{\partial \bar{c}}{\partial x^j} - U^i \bar{c}\right] + K^{ij}\frac{\partial \bar{c}}{\partial x^j}\frac{\partial \phi \Delta v_0/\partial x}{\phi \Delta v_0} \qquad [2.2.5]$$

the fraction on the right-hand side accounting for the medium heterogeneity.

(2) the continuity equation of the heterogeneous fluid:

$$\frac{\partial \bar{\rho}}{\partial t} = \frac{\partial}{\partial x^i}\left[(DT^{ij} + K^{ij})\frac{\partial \bar{\rho}}{\partial x^j}\right] - U^i \cdot \frac{\partial \bar{\rho}}{\partial x^i} + K^{ij}\frac{\partial \bar{\rho}}{\partial x^j}\frac{\partial(\phi \Delta v_0)/\partial x^i}{\phi \Delta v_0} \qquad [2.2.6]$$

where $\bar{\rho}$ is the fluid density.

(3) the movement equation:

$$U^i = -\frac{k^{ij}}{\phi \mu}\left(\frac{\partial P}{\partial x^j} + \bar{\rho} g \frac{\partial z}{\partial x^j}\right) - \frac{B\bar{\rho}}{\mu}\frac{\partial U^i}{\partial t} \qquad [2.2.7]$$

where B is the channel conductance and $k^{ij} = \overline{\phi B T^{ij}}$ is the permeability. This equation has been obtained by assuming that density and viscosity depend linearly upon the concentration, that no correlations exist between pressure and medium and between liquid and medium and that diffusion can be neglected.

Another approach, purely probabilistic, also yielded a dispersion equation similar to [2.2.5]; but the physical meaning of the dispersion coefficients as expressed in [2.2.4] does not appear so clearly in this probabilistic approach.

To make the smallest number of assumptions about the geometry of the porous medium seems to be a very natural conceptual approach to a general representation of dispersion. This leads to deriving probabilistic models (Scheidegger, 1963), based on the idea that although a porous medium is completely determined, the knowledge we have of this porous medium is random; and the most general way of modelling such a situation is to represent the medium by a set of random variables. Scheidegger gives some conceptual rules for this type of model:

(1) An assumption must be made on the averaging properties of the porous medium.

(2) The relationships between the forces acting on the fluid, the properties of the fluid and the velocity during an elementary time interval must be given.

(3) The probability laws of each event during elementary time intervals must be chosen.

He derives a random-walk model in a homogeneous and isotropic porous medium. Time is divided up into elementary intervals and an event during an interval is independent from the same event during another interval. An ergodic hypothesis is valid: the average of a quantity in the porous medium is equal to the limit of the averages of the same quantity at a given point of the medium with respect to time for increasing time. The velocity variations with respect to the mean velocity are random and the flow is laminar. The dispersing fluid concentration at a point is the probability of finding a particle of dispersing fluid at that point. It verifies the diffusion equation:

$$K\frac{\partial^2 c}{\partial x^2} - u\frac{\partial c}{\partial x} = \frac{\partial c}{\partial t}$$

for a monodimensional flow at a constant velocity. Experimental studies allow a generalization of this equation:

$$\frac{\partial c}{\partial t} + U \operatorname{grad} c = \operatorname{div}(\mathsf{K} \operatorname{grad} c)$$

where U is the pore velocity and K the dispersion tensor. This equation is similar to Bear's equation for a homogeneous medium and a constant flow velocity.

This dispersion equation can be refined (Fried and Combarnous, 1971) by analogy to diffusive mass transfer. In the case of a molecular diffusion phenomenon, the mass transfer depends on the gradients of c^*, a dimensionless number expressed in mass per mass. The diffusion equation is:

$$\operatorname{div}(\mathsf{D}\rho \otimes \operatorname{grad} C^*) - \operatorname{div}\left(\frac{C^* U}{\rho}\right) = \frac{\partial (C^*/\rho)}{\partial t}$$

$$\text{or: } \operatorname{div}(\mathsf{D}\rho \otimes \operatorname{grad} C^*) - \operatorname{div}(CU) = \frac{\partial C}{\partial t}$$

Such a form suggests that, in the general case, a good representation of dispersion phenomena may be obtained by:

$$\operatorname{div}(\mathsf{K}\rho \otimes \operatorname{grad} C^*) - \operatorname{div}(CU) = \partial C/\partial t \qquad [2.2.8]$$

In the tracer case, this form is equivalent to the usual form as ρ is constant:

$$\operatorname{div}(\mathsf{K} \otimes \operatorname{grad} C) - \operatorname{div}(CU) = \partial C/\partial t \qquad \rho C^* = C$$

Equation [2.2.8] should be used when ρ depends on concentrations, as in the case of miscible fluids of different densities. It should be noticed that there exists a correlation between the continuity equation of the fluid phase and the dispersion equation.

In the diffusion of two compounds 1 and 2, the Onsager reciprocity relationships infer that the diffusion coefficient of compound 2 in compound 1 is the same as the diffusion coefficient of compound 1 in compound 2. In the same way, it may be induced that the dispersion coefficients do not depend on the constituents.

Given a mixture of two compounds, the dispersion equations are:

$$\operatorname{div}(\mathsf{K}\rho\otimes\operatorname{grad} C_i^*) - \operatorname{div}(C_i U) = \frac{\partial C_i}{\partial t}(i = 1 \text{ and } 2) \qquad [2.2.9]$$

According to a previous remark, K does not depend on i. Taking into account the definitions of C and C^*, $C_1 + C_2 = \rho$ and $C_1^* + C_2^* = 1$, the continuity equation may be derived by adding the terms of (2.2.9) for $i = 1$ and $i = 2$:

$$\operatorname{div}[\mathsf{K}\rho\otimes\operatorname{grad}(C_1^* + C_2^*)] - \operatorname{div}[(C_1 + C_2)U] = \partial(C_1 + C_2)/\partial t$$

$$\text{or: } \operatorname{div}(\rho U) + \partial\rho/\partial t = 0$$

This result implies that the system of only one dispersion equation and the continuity equation will be sufficient to formulate a dispersion problem well.

2.3. CRITIQUES OF THE CLASSICAL FOUNDATIONS OF THE DISPERSION EQUATION

By various methods, an equation called "the general equation of dispersion" has been derived. This equation of dispersion is the mathematical model currently used to represent real cases of dispersion, found in groundwater pollution.

As the name "model" implies it, this equation is a simulation of the real phenomenon and as such provides an approximation only of dispersion, based upon the various assumptions developed in the previous paragraph. The problem is to find out whether the errors in this approximation are consistent with the errors allowed in the various experimental studies of dispersion.

We shall see that, with respect to the type and precision of the field results, as well as to the precision in the in-situ determination of the coefficients of this model, this equation is good and yields results consistent with the experimental errors. Yet some discrepancies between theoretical and experimental results appear at the level of the fine laboratory experiment. Now we shall display these discrepancies and suggest possible means of improving the conceptual representation of dispersion phenomena.

2.3.1. *Experimental results*

A series of experimental laboratory results, obtained by scientists working independently, is considered as the origin of the questioning of the validity of the classical dispersion equation. These scientists have noticed discrepancies between experimental results and theoretical results from the modelling by means of the classical dispersion equation of their laboratory experiments. They have shown that more than the current experimental errors is at the origin of these differences.

Scheidegger (1963) has shown the occurrence of systematic errors (Fig. 2.3.1). He has tried the assumption of computation errors due to boundary conditions at a finite distance, which did not prove satisfactory.

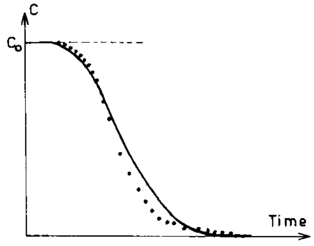

Fig. 2.3.1. Scheidegger's computed curve versus experimental results.

He also thought that, in his theory, time steps were not independent and assumed the existence of an autocorrelation between subsequent time-steps. In order to take care of the correlations between the directions that a particle possesses at time t and at time $t + \tau$, he introduced the *Lagrangian correlation coefficient* $R(\tau)$ defined as follows in a coordinate system moving with the mean velocity of flow:

$$R(\tau) = \overline{[\tilde{u}(t)\cdot\tilde{u}(t+\tau)]}\,/(\overline{\tilde{u}^2})$$

Scheidegger ended up with a *telegraph equation*:

$$\frac{\partial\psi}{\partial t} + U\frac{\partial\psi}{\partial x} = K\frac{\partial^2\psi}{\partial x^2} - A\left(U^2\frac{\partial^2\psi}{\partial x^2} + 2U\frac{\partial^2\psi}{\partial x\,\partial t} + \frac{\partial^2\psi}{\partial t^2}\right)$$

where A and K depend on the dynamic parameters such as pressure drop.

Unfortunately, this equation yields solutions which do not fit experimental results (Fig. 2.3.2). There is a sharp cut-off at $x' = (K/A)^{1/2}t$, travelling in the porous medium at velocity $(K/A)^{1/2}$.

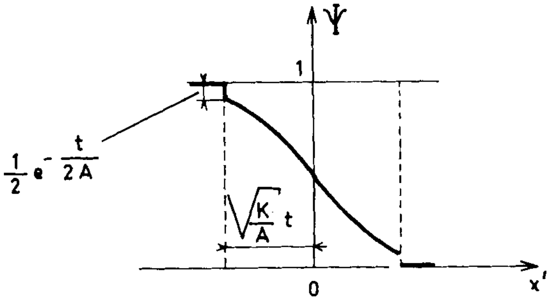

Fig. 2.3.2. Scheidegger's telegraph equation solution (1963).

Goodknight et al. (1960), Goodknight and Fatt (1963), and Coats and Smith (1964) have tried to explain these observed differences between theory and experiment by the occurrence of *dead-end pores* (Fig. 2.3.3) which are pores where the fluids are static and mass transfers are only due to molecular diffusion.

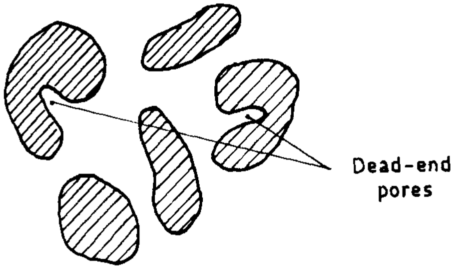

Fig. 2.3.3. Dead-end pores in a granular medium.

Fatt derives a general diffusion equation, taking into account the existence of dead-end pores and assuming a uniform distribution of dead-end pores in the medium, no communications between them and a steady-state diffusion flow through the necks of dead-end pores. He obtains the system:

$$\frac{\partial C}{\partial t} = \frac{D}{\theta^2}\frac{\partial^2 C}{\partial x^2} - \frac{V_d}{V_1}\frac{\partial C_1}{\partial t}$$

$$\frac{\partial C_1}{\partial t} = \frac{DA_0}{l_0 V_c}(C - C_1)$$

where D is the diffusion coefficient, $C_1(x,t)$ is the concentration in dead-end pores, θ is the tortuosity of the medium, V_1 is the volume of flow channels, V_d is the total volume of dead-end pores, V_c is the volume of one dead-end pore, l_0 and A_0 are the length and the cross-sectional area of the neck of a dead-end pore (Fig. 2.3.4). These equations are restricted to a diffusion process.

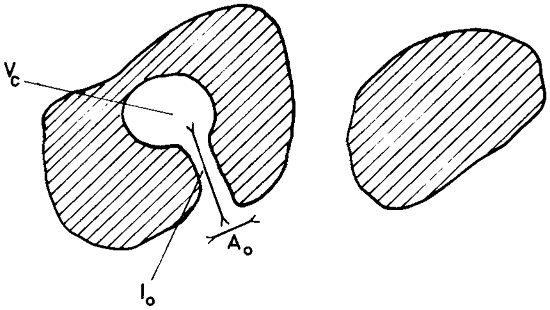

Fig. 2.3.4. Neck of a dead-end pore.

In the same way, but generalizing to a dispersion process, Coats and Smith derive the following macroscopic equation:

$$\frac{\partial c}{\partial t} + U\frac{\partial c}{\partial x} = K_L \frac{\partial^2 c}{\partial x^2} - (1-f)\frac{\partial c_1}{\partial t} \qquad [2.3.1]$$

where f is the fraction of pore volume occupied by the moving fluid. This means that, without dead-end pores, [2.3.1] is the classical macroscopic equation ($f = 1$) and $c_1(x,t)$ is the concentration in the dead-end pores at point x and time t.

The equation of diffusion in a dead-end pore should be added to [2.3.1]:

$$\gamma(c_1 - c) = (1-f)\frac{\partial c_1}{\partial t}$$

γ is a transfer coefficient between dead-end pores and other pores. These equations are easily extended to multidimensional flow and lateral dispersion.

As an explanation of the discrepancies, this theory is not quite satisfactory as conceptually molecular diffusion is a component of dispersion, already taken into account in the derivation of the classical equation, which holds for vanishing velocities when the dispersion coefficients become the coefficients of diffusion in porous media (cf. § 2.4).

Simpson (1962) and Crane and Gardner (1961) have shown the existence of discrepancies between theory and experiments for extreme concentration values. Simpson assumed then that the concentration distribution does not fit a normal law, which means that the classical equation (solutions of which are Gaussian) does not hold. Some experimentalists have recorded such discrepancies without explaining them (Blanc, 1967; Ben Salah, 1965, Pfannkuch, 1963) (Fig. 2.3.5).

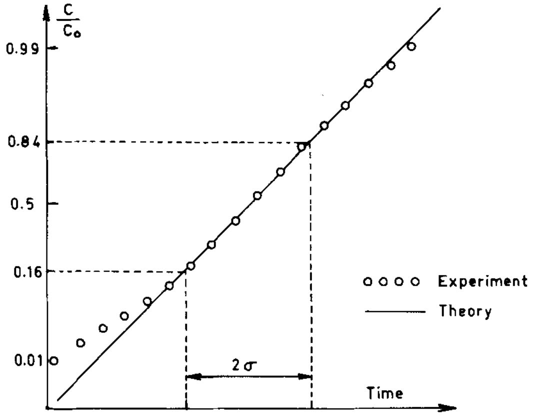

Fig. 2.3.5. Pfannkuch's computed curve versus experimental results.

Discrepancies between experimental and theoretical results have been recorded; in a few cases an interpretation of this phenomenon has been given, leading to a tentative improvement of the dispersion equation. We give now general ideas on the origin and treatment of these differences.

2.3.2. *Critiques of the concept of continuous medium*

Classical mathematical models simultaneously use the three following notions:

(1) The mean velocity of the set of particles is the real macroscopic velocity or pore velocity. Roughly, the pore velocity is the Darcy's velocity divided by the porosity of the medium (the student is referred to Appendix 1 for all hydrologic definitions).

(2) The macroscopic porous medium is continuous, i.e. any infinitesimal element of a porous medium contains both solid and void.

(3) Concentration is a function twice continuously differentiable everywhere.

These three notions can be contradictory. In mathematical language, the second notion expresses the fact that the solid space is without interior point, i.e. the boundary between solid space and void space is everywhere dense. This implies that the real velocity, which is a continuous function of the space variables and is zero on the boundary, is zero everywhere. Thus, using the mathematical definisions strictly, we see that the pore velocity does not make sense, and the first and second notions contradict themselves.

In order to remove this difficulty, the continuity of the porous medium is defined in a less strict way: the infinitesimal element of macroscopic medium is approached by a *finite* element of porous-medium volume containing *finite* volumes of solid and void: this is the case of Bear's R.E.V. But then concentration, which is a measure of the void space, is no longer differentiable everywhere, because it is discontinuous at the boundary between solid and void: indeed concentration actually measured during experiments is twice continuously differentiable at every point of the void space; it is extended by a constant in the solid and is discontinuous at the boundary (Fig. 2.3.6).

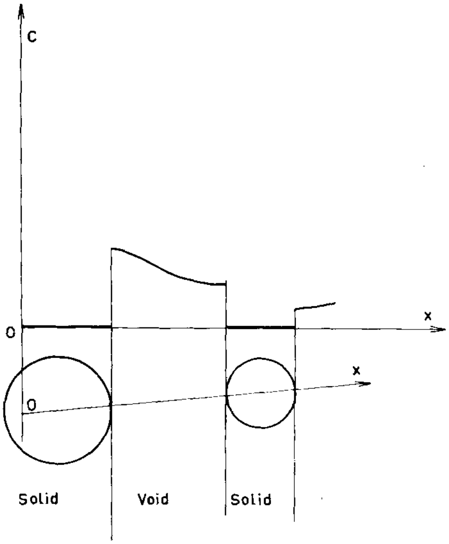

Fig. 2.3.6. Concentration discontinuities in a porous medium.

This set of contradictions shows what appears to be a major difficulty in the theory of dispersion: how should the influence of the boundary between solid space and void space be taken into account?

We wish to emphasize again here that it is a basic question in the study of porous media: the porous medium is very complex and although, in most cases, the basic equations (motion, continuity, etc.) are well known in the pores, their boundary conditions are difficult to establish because of the high complexity of the boundary. We have said (§2.2) that modelling flow in a porous medium is to replace a system of well-known equations with simple conditions on very complex boundaries, by a system of equations with simple conditions on simple boundaries. We now see that to obtain the equivalence between the two systems is not a simple problem and probably still is an interesting field of research.

The random-walk models do not take the boundary into consideration and Bear's model implies that the mean variables (computed in R.E.V., which is the approximation of an infinitesimal element of macroscopic medium in the sense we just defined) are twice continuously differentiable except at some points, curves and surfaces of the porous medium, which is not consistent with the assumption that these variables verify second-order partial differential equations everywhere.

Thus our purpose is to give some hints at possible developments of this field of research, showing that if the boundary is taken into account, an equation is derived, which is not the classical dispersion equation. These indications are given, using a scheme of spatial averaging.

2.3.3. Influence of the boundary (Fried, 1972a)

We call *microscopic* space the porous medium observed at the granulometric level (the local level of §2.1.4). The equations of molecular diffusion and Navier-Stokes hold at this level.

We call *macroscopic* space the porous medium observed at the macroscopic level. At this level, fluid velocities may obey Darcy's law (Appendix I) and dispersion makes sense.

An infinitesimal element of macroscopic space is approached by a R.E.V. in the sense of Bear: we choose a ball of radius r centered at each point x of the microscopic space; r may be determined from a graph similar to Fig. 2.3.7c. Microscopic concentration verifies the convective diffusion equation:

$$\operatorname{div}(\mathsf{D} \operatorname{grad} c) - \operatorname{div}(uc) = \frac{\partial c}{\partial t} \qquad [2.3.2]$$

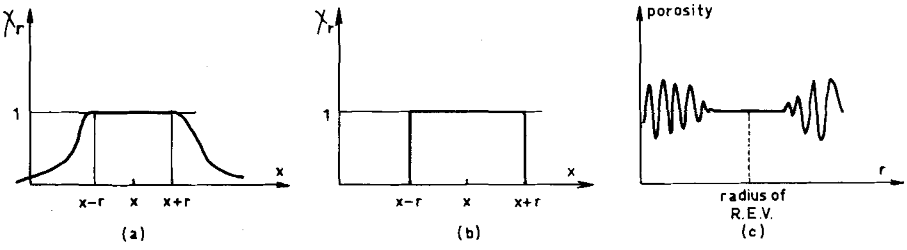

Fig. 2.3.7. (a) Example of a $C^\infty \chi_r$-function. (b) Bear's regularizing function.

where D is the diffusion tensor and u the convective velocity of the particles. For the sake of simplicity, D is taken as constant in the whole medium and spherical. Concentration c is defined in the void space (zero for instance). Function $(x,t) \to c(x,t)$ is then a discontinuous function of x on the boundary S between void space and solid space and the diffusion equation [2.3.2] does not hold on this boundary. Being locally integrable, c defines a distribution (Schwartz, 1973); then it is possible to extend the diffusion equation to the whole space by subtracting superficial distributions with their support on the boundary S and due to the discontinuities of function c.

Assume S is regular, i.e. differentiable. Applying the Laplace operator to c, in the sense of distributions, we obtain (Schwartz):

$$\Delta c = [\Delta c] + \sigma_\nu \delta_{(S)} + \frac{\partial}{\partial \nu} \sigma_0 \delta_{(S)}$$

where $[\Delta c]$ is the usual derivative of function c (where it exists), σ_ν and σ_0 are respectively the jump of the normal derivative of c and the jump of c at the boundary S. $\delta_{(S)}$ is a symbol meaning that distribution $\sigma_\nu \delta_{(S)}$ has its support on S. It may be called the "Dirac measure" of S.

The diffusion equation, taken now in the sense of distributions and valid in the whole microscopic space, is written:

$$D\Delta c - \operatorname{div}(uc) = \frac{\partial c}{\partial t} + \sigma\nu\delta_{(S)} + \frac{\partial}{\partial \nu} \sigma_0 \delta_{(S)} \qquad [2.3.3]$$

Call χ_r a family of functions converging towards the Dirac δ-measure when r tends to 0. We call macroscopic equation of dispersion the equation obtained by regularization of [2.3.3] by χ_r for small r (i.e. by a convolution by χ_r):

$$\chi_r * (D\Delta c) - \chi_r * \operatorname{div}(uc) = \chi_r * \frac{\partial c}{\partial t} + \chi_r * \sigma_\nu \delta_{(S)} + \chi_r * \frac{\partial}{\partial \nu} \sigma_0 \delta_{(S)} \qquad [2.3.4]$$

r is the radius of the ball of center x and according to the definition of the R.E.V. is a finite quantity different from zero. The macroscopic space is made up of the x-points of the microscopic space and physical quantities at these points are the averages, weighted by χ_r, of the corresponding microscopic quantities in the ball. If we choose χ_r to be c^∞ (Fig. 2.3.7a), the regularized functions are c^∞.

Remark. Bear's theory uses a classical average, i.e. a convolution with the indicator of the R.E.V., which yields a regularized function which is not c^∞.

The regularized function C of c is called macroscopic concentration and verifies the equation:

$$D\Delta C - \operatorname{div}(\chi_r * uc) = \frac{\partial C}{\partial t} + \chi_r * \sigma_\nu \delta_{(S)} + \chi_r * \frac{\partial}{\partial \nu} \sigma_0 \delta_{(S)} \qquad [2.3.5]$$

Using Bear's interpretation of the instantaneous microscopic mass flux uc as the sum of a mass flux due to the average velocity and of a mass flux due to the fluctuations of velocity (§ 2.2), and retaining his phenomenological interpretation of the last flux in terms of dispersion coefficients, we obtain the classical dispersion equation with supplementary terms due to σ_0 and σ_ν:

$$\operatorname{div}(D + K^{ij}) \operatorname{grad} C - \operatorname{div}(UC) = \frac{\partial C}{\partial t} + \chi_r * \sigma_\nu \delta(s) + \chi_r * \frac{\partial}{\partial \nu} \sigma_0 \delta(s) \quad [2.3.6]$$

$\chi_r * \sigma_\nu \delta(s)$ is a distribution with support on S and $\chi_r * \partial/\partial\nu[\sigma_0 \delta(s)]$ is the resultant of a set of doublets of moment densities $-\sigma_0$ on the normal to S at each point of S. They represent the influence of the boundary.

It seems thus that even if the boundary S between void space and solid space is physicochemically inert, it has an effect as a set of discontinuity for some physical quantities: on this set, microscopic equations do not hold and any regularizing process should take this into account.

2.3.4. Critiques of the concept of spatial averaging

Spatial averaging is a natural regularizing process, but which is not intrinsic: the macroscopic quantities depend on the regularizing method.

The determination of the R.E.V. depends, at least, on the precision of porosity measurements and on the methods of estimation of the homogeneity scales of the medium. In addition, the covering of the microscopic space by R.E.V. should be defined, i.e. the choice of the geometries of the R.E.V. (balls, parallelepipeds, etc.) and how they cover the space (overlapping or not, for instance).

Remark. Regularization of the diffusion equation by convolution usually changes the equation. Here is a simple proof. Assume:

$$A = \sum_{ij} a_{ij}(x) \frac{\partial^2}{\partial x^i \partial x^j} + \sum_j b_j \frac{\partial}{\partial x^j} + \gamma$$

The diffusion equation is then written:

$$Ac = \frac{\mathrm{d}c}{\mathrm{d}t}$$

χ being a rapidly decreasing C^∞ function, we state $C = \chi * c$ and we regularize $Ac = \mathrm{d}c/\mathrm{d}t$ by χ:

$$\chi * Ac = \frac{\mathrm{d}C}{\mathrm{d}t}$$

Defining the operator L by:

$$L(\chi *) = (\chi *)A - A(\chi *)$$

we have:

$$\chi * Ac = LC + AC$$

and:

$$\frac{\mathrm{d}C}{\mathrm{d}t} = AC + LC$$

If A has constant coefficients, L is zero and we find the diffusion equation. Otherwise, $A + L$ usually does not yield a diffusion equation. L may be computed using composition theorems of pseudo-differential operators (Unterberger and Unterberger, 1970, 1971).

2.3.5. Conclusion

There are systematic discrepancies between the solutions of the classical dispersion equation and experimental results. Classical processes modelling dispersion in porous media by a diffusion equation present some weaknesses, especially in the way the boundary between void and solid is taken into account.

The reader, especially when working on fine research problems, is invited to give some thoughts to the various criticisms that have been developed in the chapter and also to the hints as to further research which we give here as a conclusion.

The basis of dispersion theory is a *measurement* problem. In a porous medium, concentrations are measured in some way. First, it should be verified that the physical quantity that is measured (concentration for instance) does not depend on the experimental method. Theoretical macroscopic concentration, for instance, which appears in mathematical models, should correspond to the experimental concentration; this is not simple, as we have just seen.

The model of dispersion then could either be: (1) a new global equation, starting directly from some phenomenological relationships valid at the global level and considering the local level as a black box: or (2) a refinement of the classical dispersion equation, trying to identify measured concentration and mean theoretical concentration of the model.

The various conceptual approaches to dispersion and the criticisms of the existing models show that the domain of research in the field of dispersion is part of the problem of change of scale, which is a very general problem in physics.

2.4. LABORATORY INVESTIGATIONS OF THE FOUNDATIONS OF DISPERSION (HOMOGENEOUS MEDIA)

In order to verify the conceptual representations of dispersion, many laboratory experiments have been derived. Actually they serve two purposes: (1) to verify and refine the concepts and theoretical models of dispersion; and (2) to study the influence on dispersion of the various parameters, such as the characteristics of the fluids and the properties of the porous medium.

We have already seen how the experiments lead to question the representativity of the models and to suggest possible refinements (§ 2.3). The second aspect of laboratory investigations is of prime importance for pollution studies: its results consist in relationships between dimensionless numbers which are of direct use in real problems.

Most of these laboratory experiments have been conducted in homogeneous porous media. Of course field problems involve heterogeneous porous media (even if, at some scale, we shall see that they may be considered as homogeneous) and series of laboratory tests were performed in heterogeneous porous media of some sort. Although many authors would consider these tests as part of the description of the foundations of dispersion theory and within the scope of this paragraph on pollution fundamentals, we feel that they also represent a transition between the laboratory and the field and as such they are presented separately in § 2.5. Thus, it should be clear that the results presented now were obtained with homogeneous soils.

Experiments are realized under some restrictive conditions: (1) the dispersion tensor K is reduced to its principal coefficients K_L or K_T; (2) boundary conditions are usually chosen so that either lateral or longitudinal dispersion may be neglected; (3) the flow in the model is uniform and fingering is prevented; and (4) initial concentration profiles are generally step functions. The adopted model is the classical dispersion equation:

$$\operatorname{div}\left(\mathsf{K}\rho \operatorname{grad} \frac{C}{\rho}\right) - \operatorname{div}(UC) = \frac{\partial C}{\partial t} \qquad [2.4.1]$$

The main experimental results have been obtained in the tracer case (for instance, with a low concentration of NaCl) which allows an easy theoretical interpretation, as the basic equations have been derived for that case. Moreover, some practical problems are set in the tracer case. But real problems very often deal with fluids of different densities and viscosities; for instance, the displacement of crude oil by a miscible gas. Even in a pollution by seawater intrusion, the salt content is such that the problem cannot be reduced to a tracer problem. In the latter case, there exist laboratory results which allow some useful interpretations.

In this section we present experimental results, starting by a dimensional analysis and then studying the determination techniques of the dispersion coefficients. The results are then given in the tracer case and in the general case. The last part of the section is devoted to a thorough study of the technical aspects of the experiments.

2.4.1. Dimensional analysis

Physical reasons show that dispersion depends upon the following parameters: viscosities μ_i and densities ρ_i of both fluids ($i = 1$ or 2), gravity g, average pore velocity U, diffusion coefficient D, and texture parameters such as permeability k.

This dimensional analysis is worked out for a simple case answering some restrictive assumptions:

(1) With the assumption that mixing occurs without volume shrinkage, the influence of the difference between ρ_1 and ρ_2 due to the action of gravity, may be described by one parameter: $g(\rho_1 - \rho_2) = g\,\Delta\rho$.

(2) One coefficient, D, accounts for molecular diffusion. D is moreover assumed independent of concentration. In a porous medium, molecular diffusion is observed as K_0.

(3) Dispersion depends only upon the viscosities μ_1 and μ_2 of both fluids before they mix, i.e., dispersion does not depend upon the function $\mu(C)$, the resulting viscosity of the mixture. This assumption is not very accurate, especially when this function is not monotonic (Fig. 2.4.1).

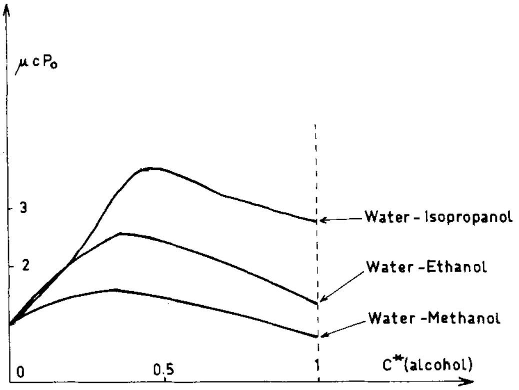

Fig. 2.4.1. Viscosity of a mixture as a function of concentration ($\theta = 20°$ C)

Dispersion may be described by a relationship between seven parameters:

$$K = f(g\Delta\rho, \mu_1, \mu_2, U, K_0, k)$$

The Pi-theorem says that this equation may be written as a relationship between four dimensionless numbers. The study of the equations describing the phenomenon and the analysis of the experimental results reveal that the dimensionless numbers, which yield the best description of the phenomenon, are:

$$K/K_0, \quad Uk^{1/2}/K_0, \quad \mu_1/\mu_2, \quad (g\Delta\rho k^{3/2})/(\mu_1 K_0) \qquad [2.4.2]$$

where K/K_0 is a dimensionless dispersion coefficient, $Uk^{1/2}/K_0$ is a Peclet number, which characterizes the influences of velocity, μ_1/μ_2 is the quantitative evaluation of the contrast of viscosities, and $(g\ \Delta\rho k^{3/2})/(\mu_1 K_0)$ is a quantitative evaluation of the contrast of densities, which has the same form as the Rayleigh number used to describe free thermal convection. The choice of μ_1 is arbitrary, as μ_2 could do as well. For the sake of symmetry, the viscosity μ of the mixture at concentration 0.5 is generally used.

The choice of K_0 appearing in the dimensionless numbers may amaze the physicist who is used to studying dispersion problems in terms of K/D. Actually there are two reasons which justify the choice of K_0 instead of D.

(1) Molecular diffusion in the fluid phase never appears alone without being influenced by the solid matrix. At low mean velocities, only K_0 reflects the action of molecular diffusion.

(2) For fluid couples, the values of D are difficult to find in the literature and D is difficult to measure experimentally. The simplest way, often used, is to measure K_0 for vanishing velocities and to deduce D by the formula:

$$(K/D)_0 = K_0/D = 1/(F\phi)$$

where F is the formation factor.

In (2.4.2) $k^{1/2}$ accounts for the texture of the medium. It is a simple way to introduce a characteristic length of the porous medium. For an unconsolidated medium made up of spherical beads, a grain diameter d may be used and sometimes the dimensionless numbers appear as:

$$K/D, \quad Ud/D, \quad \mu_1/\mu_2, \quad (g\ \Delta\rho d^3)/(\mu_1 D) \qquad [2.4.3]$$

In the tracer case only the first two numbers of the sets [2.4.2] or [2.4.3] are evidently taken into account. The numerical determination of K from the experiments is based upon analytical or numerical resolution of [2.4.1]. Resolutions of [2.4.1] are presented in § 4.1.

2.4.2. Tracer case: longitudinal dispersion

Most of the experimental studies have been performed in unconsolidated porous media, mainly for technical laboratory purposes. As previously mentioned, the experimental results are presented in a dimensionless form on two types of graphs: K/D versus Pe_D (Fig. 2.4.2) and $K/(Ud)$ versus Pe_D (Fig. 2.4.3), where Pe_D is the Peclet number of dispersion ($Pe_D = Ud/D$).

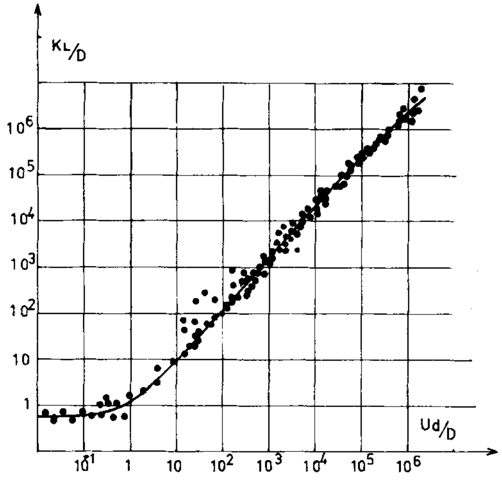

Fig. 2.4.2. Experimental results in the tracer case (longitudinal dispersion)

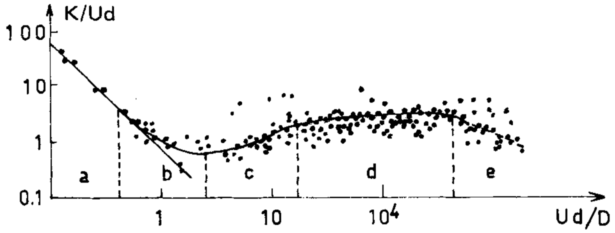

Fig. 2.4.3. The various dispersion regimes: a = pure molecular dispersion, b = superposition regime, c = predominant mechanical dispersion, d = pure mechanical dispersion, e = dispersion out of Darcy's domain, Experimental results.

It should be emphasized that it is impossible to draw a unique set of curves, valid for all types of porous media. For unconsolidated porous media, all experiments were performed in media made up of convex beads. Such media may be characterized by a geometrical parameter chosen either in the pore space or in the solid phase; usually this parameter is the grain size, which is most easily reached.

The set of experimental results obtained for longitudinal dispersion in unconsolidated media is the most complete set of quantitative results on dispersion. It allows a thorough physical analysis of the phenomena and the derivation of general formulas.

In the study of dispersion in porous media different from spherical bead packings, these results are used as the first step. Assuming that the graph "dispersion coefficient versus mean velocity" has the same structure for all porous media, the physicist may draw the real graph from a very small number of experiments (Fig. 2.4.4).

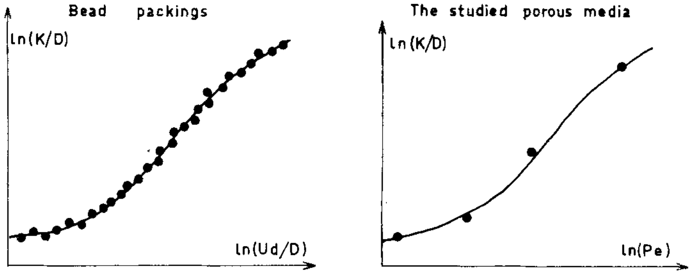

Fig. 2.4.4. Extrapolation of the curve (K/D = Peclet number) for an unknown medium by use of the large number of results obtained for bead packings.

Of course such an extrapolation is made possible by the use of dimensionless numbers.

Unconsolidated Porous Media

From the graphs presented in Figs. 2.4.2 and 2.4.3 it may be inferred that there exist five dispersion regimes.

Regime a: Pure molecular diffusion. This regime occurs when the mean velocity is small. Molecular diffusion is the unique component of dispersion and K_L/D is then constant. As previously mentioned in Fried and Combarnous (1971, p. 192), the porous medium slows down the diffusion processes. For instance, for an homogeneous medium made up of identical spheres, the ratio K_L/D is equal to:

$$(K_L/D)_0 = 0.67 \qquad [2.4.4]$$

Regime b: Superposition. The contribution of mechanical dispersion becomes appreciable.

Regime c: Major mechanical dispersion. The contribution of mechanical dispersion is predominant. But molecular diffusion cannot be neglected and reduces the effects of mechanical dispersion. Taking into account the linear relationship observed between $\log_{10}(K_L/D)$ and $\log_{10} Pe_D$, a formula may be derived:

$$K_L/D = (K_L/D)_0 + \alpha(Ud/D)^m \qquad [2.4.5]$$

Regime d: Pure mechanical dispersion. The following relationship holds:

$$K_L = (K_L/D)_0 + \beta Ud \qquad [2.4.6]$$

Due to the lack of precision of log-log curves, even though the fitting is fairly good (Fig. 2.4.2), the value of β is 1.8 ± 0.4. The influence of molecular diffusion is negligible; $(K_L/D)_0$ may be neglected. This type of formula ($K_L = \alpha U$) is also often used in regime c for practical purposes.

Regime e: Mechanical dispersion where the flow regime is out of the domain of Darcy's law. We recall that a filtration Reynolds number may be defined as Ud/ν and the domain of validity of Darcy's law ranges from 0 to a critical value about 1—10. It may be emphasized that real turbulence appears for a Reynolds number greater than 100. For this regime of dispersion, a few results are available. The change of regime is easily depicted on the graphs in Figs. 2.4.2 and 2.4.3.

Consolidated porous media

Very few experiments have been performed in the case of consolidated porous media. It can be foreseen that dispersion will be greater in consolidated than in unconsolidated media. As a matter of fact, the pore-size distribution is wider in consolidated than in unconsolidated media, and thus, the distribution of velocities is also wider. Different formulas analogous to [2.4.5] are used, such as:

Legatski and Katz (1966) $$K_L/D = (K_L/D)_0 + 0.5[(U\eta d)/D]^m \qquad [2.4.7]$$

Raimondi et al (1959) $$K_L = (K_L)_0 + \eta' dU \qquad [2.4.8]$$

These formulas have been derived by analogy with an unconsolidated medium, which is the reason why the pore-size distribution has been represented by the parameter ηd (or $\eta' d$). η or η' is a dimensionless constant which varies with the standard deviation of the distribution of velocity; d has no quantitative meaning for a consolidated medium. For an unconsolidated medium made up of identical spherical beads, $\eta = 1$, d is the bead diameter, and [2.4.7] holds. $\eta' d$ varies much from one medium to another which justifies the performance of experiments to obtain quantitative results; for instance, Raimondi et al. (1959) give values of $\eta' d$ as different as 0.001 (unconsolidated medium) and 0.2 (consolidated medium) for media with the same permeabilities.

A series of tests conducted by Klotz and Moser (1974) show how dispersion increases with decreasing porosity, i.e. with greater compactness, the explanation being that growing compactness leads to a greater branching of the flow paths. K_L corresponds more or less to ϕ^{-3}, ϕ being the total porosity (Fig. 2.4.5).

2.4.3. Tracer case: lateral dispersion

The studies of lateral dispersion are less numerous but more recent than

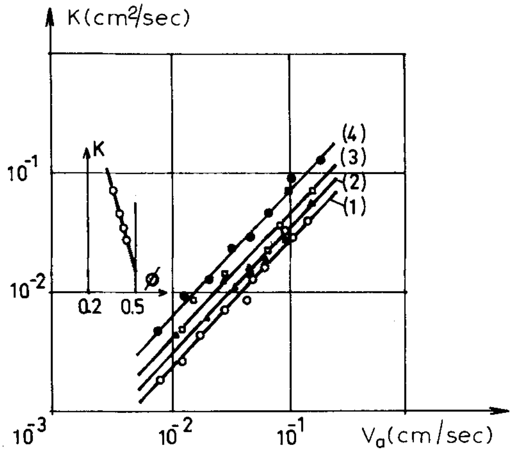

Fig. 2.4.5. Longitudinal dispersion coefficient K in relation to distance velocity V_a for different degrees of compactness given by the total porosity of the medium (sand (0.5 – 1.5 mm), $d_{50} = 0.75$) and in relation to the total porosity ϕ for $V_a = 10^{-1}$ cm/s Water temperature 20° C.
(*1*) $\phi = 0.418$, (*2*) $\phi = 0.399$, (*3*) $\phi = 0.368$, (*4*) $\phi = 0.336$. (Klotz and Moser, 1974).

longitudinal-dispersion studies. The experimental techniques are thus better and, though fewer in number, results are as valid and as accurate as those obtained for longitudinal dispersion. The experiments are mostly performed in unconsolidated media made up of convex beads, for the reasons developed in § 2.4.2.

Unconsolidated porous media

The experiments have been performed for Peclet numbers ranging from 10^{-2} to 10^{+4} and have shown the existence of four regimes of dispersion (Fig. 2.4.6).

Regime a: Pure molecular diffusion, which occurs at low mean velocities. For an homogeneous medium made up of identical spheres $(K_T/D)_0$ is roughly equal to 0.7.

Regime b: Superposition, when the influence of mechanical dispersion can be felt.

Regime c: Mechanical dispersion, when the influence of mechanical dispersion becomes predominant. The following formula may then be derived:

$$K_T/D = (K_T/D_0) + \alpha(Ud/D)^m \qquad [2.4.9]$$

with $\alpha = 0.025$ and $m = 1.1$.

Regime d: Pure mechanical dispersion where [2.4.9] holds with $m = 1$.

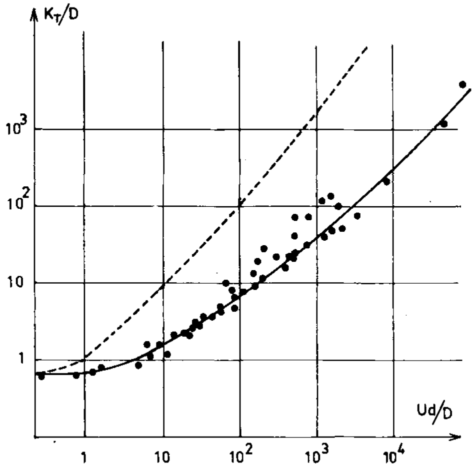

Fig. 2.4.6. Experimental results in the tracer case. Lateral dispersion — Longitudinal dispersion — — — —.

Consolidated porous media

To our knowledge, no experiment has been performed in the case of highly consolidated porous media. Simpson (1962) used a medium very loosely consolidated and, in this case, consolidation does not influence dispersion phenomena. This is the reason why his results are shown in Fig. 2.4.6.

2.4.4. General case: longitudinal dispersion (unconsolidated media)

All the results presented in the preceding sections are very useful in field studies with tracers and especially with radiotracers. Many practical cases, such as pollution problems or oil recovery, are set for fluids of different densities and viscosities. This is the reason why such a case has also been studied experimentally in laboratories.

Stability of the displacement

The first point and, for our purpose, one of the most important, is to determine the stability condition of the miscible displacement. Stability depends upon the density, viscosity, and the velocity U of the fluids. For given densities and viscosities there exists a critical velocity limiting the stability domain. The study of the growth conditions of an arbitrary perturbation yields a very approximate formula of the critical velocity U_c (Marle, 1968):

$$U_c = [kg(\rho_2 - \rho_1)]/[\phi(\mu_2 - \mu_1)] \qquad [2.4.10]$$

where g is the gravity vector and the subscripts 1 and 2 refer respectively to the upper fluid and the lower fluid. In what follows, the z-axis is oriented upward, and velocities U and U_c are algebraic.

There exist two cases depending upon the viscosity ratio: (1) if $\mu_2/\mu_1 > 1$, the displacement is stable for $U > U_c$ and unstable for $U < U_c$; (2) if $\mu_2/\mu_1 < 1$, the displacement is unstable for $U > U_c$ and stable for $U < U_c$. The difference $(\rho_2 - \rho_1)$ influences the sign of U_c: for instance, the upward vertical displacement ($U>0$) with μ_2 greater than μ_1 and ρ_2 greater than ρ_1, is always stable (Fig. 2.4.7) because U_c is negative.

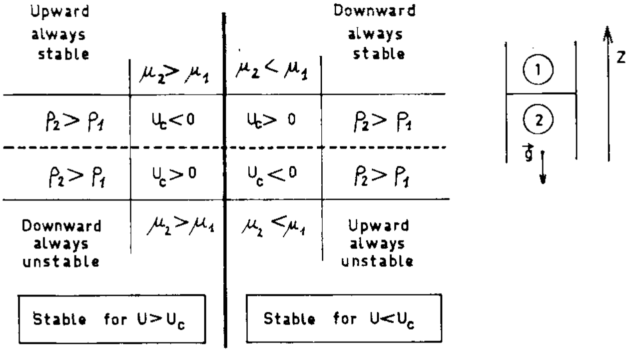

Fig. 2.4.7. Stability conditions for a miscible displacement.

When the displacement is unstable, some fingering appears which at a large scale (larger than the macroscopic scale) may be considered as an extension of the dispersion phenomenon.

Experimental versus theoretical results

As a second point it should be noted that the general dispersion equation derived in the tracer case can be used as such even when density and viscosity contrasts are important. Yet when the initial concentration profile is a step function, the observed solution deviates from the theoretical error-function profile slightly more than in the tracer case.

The last point is devoted to the study of the influence of the various parameters. As shown in § 2.4.1 the influence of these parameters may be described as the influence of three dimensionless quantities. Evidently, the first one is the Peclet number Ud/D. Two other numbers M and R account for the influences of viscosity and density:

$$M = \mu_1/\mu_2 \qquad R = [g\Delta\rho(k)^{3/2}]/(\mu D).$$

where μ is the viscosity of the mixture at concentration 0.5. The subscript 2 refers to the displacing fluid. Published results up to now treat the case of unconsolidated media. Experiments have been conducted by setting M or R constant and by working out several runs with different R or M-values.

The displacement is vertical either upward (Ben Salah, 1965) or downward (Tahar, 1968, Klotz and Moser, 1974).

Influence of the viscosity ratio M

A set of experiments has been made by Tahar (1968) with R at about 6700. This value of R may seem high, but often higher values are found in the field (up to 100,000 in some oil-recovery techniques). The results are plotted in Figs. 2.4.8 and 2.4.9.

The greater the relative viscosity of the displacing fluid, the smaller the dispersion coefficient. Moreover, M has no influence in the zone of pure molecular diffusion. Klotz and Moser (1974) show how dispersion depends on temperature, through viscosity variations. The dispersion coefficient grows when viscosity increases as water temperature decreases. K_L is approximately proportional to $\nu^{0.3}$ (Fig. 2.4.10).

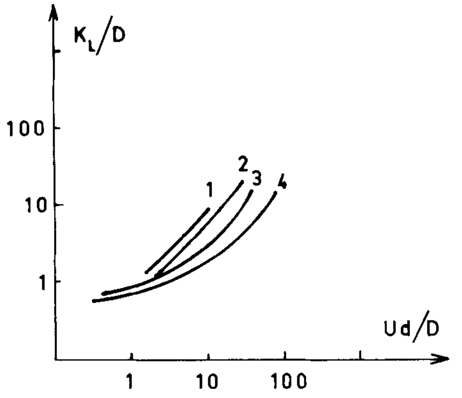

Fig. 2.4.8. Influence of the viscosity contrast for a vertical miscible displacement. (*1*) $M = 2.79$, (*2*) $M = 1$, (*3*) $M = 0.358$, (*4*) $M = 0.047$. (Tahar, 1968.)

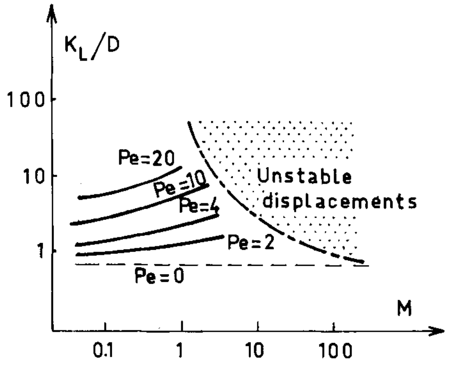

Fig. 2.4.9. Influence of the viscosity contrast for a vertical miscible displacement (Tahar, 1968).

Influence of R

In the experiments made by Ben Salah (1965), M was set equal to 0.214. The results are plotted on Figs. 2.4.11 and 2.4.12. It can be seen that the greater the density contrast, the smaller the dispersion coefficient. This effect is felt even in the pure molecular diffusion zone.

2.4.5. General case: lateral dispersion

The results are analogous to those obtained in the case of longitudinal dispersion. The existence of viscosity and density contrasts decreases the lateral dispersion coefficient. The density contrast even influences the zone of pure molecular diffusion.

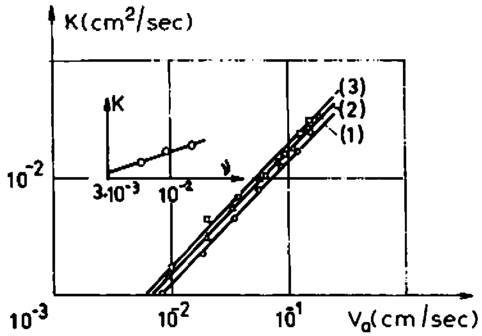

Fig. 2.4.10. Longitudinal dispersion coefficient K in relation to distance velocity V_a for different water temperatures T, and in relation to kinematic viscosity ν for $V_a = 10^{-1}$ cm/s, porous medium sand (0.9 – 1.12 mm); $d_{50} = 1.0$ mm, compact bedding. (*1*) $T = 45°$ C, (*2*) $T = 21°$ C, (*3*) $T = 5°$ C. (Klotz and Moser, 1974).

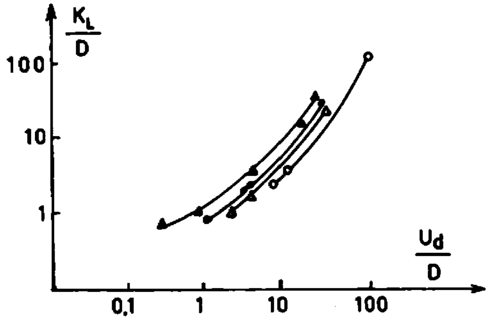

Fig. 2.4.11. Influence of the density contrast for a vertical miscible displacement $R = 650$; $R = 2450$; $R = 5200$; $R = 19{,}600$. (Ben Salah, 1965; Tahar, 1968).

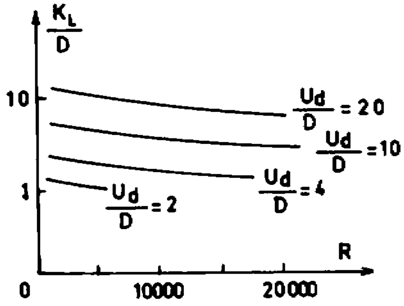

Fig. 2.4.12. Influence of a density contrast for a vertical miscible displacement. (Ben Salah, 1965, Tahar, 1968.)

The effects of density contrasts have been studied in a porous medium such that the mean velocity direction could be set at various angles with the horizontal plane (Blanc, 1967).

2.5. *LABORATORY INVESTIGATIONS IN HETEROGENEOUS MEDIA*

Real problems occur in heterogeneous media. Homogeneous media have provided simple conditions and allowed a fairly easy separation of the respective influences of various parameters: a good insight into the fundamental mechanisms was therefore obtained. In a heterogeneous medium, the parameters vary together; they interfere and the results could be rather different from those expected according to the homogeneous-medium theory.

Why then waste time in studying perfect academic media, if they are not consistent in some way with reality? Very luckily (especially for all those scientists who devoted so much work to these phenomena), there is a link between theories and practical results. Everyone can breathe easily!

Intuitively, we imagine a process equivalent to the change of scale from microscopic to macroscopic levels: in the same way as molecular and convective diffusion effects may be averaged to yield dispersion, is it possible to average dispersion effects to reach some super macroscopic phenomenon in an equivalent homogeneous medium? In order to answer this question, we present here some typical experiments.

Remark. This book is not a detective story; before reaching the end of the paragraph, it is good to know that the answer will be yes!

2.5.1. A stratified medium

The simplest case of a heterogeneous medium is a stratified medium. Besides, this is a frequent case as a sedimentary formation may often be considered as stratified, composed of plane strata of different porosities and permeabilities. For the sake of simplicity, the flow is taken as unidirectional and parallel to the layers and the density ρ of the fluid phase is constant. The equations are then bidimensional, the x-axis being taken along the flow direction and the y-axis perpendicular to the strata (Fig. 2.5.1).

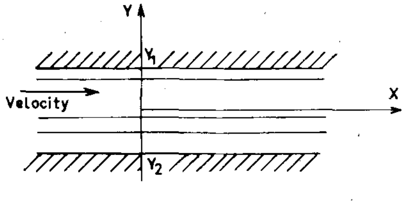

Fig. 2.5.1. Coordinate system.

In this simple case, the dispersion tensor is reduced to two components K_L and K_T, longitudinal and transverse coefficients, which depend on y. ρ being constant and the flow unidirectional, velocity U does not depend on x. We moreover assume ϕ to be dependent on y.

The equation and the boundary conditions are:

$$K_L(y)\phi(y)\frac{\partial^2 C}{\partial x^2}+\frac{\partial}{\partial y}\left[K_T(y)\phi(y)\frac{\partial C}{\partial y}\right]-\phi(y)\left(U\frac{\partial C}{\partial x}+\frac{\partial C}{\partial t}\right)=0$$

$$\partial C/\partial y = 0 \quad \text{for} \quad y=y_1 \quad \text{and} \quad y=y_2 \qquad [2.5.1]$$

It will be now shown that for large times, i.e. for an asymptotic regime in the concentration profile, it is possible to replace [2.5.1] by a unidimensional equation:

$$K_M \frac{\partial^2 \bar{C}}{\partial x^2} - U_M \frac{\partial \bar{C}}{\partial x} = \frac{\partial \bar{C}}{\partial t} \qquad [2.5.2]$$

where K_M is an equivalent dispersion coefficient and $\bar{C}$ and U_M are the average concentration and velocity.

Theoretical works use Aris' moment method, which is developed hereafter. Experiments were performed on models made up of two homogeneous strata of different characteristics and they confirm the theoretical results.

Remark. The idea of replacing a complex problem by an elementary well-known equivalent problem is very natural and is the base of the philosophy of the scale change. This is what we do when, in electricity, we replace a set of resistors by an equivalent resistor.

Aris' moment method

The solution of [2.5.1] is a concentration distribution $C(x, y, t)$. This solution (Marle et al., 1967) may be approached by deriving the moments $C^{(n)}(y;t)$ with respect to x of the distribution $C(x,y,t)$. These moments are defined by:

$$C^{(n)}(y,t) = \int_{-\infty}^{+\infty} x^n C(x,y,t)\, dx$$

Of course a mathematical problem is then raised: do these integrals converge? Convergence is obtained when C decreases faster than any power of x, which is the case when C, resulting from an initial step impulse, is a Gaussian function (Fig. 2.5.2).

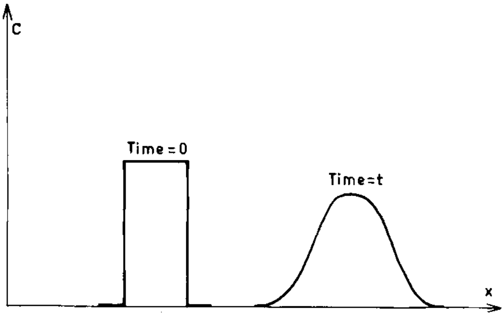

Fig. 2.5.2. Evolution of a step impulse by dispersion. C is the concentration for a given y.

This condition is not restrictive because new solutions may be obtained by superposition, [2.5.1] being linear. It is of interest to observe the physical meaning of the first moments: $C^{(0)}$ is the total amount of dispersing fluid; $C^{(1)}$ is the x-coordinate of the center of mass; and $C^{(2)}$ is a characteristic of the transition zone.

Let the moments be computed in a reference system in translation with a constant velocity $\bar{U}$ defined by:

$$\bar{U} = \left(\int_{y_1}^{y_2} \phi U \,\mathrm{d}y\right) \Big/ \left(\int_{y_1}^{y_2} \phi \,\mathrm{d}y\right)$$

In this system the velocity is $W = U - \bar{U}$.

Aris computes the various moments of the concentration distribution, solution of [2.5.1], from a set of moment equations obtained from [2.5.1] by deriving the moments of various orders of each of its terms:

$$\begin{aligned} &\frac{1}{\phi}\frac{\partial}{\partial y}\left(K_T\phi\frac{\partial C^{(n)}}{\partial y}\right) - \frac{\partial C^{(n)}}{\partial t} = -nWC^{(n-1)} - n(n-1)K_L C^{(n-2)} \\ &\partial C^{(n)}/\partial y = 0 \quad \text{for} \quad y = y_1 \quad \text{and}\; y = y_2 \end{aligned} \qquad [2.5.3]$$

This system is then solved by induction, starting at $n = 0$. For $n = 0$, [2.5.3] yields:

$$\begin{aligned} &\frac{1}{\phi}\frac{\partial}{\partial y}\left(K_T\phi\frac{\partial C^{(0)}}{\partial y}\right) - \frac{\partial C^{(0)}}{\partial t} = 0 \\ &\partial C^{(0)}/\partial y = 0 \quad \text{for} \quad y = y_1 \quad \text{and} \quad y = y_2 \end{aligned} \qquad [2.5.4]$$

Equation [2.5.4] is solved by the method of separation of variables and yields a countable sequence of solutions of the form:

$$a_i(y)\exp(-\omega_i t), \qquad i = 0, 1, 2, \ldots \qquad 0 < \ldots < \omega_{i-1} < \omega_i < \ldots$$

For $n = k$, the right-hand side of [2.5.3] is known from the solutions obtained for $n < k$. Hence the general solution of [2.5.3] for $n = k$ is the sum of the general solution of the homogeneous equation in $C^{(n)}$ on the left-hand side (which is identical to [2.5.4]) and a particular solution of the complete equation. The general solution of the homogeneous equation:

$$\frac{1}{\phi}\frac{\partial}{\partial y}\left(K_T\phi\frac{\partial C^{(n)}}{\partial y}\right) - \frac{\partial C^{(n)}}{\partial t} = 0$$

is a series $\Sigma_i a_i(y)\exp(-\omega_i t)$ defined previously.

The particular solution is a superposition of the solutions of [2.5.3] where the right-hand side is replaced successively by the terms of the series defining $C^{(n-1)}$ and $C^{(n-2)}$, computed by induction from $C^{(0)}$. It is easy to obtain the principal term for $t \to \infty$. The different moments are then:

$$\begin{aligned} C^{(0)} &= a_0 + 0(y,t) \\ C^{(1)} &= a_0\psi(y) + 0(y,t) \\ C^{(2)} &= 2\bar{K}a_0t + Q(y) + 0(y,t) \\ &\cdot \\ &\cdot \\ &\cdot \\ C^{(2p)} &= \frac{(2p)!(2\bar{K}t)^p}{2^p p!}\,a_0 + t^p \cdot 0(y,t) \\ C^{(2p+1)} &= \frac{(2p+1)!(2\bar{K}t)^p}{2^p p!}\,a_0\psi(y) + t^p \cdot 0(y,t) \\ &\cdot \\ &\cdot \\ &\cdot \end{aligned} \qquad [2.5.5]$$

where $0(y,t)$ is a function decreasing towards 0 when t goes to infinity.

$$\begin{aligned} \psi(y) &= -\int_{y_1}^{y} \frac{\varphi(y)}{K_T\phi}\,\mathrm{d}y + \text{constant} \\ \varphi(y) &= \int_{y_1}^{y} \phi W\,\mathrm{d}y \text{ with } \varphi(y_1) = \varphi(y_2) = 0 \\ \bar{K} &= \frac{1}{(y_2-y_1)\bar{\phi}}\left(\int_{y_1}^{y_2} K_L\phi\mathrm{d}y + \int_{y_1}^{y_2}\frac{\varphi^2}{K_T\phi}\,\mathrm{d}y\right) \\ Q(y) &= \int_{y_1}^{y}\frac{2}{K_T\phi}\left[\int_{y_1}^{y}(\bar{K}-W\psi(\xi)-K_L)\phi\,\mathrm{d}\xi\right]\mathrm{d}y \\ \bar{\phi} &= \frac{1}{y_2-y_1}\int_{y_1}^{y_2}\phi\,\mathrm{d}y \end{aligned} \qquad [2.5.6]$$

Equivalent dispersion coefficient

The moments $C^{(n)}$ are compared, for large values of t, to the moments of a concentration-distribution solution of a simpler system. A good choice is to take the equation of unidirectional dispersion in a homogeneous layer, which yields the equivalent dispersion coefficient. This equation is repeated here:

$$K_M\,\frac{\partial^2\bar{C}}{\partial x^2} - \left(U_M\,\frac{\partial\bar{C}}{\partial x} + \frac{\partial\bar{C}}{\partial t}\right) = 0$$

In the reference system, in translation with velocity U_M, the moments of the solution of this equation are:

$$\begin{aligned}
\bar{C}^{(0)} &= \text{constant}\\
\bar{C}^{(1)} &= \text{constant}\\
\bar{C}^{(2)} &= 2K_M t + \text{constant}\\
\bar{C}^{(2p)} &= \frac{(2p)!(2K_M t)^p}{2^p p!}\,\bar{C}^{(0)} + t^p 0(t)\\
\bar{C}^{(2p+1)} &= \frac{(2p+1)!(2K_M t)!}{2^p p!}\,\bar{C}^{(1)} + t^p 0(t)
\end{aligned} \qquad [2.5.7]$$

The systems [2.5.5] and [2.5.7] are identical when:

$$\begin{aligned}
\bar{C} &= \frac{1}{\bar{\phi}(y_2 - y_1)} \int_{y_1}^{y_2} \phi C \mathrm{d}y\\
U_M &= \bar{U} = \int_{y_1}^{y_2} \phi U \mathrm{d}y \Big/ \int_{y_1}^{y_2} \phi \,\mathrm{d}y\\
K_M &= \bar{K} = \frac{1}{\bar{\phi}(y_2 - y_1)} \left(\int_{y_1}^{y_2} K_L \phi \mathrm{d}y + \int_{y_1}^{y_2} \frac{\varphi^2}{K_T \phi} \mathrm{d}y \right)
\end{aligned} \qquad [2.5.8]$$

Thus, the asymptotic behavior of a stratified porous medium is identical to the behavior of an equivalent homogeneous medium defined by [2.5.8]. In real problems, a good knowledge of the asymptotic behavior of dispersion phenomena is often required and the previous result is important.

The example of two strata (Marle et al. 1967)

The characteristics of the strata are given in Fig. 2.5.3. Equation and boundary conditions [2.5.1] are then written:

$$\begin{aligned}
&K_{L_1} \frac{\partial^2 C_1}{\partial x^2} + K_{T_1} \frac{\partial^2 C_1}{\partial y^2} - U_1 \frac{\partial C_1}{\partial x} = \frac{\partial C_1}{\partial t}\\
&K_{L_2} \frac{\partial^2 C_2}{\partial x^2} + K_{T_2} \frac{\partial^2 C_1}{\partial y^2} - U_2 \frac{\partial C_2}{\partial x} = \frac{\partial C_2}{\partial t}\\
&y = y_1, \quad \partial C_1/\partial y = 0; \qquad y = y_2, \quad \partial C_2/\partial y = 0\\
&y = 0, \quad \phi_1 K_{T_1}(\partial C_1/\partial y) = \phi_2 K_{T_2}(\partial C_2/\partial y)
\end{aligned} \qquad [2.5.9]$$

The mean velocity U_M is defined by:

$$U_M = (\phi_1 e_1 U_1 + \phi_2 e_2 U_2)/(\phi_1 e_1 + \phi_2 e_2)$$

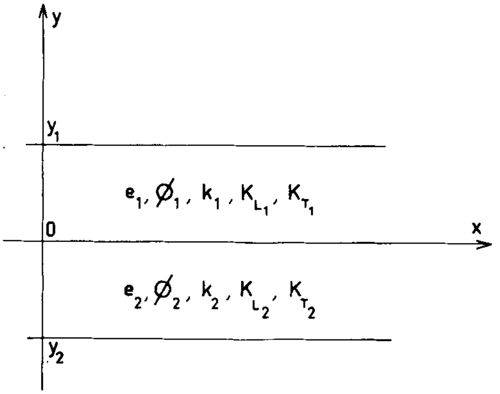

Fig. 2.5.3. Characteristics of the two-strata model: thickness, porosities, permeabilities and dispersion coefficients.

where U_1 and U_2 are the mean velocities in each stratum. Application of Aris' method leads to the following result: the asymptotic behavior of the mean concentration distribution is the solution of the equivalent equation [2.5.2] where K_M is given by:

$$\begin{aligned} K_M &= \frac{\phi_1 e_1 K_{L1} + \phi_2 e_2 K_{L2}}{\phi_1 e_1 + \phi_2 e_2} + \frac{1}{3} \frac{\phi_1^2 \phi_2^2 e_1^2 e_2^2}{(\phi_1 e_2 + \phi_2 e_2)^3} \\ &\quad \times \left[\frac{e_1}{\phi_1 K_{T1}} + \frac{e_2}{\phi_2 K_{T2}} \right] (U_1 - U_2)^2 \end{aligned} \qquad [2.5.10]$$

Another interesting result, which characterizes the asymptotic regime, is that in each streamtube $(y, y + dy)$ the center of mass of the concentration profile has a fixed position in the moving coordinate system. Also, the concentration profile on the axis of stratum 2 may be obtained by translating the concentration profile on the axis of stratum 1.

Laboratory experiments have been performed in two strata with gases (hydrogen—nitrogen, ethylen—nitrogen) which have high diffusion coefficients (the asymptotic regime is quickly reached). The results appear in Figs. 2.5.4 and 2.5.5.

(1) There exists an asymptotic regime, as proved by the observation of two identical concentration profiles in each stratum, the distance between both profiles being constant (Fig. 2.5.4).

(2) The asymptotic regime is identical to the regime observed in a homogeneous medium. Classical straight concentration profiles in Galtonian coordinates (Fig. 2.5.5) are obtained.

Formula [2.5.10] is verified experimentally.

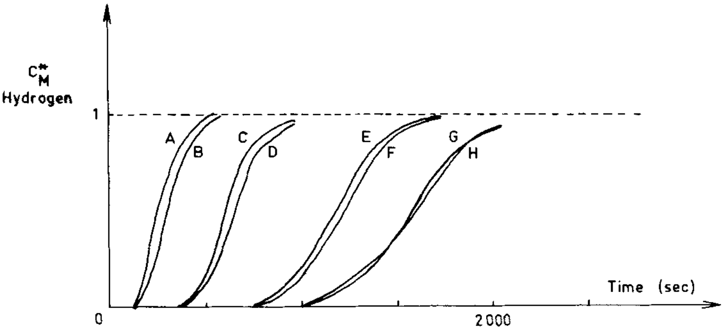

Fig. 2.5.4. Evolution of the concentration versus time at eight measurement points, in four sections of the two-strata model (initial step-input concentration and uniform velocity).

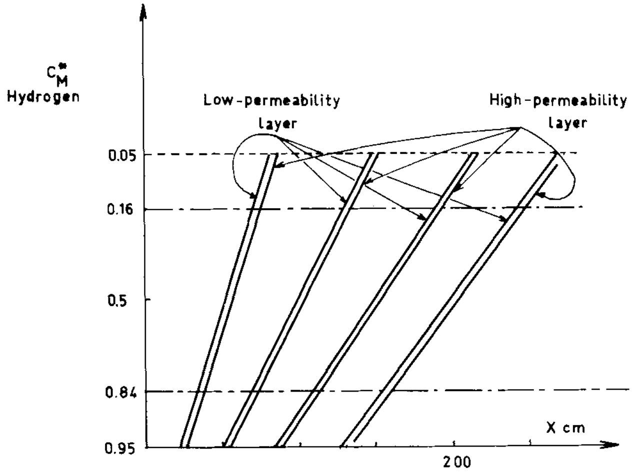

Fig. 2.5.5. Concentration profiles in the two strata at different times. (*1*) $t = 400$s, (*2*) $t = 700$s, (*3*) $t = 1000$s, (*4*) $t = 1300$s.

2.5.2. A heterogeneous non-stratified medium

Experimental studies have been conducted (Martin, 1971) on blocks of Fontainebleau sandstone of various lengths with NaCl solutions, and also nitrogen and CO_2. They show that:

(1) An asymptotic regime is reached, equivalent to the asymptotic regime in homogeneous media. It is reached only if the distance travelled by the transition zone is large with respect to the dimensions of heterogeneities.

(2) Values of the equivalent dispersion coefficient are larger than values of a dispersion coefficient in a homogeneous medium (Fig. 2.5.6).

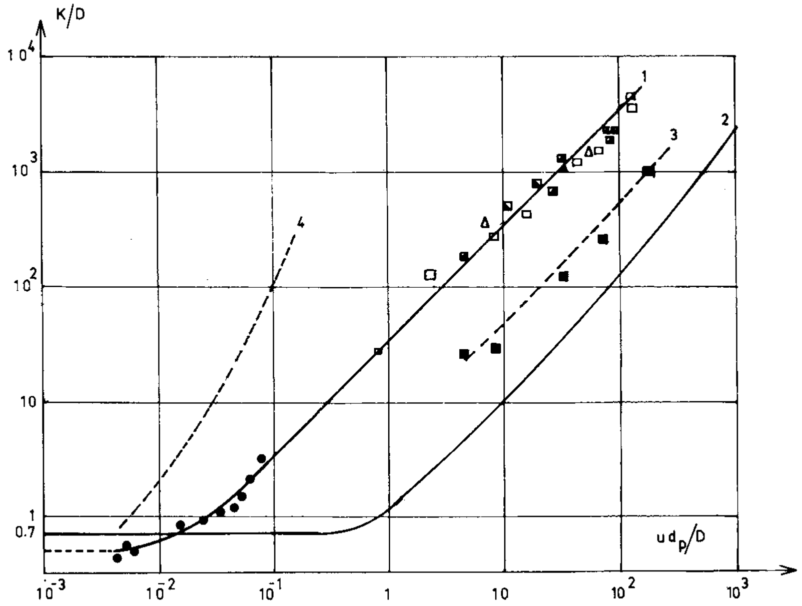

Fig. 2.5.6. Comparison between the values of the longitudinal-dispersion coefficients obtained for heterogeneous media (*1* and *3*) and for homogeneous media (*2* and *4*) = two-strata model. (Martin, 1971.)

(3) Formulas identical to [2.4.5] are proposed:

$$K = \left(\frac{K}{D}\right)_0 D + \beta U^m D^{1-m}$$

where β is a dispersivity coefficient, depending on the homogeneities of the medium.

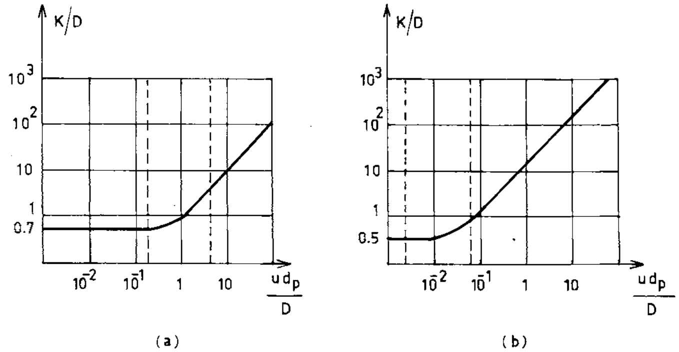

Fig. 2.5.7. The dispersion regimes: (a) homogeneous medium; (b) heterogeneous medium. (Martin, 1971.)

Remark. For practical purposes, m is usually taken equal to 1.

2.5.3. Conclusion

The theory of dispersion can be extended to general media. The results obtained for homogeneous media are valid but the domain of numerical values has changed. Semi-empirical formulas such as [2.4.5] will be retained, coupled with the various dispersion regimes, remarking that the pure diffusion domain may be somewhat smaller for heterogeneous media than for homogeneous media (Fig. 2.5.7).

CHAPTER 3

THE METHODOLOGY OF TECHNICAL STUDIES OF GROUNDWATER POLLUTION

The methodology of groundwater pollution is based upon the fact that, in most cases, the pollution is miscible with groundwater or at least behaves like a tracer and that the spreading of some transition zones cannot be neglected. We have seen in the previous chapter that the miscible flow of pollutants is governed by the dispersion theory. Of course, the evolutions of some pollutants definitely cannot be represented by the theory of dispersion, but then, as in most practical cases their movements answer Darcy's law and the continuity equation, we shall see that they are automatically part of the general methodology, one aim of which is to distinguish between dispersive and purely convective phenomena.

The scale of a pollution phenomenon determines the methods used to cope with it. Thus, the methodology is built to determine this scale and to provide means of changing it, leading to the use of the various experimental and mathematical tools necessary to study the pollution phenomenon.

3.1. THE SCALE PROBLEM

The scale problem presents two aspects:

(1) It is sometimes possible to neglect the dispersion effects and to treat the phenomenon as an immiscible transport of pollution.

For example, imagine a one-dimensional flow at a constant velocity and an injection of pollution at a constant rate. The spreading of the transition zone is proportional to the square root of time (§ 4.1.1), the travelled distance L is proportional to time, through formula $L = ut$; thus, the width e of the transition zone is proportional to $L^{1/2}$ and the relative width e/L is proportional to $L^{1/2}/L$. When L increases, $L^{1/2}/L$ decreases, which means that, on long distances, dispersion effects become less and less important compared to convective effects; a miscible pollution flow can be treated as an immiscible displacement, i.e. piston flow at the mean aquifer velocity, if the travelled distances are large with respect to the dimensions of the pollution source.

(2) Laboratory studies and many field experiments yield local results, such as dispersion coefficients for instance. A real pollution may be rather extensive and a great amount of experiments, usually costly, will be required to collect all the necessary characteristic parameters. Significant field parameters have to be determined in a rather small number to put the experimental

costs at a reasonable level, without loosing too much accuracy in the modelling. Thus a methodology had to be defined to apply the groundwater-pollution theory, developed in the laboratory within dispersion studies, to real field problems. It is mostly a change-of-scale problem, which appears when the laboratory theory of dispersion is applied to field pollution and also, in the field, when several scales of pollution are simultaneously studied (a scale of pollution being defined by the total amount of transient pollution, the strength of the pollution source and the invaded volume of soil).

3.2. THE METHODOLOGY

3.2.1. Decision criteria

When confronted with a groundwater-pollution problem, the people responsible for its solution will ask several questions:

(1) what is the nature of the pollution:
   - is it miscible or not to the water?
   - what are its physical and chemical properties?
   - what sort of danger does it present?

(2) What is the scale of the pollution:
   - what is the total amount of pollution?
   - what is the strength of the pollution source?
   - what are the dimensions and the geometrical characteristics of the pollution source?
   - what is the invaded volume of soil?
   - what is the duration of the pollution?

Preliminary answers to these questions, even only rough answers, are the decision criteria necessary to choose the adapted models and investigation techniques. These answers result from a study of the available data; yet it may sometimes be hard to decide. For instance, dispersion coefficients are essentially local (a complete mathematical proof of this feature is given in Chapter 8); this implies that dispersion phenomena are also local, that the transition zone increases slowly and that eventually dispersion theory makes sense only for large times (which explains why most of the laboratory work on dispersion has been performed for the asymptotic regime, when some sort of steady state has been reached, as seen in Chapter 2), but conversely, as we have just shown in § 3.1, that for very large times dispersion becomes negligible with respect to the dimension of the polluted area. Of course, in reality the asymptotic regime is usually quickly obtained, which allows easier decisions about the type of pollution model to be chosen.

A typical problem is the determination of the amount of pollution flowing through an aquifer to the streams and the mean residence-time of this pollution in the aquifer. This is a regional study; it can be estimated that the width of the transition zone is small with respect to the dimensions of the studied area and a convective model (i.e. a model of movement without dispersion) is good. Another problem is the definition of the protection zone of a pumping well: this is a local problem and dispersion has to be taken into account. Imagine an accidental pollution: because of dispersion, either the critical concentration in the well may be reached before the pollution front (as computed by considering piston flow) goes past, or no critical concentration will be reached at all in the well because of dilution. In this last case, a hydrodispersive model (a model taking dispersion and convection into account) fits well.

In general, the first decision will be to choose the type of structure of the pollution and its modelling having in mind that most dangerous and frequent pollutions of an aquifer are miscible with the water of the aquifer but that immiscible compounds may behave like tracers and also be treated as miscible substances. Scale factors are most important decision criteria and can be hard to study. For instance, dispersion will have to be taken into account in the case of important sources, but also in the case of sources with small dimensions when a critical concentration has to be found.

3.2.2. The dispersion scheme

We call "dispersion" scheme the following set of equations.

(1) dispersion equation:

$$\operatorname{div}\left[\mathsf{K}\rho\cdot\left(\operatorname{grad}\frac{c}{\rho}\right)\right]-\operatorname{div}(uc) = \frac{\partial c}{\partial t}$$

(2) continuity equation:

$$\operatorname{div}(\rho u) = -\frac{\partial \rho}{\partial t}$$

(3) Darcy's equation:

$$u = -\frac{\mathsf{k}}{\mu\phi}\cdot(\operatorname{grad} p + \rho g \operatorname{grad} z)$$

(4) State equations of the mixture:

$$\rho = f(c) \quad \mu = g(c) \quad D = D(c)$$

where c is the pollution concentration, D its molecular-diffusion coefficient,

K the dispersion tensor, k the permeability tensor, p the pressure, t the time, u the pore velocity, ϕ the porosity, μ the dynamic viscosity, ρ the density of the mixture. The dispersion scheme is completed by boundary and initial conditions depending on the problem.

Remark. Temperature does not vary much in an aquifer and is not accounted for in the state equations.

Mathematically, the dispersion scheme is a non-linear system of partial differential equations, because the coefficients of the dispersion equation depend on the solution c of this equation through density and velocity of the mixture. There is no direct method available to solve the system and simplifying assumptions have to be introduced to reach a practical method yielding *practical* solutions, i.e. solutions which, although correct mathematically, are probably not the most beautiful, but which can be handled with good accuracy by people responsible for the treatment of a pollution problem. The simplification of this dispersion scheme is performed according to an ordered set of rules, which is codified in a sub-methodology called the practical use of the dispersion scheme.

3.2.3. Practical use of the dispersion scheme

There are two basic ways of applying the dispersion scheme: (1) the density and the viscosity of the mixture vary with concentration (this is the general case); and (2) the density and the viscosity of the mixture are constant (this is the tracer case).

Remark. In the case histories presented in Chapter 6, the variation of the viscosity could always be neglected.

Both cases are presented on flow charts (Figs. 3.2.1 and 3.2.2) which display their fundamental differences (Fried and Combarnous, 1971).

(1) In the tracer case, the hydrodynamic equations are independent of the dispersion equation, because, density and viscosity being constant, the velocity of the mixture does not depend on the pollution concentration. The dispersion scheme becomes a linear system of partial differential equations and is solved according to the following procedure. First solve the hydrodynamic equations (the Darcy equation and the continuity equation), usually in terms of heads or pressures with pressure boundary and initial conditions. The velocity distributions in space and with time are thus obtained for all time-steps of the experience. Then express the coefficient of the dispersion equation in terms of the velocities at each time step and compute the concentration distributions in space and with time for all time steps from the dispersion equation and its boundary and initial conditions (Chapter 5).

(2) In the general case, the hydrodynamic and dispersion equations depend one on the other, because the coefficients of the dispersion equation are functions of the mixture velocity which itself is a function of the pollution concentration through viscosity and density. It is not possible to obtain the

simultaneous solutions of the equations of the dispersion scheme, as required mathematically, but an approximate procedure has been derived: a distribution of concentration is known at time t; the corresponding distribution of viscosities and densities is computed; viscosity and density are assumed to remain constant during the time-step $\mathrm{d}t$, and from the corresponding velocity distribution, concentrations at time $t + \mathrm{d}t$ are computed; of course, within the same time-step, the procedure is iterated with a convergence test on c (Chapter 5).

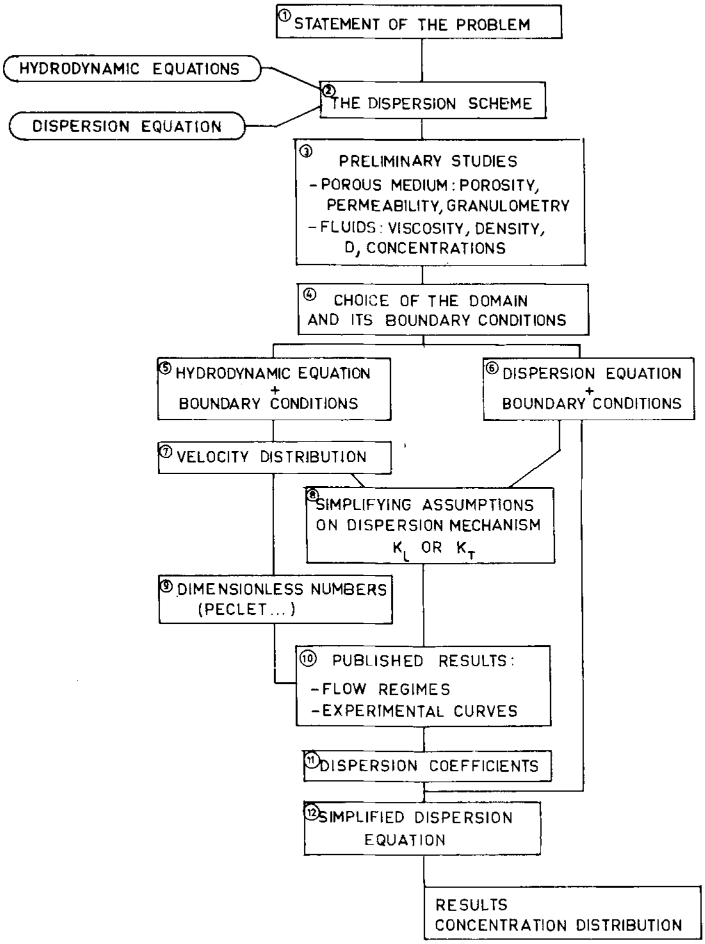

Fig. 3.2.1. Use of the dispersion scheme: the tracer case.

These flow charts require some explanatory remarks.

(1) Theoretically all the dispersion tensor coefficients can be computed either by direct experiments or from the principal coefficients determined experimentally, by the tensor change of coordinate formulas. But the general

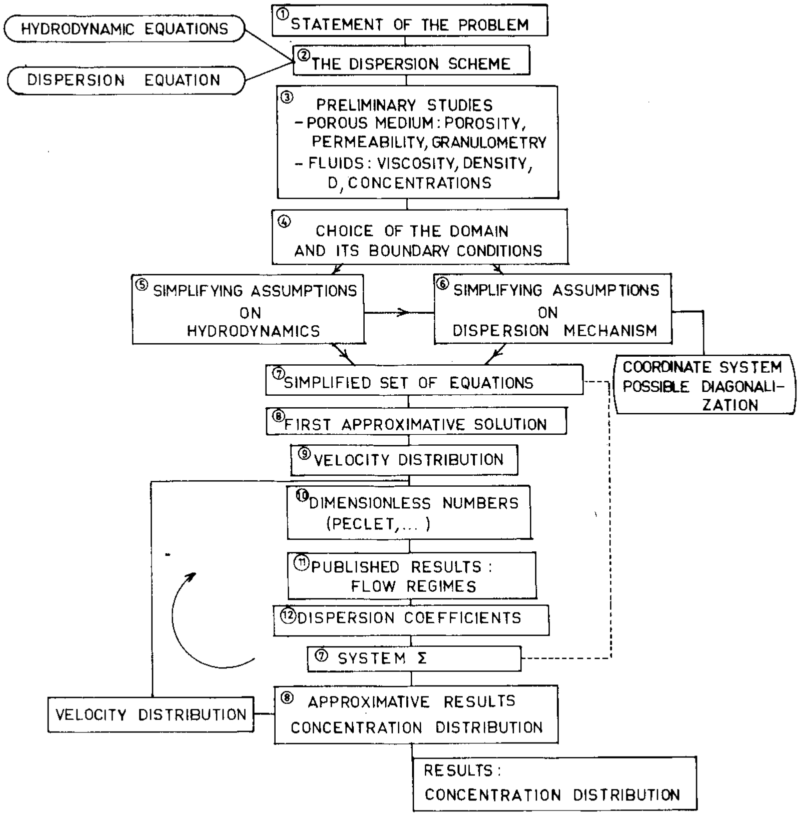

Fig. 3.2.2. Use of the dispersion scheme: the general case.

dispersion equation, with rectangular second-order partial derivatives (i.e. terms like $\partial/\partial x \partial y$), is rather difficult to solve numerically; thus it is very interesting to try to simplify this equation by suppressing the rectangular derivatives; this is obtained by writing the equation in the principal directions of the dispersion tensor, introducing the principal dispersion coefficients K_L and K_T (blocks *8* on Fig. 3.2.1 and *6* on Fig. 3.2.2).

(2) Greater simplification of the dispersion scheme can be obtained by decomposing the tridimensional scheme into two bidimensional schemes, each one being written in the plane of two principal dispersion directions.

(3) There are five dispersion regimes depending on the Peclet dispersion number. A semi-empirical formula describes the dispersion coefficients:

$$K/D = \alpha(Ud/D)^m + \beta$$

and each regime is characterized by the values of the coefficients α, β, m and a domain of the graph (K/D and Ud/D) which is detailed in § 2.4.

In each experiment, a dispersion regime is looked for by the determination of the Peclet number. The comparison with already published curves (Figs. 2.4.2 and 2.4.6) yields the values of α, β, m (blocks *9*, *10*, *11* of Fig. 3.2.1 and *10*, *11*, *22* of Fig. 3.2.2).

Remark. It has been noticed that in most alluvial aquifers, the pollution occurs in the dynamic dispersion regime and the coefficients K are proportional to the pore velocity. They are written $K = \alpha U$ where α, called the intrinsic-dispersion coefficient, depends on the soil, the permeability contrasts and the consolidation. In other cases, the formula $K = \alpha U$ can often be used as a sufficient approximation.

Here is a summary of the *practical rules* that have to be kept in mind for a dispersion study.

(1) There are two cases: (a) a tracer case where the molecular diffusion coefficient, the density and the viscosity are constant; the dispersion scheme is linear, and the hydrodynamic equations do not depend on the dispersion equation and will be solved first for all time-steps; and (b) a general case where the system is not linear; the equations are linked and only numerical methods taking this interdependence into account, such as iterative procedures, should be used.

(2) The dispersion tensor is diagonalized in the system formed by the tangent to the mixture flow velocity and the perpendicular to this velocity.

(3) Then the principal coefficients K of the dispersion tensor can be written as:

$$K/D = \alpha(Pe)^m + \beta$$

where all coefficients have been defined in §2.4.2.

(4) Dispersion coefficients and velocities must be known in space and time to determine the pollution concentration distribution: velocities are derived from field measurements (direct methods) or hydrological models (piezometric methods) and the dispersion coefficients are derived from field measurements using existing pollution or tracer methods.

3.2.4. *The general methodology*

In brief, the general methodology is organized in four stages.

(1) A preliminary study of existing data to estimate the flow and the possible pollution type (local, global, horizontal, vertical, etc.). These data usually comprise permeabilities, morphological parameters of the soils, pollution concentrations.

(2) The formulation of a working assumption from the preliminary study: a mathematical representation is chosen according to the scale of the domain and of the pollution; usually it is either a hydroconvective model (immiscible flow, without dispersion) or a hydrodispersive model. If the chosen model is

hydroconvective, the pollution problem becomes a classical hydrological problem, where only groundwater motions have to be determined. If the chosen model is hydrodispersive, the methodology comprises two more stages:

(3) the use of the dispersion scheme, and

(4) the collection of field parameters. Very often, at this stage there are two possibilities: either there are pollution sources and models are adjusted to these environmental tracer-concentration distributions, yielding dispersion coefficients, or there is no pollution and tracers of some sort must be injected. The field parameters that have to be determined are usually the velocities and the dispersion coefficients.

3.3. *EXAMPLES: TYPE-PROJECTS*

As an illustration of the possible applications of the methodology, we present type-projects that can be used as a basis for pollution-study contracts.

3.3.1. *A study of pollution hazards in a large aquifer feeding an urban community*

Aims of the study

The general aim of the study is to ensure the protection of pumping wells against the various possible pollutions which occur as:

— injections localized in time and space (accidents)

— injections localized in space but long-lasting (sanitary landfills)

— injections in large areas and long-lasting (fertilizers, for instance).

The objectives will be:

(1) To quickly estimate the probability of pollution flowing accidentally through a pumping well.

(2) To define the influence of present or unavoidable pollutions in the wells especially as a function of pumping regimes.

(3) To define pollution-sensitive zones in order to adjust the setting of new wells.

(4) To derive a large-scale model, as a quantitative support of prediction and management.

(5) To inform the public by simple visualization of the evolution of pollution.

The problem

In order to draw up a tentative study programme, the problem must be correctly defined: at this stage, some choice of the models has to be made and decision criteria derived from rough preliminary studies.

These preliminary studies consist of inquiries with local authorities to gather some knowledge of the type of existing and expected pollution. Also, from the statement of objectives, we see that it is a multi-scale problem. Most probably then, both convective and dispersive models will be necessary and the sequence of the options should be included in the programme. In brief the problem is multi-scale, dispersive on both small and large scales and convective at large scales.

The programme

The programme is organized in a sequence of steps which reflect the necessity of carefully separating the various scales and of proceeding from the local to the regional scale.

The domain is partitioned in zones presenting some geological homogeneity as displayed by the preliminary studies. Each zone is divided up into experimental areas, comprising one or several wells. To give an order of magnitude, experiments have been conducted on alluvial aquifers, on experimental areas of 0.002—3 km^2, on zones of 10—50 km^2 and in domains of 50—300 km^2 and, on fissured aquifers, in domains up to 3000 km^2 (Cf. Chapter 6).

On each experimental area, then, experiments will be performed to collect hydraulic parameters (such as porosities and permeabilities) and pollution parameters (such as dispersion coefficients). These parameters will be used as such in predictive models answering objectives 1 and 2.

Such an experimental area is an elementary block of a larger model representing the zone. First, compatibility conditions at the boundaries of the blocks, especially flux conservations, are derived between the experimental-area models, then a mean equivalent model is derived, by computing new sets of equivalent dispersion coefficients, absorbing block boundary conditions and using new zonal boundary conditions.

The zonal models will be adjusted on existing pollution and answer objective 3. The zones are then used as elementary blocks of a model of the domain, first as a juxtaposition of zonal models with compatibility conditions at the zonal boundaries, then within a domain-equivalent model with large-scale equivalent coefficients.

At this stage, dispersion may sometimes be neglected and the domain model will consist of a convective model, i.e. a balance of matter. Objectives 4 and 5 are then answered.

This programme has been summarized on the flow chart Fig. 3.3.1.

The models

These are bidimensional, for general domains. The complete dispersion matrix will be used (and not only a diagonal form) in canonical rectangular axes, with classical change of coordinate formulas to switch from the general form to the diagonal form and conversely.

The results

The results will be forecasting models, the maps of pollution-sensitive

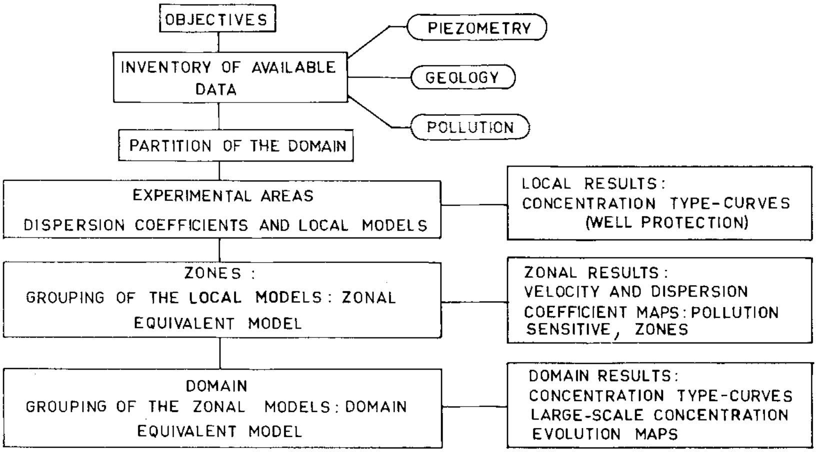

Fig. 3.3.1. Type-project: pollution of an aquifer feeding an urban community.

zones (velocity and dispersion coefficient maps) and type-curves of concentrations.

3.3.2. The setting of sanitary landfills near an urban community

The problem

A town is developing rapidly and increasing its reliance on an underlying unconfined aquifer by setting new grids of pumping wells; at the same time it has to build two new sanitary landfills near an existing one, not too far from the wells. The local authorities wish to forecast the pollution coming from the existing and future landfills and the influence of the various pumping programmes, and the seasonal nature of the surface recharge on its evolution. It is a highly transient, non-steady problem that can be most accurately handled by a mathematical model of the pollution.

Even if no accurate information has been provided concerning the composition of the wastes, it can be assumed (unless stated otherwise by the authorities) that they consist chiefly of wastes from urban areas which generate compounds such as sulfates, sulfites, etc., miscible with the water of the aquifer and a dispersion model will be suitable to determine the pollution concentration levels compared to an admissible pollution threshold in the water of the aquifer.

The programme

It is divided up into three stages, each stage providing a set of usable results allowing evaluations of the pollution with increasing accuracy, which allows of considering one stage after the other in the financial planning of the operation: this procedure is interesting for urban communities which do not have to plan large expenses immediately.

Stage 1 is an initial field study, corresponding to the preliminary studies of the general methodology. It consists of studying the available data in order to determine the various pollution thresholds, the geological features (especially the zones where significant vertical permeability contrasts may be expected), the piezometry and the expected flow lines.

Also, and this is most important, the existing landfill may be considered as a source of environmental tracers and should be monitored by using already existing wells and sampling their water for chemical analysis, and by drilling new multiple-level wells at positions given by the piezometric map.

Stage 2, corresponding to the determination of the pollution-modelling parameters (velocities, dispersion coefficients) in the field, consists of monitoring the existing pollution (by measuring water resistivities with electrical logging, for instance, if stage 1 shows that pollution changes the water resistivity), refining the geological knowledge in the proposed sites (by drilling new wells or by geophysical methods), collecting the necessary data for the determination of dispersion parameters (by injecting an artificial miscible pollutant, such as salt water, and recording its spreading, by surface-resistivity measurements for instance and trying to separate the influence of the lower and the upper aquifer strata), determining the dispersion coefficients (by interpreting the field experiments with a numerical model).

Stage 3, corresponding to the derivation and use of a forecasting and mathematical model, consists of integrating the various results of stages 1 and 2 into hydrologic and dispersion models representing the whole domain influenced by the landfills.

The results

Stage 1 will yield general knowledge of the behaviour of the pollution on the proposed landfills (such as the nature of potential pollutions, the possible average horizontal extension of pollution clouds with time, the possible average vertical extension of pollution clouds and the determination of the layers most sensitive and most affected by pollution) and guidelines to the choice of the forecasting model and its scale (such as the determination of the behaviour of the pollution in a vertical section, the choice of the field experiments with tracers to collect dispersion parameters and the determination of the position and of the number of necessary wells for further experiments to collect dispersion parameters).

Stage 2 will yield numerical values of the dispersion coefficients at the various sites, numerical values of water velocities in the aquifer and a refined map of flowlines, a detailed knowledge of the geological features near the sites, a thorough knowledge of the pollution paths vertically and horizontally and a set of rules of thumb allowing the forecasting of the pollution for steady-state conditions and various well distributions.

Stage 3 will yield a mathematical model, composed of a hydrological model and of a dispersion model, to manage water quality in the landfill zone and the determination of a belt of warning stations to continuously adjust and correct the forecasting tools in case of local variations.

CHAPTER 4

THE EXPERIMENTAL DETERMINATION OF GROUNDWATER POLLUTION PARAMETERS

Laboratory experiments have shown that the parameters that must be determined in the field are *pore velocities* and *dispersion coefficients.* Of course, in Chapter 3, it has been shown that other aquifer characteristics (such as geology and lithology) should be known; their determinations being classical and well described elsewhere, within the scope of this book we shall keep to methods that are specific to pollution studies and which were developed during research on pollution problems (which does not mean that they should be restricted to pollution studies, of course).

This chapter is divided into two parts:

§ 4.1 presents formulas that are explicit, i.e., expressed with simple functions (some authors would call them "analytical formulas"). These formulas represent the solutions of simple, idealized mathematical models and they are very often used in laboratory studies (§ 2.4 and 2.5) where experimental conditions may be chosen to be simple. For non-academic problems, they are difficult to use because approximations are too large. Anyway, in some cases, they are of interest either as means of verification of the magnitude orders or as direct computational tools when natural conditions can be idealized without too great a loss of accuracy.

§ § 4.2 and 4.3 present field methods which usually consist of some experimental devices and a treatment of the results on a mathematical model solved numerically by computer methods.

The principal characteristic of these field methods is that they vary with the scale of the problem (§ 3.1): at each usual scale some experiments correspond and without completely detailing the techniques, we give enough material and references to determine pollution parameters in the most usual pollution problems.

The experimental determination of dispersion coefficients may be summarized in the following flow chart (Fig. 4.0.1).

4.1. EXPLICIT FORMULAS FOR THE ESTIMATE OF DISPERSION COEFFICIENTS

A dispersion phenomenon is estimated from a variation of concentration either in space at a given time or at a given point with time. In order to compute the coefficients, one uses formulas derived from the analytical

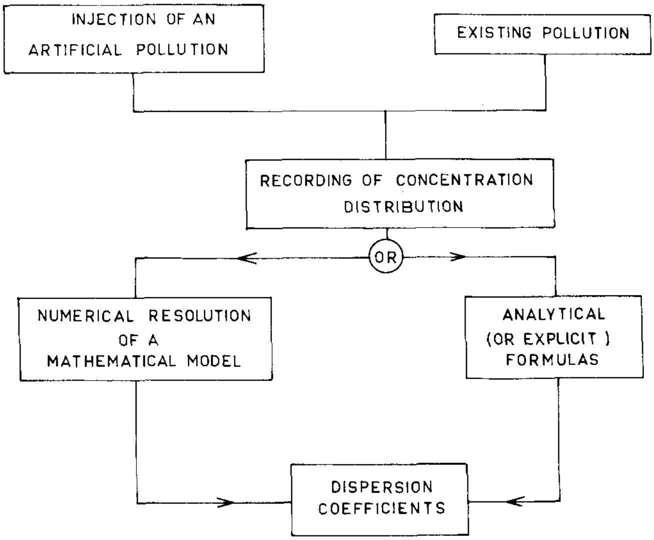

Fig. 4.0.1. Flow chart

solution of the classical dispersion equation for simple experimental conditions: a unidirectional displacement, at constant velocity, an initial step-input function. Density and viscosity are constant.

4.1.1. *The longitudinal dispersion coefficient*

Continuous injection

Consider the system:

$$
\begin{aligned}
&K_L \frac{\partial^2 C}{\partial x^2} - u\frac{\partial C}{\partial x} = \frac{\partial C}{\partial t}\\
&C(x, 0) = 0 \qquad\qquad [4.1.1]\\
&C(0, t) = C_0\\
&C(\infty, t) = 0
\end{aligned}
$$

The solution of [4.1.1] is:

$$\frac{C}{C_0} = \frac{1}{2}\left[\operatorname{erfc}\left(\frac{x - Ut}{2(K_L t)^{1/2}}\right) + \exp\,(Ux/K_L)\operatorname{erfc}\left(\frac{x + Ut}{2(K_L t)^{1/2}}\right)\right] \qquad [4.1.2]$$

The second term is very small compared to the first one and may be neglected; thus:

$$\frac{C}{C_0} = \frac{1}{2}\,\mathrm{erfc}\left(\frac{x - Ut}{2(K_L t)^{1/2}}\right) = \pi^{-1/2}\int_{\frac{x-Ut}{2(K_L t)^{1/2}}}^{\infty} \exp(-\eta^2)\,d\eta \qquad [4.1.3]$$

C/C_0 may be written as:

$$\frac{C}{C_0} = (2\pi)^{-1/2}\int_{\frac{x-Ut}{(2K_L t)^{1/2}}}^{\infty} \exp(-\eta^2/2)\,d\eta \qquad [4.1.4]$$

Then, at a given time, x being the variable, the solution is a normal distribution function $1 - N[(x - m)/\sigma]$ with expectation $m = Ut$ and standard deviation $\sigma = (2K_L t)^{1/2}$. A classical property of the normal distribution function $N[(x - m)/\sigma]$ is that:

$$N(1) = 0.8413 \sim 0.84, \qquad N(-1) = 0.1587 \sim 0.16 \qquad [4.1.5]$$

This property is used because it allows an easy computation of the standard deviation σ from the graph of concentrations versus x, and very often the width of the transition zone is defined as the difference between x at concentration 0.84 and x at concentration 0.16 (Fig. 4.1.1).

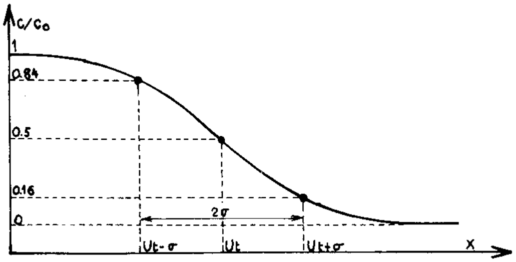

Fig. 4.1.1. The classical error-function concentration profile.

Thus, at a given time, the width e of the transition zone is:

$$e = 2\sigma = x_{0.16} - x_{0.84} = 2(2K_L t)^{1/2} \qquad [4.1.6]$$

and K_L is given by:

$$K_L = (x_{0.16} - x_{0.84})^2/(8t) \qquad [4.1.7]$$

Measurements are very often performed at a given x (for instance at the lower end of the porous medium), and then the evolution of concentration with time is recorded.

Letting $X_i = (x - Ut_i)/(2K_L t_i)^{1/2}$, relationships [4.1.4] and [4.1.5] yield:

$$(x - Ut_{0.16})/(2K_L t_{0.16})^{1/2} - (x - Ut_{0.84})/(2K_L t_{0.84})^{1/2} = 2$$

and K_L is given by the formula:

$$K_L = \tfrac{1}{8}[(x - Ut_{0.16})/(t_{0.16})^{1/2} - (x - Ut_{0.84})/(t_{0.84})^{1/2}]^2 \qquad [4.1.8]$$

It often happens that the transition zone is small with respect to the distance travelled from the upper end of the medium to the measurement point; then $t_{0.16}$ and $t_{0.84}$ may be assumed to be roughly equal to $t_{0.5}$. Thus the relationship becomes:

$$K_L = (8t_{0.5})^{-1}U^2(t_{0.84} - t_{0.16})^2 \qquad [4.1.9]$$

Defining σ' as $(t_{0.84} - t_{0.16})/(2t_{0.5})$ and $t_{0.5}$ as x/U, we derive another useful form of [4.1.9]:

$$K_L = \tfrac{1}{2}\sigma'^2 xU \qquad [4.1.10]$$

This form may be convenient when, at the lower end of the medium, instead of time, injected volumes are measured. Injected volumes, per unit sectional area of porous medium, are related to time by $V_i = Ut_i$. Thus, with C as the concentration at the lower end, the graph C/C_0 versus the injected volumes is roughly represented by a normal distribution function with standard deviation $(V_{0.84} - V_{0.16})/(2V_{0.5})$.

Crenel-type injection

Consider the system:

$$K\frac{\partial^2 C}{\partial x^2} - u\frac{\partial C}{\partial x} = \frac{\partial C}{\partial t}$$

$$\begin{aligned} C(x,0) &= 0 \\ C(0,t) &= 1 \quad t < t_0 \\ C(0,t) &= 0 \quad t > t_0 \\ C(\infty,t) &= 0 \end{aligned} \qquad [4.1.11]$$

It represents the injection of a crenel-type concentration (Fig. 4.1.2).

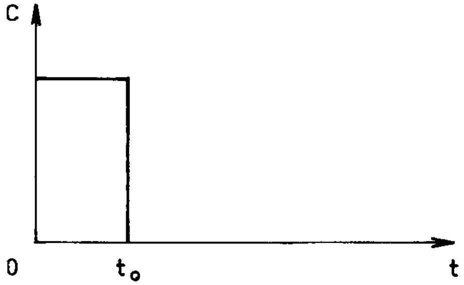

Fig. 4.1.2. Crenel-type input function.

The solution of [4.1.11] is:

$$C = (2\pi)^{-1/2} \int_{\frac{x-ut}{\sqrt{2Kt}}}^{\frac{x-u(t-t_0)}{\sqrt{2K(t-t_0)}}} \exp(-\eta^2/2)\mathrm{d}\eta$$

From this expression of C, we derive some results which we use to adjust mathematical models to experimental concentration distributions, as the crenel-type injection is a classical boundary condition.

We compute C maximum in space at a given time, from the derivative C' of C with respect to x:

$$c' = \frac{1}{\sqrt{2\pi}} \left[\frac{1}{\sqrt{2K(t-t_0)}} \exp\left\{-\frac{[x-u(t-t_0)]^2}{4K(t-t_0)}\right\} - \frac{1}{\sqrt{2Kt}} \exp\left\{-\frac{(x-ut)^2}{4Kt}\right\}\right] = 0$$

$$\text{thus: } \frac{(x-ut)^2}{4Kt} - \frac{[x-u(t-t_0)]^2}{4K(t-t_0)} = \log\sqrt{\frac{t-t_0}{t}}$$

$$\text{and: } x^2\left[-\frac{t_0}{t(t-t_0)}\right] + u^2 t_0 = 2K\log\frac{t-t_0}{t}$$

$$\text{and: } x^2 = \frac{2K\log\dfrac{t-t_0}{t} - u^2 t_0}{-\dfrac{t_0}{t(t-t_0)}}$$

For the asymptotic regime (when t is large enough), we have:

$$x^2 \approx 2K(t - t_0) + u^2 t(t - t_0) \approx u^2 t(t - t_0) + 2\alpha u(t - t_0) \qquad [4.1.12]$$

with $K = \alpha u$.

Result 1. This formula can be used to compute the mean pore velocity u when α is known, with the assumption that the variation of the transition zone can be neglected with respect to the width of this zone. Then x is the distance between injection and observation wells and t_m is the occurrence time of the maximum and we have:

$$u = [-\alpha(t_m - t_0) + \{\alpha^2(t_m - t_0)^2 + x^2(t_m - t_0)t_m\}^{1/2}]/[t_m(t_m - t_0)]$$

It should be noticed that u is different from the velocity of the maximum x/t_m. As α is usually computed by methods requiring a preliminary knowledge of u, this formula will be used for checking purposes.

Result 2. With the assumptions of an asymptotic regime and small variations of the transition zone with dispersion, the dispersion coefficient K is derived as a function of the tracer flow velocity, from [4.1.12]:

$$K = [x^2 - u^2 t_m(t_m - t_0)]/[2(t_m - t_0)] \qquad [4.1.13]$$

where x is the abscissa of the measurement point and t_m the occurrence time of the maximum. The maximum concentration c_m can also be measured, which yields another relationship between K and u:

$$c_m = \frac{1}{\sqrt{2\pi}} \int_{\frac{x - u t_m}{\sqrt{2K t_m}}}^{\frac{x - u(t_m - t_0)}{\sqrt{2K(t_m - t_0)}}} \exp(-\eta^2/2)\mathrm{d}\eta$$

K is positive, by physical considerations. Hence:

$$u < x/[t_m(t_m - t_0)]^{1/2} = u_0$$

It can be shown (Fried, 1972a) that these three relationships yield one couple (K, u) and only one, because the function $c_m(u)$ is monotonous for positive K. From this result, an adjustment method has been derived in the case of a crenel-type boundary condition; the maximum of the concentration curve will be adjusted, which yields one dispersion coefficient only, with the following assumptions: (1) the occurrence time of the tracer is large with respect to the end of the injection time; and (2) the transition zone displays almost no variation by dispersion at the measurement point.

These results have been extended to radial flow by analogy on numerical examples.

Besides, this adjustment is justified because the maximum occurs in the medium zone of the concentration curve which represents well the dispersion phenomenon as seen in § 2.3.

Remark. The error on K, from [4.1.13] is:

$$|dK| = Ut_m du + \frac{x^2}{2(t_m - t_0)^2} dt_0$$

as x and t_m are usually measured with precision.

4.1.2. The lateral dispersion coefficient

The classical experimental setting is described in Fried and Combarnous (1971). The concentration regime is asymptotic, which means that the concentration profile in the measurement section is steady for large values of time; the displacement is unidirectional. Thus the dispersion equation becomes:

$$U(\partial C/\partial x) = K_T(\partial^2 C/\partial y^2) \qquad [4.1.14]$$

Computations are made in the tracer case and in the general case of fluids with different viscosities and densities. In the first case, the velocity through a section is constant. To solve the second problem, where velocities vary in a section, two methods may be used: (1) the "local method" which takes into account the velocity distribution, and for each experiment yields a curve of dispersion coefficients versus local Peclet numbers; and (2) the "global method" reducing this case to the tracer case by the introduction of a mean velocity.

This second method yields a good approximation of the solution (Fig. 4.1.3). Thus, in this section, only the tracer case is described.

The porous medium, which is bidimensional, is assumed to be infinite in the two principal directions. Equation [4.1.14] is solved for the boundary conditions:

$$\begin{aligned} \partial C/\partial y &= 0 \quad &&\text{for} \quad y = \pm\infty \\ C(0,y) &= C_0 \quad &&\text{for} \quad 0 < y < +\infty \\ C(0,y) &= 0 \quad &&\text{for} \quad -\infty < y < 0 \end{aligned} \qquad [4.1.15]$$

The solution of [4.1.15] is:

$$\frac{C}{C_0} = \frac{1}{2}\left[1 + \text{erf}\,\frac{y}{2(K_T x/U)^{1/2}}\right] \qquad [4.1.16]$$

Let σ be the standard deviation at $x = x_0$, defined by:

$$\sigma = \tfrac{1}{2}[y(x_0, C/C_0 = 0.84) - y(x_0, C/C_0 = 0.16)]$$

From [4.1.16] we derive the formula:

$$K_T = \tfrac{1}{2}\sigma^2(U/x_0) \qquad [4.1.17]$$

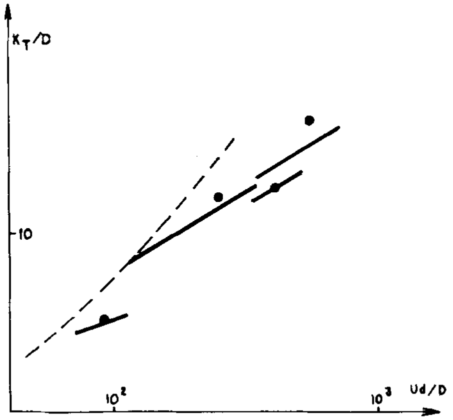

Fig. 4.1.3. Local and global methods (transverse dispersion), – – – = the tracer case, ——— = local method, • = global method.

4.1.3. *Radial flow*

The formulas just derived can actually be applied with very restrictive conditions, such as a unidirectional flow, homogeneous media, step-input initial functions and a constant velocity. In the field, it is rather difficult to obtain all these conditions. For some experiments, however, at a consistent scale of homogeneity, [4.1.1] is a fairly sufficient approximation and then the formulas of §4.1.1 may be used.

What often happens is that field investigations are conducted from wells and imply radial flows. A few authors (Lau et al., 1959; Raimondi et al., 1959) have tried to derive formulas analogous to the unidirectional flow formulas, expressing the dispersion equation in cylindrical coordinates:

$$\frac{1}{r}\frac{\partial}{\partial r}\left[\rho K_r r \frac{\partial}{\partial r}\left(\frac{c}{\rho}\right)\right] - \frac{1}{r}\frac{\partial}{\partial r}(ruc) = \frac{\partial c}{\partial t} \qquad [4.1.18]$$

where K_r is the longitudinal dispersion coefficient, u the pore velocity and ρ the density of the mixture.

They assume some dynamic dispersion regime, u and K_r being given by:

$u = \frac{A}{r}$: velocity of a steady-state flow

$K_r = \alpha \frac{A}{r}$: α is the intrinsic dispersion coefficient

and constant density. Equation [4.1.14] then yields:

$$\alpha \frac{A}{r} \frac{\partial^2 c}{\partial r^2} - \frac{A}{r} \frac{\partial c}{\partial r} = \frac{\partial c}{\partial t} \qquad [4.1.19]$$

They then assume that dispersion may be neglected with respect to convection at some distance from the source, which yields the relationship:

$$\frac{\partial}{\partial r} = -\frac{r}{A} \frac{\partial}{\partial t} \qquad [4.1.20]$$

Under condition [4.1.20], [4.1.19] becomes:

$$\alpha \frac{r}{A} \frac{\partial^2 c}{\partial t^2} - \frac{A}{r} \frac{\partial c}{\partial r} = \frac{\partial c}{\partial t} \qquad [4.1.21]$$

the solution of which will be:

$$c(x, t) = \frac{c_0}{2} \operatorname{erf} \left[\left(\frac{r^2}{2} - At \right) \Big/ \frac{4}{3} \alpha r^3 \right] \qquad [4.1.22]$$

From [4.1.22] a formula may be deduced:

$$\sigma = (2/3\, \alpha r)^{1/2} \qquad [4.1.23]$$

σ being the standard deviation of the concentration distribution. When the well radius r_0 is other than zero, Lau gives the relationship:

$$\sigma = [2/3\, \alpha(r - r_0^3/r^2)]^{1/2} \qquad [4.1.24]$$

From a mathematical point of view, problems arising from the use of a second-order equation in t are completely different from the problems with a second-order equation in r (especially with a singularity at the origin) and mathematicians will strongly object to this change of equations.

Another philosophy is that as long as a mathematical model is a good representation of the phenomenon, it may be accepted. When the rather crude physical approximation [4.1.20] is valid, one may get a very rough estimate of α by measuring σ from experimental curves. But in most cases and when possible, it seems more prudent to maintain the classical form [4.1.19] and use direct methods of comparing the experimental solutions with the numerical solutions of [4.1.19] obtained by computer methods.

4.1.4. *Remarks about heterogeneous media*

When the asymptotic regime is reached, previous computations hold for the equivalent homogeneous medium. Formulas [4.1.10] and [4.1.17] can be used.

When the geology and lithology of the various layers of a stratified porous medium are known, one could attempt to reach a value of the equivalent dispersion coefficient using [2.5.8]. Due to uncertainties about the local dispersion coefficients, this formula only yields rough estimates of K and has only been used to verify the order of magnitude of the dispersion coefficient.

4.2. *FIELD METHODS FOR THE DETERMINATION OF DISPERSION COEFFICIENTS*

Field methods are usually classified into four sets, corresponding to the four usual scales of pollution problems. These scales are given as a function of the mean travelled distance:
— a local scale, between 2 and 4 meters
— a global scale 1, between 4 and 20 meters
— a global scale 2, between 20 and 100 meters
— a regional scale, more than 100 meters (usually several kilometers).

4.2.1. *Local scale: a single-well pulse technique*

Consider a well screened on its whole depth and fully penetrating the aquifer. It is filled with water traced by a radio-tracer at a constant concentration over the whole depth. This traced water is pushed by water traced at the same concentration, then by fresh water. Then it is pumped back into the injection well. At each level, tracer concentration is recorded with respect to time and these measurements are interpreted in two ways: (1) concentration variations at a given level with respect to time and at a given time with respect to depth yield the relative permeabilities of the strata (Levêque et al., 1971, 1974); and (2) concentration variations at a given level with respect to time allow a quantitative evaluation of the longitudinal dispersion coefficient at each level, using the dispersion scheme (§ 3.2) and mathematical models (Fried, 1971a; Fried et al., 1972).

Experimental studies

The radioactive tracer is injected into the aquifer from a screened piezometer. The radioactivity is measured along the whole depth of a screened pipe. At each point, the activity is a function of: (1) the concentration of the tracer in the piezometer itself; (2) the volume of the aquifer invaded by tracer around the point. The cloud of tracer is distorted according to the hydrodynamic properties of each stratum: it penetrates easily transmissive layers; its extension is far smaller in semi-pervious strata; and (3) the volumic radiation emitted by the invaded aquifer: in addition to the tracer concentration, this radiation depends on the effective porosity and on the density of the solid matrix.

The characteristics of the probe and the mathematical simulation show that the effects pointed out in (1) and (3) are widely predominant.

Different radioactive tracers have been tried:

^{82}Br half-life = 36 hours; peak of energy = 0.78—1.47 MeV
^{131}I half-life = 8.05 days; peak of energy = 0.36—0.64 MeV
^{57}Cr half-life = 27.8 days, peak of energy = 0.32 MeV.

^{131}I or ^{82}Br are the most often used. The required activity is very low, not exceeding some microcuries. These isotopes are respectively in the form of sodium bromide and sodium iodide solutions contained in a medical flask. The solution is taken out from the flask, using two hypodermic needles, by means of a water flow. The traced water is mixed with about 4 m^3 of water (for a well 30 meters deep) by feed-back pumping. During this mixing, the carrier is added. The apparatus needed for such a process is very simple and safe, and especially suitable as a field device.

Such a tracer has some very interesting properties:

— it does not present any danger for the field staff nor for the environment because of its short half-life and its low activity;
— it has a good detectability;
— it does not modify the water density.

The probe measures activities by a solid-medium scintillation process. The impulse sent by the probe through the supporting cable is received by an integrator and a counting scale. A recorder controlled by the downwards movement of the probe draws the log (Fig. 4.2.1).

Remarks. In some way the probe transforms the signal it receives. Thus the properties of the probe have to be investigated before the experiment itself. Two points are important: the power of resolution of the probe and the size of the volume of influence. Here follows an example of a possible method.

Investigation of the power of resolution of the probe. Measurements are done with a loss of information which characterizes the power of resolution of the probe; a deconvolution process may avoid this effect, assuming:

$$s(j) = \sum [e(j-i)\phi(i)]$$

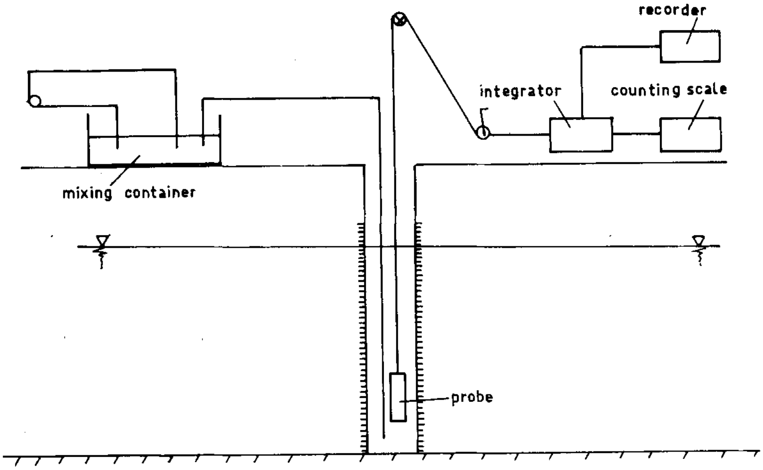

Fig. 4.2.1. Injection device; single-well pulse method.

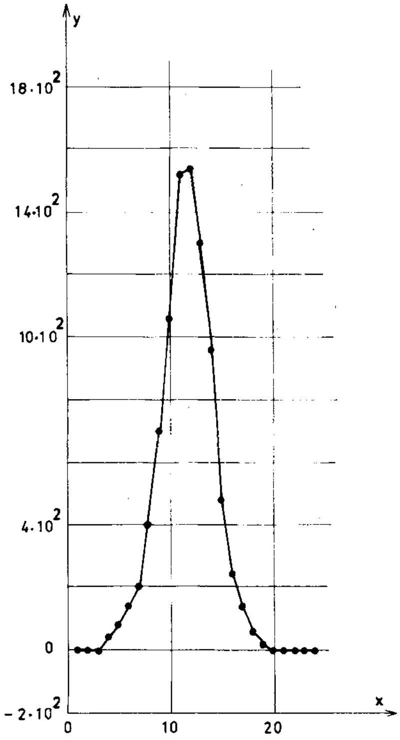

Fig. 4.2.2. Impulse-response of this probe. y = activity (impulse(s)); x = distance (5-cm increments).

where $s(j)$ is the activity measured with the apparatus at depth j, e is the distribution of tracer along the piezometer, ϕ is the kernel function characteristic of the probe working with a given isotope.

The experimental device consists of a stratified medium with one layer saturated by the tracer and put at concentration 1. By the numerical deconvolution process (Emsellem et al., 1971), ϕ is computed (Fig. 4.2.2) for steps of 5 cm. Then by deconvolution of s by ϕ, it is possible to find the distribution of tracer in an invaded borehole. Fig. 4.2.3 shows the results of a series of measurements made every 10 cm, concentration 1 being activity 1000. A log is measured in the field, deconvoluted by ϕ to get e and then e is numerically convoluted by ϕ to verify the method.

The size of the volume of influence. This investigation has been carried out on a cubic meter container divided in cylindrical coaxial sectors. It was possible to inject a radioactive tracer in each sector. We found that a concentric cloud around the piezometer was not seen, in the optimum case, at a greater distance than one meter (Fig. 4.2.4).

The diameter of the piezometer must take into account the diameter of the probe. It must be screened ($> 20\%$) over the whole length of the investigated aquifer. The screened pipe is covered with nylon linen the mesh of which is about 0.5—1 mm large. There must not exist any gravel pack that would screen the information sent by the injected aquifer and the probe.

The experiment is performed in four steps. The piezometric column is filled up with traced water by pumping at the head of the borehole and injecting at its bottom. When the activity of the pumped-out water stays constant, pumping out is stopped and injection of traced water begins. In unconfined aquifers, one must make sure that the elevation of the water table is small to insure safety and to prevent any injection of tracer above the investigated aquifer. Then untraced water is injected. The fourth step is pumping back into the injection borehole and the investigation of the returning radioactive cloud in each stratum.

At each step, the flow rate must be small, to assure that time necessary to draw a log is short with respect to the evolution of the traced aquifer: then logs may be considered as instantaneous. Of course as many logs as possible are made. Examples carried out with ^{82}Br are shown on Figs. 4.2.5 and 4.2.6.

Remark. A qualitative evaluation of permeabilities can be derived from these results. Two strata may be pointed out, characterized by:
— peaks of activity during the injection
— nodes during injection of non-active water
— the fact that during the pumping, these strata send back more activity than others.

It is obvious that the transmissivity calculated by a classical pumping test is due, in greatest part, to these strata. Fig. 4.2.6 shows the evolution of

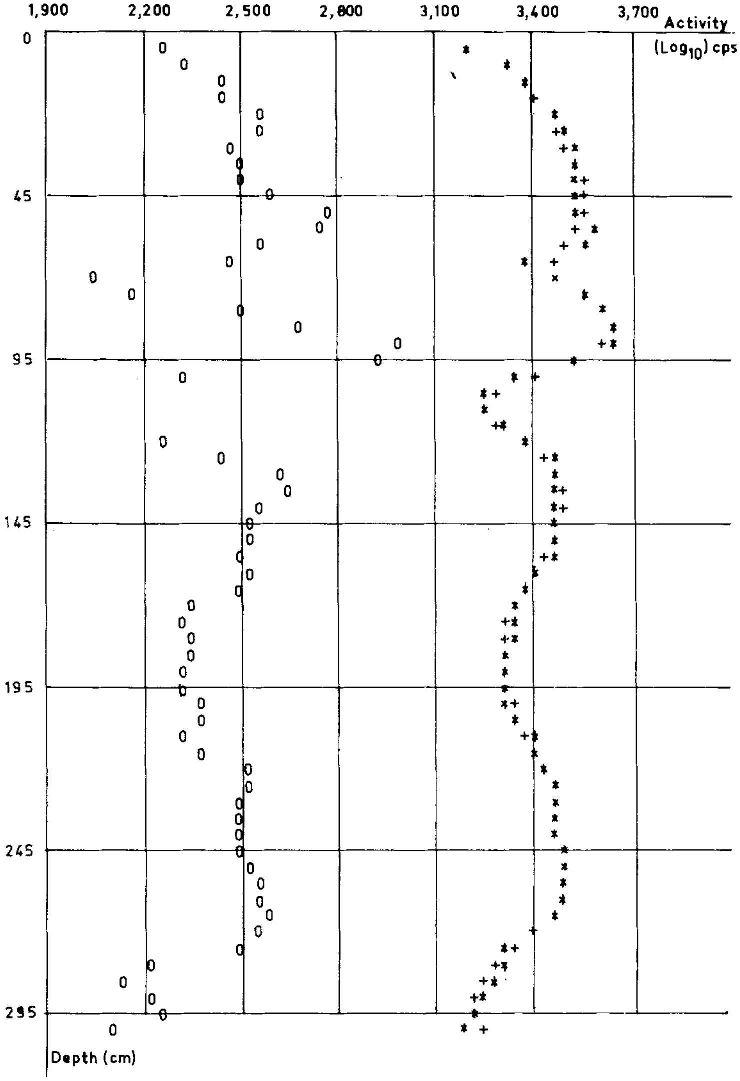

Fig. 4.2.3. Deconvolution results (activities versus depth).
*** = field data, ooo = deconvolution results (input function), +++ = output function computed by the convolution of the computed input function with the probe impulse-response.

activity for various permeable layers during the pumping back. It should be noted that in most cases the recovery rate of activity is about 85—95%.

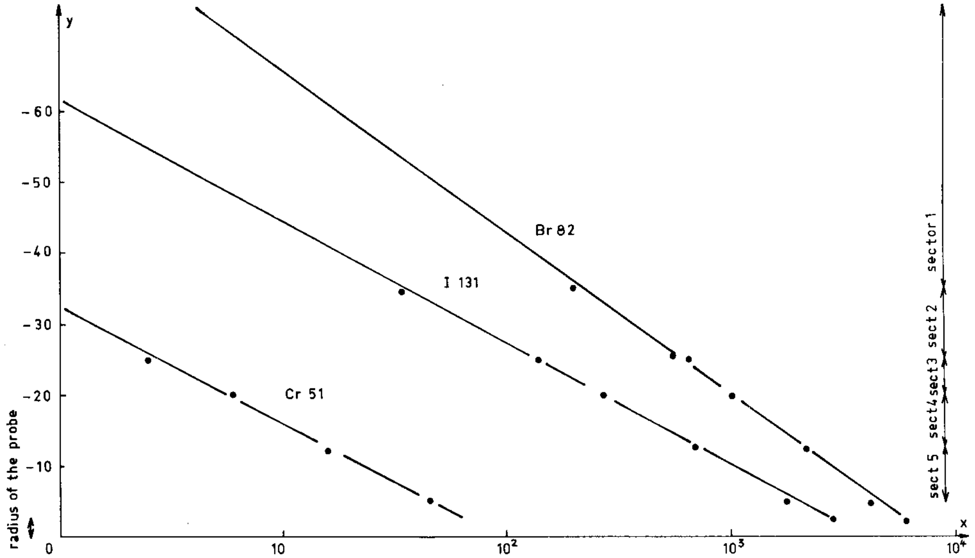

Fig. 4.2.4. Investigation of the volume of influence of the probe (laboratory). The sectors invaded successively are: 1; 1,2; 1,2,3; 1,2,3,4; 1,2,3,4,5. The tracer concentration and the level of energy of measurement are the same as in the field. y = activity (impulse(s)).

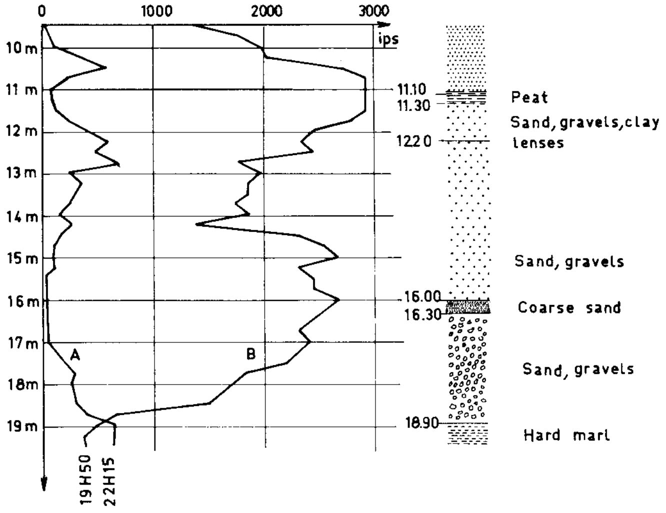

Fig. 4.2.5. Bromide injection. A = end of freshwater injection, B = end of tracer injection.

The mathematical models

These are based upon the general dispersion equation:

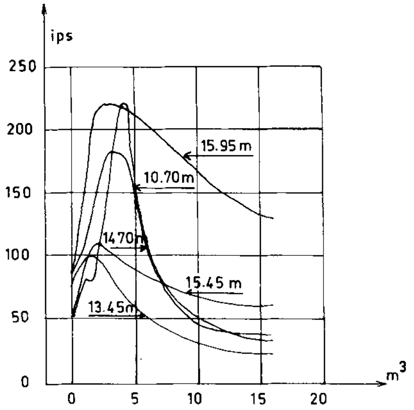

Fig. 4.2.6. Activity vs. pumped volume for various permeable layers.

$$\operatorname{div}\left[K\rho \cdot \left(\operatorname{grad}\frac{c}{\rho}\right)\right] - \operatorname{div}(uc) = \frac{\partial c}{\partial t}$$

simplified according to the following remarks and assumptions.

The medium is made up of homogeneous, horizontal, independent strata. Only small quantities of radioactive tracer are used, which implies that the density and viscosity of the mixture do not vary and are equal to those of fresh water. The coordinate system is chosen to coincide with the principal axes of the dispersion tensor, which is then put in its diagonal form.

The velocity regime is that of dynamic dispersion and the dispersion coefficients K can be written as:

$$K = \alpha|u|$$

where u is the pore velocity and α the intrinsic dispersion coefficient (which has the dimension of a length).

We intend to measure α_L, the longitudinal-dispersion intrinsic coefficient, which is equal to the longitudinal intrinsic coefficient for radial flow (Hoopes and Harleman, 1967a). We assume that horizontal and vertical transverse dispersion are negligible. The model is then:

$$\operatorname{div}(\alpha|u|\operatorname{grad} c) - \operatorname{div}(uc) = \frac{\partial c}{\partial t} \qquad [4.2.1]$$

$$\frac{\partial^2 h}{\partial r^2} + \frac{1}{r}\frac{\partial h}{\partial r} = \frac{S}{T}\frac{\partial h}{\partial t} \qquad [4.2.2]$$

$$u = u_n - \frac{k\rho g}{\mu\phi}\operatorname{grad} h \qquad [4.2.3]$$

where h is the piezometric head during the injection or the pumping and u_n the natural aquifer velocity. μ is the dynamic viscosity, ϕ the porosity, k the permeability coefficient, T the transmissivity and S the storage coefficient. Convenient boundary and initial conditions are added. Two cases are considered: either the aquifer velocity may be neglected with respect to the imposed velocity or u_n is taken into account.

(1) u_n is neglected: dispersion is purely radial and we use cylindrical coordinates to write the dispersion equation as:

$$\frac{1}{r}\frac{\partial}{\partial r}\left(\alpha r|u|\frac{\partial c}{\partial r}\right)-\frac{1}{r}\frac{\partial(ruc)}{\partial r}=\frac{\partial c}{\partial t} \qquad [4.2.4]$$

(2) u_n cannot be neglected: the principal directions of the dispersion tensor are respectively tangential to the streamlines and the equi-potential lines and [4.2.1] reduces to (§5.2):

$$u^2\frac{\partial}{\partial \phi}\left(\alpha|u|\frac{\partial c}{\partial \phi}\right)-u^2\frac{\partial c}{\partial \phi}=\frac{\partial c}{\partial t} \qquad [4.2.5]$$

in the ϕ, ψ-coordinates system, where ϕ = constant are equi-potential lines and where ψ = constant are streamlines.

Two methods may be used to determine the dispersion coefficients: a semi-analytical formula derived from [4.2.4]; and direct simulation and curve fitting.

Semi-analytical formula. We assume to be in case (1) where u_n is neglected. We have shown that the steady-state velocity is obtained after a relatively short lapse of time (a few minutes of injection or pumping), thus we take the velocity as:

$$u=\frac{A}{r}$$

with $A=Q/2\pi b\phi$, where b is the aquifer width, Q the injection rate and ϕ the porosity. Velocities are oriented outwards from the well (we put a minus sign for pumping). α is deduced from [4.2.4] as:

$$\alpha=\frac{r\dfrac{\partial c}{\partial t}+A\dfrac{\partial c}{\partial r}}{A\dfrac{\partial^2 c}{\partial r^2}} \qquad [4.2.6]$$

$\partial c/\partial t$ is given by the experiment and [4.2.6] yields:

$$\alpha = \frac{r_2 \dfrac{c_{n+2}(1) - c_{n+1}(1)}{\mathrm{d}t} + \dfrac{c_{n+3}(1) - c_{n+2}(1)}{r_3 - r_2} A}{\dfrac{2A}{r_3 - r_1} \left[\dfrac{c_{n+3}(1) - c_{n+2}(1)}{r_3 - r_2} - \dfrac{c_{n+2}(1) - c_{n+1}(1)}{r_2 - r_1} \right]} \qquad [4.2.7]$$

where $c_n(i)$ is the concentration at time t_n at a point i lying at the distance r_i from the well axis; r_1 is the well radius.

Formula [4.2.7] has been obtained from a discretization of [4.2.6], assuming that the transition-zone variation during a relatively short time step $\mathrm{d}t$ may be neglected with respect to its width. Then, the tracer moves without dispersion and, under this assumption, the concentration at the well at time $t + \mathrm{d}t$ is the concentration at time t at a point $r_1 + \mathrm{d}r$ where $\mathrm{d}r$ is given by the formula:

$$\mathrm{d}r = \int_t^{t+\mathrm{d}t} u\mathrm{d}t$$

$$c_{n+1}(3) = c_{n+3}(1)$$

$$c_{n+1}(2) = c_{n+2}(1)$$

For instance:

$$c_n(2) = c_{n+1}(1)$$

$$r_3 = \sqrt{4A\mathrm{d}t + r_1^2}$$

$$r_2 = \sqrt{2A\mathrm{d}t + r_1^2}$$

The smaller $\mathrm{d}t$ is, the better is α. If A is precisely known, [4.2.7] provides a very quick estimate of the order of magnitude of α, with simple computations.

Simulation. A finite-difference form of [4.2.1], [4.2.2] and [4.2.3] is used, Because of symmetry, these equations are reduced to monodimensional (in space variables) equations (§ 9.6).

The adopted scheme is totally implicit, with backward differences in the velocity direction for [4.2.1]. A tridiagonal Gaussian elimination method is used to solve the linear system of discretized equations directly.

Computed solutions are fitted to experimental solutions by curve fitting. Fig. 4.2.7 represents concentration variations at the well versus time at a given level; during this experiment dispersion coefficients were measured every 25 cm (§ 6).

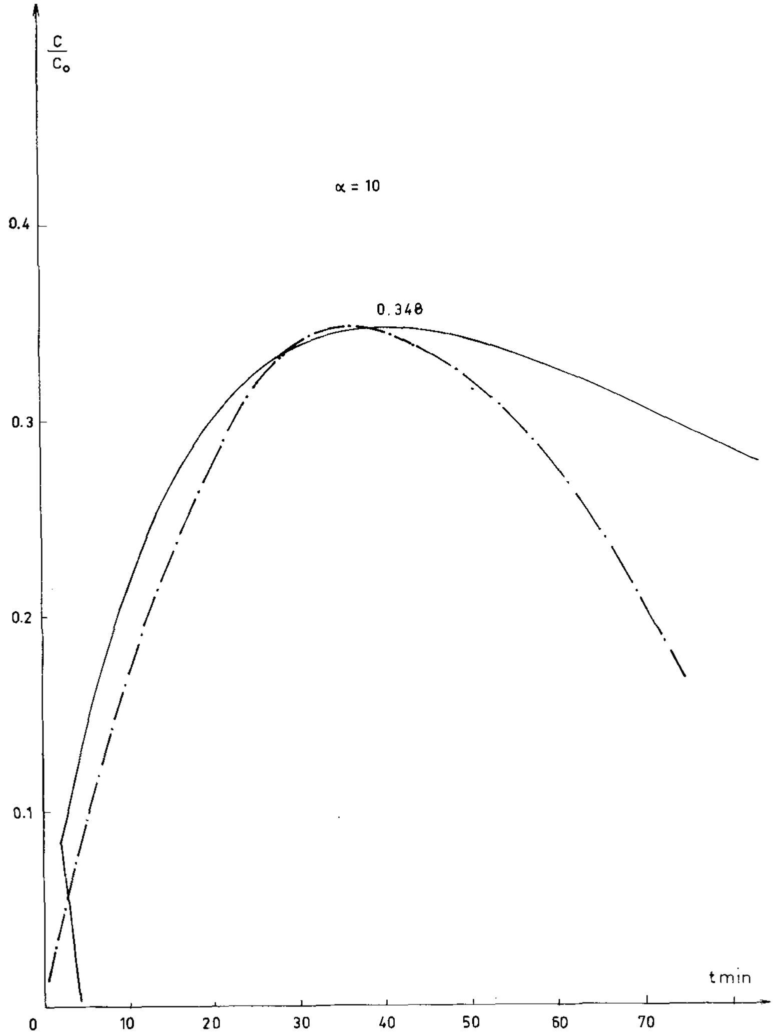

Fig. 4.2.7. Concentration variations vs. time at a given depth.
—·— = experimental curve, —— = computed curve for α = 10 cm.

Conclusion

This single-well pulse technique provides a quantitative evaluation of the longitudinal dispersion coefficient in each stratum, at a scale of 2—4 m. Detection of the most pollutable strata and their modelling for prediction purposes, are then possible.

It is also interesting to notice that most of the radioactive tracer is pumped out of the aquifer and if the lifetime of the radioactive elements is short, these experiments with radioactive tracers are quite safe and there is no danger of contamination.

4.2.2. Global scale 1: multiple-well methods

The principle of these methods is very simple. Traced water injected in the aquifer is spotted in a set of observation wells; the curves of concentration versus time are interpreted quantitatively to yield the longitudinal dispersion coefficient.

Remark. Multiple-well experiments in dispersion have also been conducted in laboratories (Hoopes and Harleman, 1967a). Of course, the methods of investigation differ from field experiments, as financial stresses are of prime importance on the latter: the scale of the financial investments is usually well adjusted to the scale of the experiment.

The methodology

The methodology consists of the following points. Consider an injection well and concentric rings of observation wells, centered at the injection well. All the wells are fully penetrating and screened over their whole depth. A tracer is put in the injection well, its concentration is homogenized and traced water is brutally injected into the aquifer. A step-input initial condition is thus realized and the impulse response is analyzed in the observation wells. The studied function is the tracer concentration versus time at a point in space.

Traced water has been injected in the aquifer; what becomes of it? There are two possibilities: either it flows with the proper velocity of the aquifer or it is pushed at a greater velocity.

In the first case simple models can be used: at a scale of 6—12 meters, the aquifer velocity does not fluctuate and usually a bidimensional unidirectional model is adequate. Explicit formulas, such as those presented in § 4.1, may also be used and sometimes an analytical resolution of the equations. Some examples will be discussed later in this section. But the duration of such an experiment is rather long and this will prevent the use of short-lived radioactive tracers; besides if the tracer is heavy and highly concentrated, gravity may become a disturbing factor which is to be taken into account.

In the second case, either the imposed tracer velocity is high enough to neglect the proper velocity of the aquifer or these two velocities have to be composed. Although it is interesting to be able to neglect the aquifer velocity (the experiment is rapid and the model is simply radial), this condition is not easy to obtain: the imposed velocity is radial and is, thus, more or less proportional to $1/r$ (r is the distance from the injection well) and it decreases rather quickly; a high head is necessary or a high injection rate which is not always compatible with the experimental conditions.

In both cases, preliminary knowledge of the direction and intensity of

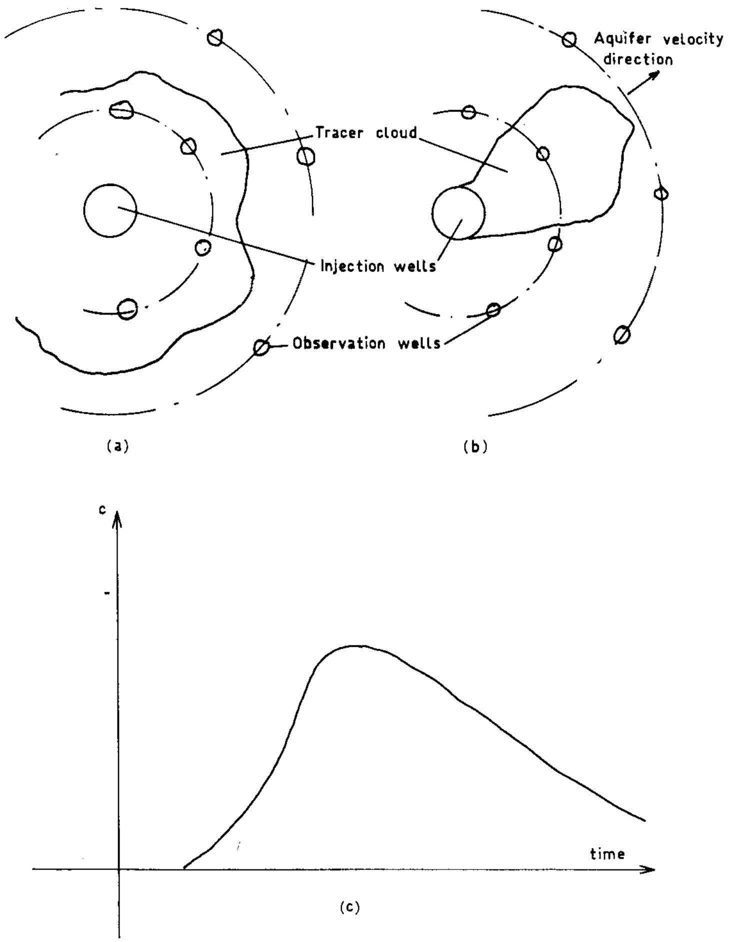

Fig. 4.2.8. The multiple-well methods.
(a) Forced injection. (b) Injection at the aquifer velocity. (c) Impulse response at an observation well.

the aquifer velocity is essential. These data also yield the injection rate and the optimal setting of the observation wells:

(1) A good knowledge of the velocity field, allows the drilling of the observation wells on the mean run of the traced water only, thus decreasing the number of wells and consequently the costs.

(2) If the aquifer velocity is known, an injection rate can be chosen, so that the tracer flow be radial. Then it is not necessary to know the direction of the aquifer velocity and observation wells may be drilled anywhere in the vicinity of the injection well.

Remark. At the chosen scale, the aquifer velocity can usually be taken parallel to a given direction.

Usual simplifying assumptions and mathematical models

Initial tracer concentrations are chosen in such a way that the density and the viscosity of the mixture remain constant and do not differ from pure-water density and viscosity. The mean velocity of the mixture is then constant during the experiment and equal either to the aquifer pore velocity or to the superposition of the aquifer pore velocity and the radial velocity imposed by constant flow rate or constant well-head conditions (as has been said, sometimes the aquifer pore velocity may be neglected before the radial velocity). The velocity of the mixture is therefore either measured or given once and for all at the beginning of the experiment.

The velocity regime is such that dispersion be dynamic, i.e., the dispersion coefficients are linear functions of the mixture velocity (§ 2.4.2):

$$K_L = \alpha_L u$$

Both longitudinal-dispersion intrinsic coefficients α_L in radial flow and uniform unidirectional flow are equal (Hoopes and Harleman, 1967).

The flow is horizontal, transverse vertical and horizontal dispersions can be neglected with respect to longitudinal dispersion.

First case. The model is monodimensional and unidirectional. A concentration crenel is injected and the dispersion coefficient is derived from [4.1.13].

Second case. When the aquifer pore velocity can be neglected, dispersion is radial and plane in a homogeneous medium. It is represented by:

$$\frac{1}{r}\frac{\partial}{\partial r}\left[\rho K_r r \frac{\partial}{\partial r}\left(\frac{c}{\rho}\right)\right] - \frac{1}{r}\frac{\partial}{\partial r}(ruc) = \frac{\partial c}{\partial t} \qquad [4.2.8]$$

where K_r is the longitudinal-dispersion coefficient, u the pore velocity and ρ the mixture density. With the simplifying assumptions, [4.2.8] becomes:

$$\frac{\alpha A}{r}\frac{\partial^2 c}{\partial r^2} - \frac{A}{r}\frac{\partial c}{\partial r} = \frac{\partial c}{\partial t} \qquad [4.2.9]$$

with $u = A/r$ and $A = Q/2\pi b\phi$ where Q is the injection rate, b the width of the aquifer, ϕ the porosity. A concentration is injected and the obtained impulse response is adjusted on the experimental curve, noticing that the position of the maximum depends on the flow velocity and its amplitude depends on dispersion (§ 4.1.1., crenel-type injection). The model is then:

$$\begin{aligned} &\frac{\alpha A}{r}\frac{\partial^2 c}{\partial r^2}-\frac{A}{r}\frac{\partial c}{\partial r}=\frac{\partial c}{\partial t} \\ &c(r,0)=0 \\ &c(r_0,t)=c_0 \quad 0<t<T \\ &c(r_0,t)=0 \quad T<t \\ &c(\infty,t)=0 \end{aligned} \qquad [4.2.10]$$

where T is the time when injection ends and r_0 is the well radius. A is kept constant during the experiment by injecting pure water at the same rate for $t>T$.

Remark. The steady-state assumption for imposed velocities is correct as the permanent regime is reached within a few minutes (numerical and experimental results, Fried, 1972a). When the aquifer pore velocity cannot be neglected, the mixture velocity is the superposition of a radial velocity A/r and the uniform velocity u_n of the aquifer (Fig. 4.2.9). The model is then represented in the streamlines—equipotential line system (§ 5.2) again by [4.2.5], using symmetry properties of the velocity field.

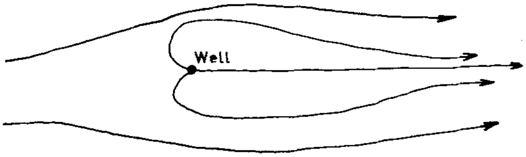

Fig. 4.2.9. Superposition of a radial forced velocity and of the aquifer velocity.

Examples

Here are some examples which illustrate the multiple-well methods.

First case. The experimental setting is defined in Fig. 4.2.10 (Agence Financière de Bassin R.M.C., 1971). It is part of the study of the Lyons aquifer and the geological setting is given in § 6.2.

100 g of I- (as I Na) was instantaneously injected. In order to measure the mean tracer concentration over the whole depth of the aquifer, a mixing device, described in Fig. 4.2.11 was set up in the injection well and in some of the observation wells. Measurements of concentration were made by chemical analysis of water samples taken from levels −6 m and −12 m of the aquifer by means of sampling bottles. A radioactive tracer (2 mCi of ^{131}I) has also been used and the continuous measurement device is shown in Fig. 4.2.11. The experiment lasted 160 hours, and concentration measurements in each of the seven observation wells were performed every 2—10 hours.

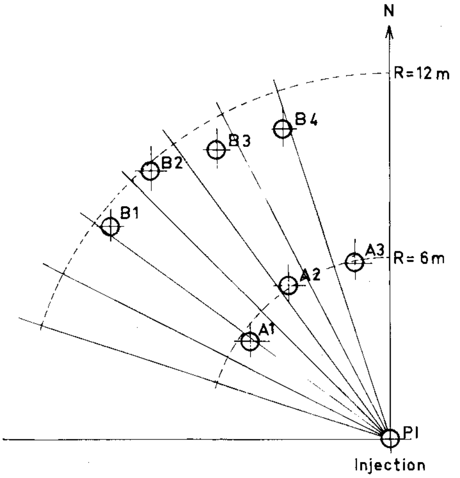

Fig. 4.2.10. Experimental setting of a multiple-well experiment (P: injection well; A and B: observation wells).

Results (concentration of I in ppb versus time) are represented in Figs. 4.2.12 and 4.2.13, in the injection well and in observation well A2 respectively. Fig. 4.2.14 shows the various concentration maxima observed in the seven wells. These curves can be interpreted in terms of aquifer velocity (§ 4.3) and in terms of mean longitudinal dispersion coefficient. In the case of this example, the dispersion coefficient α_L was computed by formula (§ 4.1.1):

$$\alpha_L = \frac{x^2 - u^2 t(t - t_0)}{u(t - t_0)} \qquad [4.2.11]$$

where t_0 is the mean injection time, t the arrival time of the maximum, x the position of the maximum and u the mean pore velocity. For this particular experiment, it has been found that $\alpha = 425$ cm.

Second case. A multiple-well method with pure radial flow was applied in the study of the pollution of the Rhine aquifer by salts (§ 6). This highly permeable aquifer is a mixture of sands and gravels. The injection and observation wells are represented in Fig. 4.2.15. Salt water at a concentration of 10 g/l was injected during 2 hours at a flow rate of 10 m^3/h which was enough to insure pure radial flow within the first ring of observation wells. The injection device, at constant flow rate, is illustrated in Fig. 4.2.16; in the observations wells, the liquid phase was homogenized. Concentrations were continuously recorded by resistivity measurements and controlled by sampling.

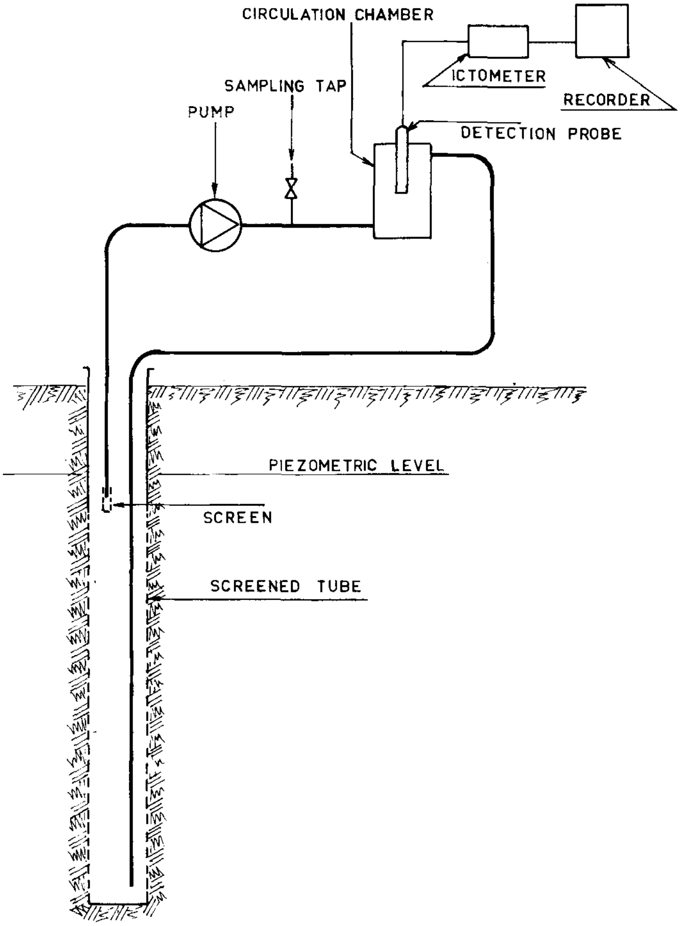

Fig. 4.2.11. Measurement device for radioactive tracing.

Measurements were carried on for 12 hours after the end of injection. Results (salt concentration versus time) were analyzed by adjusting a radial dispersion model ([4.2.10], Fig. 4.2.17) and they yielded $\alpha_L = 1100$ cm.

4.2.3. *Global scale 2: a single-well method*

The global scale 2 ranges from 20 to 100 meters. Multiple-well methods described in § 4.2.2 can be used at this scale under the following conditions.

(1) Large amounts of tracer must be injected to regularize the dispersion front. The scale of the injection has to be compatible with the scale of the studied area, otherwise only preferential paths are traced.

(2) The flow velocity results from the superposition of the natural head

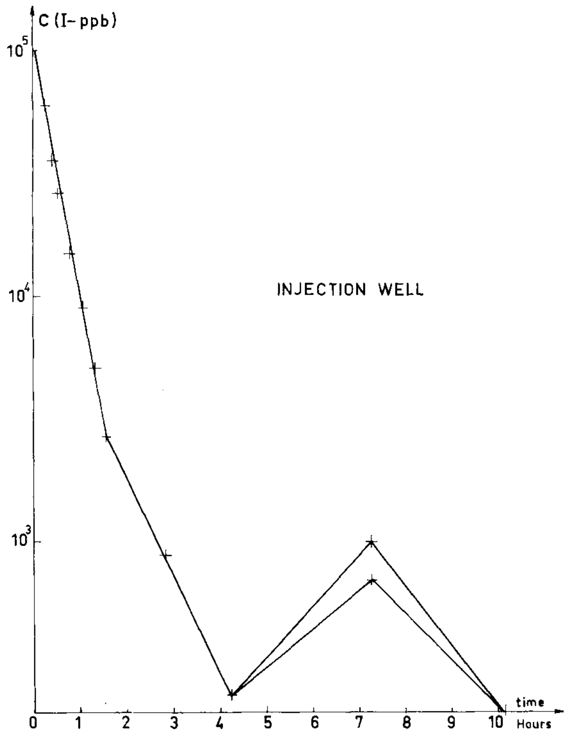

Fig. 4.2.12. Evolution of the concentration at the injection well vs. time.

of the aquifer and the imposed injection head. Usually, except near the well, only the natural aquifer velocity has to be considered; the radial flow simplification is not possible.

(3) The direction of the aquifer velocity must be known with accuracy. Even then a large number of observation wells is required, which considerably raises the costs of experimentation. Of course these conditions can be realized.

However, another method, specially developed for pollution studies, has proved very interesting both scientifically and financially and it is presented here. It is a single-well method with injection of a chemical compound spotted by tracing the resistivity variations of the aquifer by geophysical electrical means; recording of the resistivity variations is conducted from the soil surface, which leaves the medium undisturbed; flow takes place at the natural aquifer velocity. This experiment yields two sets of results: (1) the direction and intensity of aquifer velocity (§ 4.3.2); and (2) the evolution in time and space of tracer concentrations, in terms of apparent resistivities, which allows the determination of the dispersion coefficients.

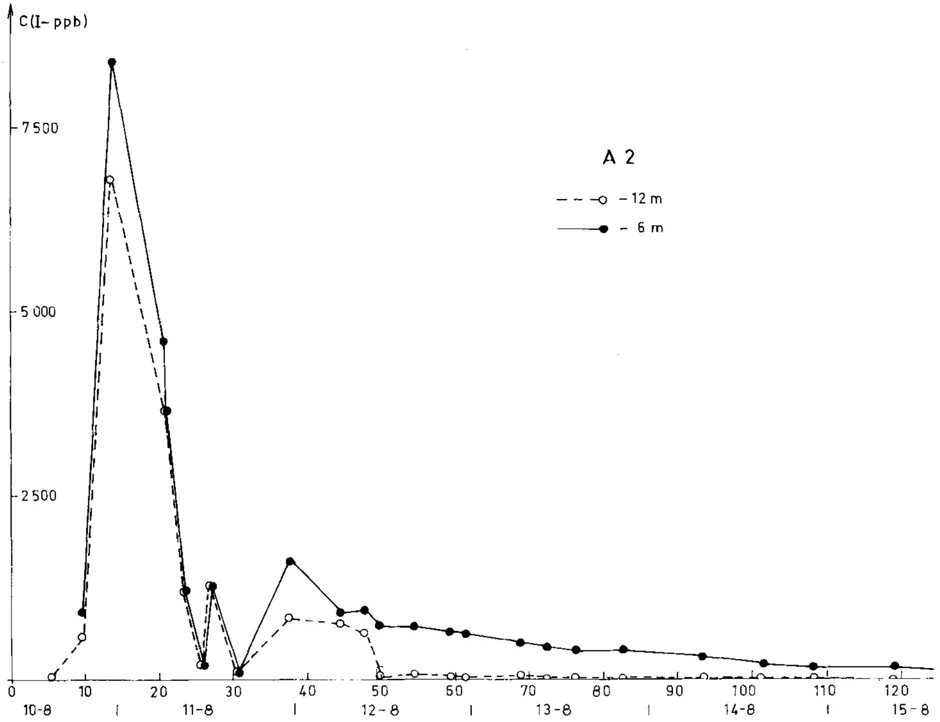

Fig. 4.2.13. Evolution of the concentration at two levels in the observation well A2.

The experiment

The electrical-measurement techniques are described in Appendix II. The currently used chemical compound is NaCl, chosen because it has good electrical properties and is cheap. Of course, other compounds could be used as well if their prices and properties are competitive with those of kitchen salt.

Remark. NaCl is used when soil resistivity is rather high; then, a reasonable amount of NaCl is sufficient to substantially modify the overall resistivity. In other cases, one could use substances that increase the resistivity: for instance, in a soil polluted by salt, one could inject fresh water and record the increase in resistivity. The salt-water injection device is illustrated in Fig. 4.2.18.

The well waters are recycled to provide better homogenization of the mixture which is injected along the whole depth of the aquifer. The hazards of salt sedimentation at the bottom of the well are reduced. The salt is dissolved at relatively high pressures and is then injected at a constant rate: due to the salt overburden, a locally radial effect might be observed in the vicinity of the well; this effect is checked during measurements.

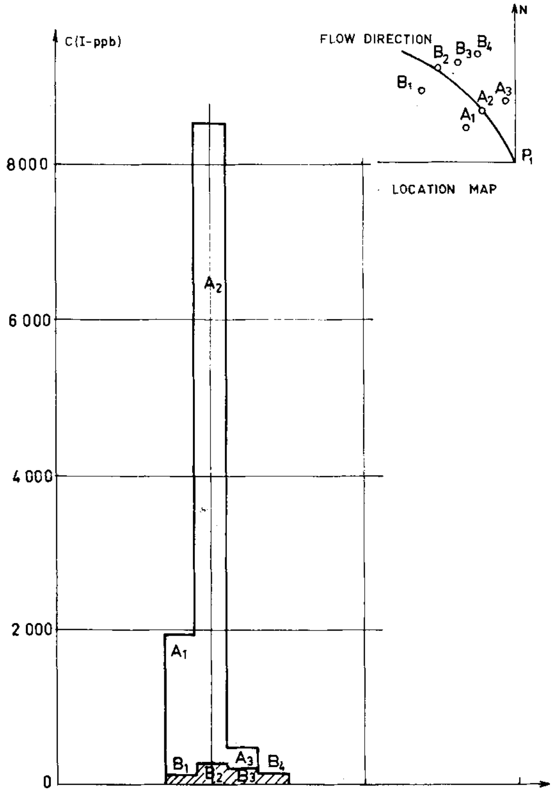

Fig. 4.2.14. Concentration maxima in the various wells — the abscissus has no quantitative meaning.

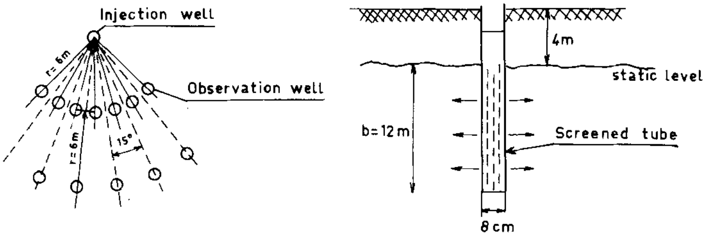

Fig. 4.2.15. Experimental setting of the Rhine aquifer multiple-well experiment.

The three following techniques (Appendix II) are used jointly: (1) electrical soundings (E S); (2) resistivity measurements (rectangle R M); (3) potential measurements (P M).

Before the injection starts, an electrical sounding, a potential measurement and a resistivity measurement are performed on the electrode mesh to determine the initial geoelectrical state of the soil before perturbation.

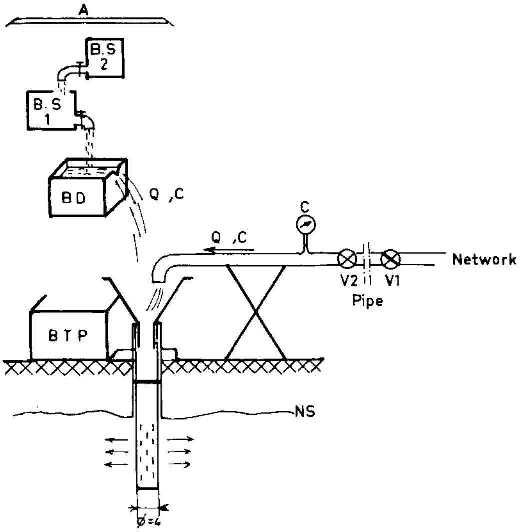

Fig. 4.2.16. Injection device of the multiple-well experiment in the Rhine aquifer. *V*1 and *V*2 = water gate, *C* = counter, *BS*1 and *BS*2 = saturated salt water tank (C = C2), *BD* = overfall gauged tank, *BTP* = tank, *A* = shelter.

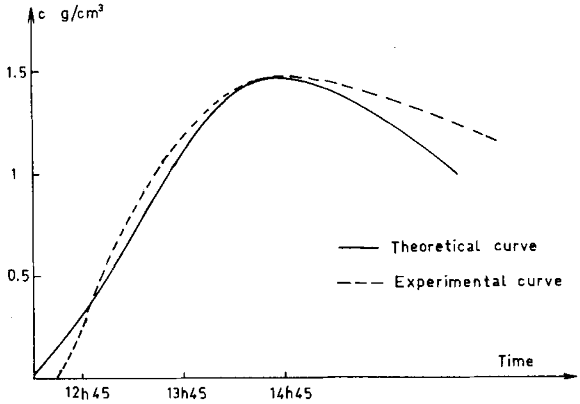

Fig. 4.2.17. Rhine aquifer multiple-well experiment and computed results.

During the injection, resistivity measurements are performed (for instance five times a day) and also one electrical sounding and one potential measurement, as a check, in the middle and at the end of the injection.

After the injection, potential and resistivity measurements are performed at points considered useful according to the previous measurements and at a frequency depending on the detection sensitivity and resistivity and potential contrasts.

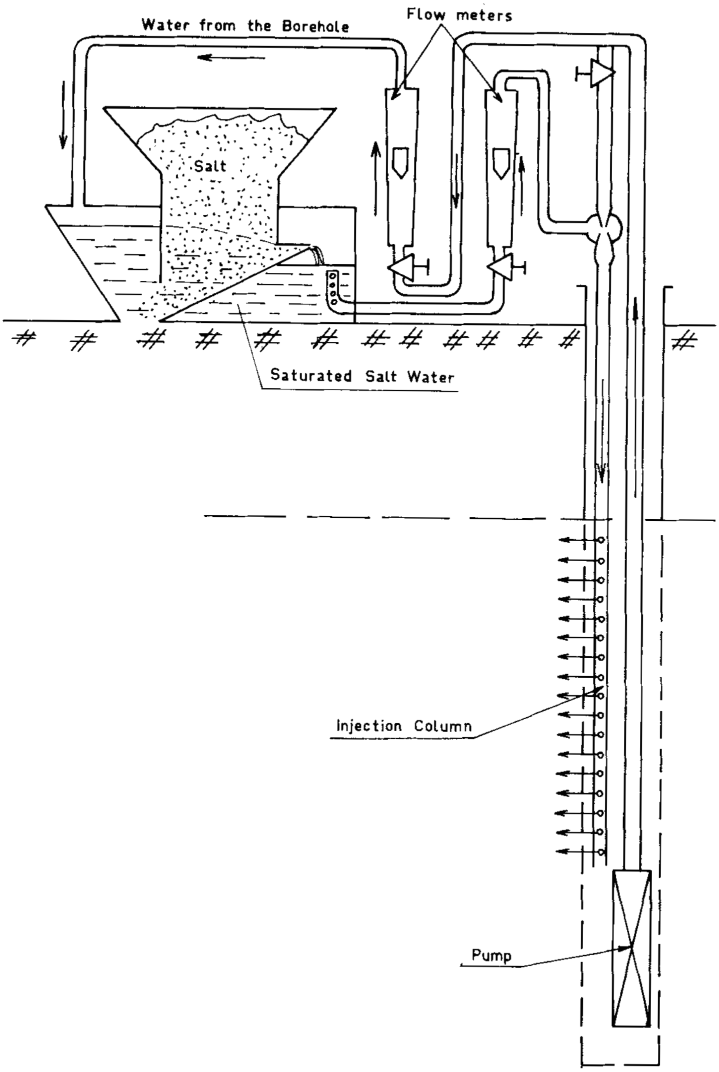

Fig. 4.2.18. Single-well geoelectrical method: injection device.

Usual simplifying assumptions and model

In such a single-well method, it is assumed that the investigation zone downstream of the well has the lithologic, geologic and hydrodynamic characteristics observed at the well. The type of model (in curvilinear or canonical rectangular coordinates) depends on the geometry of the flow lines. A usual assumption is that the flow lines are rectilinear in the investigation zone, except perhaps near the well during a rather short equilibrium phase with transverse widening of the traced zone; this effect is usually ascribed to a radial velocity due to the salt mass overburden at injection. This local effect can be neglected at some short distance from the well and the upstream boundary of the domain will be taken at that distance from the well (Fig. 4.2.19).

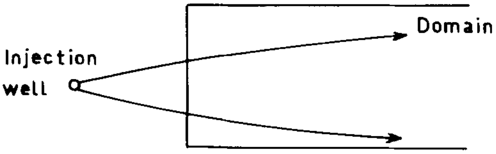

Fig. 4.2.19. Single-well geoelectrical method: definition of the modelled domain.

Other usual assumptions (in an alluvial aquifer at least) are the horizontal stratification of the aquifer, subject to confirmation by geological logs at the well, and the negligible water transfers between strata. Strata are then independent and the velocity in a stratum is constant. Gravity effects are neglected and also the density variations of the mixture.

Remark. It has been shown that these simplifying assumptions are reasonable in most cases. Of course, if needs be they should be adapted or changed. For instance, vertical water transfers can be taken into account in a bidimensional horizontal model by adding field singularities in the equation (§ 9.5.2).

Under these assumptions, the model is a set of bidimensional horizontal hydrodispersive models; velocities, dispersion coefficients and boundary conditions vary with the strata (Fig. 4.2.20). $Q(i)$ is the flow rate at the upstream boundary of stratum i.

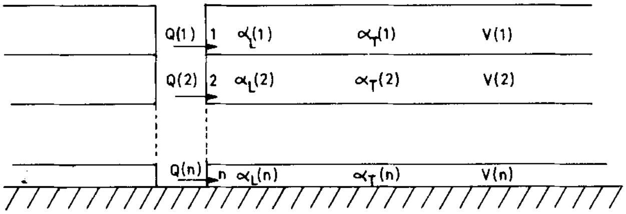

Fig. 4.2.20. The multistrata model. Q = pollution flow rate, α_L and α_T = dispersion coefficients, V = velocity of the aquifer.

Each model is based upon the dispersion equation:

$$\frac{\partial}{\partial x}\left(K_L\,\frac{\partial c}{\partial x}\right)+\frac{\partial}{\partial y}\left(K_T\,\frac{\partial c}{\partial y}\right)-\frac{\partial}{\partial x}(uc) = \frac{\partial c}{\partial t} \qquad [4.2.12]$$

written in classical rectangular coordinates, born by the mean velocity direction and its orthogonal direction in the horizontal plane xOy of the strata. The simulation domain is thus rectangular and semi-infinite, with its upstream boundary at the well.

The upstream boundary is set at the injection concentration in the salted zone and at the initial concentration elsewhere. The other boundaries are maintained at the initial concentration.

The initial and boundary conditions are thus:

$$\begin{aligned} C(x, y, 0) &= C_0(x, y) \\ C(x, \pm L, t) &= C_0(x, \pm L) \\ C(0, y, t) &= C_p(y, t) \quad -a < y < +a \\ C(0, y, t) &= C_0(0, y) \quad |y| > a \\ C(M, y, t) &= C_0(M, y) \end{aligned} \qquad [4.2.13]$$

The initial concentration C_0 can sometimes be taken as constant. The concentration at the well is computed by dilution, from the injected salt flow rate and the aquifer flow rate in each stratum. Set Qsalt as the salt injection rate (dimension MT^{-1}) and Qaquif(j) as the water flow rate through the well in stratum j (dimension L^3T^{-1}). We have:

$$Q\text{aquif}\ (j) = u(j) \cdot \text{d}y \cdot h(j)$$

where $u(j)$ is the aquifer pore velocity in stratum j, dy is the width increment, $h(j)$ is the height of stratum j. Set Qs (j) as the salt flow rate in stratum j. We then have:

$$Q\text{s}\ (j) = Q\text{salt} \cdot k(j) \cdot h(j) \Big/ \sum_j h(j) \cdot k(j)$$

where $k(j)$ is the permeability of stratum j. The concentration at the well is then:

$$C_p(j) = Q\text{s}\ (j)/Q\text{aquif}\ (j)$$

The concentration is constant over the whole depth of the well and equal to:

$$Q\text{salt} \Big/ \sum_j Q\text{aquif}\ (j)$$

The quantitative experimental data resulting from the geophysical experiments are mean values over the whole aquifer depth. To adjust the model, it

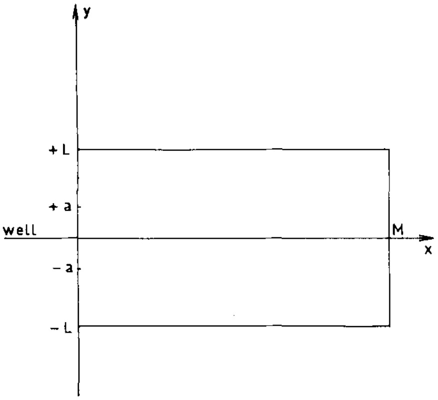

Fig. 4.2.21. The modelled domain and the well position.

is necessary to reach these mean values in some way and there the theory of composition of porous media described in § 2.5.1 can be used, with the following formulas (notations are defined in § 2.5.1):
porosities:

$$\bar{\phi} = \frac{1}{y_2 - y_1} \int_{y_1}^{y_2} \phi \mathrm{d}y$$

concentrations:

$$\bar{c} = \frac{1}{\bar{\phi}(y_2 - y_1)} \int_{y_1}^{y_2} \phi c \mathrm{d}y$$

velocities:

$$\bar{u} = \int_{y_1}^{y_2} \phi U \mathrm{d}y \Big/ \int_{y_1}^{y_2} \phi \mathrm{d}y$$

dispersion coefficients:

$$\overline{K} = \frac{1}{\bar{\phi}(y_2 - y_1)} \left(\int_{y_1}^{y_2} K_L \phi \mathrm{d}y + \int_{y_1}^{y_2} \frac{\varphi^2}{K_T \phi} \mathrm{d}y \right)$$

and:

$$\varphi = \int_{y_1}^{y_2} \phi(u - \bar{u}) \mathrm{d}y \qquad \varphi(y_1) = \varphi(y_2) = 0$$

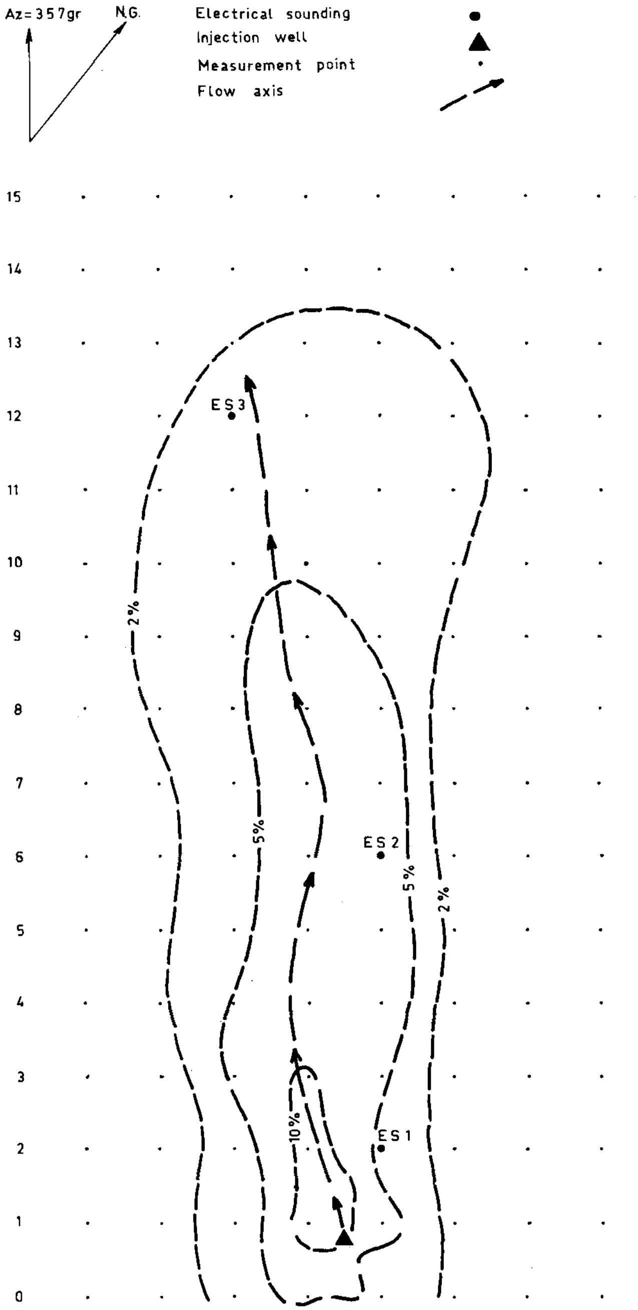

Fig. 4.2.22. Maps of the apparent-resistivity variations (%). Scale 1:400.

Adjustment of the model on the experimental curves

The model is adjusted on the representative curves of the percentage variations of apparent resistivity with the assumption of a constant initial concentration (Fig. 4.2.22).

Let C_0 be the constant initial concentration and C_1 the constant well concentration. Then [4.2.12] has a solution:

$$c = (c_1 - c_0) f(x, t) + c_0$$

where $f(x, t)$ is an error function of some form. Resistivity variations depend linearly on relative concentration variations, for weak amplitude variations (Fig. 4.2.23) which is generally the case (but this has to be checked). Thus

$$\frac{\Delta c}{c} = \frac{(c_1 - c_0) f(x, t)}{c_0} = A \frac{\Delta\rho}{\rho}$$

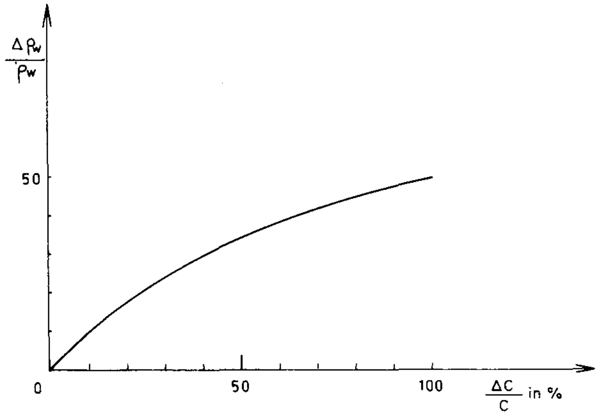

Fig. 4.2.23. Water-resistivity variations (%) vs. NaCl concentration variations (%). $T = 13°$ C.

At the well, the measured variation is:

$$\frac{c_1 - c_0}{c_0} = A \left(\frac{\Delta\rho}{\rho}\right)_p$$

Resistivity-variation maps are equivalent to relative resistivity-variation maps through the quantities:

$$\left(\frac{\Delta\rho}{\rho}\right) \Big/ \left(\frac{\Delta\rho}{\rho}\right)_p$$

and the model directly computes:

$$(c_1 - c_0) f(x, t)/(c_1 - c_0) = f(x, t)$$

The map of $f(x, t)$ is adjusted to the map:

$$\frac{\Delta\rho}{\rho} \bigg/ \left(\frac{\Delta\rho}{\rho}\right)_p$$

Concentrations are average values per stratum. Adjustment is performed in two steps:

(1) Position, width and permeability of each stratum are determined from geological logs at the well. These values are subject to modifications during adjustment. It must be noticed that the transmissivity and the depth of the aquifer are fixed given data. The trial-and-error method for the stratum characteristics is based upon direct qualitative interpretation of the geophysical results. For example, resistivity variations are small with respect to the injected quantities; this is interpreted as the occurrence of a very permeable stratum near the bedrock and the trial-and-error takes it into account. Also, details of the features of the stratum may be supplemented by other techniques such as electrical logs or radioactive tracing.

(2) A longitudinal-dispersion coefficient and a transverse-dispersion coefficient are given per stratum, as multiple or unitary coefficients, the multiplication constants resulting from tests and bibliographical studies: for instance (Fried et al., 1973), a constant equal to 1 for longitudinal dispersion and inversely proportional to permeabilities for transverse dispersion; this last result was explained by the fact that when low-permeability zones are encountered they act as buried dams, which results in a widening of the polluted zone, a hydrodynamic effect which is part of the mechanism of transverse dispersion.

Adjustment is carried out by modifying the unitary coefficients according to the following flow chart (Fig. 4.2.24).

Remark. Geophysical results are sufficient to adjust the model, because only variations are used. Real values of the concentrations cannot be determined by geophysics. A supplementary experiment is needed to verify the concentration values given by the model which depend on the dilution assumptions.

Experimental results and their interpretations on an example

Experimental results are presented on the example of the Lyons aquifer measurement campaign treated in §6.2. Schlumberger-type curves in Fig. 4.2.25 relate the concentration variations of the groundwater at a given temperature to its resistivity. The apparent relative resistivity variations are connected to the relative variations of equivalent concentrations of NaCl (the resistivities of other chemical constituents of the groundwater do not change) which are represented in Fig. 4.2.23.

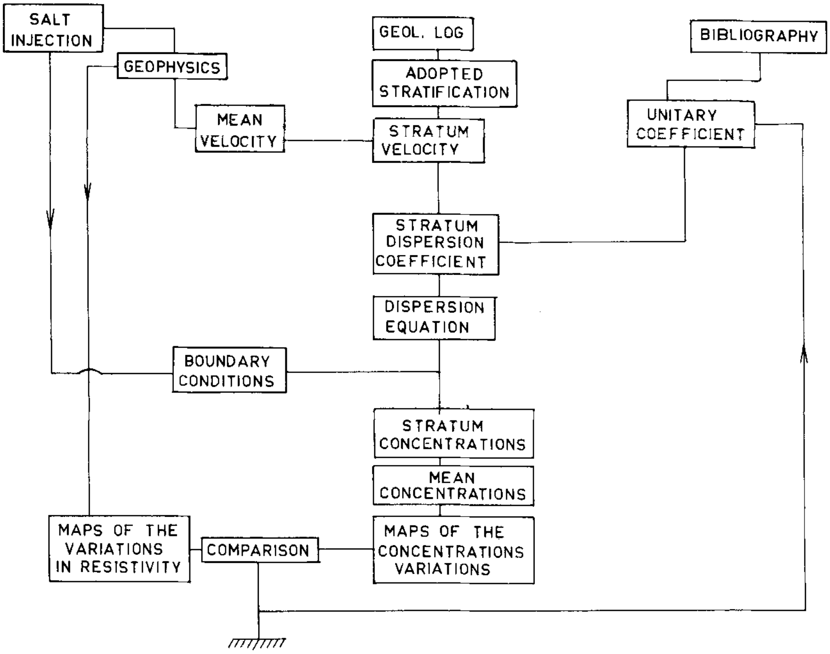

Fig. 4.2.24. Operation flow chart.

For the first step of the adjustment, the positions of the permeable layers were obtained by comparing the experimental curve of electrical sounding to the computed curves corresponding to a series of media obtained by moving a pervious layer down the aquifer (Fig. 4.2.26). In the example, it was found that medium 7 suited best. Results appear on Figs. 4.2.27, 4.2.28 and 4.2.29.

The injection lasted 225 hours and more than 40 tons of salt were introduced. The initial-resistivity map (Fig. 4.2.27), realized with a length of line $AB = 90$ m, shows a zone of higher conductibility parallel to the axis of the device. Following three electrical soundings, the apparent-resistivity variations are explained by a resistivity variation of dry alluvia. At the end of the injection period, modifications due to salt water mainly occurred along the axis of the electrode device and they can be detected up to profiles 23 and 24: beyond this, resistivities were stable during the operation (Fig. 4.2.27). The apparent-resistivity variations (Fig. 4.2.28), given in percentages, define a narrow conductive anomaly: the variations amount to 4—5% near the well and 2% at 45 m from it, at the limit of the detection threshold. Values between 1 and 2% yield the axis of flow up to profile 24.

The potential method (Fig. 4.2.29), extending up to profile 14, defines a conductive axis, corresponding to the axis of the narrow conductive anomaly. This axis is taken as the x-axis of the model, the y-axis is orthogonal. The model simulates the situation on Fig. 4.2.28, the velocities being computed from the same experiment by a method described in § 4.3.

Some conclusions about this single-well geophysical method

Global scale 2 (20—100 m) is the scale of many classical pollution accidents and also the scale of protection zones of pumping wells. Two important

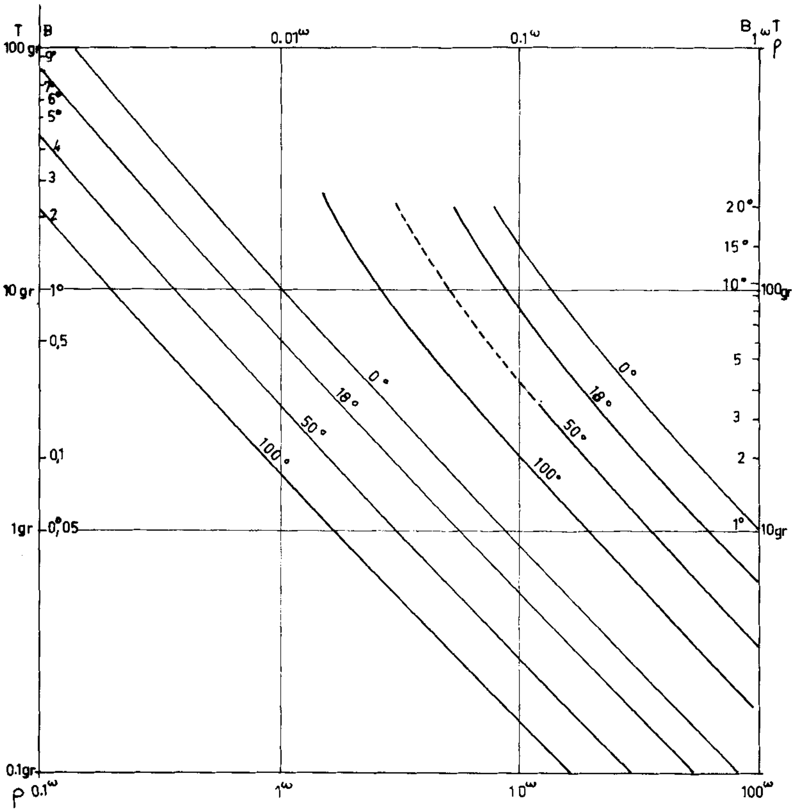

Fig. 4.2.25. Resistivity-equivalent NaCl curves for various temperatures.

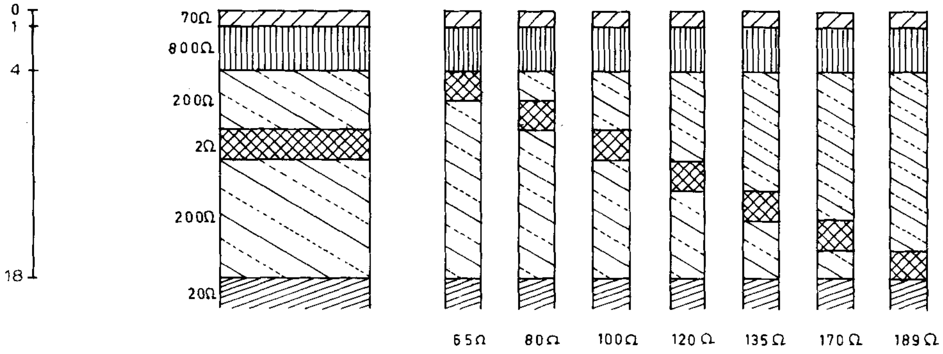

Fig. 4.2.26. Geoelectrical equivalent of various layered media.

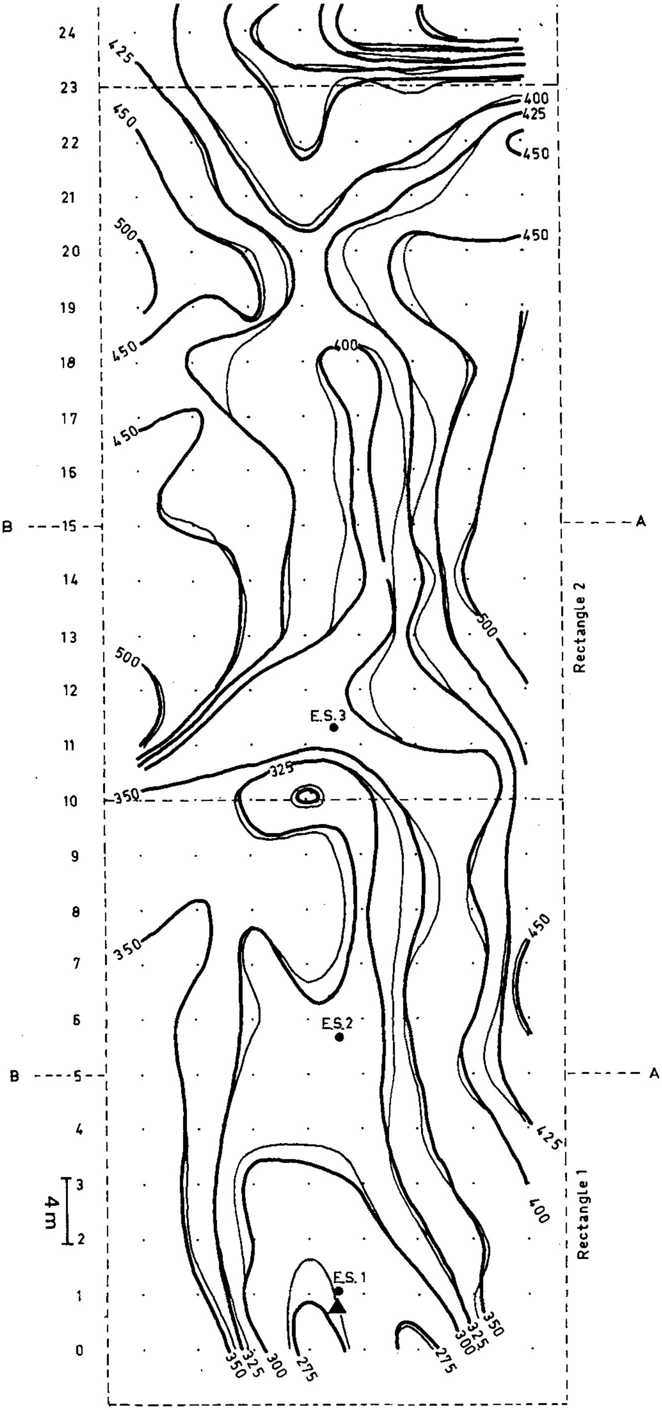

Electrical sounding	●
Injection well	▲
Measurement point	.

Fig. 4.2.27.
Apparent-resistivity map.

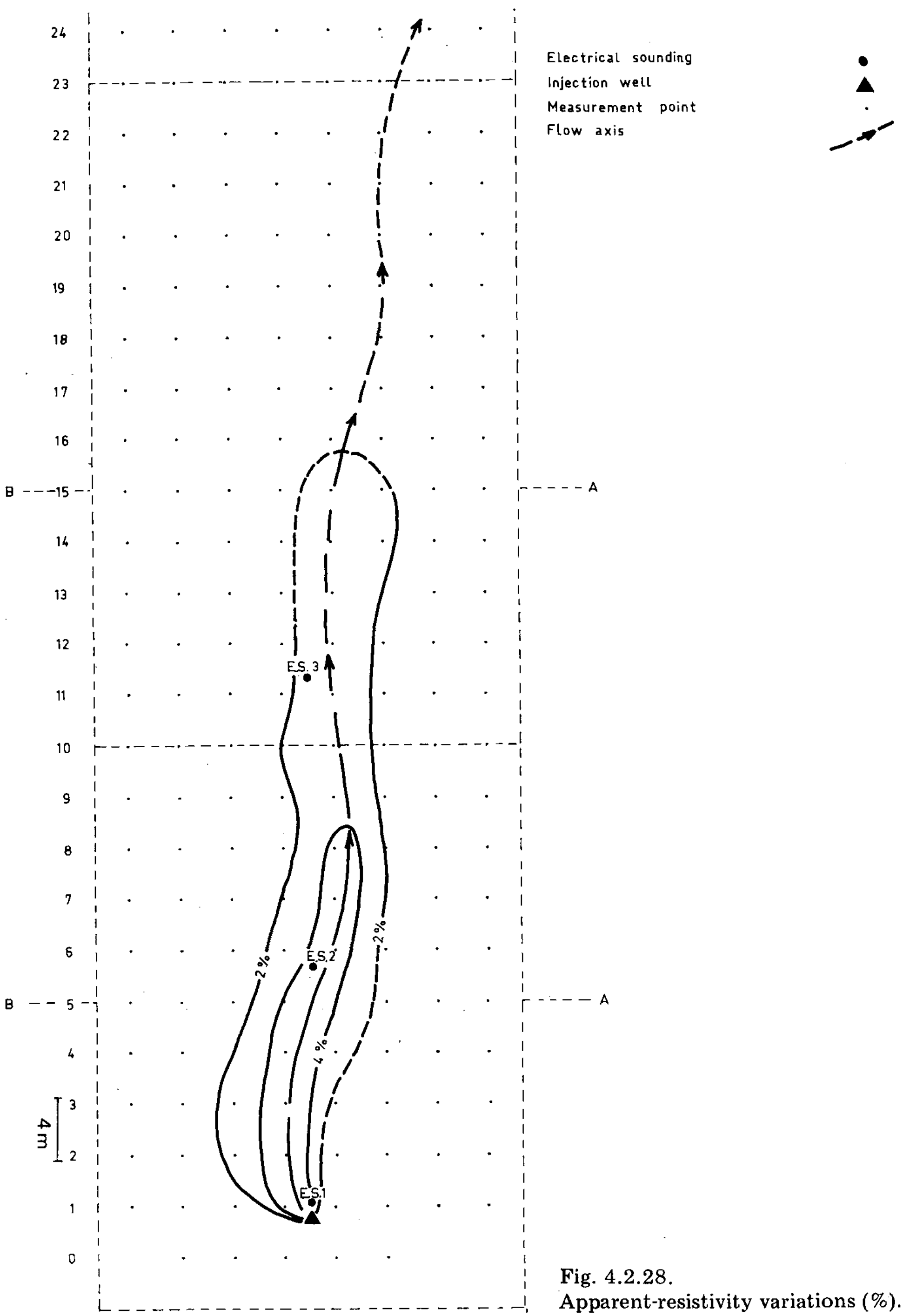

Fig. 4.2.28.
Apparent-resistivity variations (%).

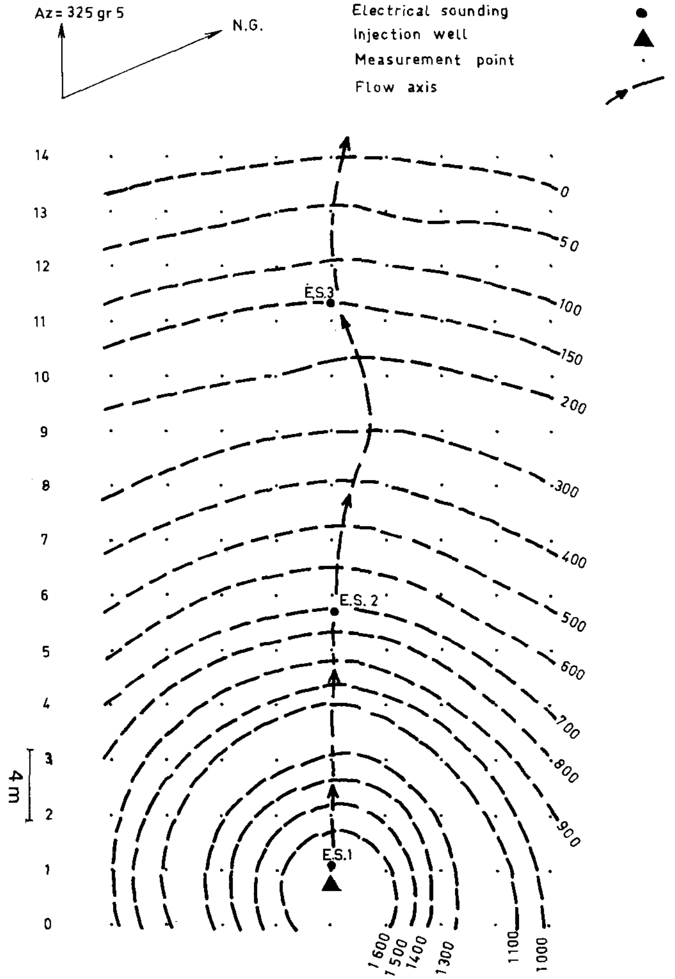

Fig. 4.2.29. Potential method results.

factors appear: stratification and transverse dispersion. Of course, for reasons explained in § 2.5, longitudinal dispersion is important also, but it already plays a role at smaller scales (§ 4.2.1 and 4.2.2).

A mean dispersion effect on the whole aquifer depth at this scale implies the use of a much too great amount of tracer which would be expensive and which also does not correspond to many pollution accidents at that scale. In the given example, more than 30 tons of salt were already required and a significant mean experimental dispersion was not obtained; experimental regularization by molecular diffusion, and vertical transverse dispersion and mechanical effects does not happen, because injected quantities are still too small and they flow through the permeable layers. Stratification must be taken into account.

The geophysical electrical measurement, however, is an artificial regularization and it is reproduced in the model by a numerical averaging process. The model simulates the stratified medium, then creates a homogeneous equivalent medium which is adjusted to the geophysical electrical measurements and then reverts to the stratified medium, which allows to infer local properties. In itself, such a mathematical process does not yield a unique solution. Uniqueness is obtained by comparing the model stratification to geological logs and to geophysical stratified media (Fig. 4.2.26).

This method requires two mathematical models, a series of geophysical measurements from a single well and geological logs at the injection wells. There is no need for any observation well. It is a rather easy and cheap method, which does not disturb the medium. Of course, as has been said, salt can be replaced by other electrical tracers.

In conclusion, the proposed methodology is as follows:

(1) Experimental step: geological logs at the injection wells; geophysical electrical measurements of a convenient tracer by a single-well method (injection in a well and detection from the soil surface).

(2) Model step: a geophysical stratification model to obtain the positions and the widths of the strata for the geophysical measurements; a dispersion stratification model to obtain the dispersion coefficients.

4.2.4. Regional scale: use of environmental tracers

At the regional scale (over 100 m), two types of pollution effects may be sought: (1) either long-distance effects of small amounts of pollution, or (2) long-distance effects of large amounts of pollution.

The first type is purely mechanical, because mixing (mechanical mixing and molecular diffusion, as described in § 2.1) does not occur: the pollution flows through preferential paths and fingering is a predominant feature. Dispersion is neglected and the evolution of the pollution can be described by measuring the velocities of the water along the preferential paths. These velocities are obtained from the minimum residence time of an injected tracer recorded in a line of wells at the required observation distance from the injection well: t being the minimum residence time and x the distance between the injection and observation well, x/t is taken as the velocity of the pollution (Fig. 4.2.30).

The second type of pollution is obviously very difficult to simulate with a pollution created for the sole purpose of measuring dispersion coefficients. This is the reason why only environmental tracers are considered, with the condition that they exist in sufficient amounts. We call "environmental tracer" a substance that exists in the soil before the investigation begins. It can be natural (a natural radioisotope for instance, or sea-water intrusion), semi-artificial (as tritium, originally produced by atom-bomb tests) or artificial (a man-made pollution).

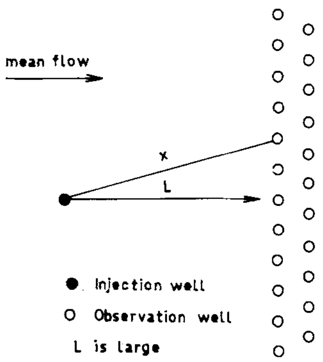

Fig. 4.2.30. Experimental setting for the determination of pollution velocities on a large scale.

Mostly artificial environmental tracers and sea-water intrusion have been used up to now. The method is to calibrate a mathematical model on the concentration curves obtained from field measurements, by adjusting the dispersion coefficients, and then to use the same model in the predictive phase to compute new concentration distributions from various boundary conditions. We give two examples to illustrate the method.

An existing pollution due to industrial wastes

The complete case history, including geological setting and mathematical models, is described in § 6.1. The bidimensional, horizontal, monolayer, hydrodispersive model in canonical rectangular coordinates (§ 6.1) is adjusted by a trial-and-error method to the concentration values measured along the mean flow axis issued from a salt dump. The adjustment is performed by varying the longitudinal and lateral dispersion coefficients, at a given mean velocity computed from the measured piezometry in the area. These adjustment operations are repeated for each salt dump which yields a map of dispersion coefficients of the whole area.

An example of computed and measured concentration curves for a given salt dump at different times and different assumed permeabilities is shown in Fig. 4.2.31 which yielded the intrinsic dispersion coefficients $\alpha_L = 15$ m and $\alpha_T = 1$ m.

Pollution due to a sanitary landfill

The setting is described in § 6.2. The geophysical measurements of resistivity have yielded the direction of the aquifer flow; the intensity of the aquifer velocity along the mean flow axis is deduced by analogy from geophysical measurements on the other sites (§ 6.2) which present an equivalent geological composition (in the sense of permeabilities). Of course, at the scale of the investigation (600—1000 m), a mean velocity value deduced from piezo-

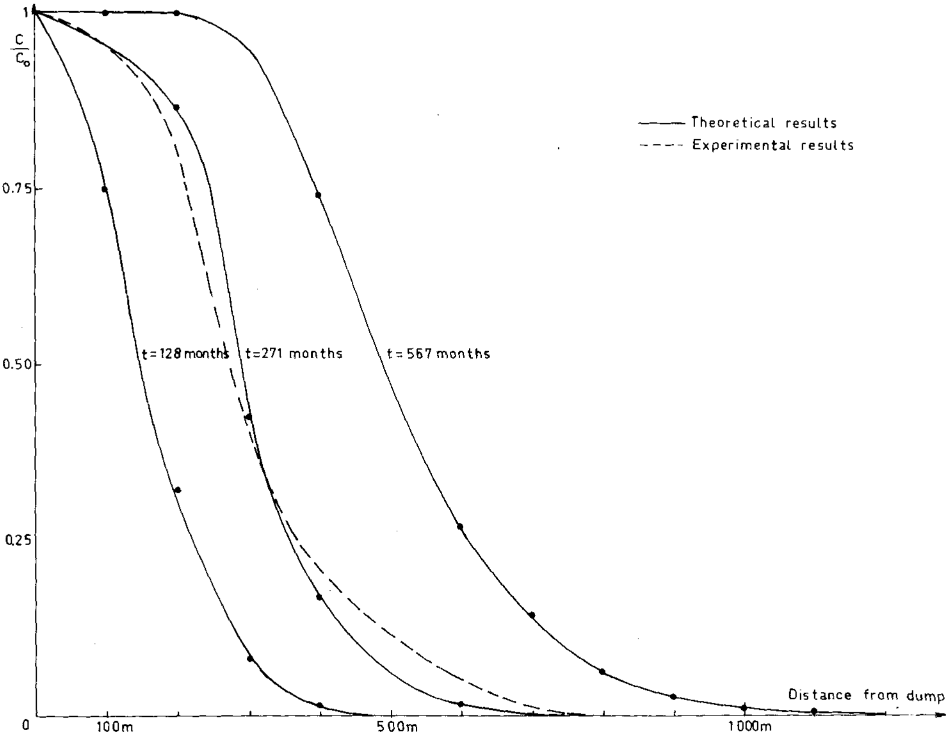

Fig. 4.2.31. Computed and observed salt concentrations vs. the distance from the dump at various times.

metric measurements already makes sense. Conductibility measurements of the water were performed in a series of observation wells downstream of the landfill and have been used to adjust a bidimensional, horizontal, monolayer hydrodispersive model analogous to the model used in the preceding example. Local authorities have provided the age of the landfill, which is taken as the calibration time of the model. The various chemical ions were not differentiated and only their global conductibility was taken into account. The calibration curves are similar to the curves drawn on Fig. 4.2.31. The values of the intrinsic dispersion coefficients were $\alpha_L = 12$ m and $\alpha_T = 4$ m.

Remark. Of course other experimental criteria could be used to calibrate the model. For instance, the amount of total dissolved solids can be computed from chemical analysis and used as an environmental tracer.

4.3. FIELD METHODS FOR THE DETERMINATION OF POLLUTION VELOCITIES

Field methods used to determine the velocity of a pollution are classified into two families: (1) indirect estimates of the velocity from the hydraulic parameters of the aquifer and Darcy's law; and (2) direct estimates of the velocity.

4.3.1. Indirect estimates of the velocities through Darcy's law

In Appendix I, we develop the basic principles of hydrogeology and introduce Darcy's law as the governing equation of aquifer movements, connecting the velocity v and the pressure gradient:

$$v = -\frac{k}{\mu}(\mathrm{grad}\, p + \rho g\, \mathrm{grad}\, z) \qquad [4.3.1]$$

where k is the permeability coefficient tensor, g the gravity, p the pressure of the fluid, μ and ρ respectively the dynamic viscosity and the density; z is the coordinate along the vertical axis $0z$ in a classical rectangular coordinate system, where the gravity vector is parallel to $0z$. In Appendix I we see that Darcy's law and the continuity equation yield the fundamental hydrologic equation of the form:

$$\mathrm{div}\,(T\, \mathrm{grad}\, h) = S\frac{\partial h}{\partial t} + q \qquad [4.3.2]$$

written here for a confined aquifer of transmissivity T and storage coefficient S; h is the piezometric potential, which can be introduced when ρ is constant, and it is equal to:

$$h = \frac{p}{\rho g} + z$$

q represents field singularities.

Remark. Constant ρ is a good and usual assumption in the case of water flow. But for pollution flow, this assumption must be handled with care and is valid in the tracer case only.

The principle of the indirect methods is to determine the permeability coefficient (or the transmissivity) and from pressure-gradient measurements compute v by means of Darcy's law.

As already seen for dispersion coefficients, various methods have to be used to determine permeability or transmissivity according to the scale of the investigation. They can be classified into two sets: (1) experimental methods, such as pumping tests or geoelectrical techniques, valid at global scale 1 or global scale 2; and (2) mathematical methods which consist in interpreting piezometric maps with the fundamental hydrologic equation either by trial-and-error adjustment of field maps and computed maps or by inverse methods. The resulting parameters are valid at global scale 2 or at regional scales.

Remark. Under special homogeneity conditions of the aquifer, transmissivity values computed by experimental methods at global scales can be used in regional-scale models.

Pumping tests

Nonequilibrium methods (Theis, 1935; Chow, 1952, Jacob, 1947) and steady-state methods (Dupuit) with their simplifying assumptions (Dupuit—Forcheimer assumptions) are extensively described in several textbooks (Todd, 1959). They are very classical; although they are used in pollution problems, they are not specific and we do not elaborate.

It should be noticed that, in addition to the pumping well, at least one observation well is needed at such a distance that errors in the hydraulic-gradient measurements are not too important.

Geoelectrical techniques

Geoelectrical techniques described in Appendix II, have been used to determine the transmissivities of an aquifer without any well. Although it is an application of geophysics still under investigation, we present here results obtained in an experimental area, as a hint for possible applications of these techniques.

The proposed technique (Ungemach, 1975, Duprat et al., 1970), is to interpret the values of the transverse resistances R_t, given by electrical soundings, in terms of transmissivities. The study has taken place in the Rhine aquifer of eastern France, which is an alluvial aquifer made up of sands and gravels and pebbles with thin clay lenses, on an impervious bedrock; it is unconfined and its free surface is a few meters deep.

A relationship between transmissivity T and transverse resistance R_t has been sought, by plotting the transmissivities computed from pumping tests in six wells versus the transverse resistances obtained by electrical soundings near the wells. Other values of T and R_t determined in other areas confirmed the graph ($R_t - T$) represented in Fig. 4.3.1. T appears to be an almost linear function of R_t.

A transmissivity map of the aquifer (Fig. 4.3.2) can be derived from the graph (Fig. 4.3.1) and the map of R_t (Fig. 4.3.3).

Remark. The values of R_t introduced here are "corrected" values. The electrical soundings yield gross values of R_t, which have to be corrected, taking into account the local resistivity of the water: the resistivity of an aquifer closely depends on the resistivity of its water. For instance, Archie's relationship can be used:

$$\rho_a / \rho_w = \phi^{-m} \qquad [4.3.3]$$

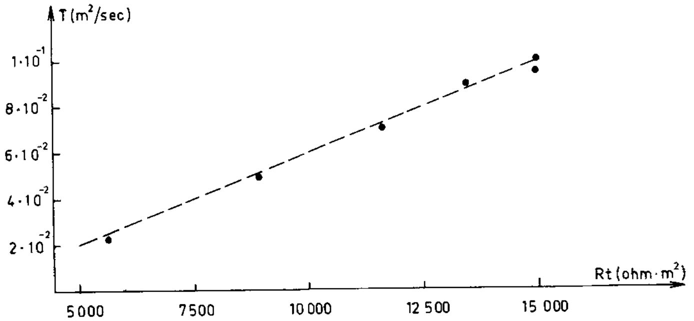

Fig. 4.3.1. Transmissivities vs. transverse resistance (Duprat et al., 1970).

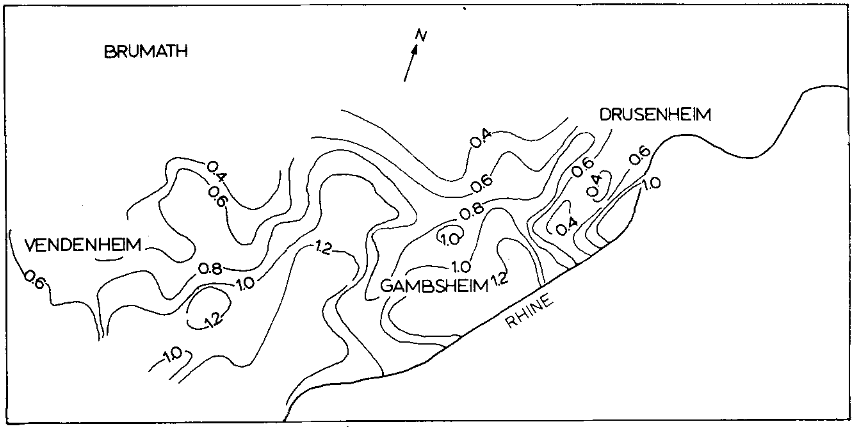

Fig. 4.3.2. Transmissivities (× 10^{-1} m^2/sec) (Duprat et al., 1970).

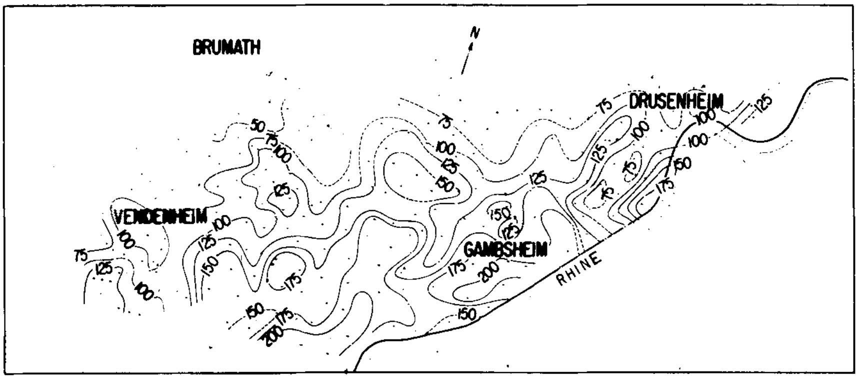

Fig. 4.3.3. Corrected transverse resistance (× 100 ohm.m^2) (Duprat et al., 1970).

where ρ_a and ρ_w are respectively the resistivities of the aquifer and of its water and ϕ its porosity and m a consolidation coefficient. This relationship shows that the resistivity of a given aquifer is proportional to the resistivity of its water. Assuming a mean water resistivity, computed from samples, the transverse resistance is computed at each sounding. These corrected values of R_t display the changes in real resistivity due to the alluvia properties, such as grain-size distribution and clay content.

4.3.2. Direct estimates of velocities

Direct estimates of velocities can be performed at the local scale and at global scales 1 or 2. They yield pore velocities.

Multiple-well method

As for dispersion-coefficient measurements, the method is based upon the experimental setting of Fig. 4.2.15. A tracer (radioactive or not, such as ^{131}I or INa) is injected at a rate small enough not to perturb the natural flow. This tracer concentration should be large enough to be detected by the measurement device; also, of course, it must not preexist in the aquifer. An injection device is presented in Fig. 4.2.11. The observation wells are located so that preferential paths can be detected.

Remark. A weakness of the multiple-well method is that it is necessary to know the mean direction of flow to locate the observation wells. This means that preliminary studies are necessary to determine this direction; of course, it could be possible to drill wells on concentric circles, which would be rather expensive. In the case history of § 6.2, we see how several methods are coupled to reduce the costs and yield the expected results.

In Figs. 4.2.12 and 4.2.13 are represented the vanishing of the tracer with time and its occurrence in an observation well, respectively. The input function is assumed to be a Dirac δ-function and the residence-time distributions $E(t)$ are directly given by the concentration curves as:

$$E(t) = \frac{c(t)}{\int_0^\infty c(t)\mathrm{d}t} \qquad [4.3.4]$$

From the residence-time distribution, a mean velocity can be computed by the formulas:

$$\bar{u} = \frac{\int_0^\infty u(t)\,c(t)\mathrm{d}t}{\int_0^\infty c(t)\mathrm{d}t}$$

$$u(t) = L/t \qquad [4.3.5]$$

$$\text{and: } \bar{u} = L\int_0^\infty \frac{1}{t}E(t)\mathrm{d}t \qquad [4.3.6]$$

where L is the distance between the injection and observation wells.

Single-well method: a point-dilution technique

The preceding experimental device can be used to compute a local velocity at the injection well, by using the vanishing concentration curve at the injection well, the tracer having been well mixed over the whole depth of the borehole (Fig. 4.2.11). The flow rate of tracer is equal to the mass of tracer leaving the well during time interval dt:

$$Suc\,\mathrm{d}t = -v\,\mathrm{d}c \qquad [4.3.7]$$

where c is the concentration at time t, S the section of aquifer intercepted by the borehole, t the observation time, u the velocity and v the volume of the borehole.

The integration of the differential equation [4.3.7] yields:

$$u = \frac{v}{St}\ln(C_0/C)$$

where C_0 is the initial tracer concentration. The horizontal flow pattern in the aquifer is distorted owing to the presence of a borehole and the different flows therein. If a correction factor θ, which accounts for the distortion of the flow lines owing to the presence of the borehole, is defined as:

$$\theta = Q_b/Q_f$$

where Q_b is the horizontal flow rate in the borehole and Q_f the flow rate in the same cross-section of the formation and in the absence of all other flows but horizontal, then the filtration velocity is:

$$u_f = \frac{v}{\theta St}\ln(C_0/C)$$

Single-well method: a geoelectrical method

The single-well method described in § 4.2.3 can be used to detect average and maximum velocities of an aquifer at global scales 1 or 2. Actually, this geoelectrical method has been first introduced to detect velocities and later only modified to collect dispersion coefficients.

The idea was to adapt the well-known potential method (Appendix II). A conducting solution (NaCl for instance) is injected into a well, resulting in the distortion of the equipotential net in the direction of flow of the conducting solution. Thus, it is possible to detect the mean direction of flow of the aquifer (Chalengeas, 1970), as a preliminary step to the boring of observation wells (as required by the multiple-well method, for instance). The method has been extended to the direct measurement of velocities

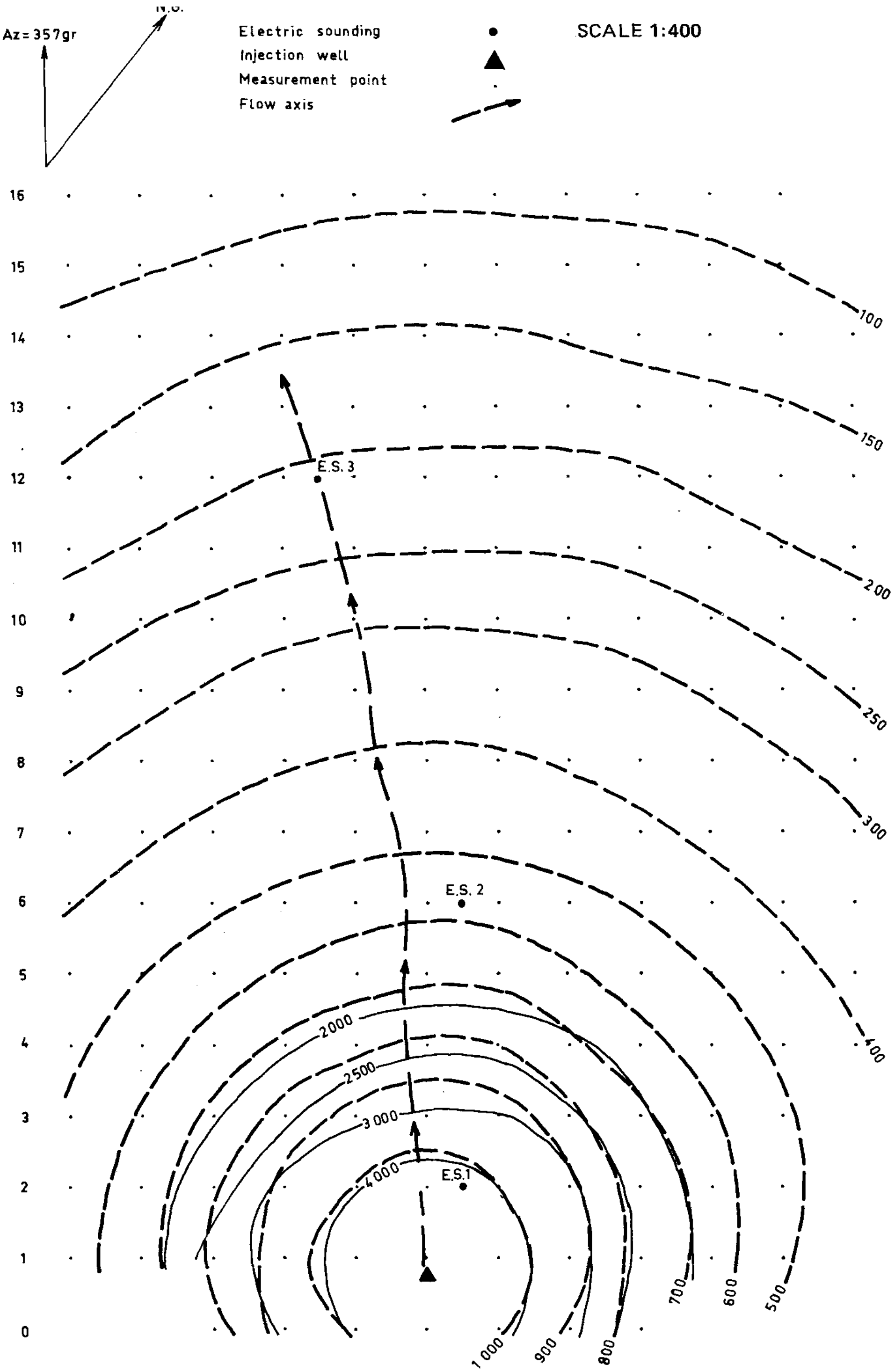

Fig. 4.3.4. Resistivity variations vs. time.

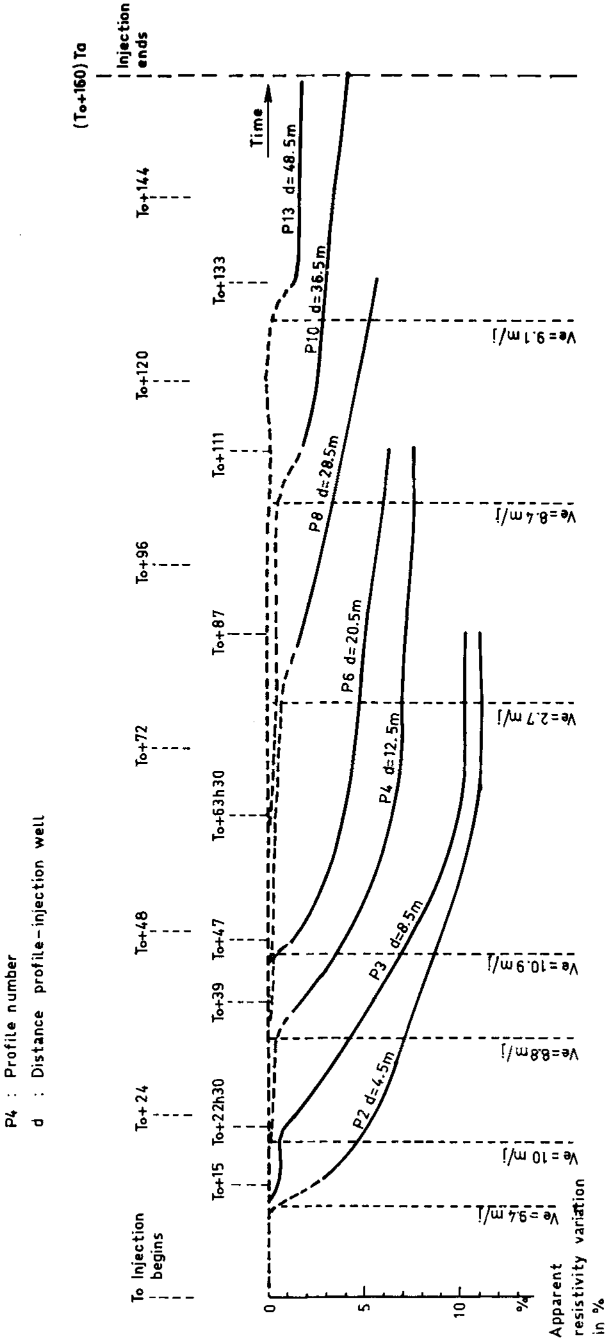

Fig. 4.3.5. Estimation of flow velocities during injection.

(Ungemach, 1975), by estimating the displacement of the distortion with time by resistivity measurements.

The potential method is used to display the direction of flow (Fig. 4.3.4) and the resistivity measurements yield the maximum and average velocities (Fig. 4.3.5). The occurrence of salt water progressively decreases the resistivity which reaches a minimal value after a period of time depending on the experiment, the velocity is the average of the maximum velocities corresponding to the first occurrence of salt water at the various observation points.

We have seen that the resistivity-variation map (Fig. 4.2.22) was interpreted in terms of dispersion (§ 4.2.3). It also yields the flow direction and can be usefully compared to Fig. 4.3.4, which it confirms.

From the technical point of view, a few precautions must be taken (as already stated in the case of dispersion measurements):

(1) The injection rate must be small enough to prevent perturbations of the natural flow.

(2) If possible, the injection should be constant with time.

(3) The amount of salt should be large enough to create modifications of the electrical properties of the medium, this can be detected by the superficial geophysical probes.

(4) The geochemical and geophysical properties of the medium must be measured before the injection; they will serve as the initial condition of any model of the experiment.

4.3.3. The single-well possibilities

Single-well methods have been introduced because they only slightly disturb the medium. We summarize their possibilities in the following flow chart (Fig. 4.3.6).

In this book, we do not elaborate on the determination of clay lenses by fixation, a technique developed by P. Levêque (Levêque et al., 1971).

The single-well techniques which have been successfully applied in many hydrological problems are now currently investigated for simplification purposes; local methods, especially by radiotracers, are under study and as an example, we describe the device derived by Drost et al. (Drost and Neumaier, 1974) which can be handled by one person with professional experience of hydrological problems, measuring techniques and the basic principles of radiation protection.

The single-borehole probe is presented in Fig. 4.3.7: the detector, the injector and the mixing coil are inside the sealed measuring volume of the probe; rubber packers with detectors monitoring vertical flow are placed above and below this measuring volume. Flow in the outside gravel pack is avoided by forcing possible vertical groundwater currents through the pressure-equalizing tube; under this condition, the influence of vertical currents on the measured filtration rates can be neglected. The probe can be

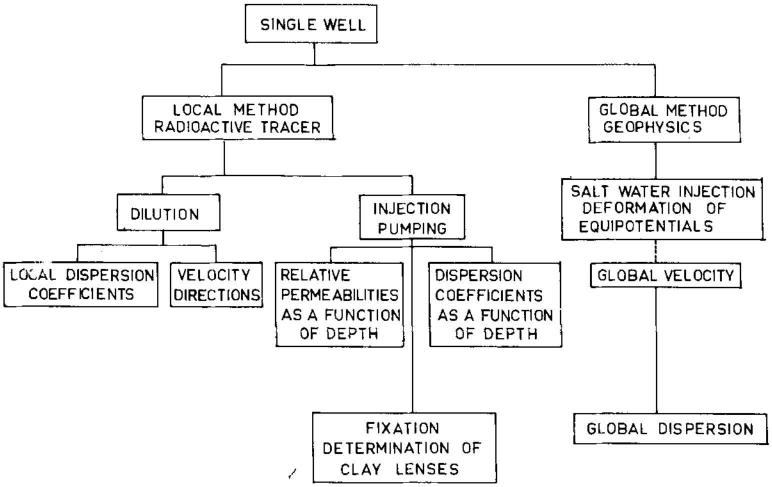

Fig. 4.3.6. Possibilities of the single-well methods.

lowered in the borehole (diameter $\geqslant 5$ cm) by means of a cable the diameter of which is 1 cm.

4.3.4. *A note on porosity measurements in the saturated zone*

When velocity is determined indirectly by means of permeability (or transmissivity) measurements and the use of Darcy's law, it is necessary to know the effective porosity ϕ, as the pollution velocity is the pore velocity. We recall the relationship between Darcy's filtration velocity v and pore velocity u:

$$u = v/\phi$$

Many methods exist to determine ϕ (Bear, 1972) but we shall restrict our note to specific methods of pollution studies, i.e. the two-well pulse method with radioisotopes and the geoelectrical single-well method.

The principle of the methods of porosity determination in the saturated zone is based on the approximate equality between porosity ϕ and partial volume of water (defined as the ratio between the volume of water and the total volume).

In the two-well method, traced water is introduced in one well and pumped at the other; dispersion is neglected and v being the volume of water pumped, we have:

$$v = \pi r^2 b\phi$$

where b is the aquifer thickness, r the distance between the wells.

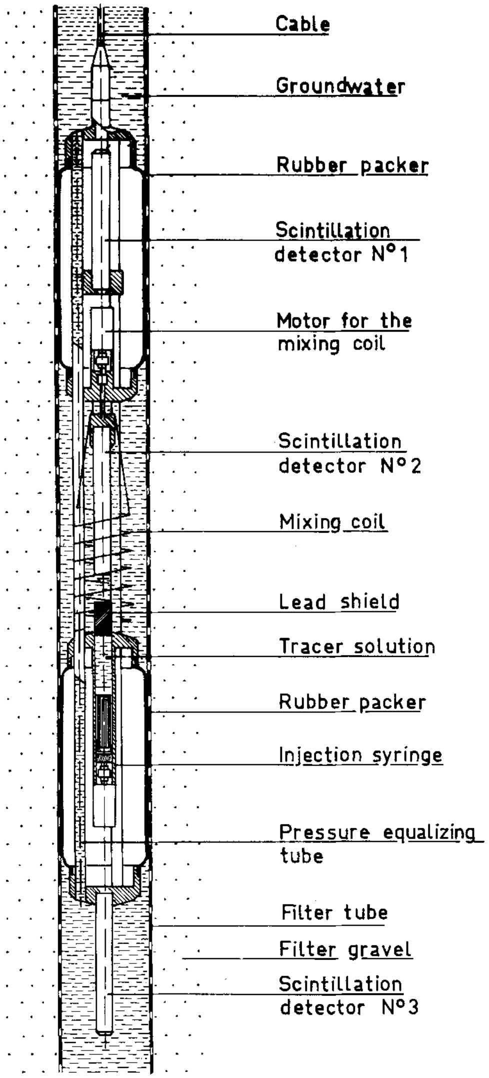

Fig. 4.3.7. Borehole probe for the determination of groundwater filtration velocity (from Drost and Neumaier, 1974).

This formula is valid under the following conditions (Int. At. Energy Agency — UNESCO, 1968, p. 187): (1) the velocity of the aquifer is neglected with respect to the radial velocities induced by pumping. The flow pattern is locally radial; (2) the thickness of the aquifer is small compared to the distance between wells; (3) the cone of depression at the pumping well is small compared to the total water volume V.

Exchange and dispersion effects between flowing and bound waters can create errors in the interpretation and might yield intermediate values between porosity and effective porosity.

Radiotracers are used and V is taken as the volume corresponding to the peak activity, this volume being determined by plotting the activity as a function of $V^{1/2}$ (Halevy and Nir, 1962). Porosity is then:

$$\phi = V/\pi r^2 b$$

The geoelectrical single-well method is based upon tracing the water by an electrolyte and recording the resistivities of the traced water ρ_w and of the total layer (solid matrix and traced water) ρ_a. The techniques used to measure the resistivities are described in Appendix II. The ratio of both resistivities is called the formation factor F and we have:

$$F = \rho_a/\rho_w = \phi^{-m}$$

This relationship is known as Archie's formula. m is a coefficient with a value between 1 and 2, depending upon the consolidation of the layer. Porosity is then given by:

$$\phi = F^{-1/m}$$

CHAPTER 5

CLASSICAL MATHEMATICAL MODELS AND THEIR NUMERICAL FORMULATION

This chapter is mainly intended for the Engineer and will provide him with practical numerical formulation and rules to treat groundwater-pollution mathematical models. It is divided into three parts: canonical rectangular coördinate models, curvilinear coordinate models, and special models (analytical, deconvolution).

The finite-difference discretization is also presented as the most used procedure (although finite-element methods begin to be used in pollution modelling, they still belong to a research stage of dispersion modelling).

5.1. CANONICAL RECTANGULAR COORDINATE MODELS

5.1.1. Bidimensional monolayer model

The pollution is horizontal, plane and transient. The mixture density is a linear function of concentration. The movement is unidirectional and pressure only depends on x. The regime is dynamic dispersion, with dispersion coefficients proportional to the velocity. The mathematical problem is defined by a system of equations:

$$\frac{\partial\left[\rho\alpha_L|u_x|\dfrac{\partial\left(\dfrac{c}{\rho}\right)}{\partial x}\right]}{\partial x}+\frac{\partial\left[\rho\alpha_T|u_x|\dfrac{\partial\left(\dfrac{c}{\rho}\right)}{\partial y}\right]}{\partial y}-\frac{\partial(u_x c)}{\partial x}=\frac{\partial c}{\partial t}$$

$$u_x = -\frac{k_x}{\mu\phi}\frac{\partial p}{\partial x}$$

$$u_y = 0$$

$$\frac{\partial(\rho u_x)}{\partial x} = -\frac{\partial\rho}{\partial t}$$

$$\rho = ac + b$$

where u_x and u_y are the components of the mixture velocity, k_x the permeability along $0x$, p the pressure, ρ,μ,ϕ respectively the density, the viscosity and the porosity; a and b are constants given by the tables.

The domain is defined in Fig. 5.1.1 and is symmetrical with respect to the x-axis.

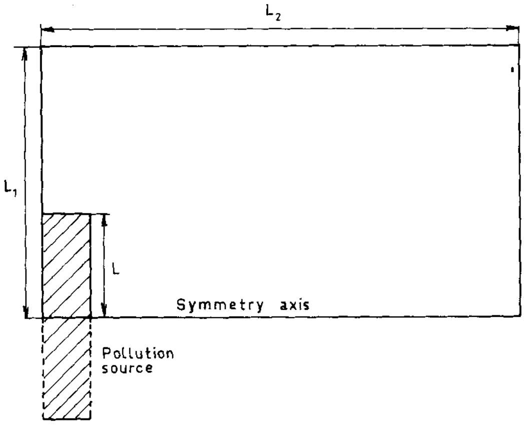

Fig. 5.1.1. Modelled domain

Initial and boundary conditions are:

$$c(x,y,0) = c_0$$

$$p(x,0) = p_W + [p_E - p_W]\,\frac{x}{L_2}$$

$$c(0,y,t) = c_s \quad \text{with} \quad 0 \leqslant y \leqslant L$$

$$c(0,y,t) = c_0 \quad \text{with} \quad L < y \leqslant L_1$$

$$c(x,L_1,t) = c_0$$

$$c(L_2,y,t) = c_0$$

$$\frac{\partial c}{\partial y}(x,0,t) = 0$$

$$p(0,t) = p_W$$

$$p(L_2,t) = p_E$$

where c_s and c_0 are constant, and represent the pollution concentration at the source and the pollution initial concentration in the domain, respectively; p_W and p_E are constant.

This system is discretized in finite differences according to the ADIP. The convection term is discretized in backward differences with the flow direction. Density ρ and velocity u are constant during a time-step. A possible discretization scheme is:

$$\frac{\alpha_L}{\mathrm{d}x^2}\left[\frac{\rho(i+1,j)|u(i+1,j)|+\rho(i,j)|u(i,j)|}{2}\left\{\frac{c^+(i+1,j)}{\rho(i+1,j)}-\frac{c^+(i,j)}{\rho(i,j)}\right\}\right.$$
$$\left.-\frac{\rho(i,j)|u(i,j)|+\rho(i-1,j)|u(i-1,j)|}{2}\left\{\frac{c^+(i,j)}{\rho(i,j)}-\frac{c^+(i-1,j)}{\rho(i-1,j)}\right\}\right]$$
$$+\frac{\alpha_T}{\mathrm{d}y^2}\left[|u(i,j)|\frac{\rho(i,j+1)+\rho(i,j)}{2}\left\{\frac{c(i,j+1)}{\rho(i,j+1)}-\frac{c(i,j)}{\rho(i,j)}\right\}\right.$$
$$\left.-|u(i,j)|\frac{\rho(i,j)+\rho(i,j-1)}{2}\left\{\frac{c(i,j)}{\rho(i,j)}-\frac{c(i,j-1)}{\rho(i,j-1)}\right\}\right]$$
$$-\frac{u(i,j)c^+(i,j)-u(i-1,j)c^+(i-1,j)}{\mathrm{d}x}=\frac{c^+(i,j)-c(i,j)}{\mathrm{d}t(n)/2}$$

$$\frac{\alpha_L}{\mathrm{d}x^2}\left[\frac{\rho(i+1,j)|u(i+1,j)|+\rho(i,j)|u(i,j)|}{2}\left\{\frac{c^+(i+1,j)}{\rho(i+1,j)}-\frac{c^+(i,j)}{\rho(i,j)}\right\}\right.$$
$$\left.-\frac{\rho(i,j)|u(i,j)|+\rho(i-1,j)|u(i-1,j)|}{2}\left\{\frac{c^+(i,j)}{\rho(i,j)}-\frac{c^+(i-1,j)}{\rho(i-1,j)}\right\}\right]$$
$$+\frac{\alpha_T}{\mathrm{d}y^2}\left[|u(i,j)|\frac{\rho(i,j+1)+\rho(i,j)}{2}\left\{\frac{c(i,j+1)}{\rho(i,j+1)}-\frac{c(i,j)}{\rho(i,j)}\right\}\right.$$
$$\left.-|u(i,j)|\frac{\rho(i,j)+\rho(i,j-1)}{2}\left\{\frac{c(i,j)}{\rho(i,j)}-\frac{c(i,j-1)}{\rho(i,j-1)}\right\}\right]$$
$$-\frac{u(i,j)c^+(i,j)-u(i-1,j)c^+(i-1,j)}{\mathrm{d}x}=\frac{c(i,j)-c^+(i,j)}{\mathrm{d}t(n)/2}$$

$$\frac{k_x}{\mu\phi\mathrm{d}x^2}\left[\frac{\rho(i+1,j)+\rho(i,j)}{2}\{p(i+1)-p(i)\}-\frac{\rho(i,j)+\rho(i-1,j)}{2}\right.$$
$$\left.\{p(i)-p(i-1)\}\right]=\frac{\rho(i,j)-\rho^-(i,j)}{\mathrm{d}t(n)}$$

$$\rho(i,j)=ac(i,j)+b$$

$$u(i,j)=-\frac{k_x}{\mu\phi}\frac{p(i)-p(i-1)}{\mathrm{d}x}\qquad\text{for all } j$$

where c^+ are intermediate values without physical meaning introduced within the theory of alternate direction methods (§ 9.4.4); ρ^- is the density at time $t(n)$ and ρ is the density at time $t(n + 1)$.

The linear systems are solved by direct Gauss tridiagonal elimination. At each time step, ρ^- is known, ρ is computed, then c and a consistency test is made on u (usually the procedure is iterated within the same time-step until good convergence is reached), then the procedure is iterated to the next time-step. This method is summarized in the flow chart of Fig. 5.1.2.

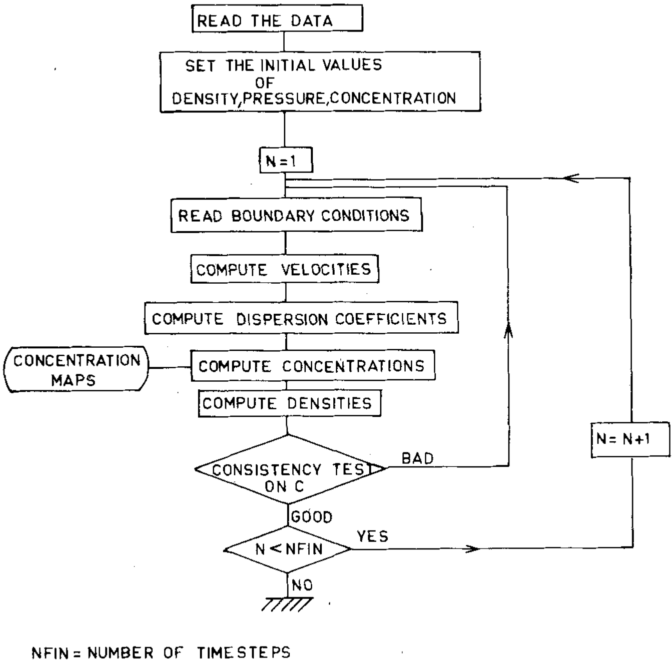

Fig. 5.1.2. Bidimensional horizontal model: computation flow chart.

Fig. 5.1.3 shows the evolution of a pollution intrusion with time as the output of the model written for constant ρ and μ (the tracer case) and a linear source all along the western boundary.

5.1.2. *Bidimensional multilayer model*

This aquifer is multi-layered and in each layer, the pollution is plane and horizontal. It is the tracer case and the movement is unidirectional at a constant measured velocity. Experimentally, only an average value of the pollution concentrations is obtained (by surface resistivity measurements for instance) and the model yields the values of concentration averaged on the depth of aquifer. The layers are independent.

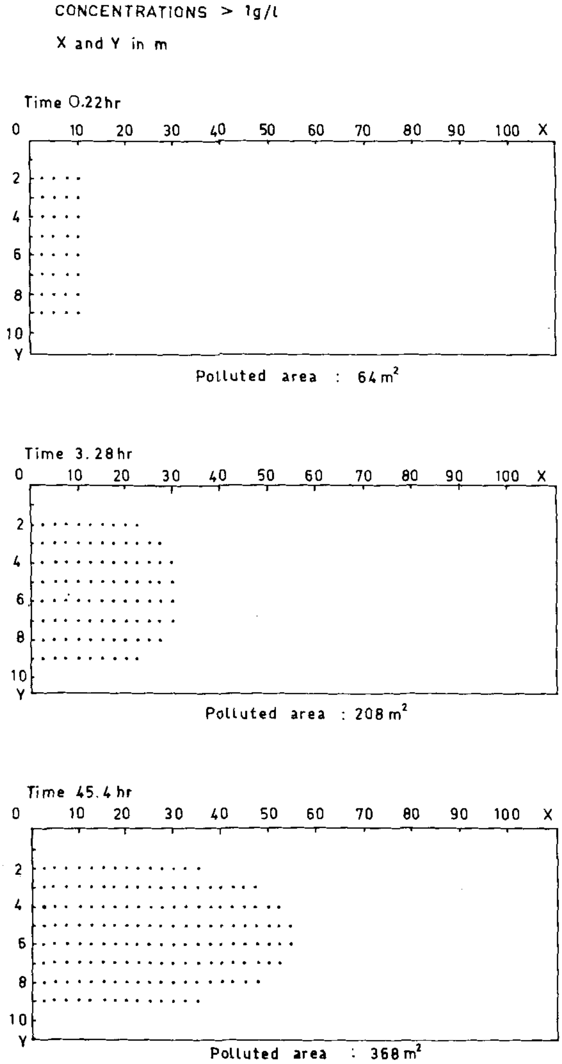

Fig. 5.1.3. Evolution of pollution with time for the bidimensional tracer case.

The mathematical problem is defined by a set of equations:

$$\frac{\partial}{\partial x}\left(\alpha_L \, |u| \frac{\partial c}{\partial x}\right) + \frac{\partial}{\partial y}\left(\alpha_T \, |u| \frac{\partial c}{\partial y}\right) - \frac{\partial}{\partial x}(uc) = \frac{\partial c}{\partial t}$$

$$\bar{\phi} = [1/(z_2 - z_1)] \int_{z_1}^{z_2} \phi \, \mathrm{d}z$$

$$\bar{c} = [1/\bar{\phi}(z_2 - z_1)] \int_{z_1}^{z_2} \phi c \, \mathrm{d}z$$

where α_L, α_T and u are the longitudinal intrinsic dispersion coefficient, the lateral intrinsic dispersion coefficient and the velocity in each layer, respectively; ϕ and $\bar{\phi}$ are the porosity in a layer and the mean porosity, c and $\bar{c}$ are the concentration in a layer and the mean concentration; z measures the thickness of the aquifer.

The discretization of the dispersion equation is identical to the discretization of the bidimensional monolayer model taking ρ and u as constant, and it is solved by ADIP for the same type of boundary conditions in each layer. Then $\bar{c}$ is directly computed by averaging the concentrations in each layer at given x and y along z. A more complex form of this multi-layer model is under study at the time of publication of this book; the problem is the same, but the pollution may transfer vertically from one layer to another and point sources are added to the dispersion equations in the meshes receiving that vertical pollution. The infiltration rate has to be first estimated.

5.2. CURVILINEAR COORDINATE MODELS

5.2.1. Curvilinear coordinates: some definitions

Let $Oxyz$ be the usual rectangular coordinate system of R^3. Suppose that the coordinates x, y, z of a point P can be expressed in terms of some variables x^1, x^2, x^3 and conversely that x^1, x^2, x^3 can be expressed in terms of x, y, z; assume further that the functions $x(x^1, x^2, x^3)$, $y(x^1, x^2, x^3)$, $z(x^1, x^2, x^3)$, $x^1(x, y, z)$, $x^2(x, y, z)$ $x^3(x, y, z)$ are single-valued and continuously differentiable. The correspondance between the set (x, y, z) and the set (x^1, x^2, x^3) is then unique. The system (x^1, x^2, x^3) is called the curvilinear coordinate system of P.

In groundwater-pollution modelling, three curvilinear coordinate systems are used:

(1) the cylindrical system (Fig. 5.2.1a) defined by the equations:

$$x = r\cos\theta \qquad x^1 = r, \quad x^2 = \theta, \quad x^3 = z$$

$$y = r\cos\theta$$

$$z = z$$

(2) the spherical system (Fig. 5.2.1b) defined by the equations:

$$x = r\sin\psi\cos\theta \quad x^1 = r, \quad x^2 = \psi, \quad x^3 = \theta$$

$$y = r\sin\psi\sin\theta$$

$$z = r\cos\psi$$

(3) the equipotential-streamline system or $\phi - \psi$ system (Fig. 5.2.1c) where $x^1 = \phi(x, y)$ and $x^2 = \psi(x, y)$.

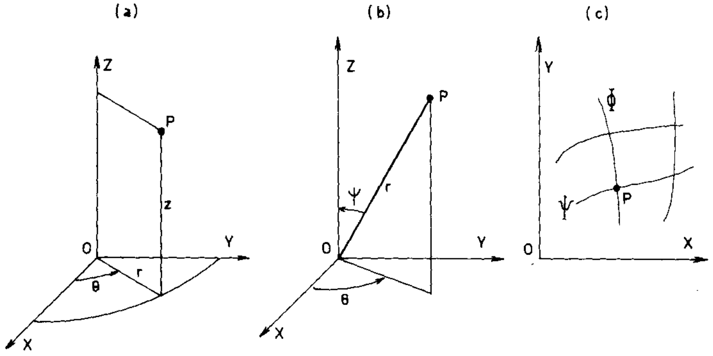

Fig. 5.2.1. Classical curvilinear coordinate systems used in groundwater pollution. (a) Cylindrical system (b) Spherical system (c) Equipotential-streamline system.

The line element ds in the curvilinear coordinate system (x^1, x^2, x^3) is defined by:

$$ds^2 = g_{ij}\, dx^i\, dx^j$$

using Einstein's summation convention ($g_{ij} dx^i dx^j = g_{11} dx^1 dx^1 + g_{12} dx^1 dx^2 + \ldots$). g_{ij} is a twice-covariant tensor (Spiegel, 1959) called the metric tensor.

In the usual rectangular system g_{ij} is defined by:

$$g_{ij} = 1 \text{ if } i = j, \quad g_{ij} = 0 \text{ if } i \neq j \quad \text{and} \quad ds^2 = dx^2 + dy^2 + dz^2$$

The twice-contravariant tensor (g^{ij}), defined by:

$$g^{ij} g_{ik} = 1 \text{ if } j = k \quad \text{and} \quad g^{ij} g_{ik} = 0 \text{ if } k \neq j$$

using the summation convention, is called the conjugate tensor of the metric tensor. Associating a square matrix (g_{ij}) to the metric tensor, we associate the inverse matrix of (g_{ij}) to the conjugate tensor. The determinant of the matrix (g^{ij}) is written as g.

These two tensors are used to shift from contravariant to covariant coordinates and conversely and they appear in the curvilinear form of the partial differential equations:
the divergence of vector $V = (v^i)$, $i = 1, 2, 3$ being given by the relationship

$$\text{div}\, V = g^{-1/2} \frac{\partial}{\partial x^i} (g^{1/2} v^i)$$

the general equation of dispersion in an orthogonal curvilinear system (i.e. a curvilinear system where $g_{ij} = 0$ if $i \neq j$) is written:

$$g^{-1/2} \frac{\partial}{\partial x^k} \left(g^{1/2} g^{kp} K^i_p \rho \frac{\partial C^*}{\partial x^i} \right) - g^{-1/2} \frac{\partial}{\partial x^k} \left(g^{1/2} \frac{U^k C}{g^{1/2}_{kk}} \right) = \frac{\partial C}{\partial t} \qquad [5.2.1]$$

where K^i_p is the component (i, p) of the dispersion tensor, U^k is the physical component k of the velocity and $C^* = c/\rho$.

The physical components of a vector are the projections of the vector on the tangent to the coordinate curves. If Vx, Vy, Vz are the components of the vector in the usual rectangular system and V^1, V^2, V^3 its components in the curvilinear system, the following relationship holds:

$$V^1 = g^{1/2}_{11}\, Vx; \quad V^2 = g^{1/2}_{22}\, Vy; \quad V^3 = g^{1/2}_{33}\, Vz$$

The metric tensor, its conjugate, the determinant g and [5.2.1] are expressed in the three usual curvilinear coordinate systems here after Lichnerowicz (1955) and Bachmat and Bear (1964).

(1) The cylindrical system:

$$(g_{pq}) = \begin{bmatrix} 1 & 0 & 0 \\ 0 & r^2 & 0 \\ 0 & 0 & 1 \end{bmatrix}, \qquad (g^{pq}) = \begin{bmatrix} 1 & 0 & 0 \\ 0 & 1/r^2 & 0 \\ 0 & 0 & 1 \end{bmatrix}$$

$$g = r^2$$

$$\frac{1}{r} \frac{\partial}{\partial r} \left[r K^1_1 \rho \frac{\partial (c/\rho)}{\partial r} \right] + \frac{1}{r^2} \frac{\partial}{\partial \theta} \left[K^2_2 \rho \frac{\partial (c/\rho)}{\partial \theta} \right] + \frac{\partial}{\partial z} \left[K^3_3 \rho \frac{\partial (c/\rho)}{\partial z} \right]$$
$$- \frac{1}{r} \frac{\partial}{\partial r} (r U^1 c) - \frac{1}{2} \frac{\partial}{\partial \theta} (U^2 c) - \frac{\partial}{\partial z} (U^3 c) = \frac{\partial c}{\partial t} \qquad [5.2.2]$$

(2) The spherical system:

$$(g_{pq}) = \begin{bmatrix} 1 & 0 & 0 \\ 0 & r^2 & 0 \\ 0 & 0 & r^2 \sin^2 \psi \end{bmatrix}, \qquad (g^{pq}) = \begin{bmatrix} 1 & 0 & 0 \\ 0 & 1/r^2 & 0 \\ 0 & 0 & 1/(r^2 \sin^2 \psi) \end{bmatrix}$$

$$g = r^4 \sin^2 \psi$$

$$\frac{1}{r^2}\frac{\partial}{\partial r}\left[r^2 K_1^1 \rho \frac{\partial}{\partial r}(c/\rho)\right] + \frac{1}{r^2 \sin\psi}\frac{\partial}{\partial \psi}\left[\sin\psi\, K_2^2 \rho \frac{\partial}{\partial \psi}(c/\rho)\right]$$
$$+ \frac{1}{r^2 \sin^2\psi}\frac{\partial}{\partial \theta}\left[K_3^3 \rho \frac{\partial}{\partial \theta}(c/\rho)\right] - \frac{1}{r^2}\frac{\partial}{\partial r}(r^2 U^1 c) - \frac{1}{r \sin\psi}\frac{\partial}{\partial \psi}(\sin\psi\, U^2 c)$$
$$- \frac{1}{r \sin\psi}\frac{\partial}{\partial \theta}(U^3 c) = \frac{\partial c}{\partial t} \qquad [5.2.3]$$

(3) The $\phi - \psi$ system (two-dimensional):

$$(g_{pq}) = \begin{bmatrix} [(\partial\Phi/\partial x)^2 + (\partial\Phi/\partial y)^2]^{-1} & 0 \\ 0 & [(\partial\Psi/\partial x)^2 + (\partial\Psi/\partial y)^2]^{-1} \end{bmatrix}$$

$$(g^{pq}) = \begin{bmatrix} (\partial\Phi/\partial x)^2 + (\partial\Phi/\partial y)^2 & 0 \\ 0 & (\partial\Psi/\partial x)^2 + (\partial\Psi/\partial y)^2 \end{bmatrix}$$

The pore velocity is given by:

$$U = -\operatorname{grad}\Phi$$

and ϕ and ψ are related by the Cauchy conditions:

$$\partial\Phi/\partial x = \partial\Psi/\partial y, \qquad \partial\Phi/\partial y = -\partial\Psi/\partial x$$

The physical components of the velocity by definition are:

$$U' = U, \qquad U^2 = 0$$

and they verify the following relationships:

$$g^{1/2} = 1/U^2, \qquad g_{11} = g_{22} = 1/U^2$$

The dispersion equation [5.2.1] becomes:

$$U^2 \frac{\partial}{\partial\Phi}\left(\rho K_\Phi \frac{\partial C^*}{\partial\Phi}\right) + U^2 \frac{\partial}{\partial\Psi}\left(\rho K_\Psi \frac{\partial C^*}{\partial\Psi}\right) - U^2 \frac{\partial C}{\partial\Phi} = \frac{\partial C}{\partial t} \qquad [5.2.4]$$

with $C^* = c/\rho$.

5.2.2. Single-well model

The aquifer is confined and stratified horizontally. The strata are homogeneous and independent. The dispersion regime is pure dynamic dispersion, and the dispersion coefficient is proportional to the mixture velocity. It is the tracer case, where the mixture density is constant. The model is used for the determination of local dispersion coefficients by a radioactive tracer injected and pumped in one well, the radioactivity being recorded in the well; near the well, the natural velocity of the aquifer can be neglected compared to the velocity imposed by injecting and pumping the tracer. Flow and dispersion are assumed to be axisymmetrical (§ 4.2.1). The mathematical problem is defined by the system of equations:

$$\begin{aligned} \frac{1}{r}\frac{\partial}{\partial r}\left(r\alpha|u|\frac{\partial c}{\partial r}\right) - \frac{1}{r}\frac{\partial}{\partial r}(ruc) &= \frac{\partial c}{\partial t} \\ \frac{1}{r}\frac{\partial h}{\partial r} + \frac{\partial^2 h}{\partial r^2} &= \frac{S}{T}\frac{\partial h}{\partial t} \qquad [5.2.5] \\ u &= -\frac{k\rho g}{\phi\mu}\frac{\partial h}{\partial r} \end{aligned}$$

where c is the tracer concentration, h the piezometric head, k the permeability coefficient, r the distance from the well, u the pore velocity of the mixture, S the storage coefficient, T the transmissivity, ϕ, ρ, μ, the porosity of the soil, the density and the viscosity of the mixture respectively.

The initial and boundary conditions are:

(1) during injection:

$c(r_0, t) = 1$ during the tracer-injection period

$c(r_0, t) = 0$ during the injection of fresh water used to push the tracer

$c(\infty, t) = 0$

where r_0 is the well radius, the origin being chosen as the center of the well.

Injection is usually performed at a constant head h_0 at the well:

$$h(r_0, t) = h_0$$
$$h(\infty, t) = 0$$

The initial conditions correspond to a step-input function:

$$c(r, 0) = 0$$
$$h(r, 0) = 0$$

(2) during pumping back:

$$\frac{\partial c}{\partial r}(r_0, t) = 0$$

$$C(\infty, t) = 0$$

The zero-flux condition at the well corresponds to the instantaneous homogenization of the tracer in the well. It means that the concentration in the well is equal to the concentration near the well. The concentration variation due to dispersion can be neglected on a space-step. The complete boundary condition would be:

$$Uc - K\frac{\partial c}{\partial r} = Uc_W$$

where c_W denotes the concentration in the well. Here we have:

$$c_W = c(r_0, t)$$

Pumping is usually performed at a constant head h'_0:

$$h(r_0, t) = -h'_0$$

$$h(\infty, t) = 0$$

The initial conditions are the conditions prevailing in the aquifer at the end of the injection period:

$$c(r, t_1) = c_1(r, t_1)$$

where t_1 is the time at the end of injection and $c_1(r, t_1)$ the solution of the system with the injection initial and boundary conditions at time t_1:

$$h(r, t_1) = 0$$

assuming that the aquifer comes back to its natural equilibrium state between the end of the injection and the beginning of the pumping.

This system is discretized according to a totally implicit finite-difference scheme; the convection term of the dispersion equation (first-order spatial derivative) is discretized as a backward difference in the velocity direction. The linear systems are solved by the direct Gauss elimination method for tridiagonal matrices (§ 9.3.2).

Here is a possible form of the discretized equations with space-varying space increments d$r(i)$ and time-varying time steps d$t(n)$.

(1) Injection period:

$$\frac{r(i)|u(i)|+r(i+1)|u(i+1)|}{2}\left[\frac{c(i+1)-c(i)}{\mathrm{d}r(i+1)}\right]$$

$$-\frac{\alpha}{r(i)}\frac{\frac{r(i)|u(i)|+r(i-1)|u(i-1)|}{2}\left[\frac{c(i)-c(i-1)}{\mathrm{d}r(i)}\right]}{\frac{\mathrm{d}r(i+1)+\mathrm{d}r(i)}{2}}$$

$$-\frac{1}{r(i)}\frac{r(i)u(i)c(i)-r(i-1)u(i-1)c(i-1)}{\mathrm{d}r(i)}=\frac{c(i)-c^{-}(i)}{\mathrm{d}t(n)}$$

(2) Pumping back period:

$$[r(i)|u(i)|+r(i+1)|u(i+1)|]\frac{c(i+1)-c(i)}{\mathrm{d}r(i+1)}$$

$$-\frac{\alpha}{r(i)}\frac{[r(i)|u(i)|+r(i-1)|u(i-1)|]\frac{c(i)-c(i-1)}{\mathrm{d}r(i)}}{\frac{\mathrm{d}r(i+1)+\mathrm{d}r(i)}{2}}$$

$$-\frac{1}{r(i)}\frac{r(i+1)u(i+1)c(i+1)-r(i)u(i)c(i)}{\mathrm{d}r(i+1)}=\frac{c(i)-c^{-}(i)}{\mathrm{d}t(n)}$$

where n is the number of the time step, $c(i)$ and $c^{-}(i)$ are the concentrations at point i at times n and $n-1$, respectively.

If the pumping or the injection are permanent, the corresponding model is obtained by setting $r(i)u(i)=A$, where A is a constant determined by the pumping and the injection conditions.

During injection and pumping, the movement and velocity equations are written:

$$\frac{1}{r(i)}\frac{h(i)-h(i-1)}{\mathrm{d}r(i)}+\frac{\frac{h(i+1)-h(i)}{\mathrm{d}r(i+1)}-\frac{h(i)-h(i-1)}{\mathrm{d}r(i)}}{\frac{\mathrm{d}r(i)+\mathrm{d}r(i+1)}{2}}=\frac{S}{T}\frac{h(i)-h^{-}(i)}{\mathrm{d}t(n)}$$

$$u(i)=-\frac{k(i)\rho g}{\phi\mu}\frac{h(i)-h(i-1)}{\mathrm{d}r(i)}$$

where $h(i)$ and $h^{-}(i)$ are the heads at point i at times n and $n-1$. At each time step, the movement equation is solved, the space-velocity distribution is determined, the velocity values are put in the dispersion equation which is then solved. The movement equation does not depend on the dispersion equation (Fig. 5.2.2).

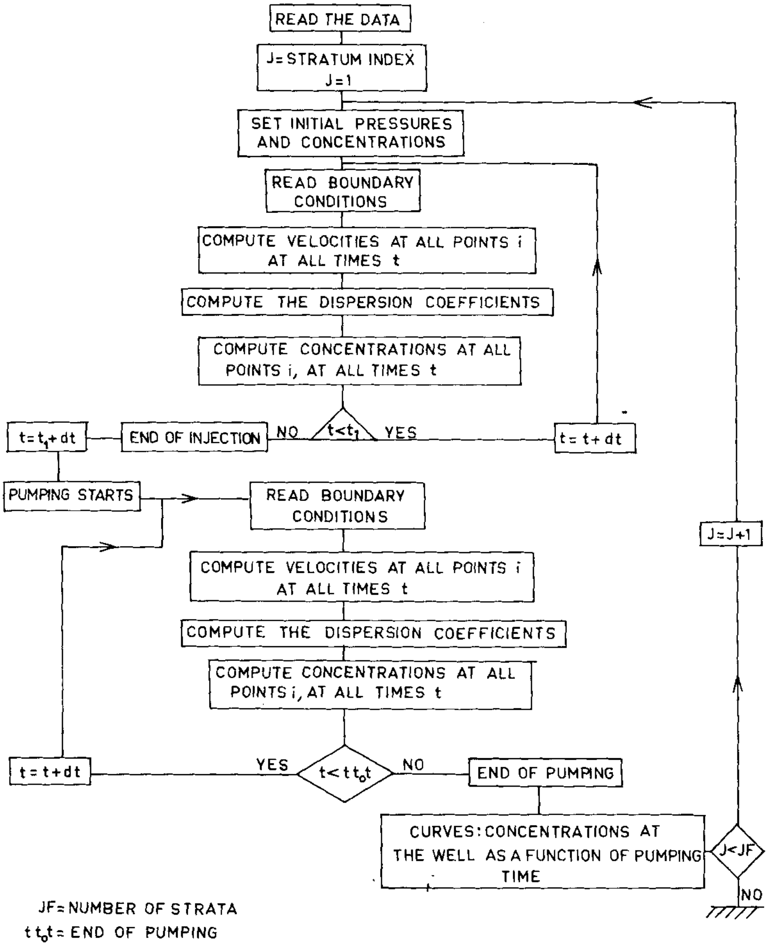

Fig. 5.2.2. Single-well pulse model: computation flow chart.

Fig. 5.2.3 shows the concentration curve obtained at the well during pumping for a permanent pumping rate; ru = constant.

5.2.3. *Multiple-well model*

The aquifer is homogeneous and confined. The dispersion regime is pure dynamic dispersion and the dispersion coefficient is proportional to the mixture velocity. The mixture velocity is composed of the natural aquifer velocity and the velocity imposed by the injection of the tracer in the well. The density of the mixture is constant (tracer case). Transverse dispersion is neglected.

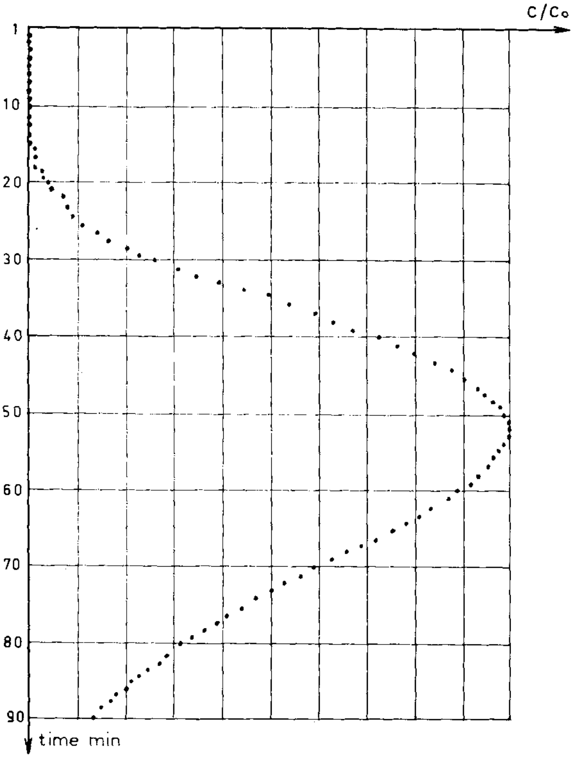

Fig. 5.2.3. Computed concentration curve vs time at the well, at a given depth. Permanent pumping rate.

The dispersion matrix is diagonalized in the system of curvilinear coordinates defined by the streamlines and equipotential lines (Fig. 5.2.3). The injection rate is constant, which implies that the water flow is steady. The mathematical problem is then defined by the system of equations:

$$u^2 \frac{\partial}{\partial \phi}\left(\alpha |u| \frac{\partial c}{\partial \phi}\right) - u^2 \frac{\partial c}{\partial \phi} = \frac{\partial c}{\partial t}$$

$$\frac{1}{r}\frac{\partial h}{\partial r} + \frac{\partial^2 h}{\partial r^2} = \frac{S}{T}\frac{\partial h}{\partial t} \qquad [5.2.6]$$

$$u_1 = -\frac{k\rho g}{\phi \mu}\frac{\partial h}{\partial r}$$

$$u = u_N + u_1$$

where u_1 is the injection velocity, and u_N the natural aquifer velocity. The initial and boundary conditions are:

c at the well $= 1$, $\quad$ c at time $0 = 0$

c at infinity $= 0$, $\quad$ h at time $0 = 0$

$h(r_0, t) = h_0$

$h(\infty, t) = 0$

here r_0 is the well radius.

Relationships between u, ϕ, and ψ have to be added:

$$u = \frac{\mathrm{d}\phi}{\mathrm{d}s} = \frac{\mathrm{d}\psi}{\mathrm{d}n} \qquad [5.2.7]$$

where ds and dn are the elements of curvilinear abscissa along the streamline and equipotential line. Usually ds = dn.

The system is discretized according to a totally implicit finite-difference scheme as in § 5.2.2. The resulting linear systems are solved by direct Gauss elimination methods for tridiagonal matrices. The movement equations are discretized as in § 5.2.2 and a possible discretization of the dispersion equation is:

$$\alpha u^2(i)\,\frac{\dfrac{|u(i)|+|u(i+1)|}{2}[c(i+1)-c(i)] - \dfrac{|u(i)|+|u(i-1)|}{2}[c(i)-c(i-1)]}{\mathrm{d}\phi^2}$$

$$-u^2(i)\,\frac{c(i)-c(i-1)}{\mathrm{d}\phi} = \frac{c(i)-c^-(i)}{\mathrm{d}t}$$

The increment dϕ is chosen as constant and small enough to reduce numerical diffusion errors. The computations are performed on the x-axis which is a streamline and is discretized by [5.2.7]. The concentration values are then extended in the x-y field along the equipotential lines.

Shamir and Harleman (1967b) discuss other various numerical schemes in $\phi - \psi$ coordinates, especially the general $\phi - \psi$ dispersion equation [5.2.4], where transverse dispersion is not neglected: discretization is analogous to the one adopted in §9.4.4 and the resolution method is the Alternate Direction Implicit Procedure (§ 9.4.4).

5.3. ANALYTICAL MODELS

Analytical solutions of the dispersion equation exist only in very few cases, extensively discussed by Bear (1972). If it is possible, an analytical solution is interesting because it does not introduce errors due to the numerical diffusion and errors due to the approximations by the finite-differences.

Various mathematical techniques can be applied to the finding of analytical solutions, such as Green functions, Laplace transforms or Fourier transforms. As an illustration, we give here two basic examples that can be used to derive pollution type-curves for mono- or bi-dimensional flow.

5.3.1. A monodimensional model

Assume longitudinal dispersion, at a constant velocity U in a semi-infinite medium, with a step initial function. The dispersion coefficient K is constant.

The mathematical problem is defined by the set of equations:

$$\begin{aligned} &K(\partial^2 C/\partial x^2) - U(\partial C/\partial x) = \partial C/\partial t \\ &C(x = 0, t > 0) = C_0, \qquad C(x = \infty, t \geqslant 0) = 0, \qquad [5.3.1] \\ &C(x \geqslant 0, t = 0) = 0 \end{aligned}$$

The problem is solved by Laplace transformation.

Note. Let f be a function of the variable x, defined for all x and equal to zero for $x < 0$. The Laplace transform of f is the function:

$$L(f) = \bar{f}(p) = \int_0^\infty e^{-px} f(x)\,\mathrm{d}x \qquad [5.3.2]$$

provided that this integral exists. p is a complex number, equal to $\eta + i\xi$. If η is zero, $\bar{f}(p)$ is the Fourier transform of f.

The properties of the Laplace transform used here are the following:

$$\begin{aligned} L(f') &= p\bar{f}(p) - f(0) \\ L(f'') &= p^2\bar{f}(p) - pf(0) - f'(0) \end{aligned}$$

easily proved by applying [5.3.2] to the functions $f'(x)$ and $f''(x)$. Setting $\bar{c}(x,p) = \int_0^\infty e^{-pt}c(x,t)\mathrm{d}t$, [5.3.1] yields:

$$\begin{aligned} &K(\mathrm{d}^2\bar{c}/\mathrm{d}x^2) - U(\mathrm{d}\bar{c}/\mathrm{d}x) = p\bar{c} \\ &\bar{c}(x=0) = c_0/p \qquad \bar{c}(x=\infty) = 0 \end{aligned} \qquad [5.3.3]$$

and [5.3.3] has the solution:

$$\begin{aligned} C &= \frac{C_0}{p}\exp\left[\frac{U-(U^2+4pK)^{1/2}}{2K}x\right] \\ &= C_0\exp\left(\frac{Ux}{2K}\right)\cdot\frac{1}{p}\exp\left[\frac{-x}{K^{1/2}}\left(\frac{U^2}{4K}+p\right)^{1/2}\right] \end{aligned}$$

From a table of Laplace transforms, we obtain:

$$C = \frac{C_0}{2}\operatorname{erfc}\left[\frac{x-Ut}{2(Kt)^{1/2}}\right] + \frac{C_0}{2}\exp\left(\frac{Ux}{K}\right)\operatorname{erfc}\left[\frac{x+Ut}{2(Kt)^{1/2}}\right] \qquad [5.3.4]$$

Fig. 5.3.1 provides the solution of this equation as type-curves.

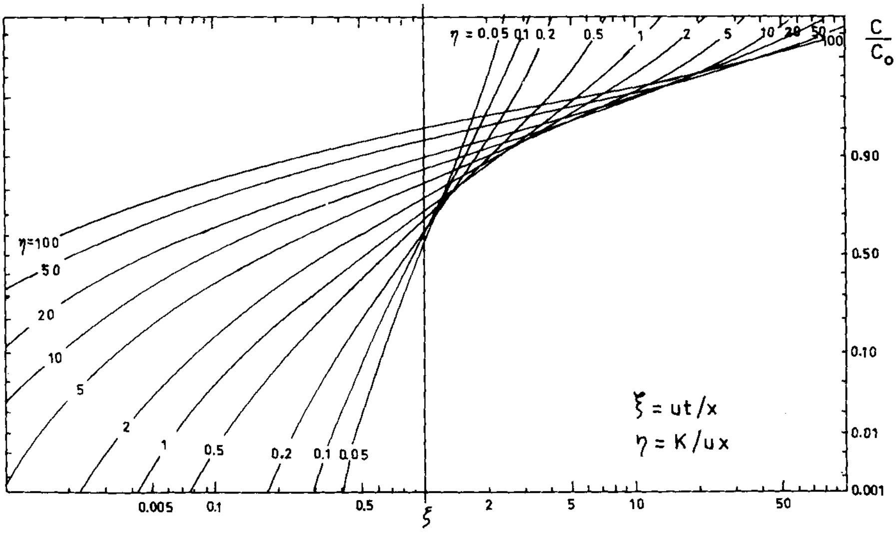

Fig. 5.3.1. Type-curves for monodimensional dispersion; constant velocity (Ogata and Banks, 1961).

5.3.2. *A bidimensional horizontal model*

The aquifer is horizontal, monolayered and homogeneous. The water velocity u is constant and parallel to $0x$. The dispersion coefficients are constant, proportional to the velocity (dynamic dispersion regime). At the origin, pollution is injected at concentration C_0 and at the rate Q; during period $\mathrm{d}t$, the mass of the injected pollution is $C_0 Q \mathrm{d}t$. The initial concentration is zero. The domain is infinite and the concentrations are equal to zero at infinity. The mathematical model is the equation:

$$\alpha_L u \frac{\partial^2 c}{\partial x^2} + \alpha_T u \frac{\partial^2 c}{\partial y^2} - u \frac{\partial c}{\partial x} = \frac{\partial c}{\partial t}$$

The Green function, i.e. the solution of this equation for the injection of a unit amount of pollution at the origin, instantaneously at $t = 0$ is:

$$G(x, y, t) = \frac{1}{4\pi u t(\alpha_L \alpha_T)^{1/2}} \exp\left[-\frac{(x-ut)^2}{4\alpha_L u t} - \frac{y^2}{4\alpha_T u t}\right]$$

and the solution of the problem is then:

$$C(x, y, t) = \frac{C_0 Q \mathrm{d}t}{4\pi u t(\alpha_L \alpha_T)^{1/2}} \exp\left[-\frac{(x-ut)^2}{4\alpha_L u t} - \frac{y^2}{4\alpha_T u t}\right]$$

For a continuous injection at rate Q, the solution at time t is:

$$C(x, y, t) = \frac{C_0 Q}{4\pi u(\alpha_L \alpha_T)^{1/2}} \int_0^t \exp\left[-\frac{(x-u\theta)^2}{4\alpha_L u\theta} - \frac{y^2}{4\alpha_T U\theta}\right] \frac{\mathrm{d}\theta}{\theta} \qquad [5.3.5]$$

The steady-state regime is obtained for $t = \infty$:

$$C(x, y) = \frac{C_0 Q}{2\pi u(\alpha_L \alpha_T)^{1/2}} \exp\,(x/2\alpha_L)\, K_0 \left(\frac{x^2}{4\alpha_L^2} + \frac{y^2}{4\alpha_L \alpha_T}\right) \qquad [5.3.6]$$

where K_0 is the modified Bessel function of the second kind and zero order. It should be noticed that on the x-axis ($y = 0$) when α_T tends to zero the concentration tends to infinity, which has no physical meaning: one should revert to the monodimensional case. If the velocity u increases, the concentration decreases everywhere: pollution is quickly washed out. If Q and u are constant, c tends to 0 when α_L tends to infinity: when dispersion increases, the concentration at a point decreases.

An interesting computation of [5.3.5] is due to Emsellem (see Arlab, 1974) and leads to practical type-curves by the introduction of the tabulated Hantush function $W(u, b)$:

$$W(u, b) = \int_u^\infty \exp(-y - b^2/4y) \frac{\mathrm{d}y}{y}$$

Equation [5.3.5] can be written:

$$C(x, y, t) = \frac{C_0 Q}{4\pi u(\alpha_L \alpha_T)^{1/2}} \exp(x/2\alpha_L) \int_0^t \exp\left[-\frac{u\theta}{4\alpha_L} - \left(\frac{x^2}{4\alpha_L u} + \frac{y^2}{4\alpha_T u}\right)\frac{1}{\theta}\right]\frac{\mathrm{d}\theta}{\theta}$$

setting $y = u\theta/4\alpha_L$ we have:

$$C(x, y, t) = \frac{C_0 Q}{4\pi u(\alpha_L \alpha_T)^{1/2}} \exp(x/2\alpha_L) \int_0^t \exp(-y - b^2/4y) \frac{\mathrm{d}y}{y}$$

with $b^2 = \dfrac{x^2}{4\alpha_L^2} + \dfrac{y^2}{4\alpha_L \alpha_T}$

and eventually:

$$C(x, y, t) = \frac{C_0 Q}{4\pi u(\alpha_L \alpha_T)^{1/2}} \exp(x/2\alpha_L) \left[W(0, b) - W(t, b)\right] \qquad [5.3.7]$$

The values of $W(t, b)$ can be found in Hantush tables (Walton, 1962), for instance. Fig. 5.3.2 provides the necessary values for most simple pollution problems, from [5.3.7].

5.4. A BLACK-BOX MODEL

As developed in Chapter 7, it is sometimes interesting to treat a pollution problem by a black-box method: the aquifer is equivalent to a black box where pollution comes in and flows out; the mechanisms inside the box are unknown and only the global effects of the box are analyzed, by studying the pollution inputs and outputs. The method will be used essentially for large-scale studies, when the influences of the aquifer on the pollution are complex but can be integrated in one representation: for instance, the physico-chemical phenomena of the non-saturated zone will not be detailed and only their results will be analyzed, if the pollution output of the watershed is to be determined. The basic principle of this method is to consider pollution as a signal $e(t)$ (or as some composition of unit signals) which is transformed into $s(t)$ by the aquifer acting as an operator A which is symbolically represented by $s = A \cdot e$, while t is the time.

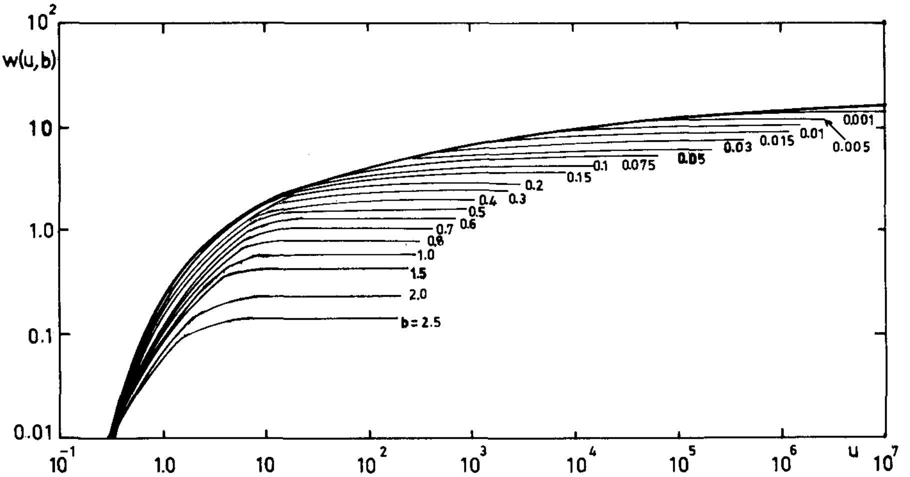

Fig. 5.3.2. Type-curves $W(u, b)$ vs u for various b (Walton, 1962).

The following assumptions are usually made:

(1) The transformation $e \rightarrow s$ exists, i.e., there is an operator A such that $s = A \cdot e$.

(2) s is a linear function of e, i.e., A is linear. So, if s corresponds to e, then λs corresponds to λe; and if s_1 corresponds to e_1 and s_2 to e_2, then $s_1 + s_2$ corresponds to $e_1 + e_2$.

(3) Any translation in time at the entrance e implies the same translation in time at the exit s (i.e., the transformation $e \rightarrow s$ commutes with translations in time).

(4) The transformation A is continuous, i.e., if the sequence $e_n(t)$ tends to 0, when n tends to infinity, then the sequence $s_n(t) = Ae_n(t)$ tends to 0.

Then it can be proved (Hörmander, 1969) that the transformation is a convolution written:

$$s = A * e$$

The pollution model is the operator A which is called "impulse-response", or "unit-response" or transfer function, of the aquifer for pollution and the problem consists in computing this unit response. Once A is known, the model can be used in two ways: either e is known and s is computed (this is a convolution) or s is known and e is computed (this is a deconvolution).

For example, consider a watershed with an aquifer and some rivers. The water of the streams is used for drinking purposes. Factories pile up their wastes which contaminate the aquifer by infiltration due to rains; the pollution input from these wastes is $e(t)$ and authorities need to forecast the output $s(t)$ from the aquifer into the rivers to establish safety rules concerning the factories (for instance, a timing of pollution piling or burning). If they know A, which characterizes the aquifer they can compute $s(t)$ for a given $e(t)$ by the convolution $A \times e$.

Now, if they want to respect pollution sanitary thresholds (which impose the function s) and determine the possible input e, they do a deconvolution on e and s. Of course preliminary deconvolution experiments with known s and e will be performed to determine A.

Although convolution is rather simple to perform numerically, it has been shown that deconvolution is an unstable numerical operation and special numerical methods have to be used. After a review of some classical numerical methods, we present a numerical method based on Emsellem's algorithm (Emsellem et al., 1971) and developed by Poitrinal (Emsellem, et al., 1971) which is stable and already in use rather extensively.

In what follows, we assume that the operator A is an integrable function and that the convolution equation is written:

$$s(t) = \int_{-\infty}^{+\infty} A(t-\tau)\, e(\tau)\, \mathrm{d}\tau$$

A further good assumption is that A and e are zero for negative times which yields the convolution equation:

$$s(t) = \int_{0}^{t} A(t-\tau)\, e(\tau)\, \mathrm{d}\tau$$

5.4.1. Classical deconvolution methods

Fourier transform

The Fourier transform of a function of f is defined by:

$$F(f) = \hat{f}(\zeta) = \int_{-\infty}^{+\infty} \exp\,(-2i\pi x\zeta)\, f(x)\, \mathrm{d}x$$

for appropriate convergence conditions on f.

The Fourier transform of a convolution product $f \times g$ is the usual product $\hat{f} \cdot \hat{g}$ and an obvious deconvolution method is to Fourier-transform the convolution product, to divide it by the known function and apply the Fourier inverse transform to obtain the unknown function:

$$s = A * e \to \hat{s} = \hat{A} \cdot \hat{e} \to \hat{e} = \hat{s}/\hat{A} \to e = F^{-1}(\hat{s}/\hat{A})$$

Direct identification

The convolution equation is discretized according to a unit time-step: the input gives $e(0)$, $e(1), \ldots, e(n)$ and the unit response A gives $A(0)$, $A(1), \ldots, A(n)$. Each $e(p)$ is an impulse of amplitude $e(p)$ which yields a response $e(p)A(n-p)$.

The convolution equation then provides the linear system:

$$
\begin{aligned}
s(0) &= e(0)A(0) \\
s(1) &= e(0)A(1) + e(1)A(0) \qquad [5.4.1] \\
s(n) &= e(0)A(n) + e(1)A(n-1) + \ldots + e(p)A(n-p) + \ldots + e(n)A(0)
\end{aligned}
$$

The unknowns are $e(0)$, $e(n)$, and the system [5.4.1] is easily solved.

These methods are highly unstable when the data present some errors and do not exactly verify a convolution equation (Fig. 5.4.1). Classical remedies, such as smoothing of the Fourier transforms, do not totally improve these methods. Some other methods are now tried, such as analog deconvolution.

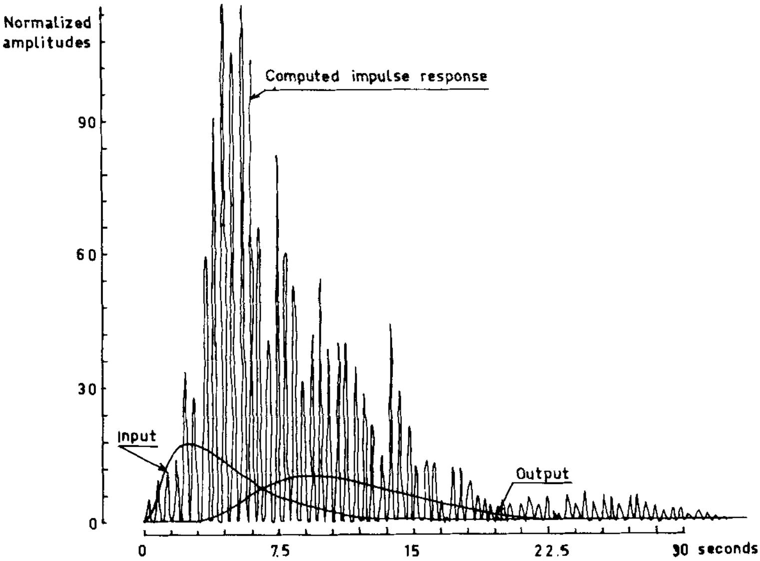

Fig. 5.4.1. Deconvolution by Fourier transform.

5.4.2. Emsellem's deconvolution method

The basic principle of this method is to derive the unit response by successive approximations, each new approximation being a correction with zero mean of the preceding approximation. These approximations are computed by projections on a special orthogonal vector basis, the best to limit the influence of experimental (measurement) errors. First, the time n when the unit response becomes zero again is computed by trials (Fig. 5.4.2).

First approximation

It is a constant function which, by convolution with the real input func-

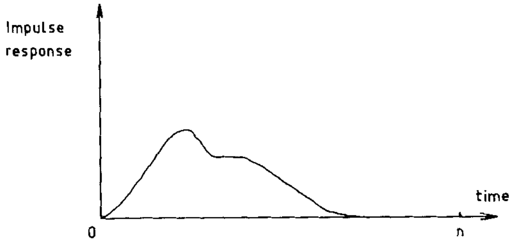

Fig. 5.4.2.

tion, gives an output on the whole measurement interval such that the difference between real output and computed output be minimum. This difference is usually minimized by a least-square method: consider a basis vector b_1 equal to 1 on $(0, n)$ (Fig. 5.4.3).

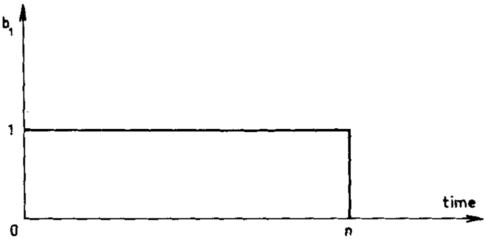

Fig. 5.4.3. Vector b_1.

The projection $A_1(i)$ of the unit response, verifies the equation:

$$A_1(i) = a_1 b_1(i)$$

and a_1 is the constant function to be determined to minimize the difference between known and computed output functions at all points j where the output is known.

$$\begin{aligned} s(j) - \sum_0^n e(j-i)\, A_1(i) &= s(j) - \sum_0^n e(j-i) a_1 b_1(i) \\ &= s(j) - a_1 \sum_0^n e(j-i)\, b_1(i) = E(j) \end{aligned}$$

The optimal a_1 is determined by:

$$\partial \left[\sum_j E^2(j) \right] / \partial a_1 = 0$$

$$a_1 = \left[\sum_j \left\{ s(j) \sum_{i=0}^n e(j-i)\; b_1(i) \right\} \right] \Bigg/ \sum_j \left\{ \sum_{i=0}^n e(j-i)\, b_1(i) \right\}^2$$

Second approximation

a is unknown, the interval $(0, n)$ is divided up into two intervals and a basis vector b_2 equal to 1 on $(0, 1/2)$ and -1 on $(n/2, n)$ is considered (Fig. 5.4.4).

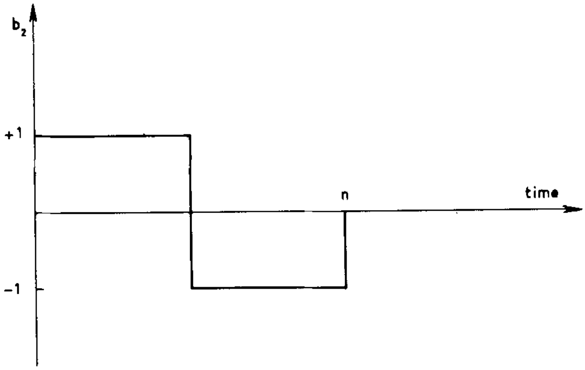

Fig. 5.4.4. Vector b_2.

The second approximation of A is A_2 defined by:

$$A_2(i) = a_1 b_1(i) + a_2 b_2(i)$$

$a_2 b_2(i)$ obviously is a correction with a zero mean of the first approximation and the aspect of A_2 is sketched on Fig. 5.4.5.

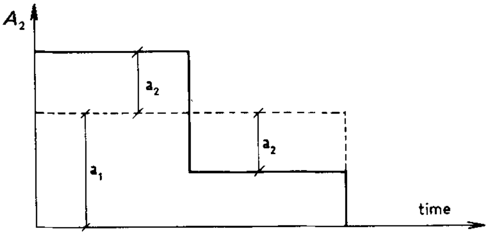

Fig. 5.4.5. Approximation A_2 with b_1 and b_2

a_2 is determined in the same fashion as a_1:

$$E(j) = s(j) - a_1 \sum_{i=0}^{n} e(j-i) b_1(i) - a_2 \sum_{i=0}^{n} e(j-i) b_2(i) \qquad \frac{\partial \sum_j E^2(j)}{\partial a_2} = 0$$

$$a_2 = \left[\sum_j \; s(j) - a_1 \sum_0^n e(j-i) b_1(i) \sum_0^n e(j-i) b_2(i) \right] \Bigg/ \sum_j \sum_0^n e(j-i) b_2(i)$$

Following approximations

They are obtained by dividing up $(0, n)$ into 3,4 ... intervals and defining the vectors b_3, b_4,... (Fig. 5.4.6).

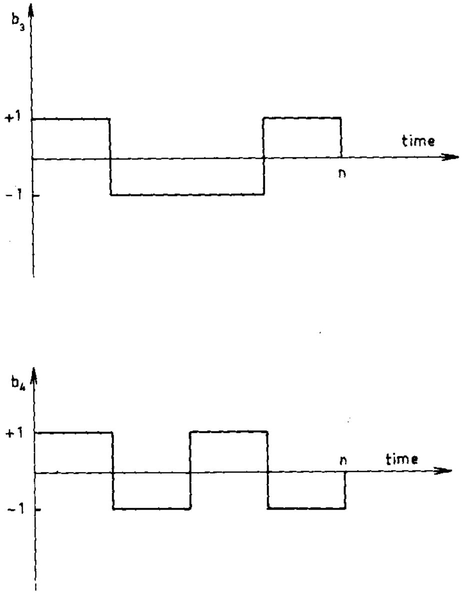

Fig. 5.4.6. Vectors b_3 and b_4.

The vectors are easily derived one from the other by an iteration process: b_3 and b_4 are derived from b_2 and b_1 by dividing up the support into four intervals and multiplying the respective values of b_2 and b_1 on each side of the new divisions by $+1, -1$; b_5 to b_8 are derived from b_4 to b_1 in the same way. These vectors are orthogonal. Of course, if $(0, n)$ is some power of 2, this will simplify the algorithm. a_3 and a_4 can be computed together from these equations:

$$A_{34}(i) = a_1 b_1(i) + a_2 b_2(i) + a_3 b_3(i) + a_4 b_4(i)$$

$$E(j) = s(j) - \sum_{i=0}^{n} e(j-i) A_{34}(i)$$

$$= s(j) - a_1 \sum_{i=0}^{n} e(j-i) b_1(i) - \dots - a_4 \sum_{i=0}^{n} e(j-i) b_4(i)$$

$$\frac{\partial \Sigma E^2(j)}{\partial a_3} = 0, \qquad \frac{\partial \Sigma E^2(j)}{\partial a_4} = 0$$

These computations are iterated to the other approximations.

A phase is the set of vectors of a given partition of the interval $(0, n)$ (for instance, phase 1 is b_1, phase 2 is (b_1, b_2), phase 3 is $(b_1 b_2 b_3 b_4)$ ....). For each phase, computations are iterated until a minimum value of the minima $\sum_j E^2(j)$ is reached: on phase 2, a_2 is computed, than a_1 is corrected by going back to phase 1, then a_2 is corrected and so on before computing a_3, a_4; when two following minima $\sum_j E^2(j)$ are almost equal, then it is time to compute the next phase, otherwise one has to go back to phase 1.

Emsellem's algorithm has the following properties:

(1) Each phase represents a finer partition of the unit response than the preceding phase: if the approximation is considered as accurate enough, the procedure can be stopped.

(2) Each vector brings a correction of zero mean to the preceding approximation.

(3) Each vector modifies the unit response on the whole interval $(0, n)$; during the convolution of the basis vector and the input function, the input errors, if not systematic, balance each other and generate lesser errors on the computed projection.

Fig. 5.4.7. Impulse-response computed by Emsellem's deconvolution method on the data of Fig. 5.4.1.

An example of this method has been given in § 4.2.1: the determination of a radioactive-probe transfer function.

Fig. 5.4.7 represents the unit response computed by Emsellem's method using the data of Fig. 5.4.1.

CHAPTER 6

CASE HISTORIES

We have chosen a series of case histories to illustrate the possible applications of the methodology. These case histories are distributed into three groups: (1) description and evolution of an existing pollution; protection against existing pollutions; (2) prediction of a potential pollution; protection against pollution hazards; and (3) seawater intrusion into a coastal aquifer.

6.1. DESCRIPTION AND EVOLUTION OF AN EXISTING CASE OF POLLUTION: POLLUTION OF THE RHINE AQUIFER BY MINING WASTES

The occurrence of a pollution by salt in the aquifer of southern Alsace (eastern France) has been known for a long time and it was detected by the increase in salt content at the pumping wells of the city of Colmar (Fig. 6.1.1).

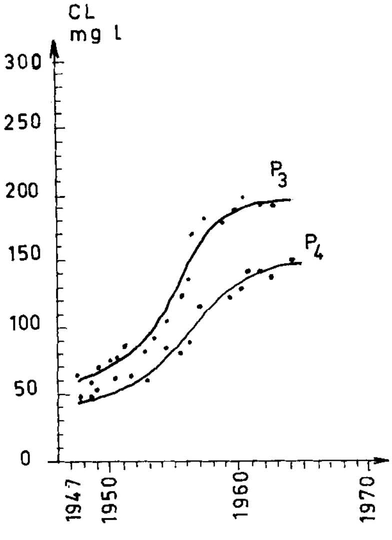

Fig. 6.1.1. Salt content in a pumping well at Colmar.

This pollution comes from residual salts in the extraction and treatment zones of potash mines, made up of sodium chlorides (85%) and clays (15%). For a very long time, these wastes have been dumped above the ground; rain, infiltrating through the dumps, carries solved NaCl into the groundwater.

Of course, to prevent such a pollution, the NaCl was progressively carried by pipeline to the Rhine and the dumps now only receive residues of residues with a very small percentage of salt. But, this policy has not really improved the situation: first the River Rhine is now heavily polluted, with consequent international implications; then these dumps were not destroyed and although they are not being renewed, they are so large (an average height of 20 m and an average base area of 100 × 100 m) that they pollute the aquifer as a continuous source of dissolved salt. Therefore, investigations of the pollution have been performed in order to

— characterize mechanisms of the contamination of ground and surface waters
— estimate the annual amounts of salt transferring into the surface hydrographic net coming from the mining district and the evolution of the salinity of groundwaters.

These investigations have displayed two types of pollution: (1) a light contamination, by well-diluted salt waters entering the aquifer by hydraulic exchanges between the streams and the aquifer; and (2) a heavy contamination by almost saturated salt waters, infiltrating the aquifer near the dumps with rain.

6.1.1. General description of the problem

The aquifer reservoir is made up of Quaternary alluvia, a mixture of sands, gravels and pebbles in variable proportions, with clay lenses on a marl substratum; it is very permeable, with a horizontal Darcy's coefficient of the order of 10^{-3} m/sec. It is 50—200 m thick. The mean annual pluviometry is 70 cm. The two types of pollution are located in two distinct zones: the light contamination is in a zone 1, where the studies are aimed at controlling the pollution charges conveyed by the streams, describing the mechanisms of the hydraulic exchanges between streams and aquifer and computing the increase of salinity of the groundwater due to the input from the streams. The heavy contamination is in a zone 2 where the studies are aimed at establishing the annual balance of infiltrated amounts in the aquifer, describing the mechanisms of the salt-water evolution quantitatively, both horizontally and vertically, downstream from the dumps and modelling the whole mining district for forecasting purposes.

The pollution cycle is described in Fig. 6.1.2.

6.1.2. The operations

The operations are described in a flow chart (Fig. 6.1.3) (Fried and Ungemach, 1973). The following commentaries help to understand the flow chart.

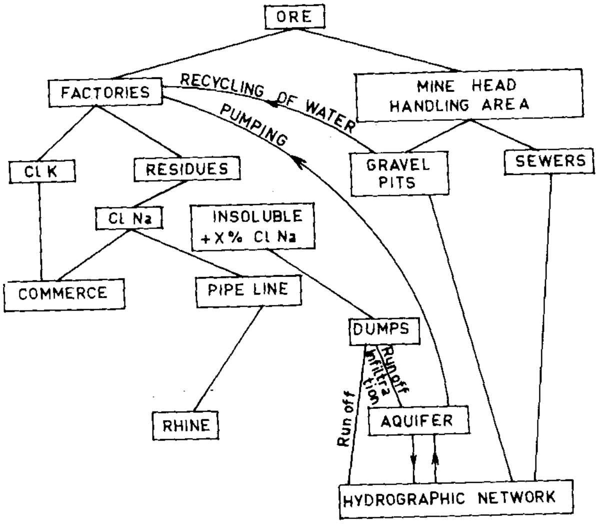

Fig. 6.1.2. Cycle of ore and pollution at the potash mines.

The detection of pollution by geophysical means

Electrical prospecting yields the geometry of the permeable reservoir. Its use is additionally justified, because on the one hand the resistivity of an aquifer formation is proportional to the resistivity of the water which it contains, and on the other hand the resistivity of the water is inversely proportional to its salt content; it follows that the real resistivity of a given formation (in our case, recent alluvia) will decrease when the dissolved salt content of its water increases. This phenomenon is quantified by the relationship:

$$\rho_c = \rho_w A/\phi$$

where ρ_c is the resistivity of the soil soaked with water, ρ_w the resistivity of the soaking water, A a coefficient depending upon the degree of consolidation of the soil and ϕ the effective porosity.

Thus sands with a porosity of 25%, soaked by water at resistivity 40 Ωm (at 18°C), equivalent NaCl pure and dry of 135 mg/l, will show a resistivity of 240 Ωm. As only a few conductive clay formations can be found in the alluvia, most of the conductive zones, displayed by the maps of apparent resistivities, correspond to the zones polluted by salt.

Figs. 6.1.4, 6.1.5 and 6.1.6 show the three types of results obtained from this geophysical campaign: a map of the substratum and resistivity distributions vertically and horizontally.

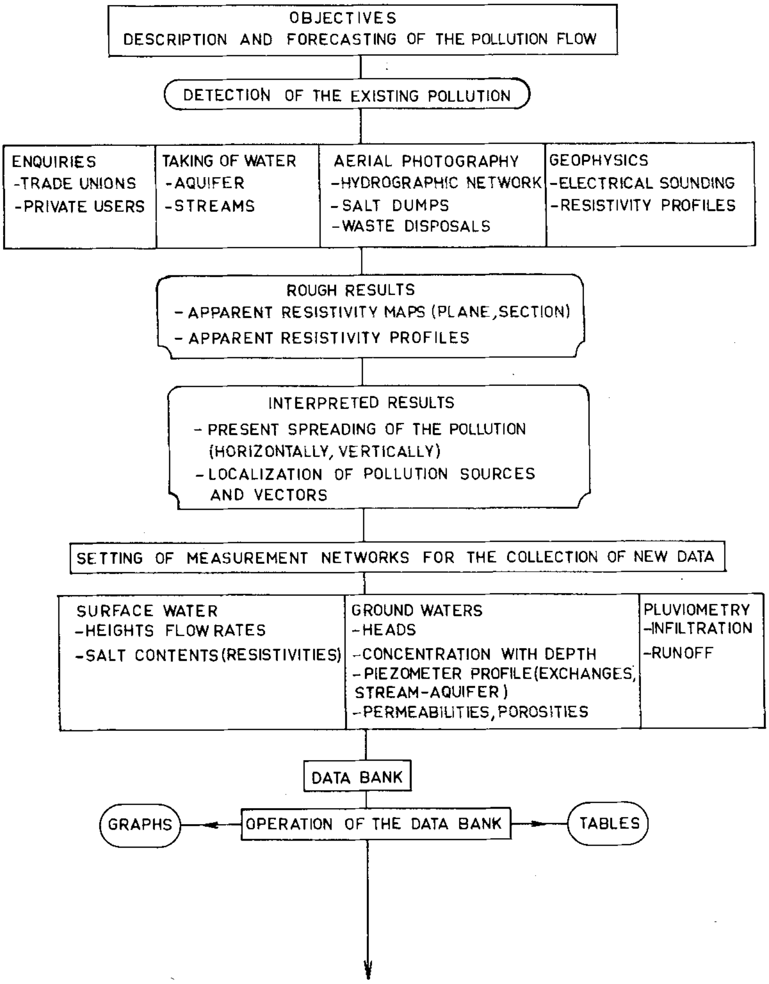
OBJECTIVES
DESCRIPTION AND FORECASTING OF THE POLLUTION FLOW
DETECTION OF THE EXISTING POLLUTION
ENQUIRIES
-TRADE UNIONS
-PRIVATE USERS
TAKING OF WATER
-AQUIFER
-STREAMS
AERIAL PHOTOGRAPHY
-HYDROGRAPHIC NETWORK
-SALT DUMPS
-WASTE DISPOSALS
GEOPHYSICS
-ELECTRICAL SOUNDING
-RESISTIVITY PROFILES
ROUGH RESULTS
- APPARENT RESISTIVITY MAPS (PLANE, SECTION)
- APPARENT RESISTIVITY PROFILES
INTERPRETED RESULTS
- PRESENT SPREADING OF THE POLLUTION (HORIZONTALLY, VERTICALLY)
- LOCALIZATION OF POLLUTION SOURCES AND VECTORS
SETTING OF MEASUREMENT NETWORKS FOR THE COLLECTION OF NEW DATA
SURFACE WATER
-HEIGHTS FLOW RATES
-SALT CONTENTS (RESISTIVITIES)
GROUND WATERS
-HEADS
-CONCENTRATION WITH DEPTH
-PIEZOMETER PROFILE (EXCHANGES, STREAM-AQUIFER)
-PERMEABILITIES, POROSITIES
PLUVIOMETRY
-INFILTRATION
-RUNOFF
DATA BANK
GRAPHS
OPERATION OF THE DATA BANK
TABLES

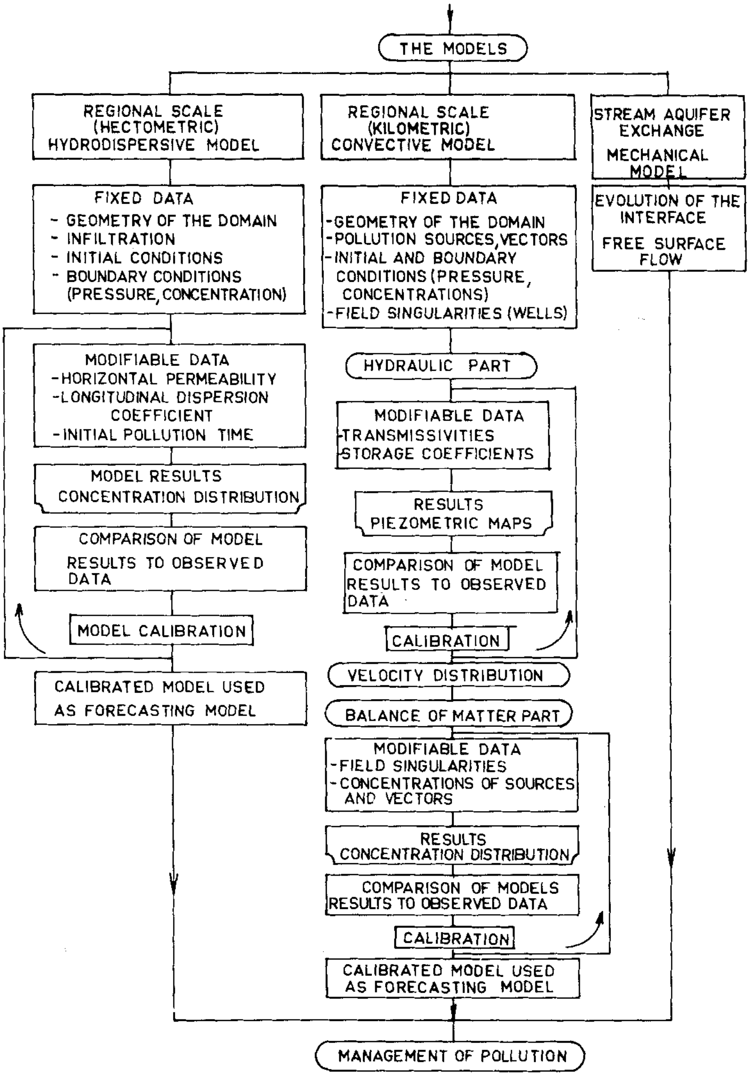

Fig. 6.1.3. Pollution by industrial wastes: operation flow chart.

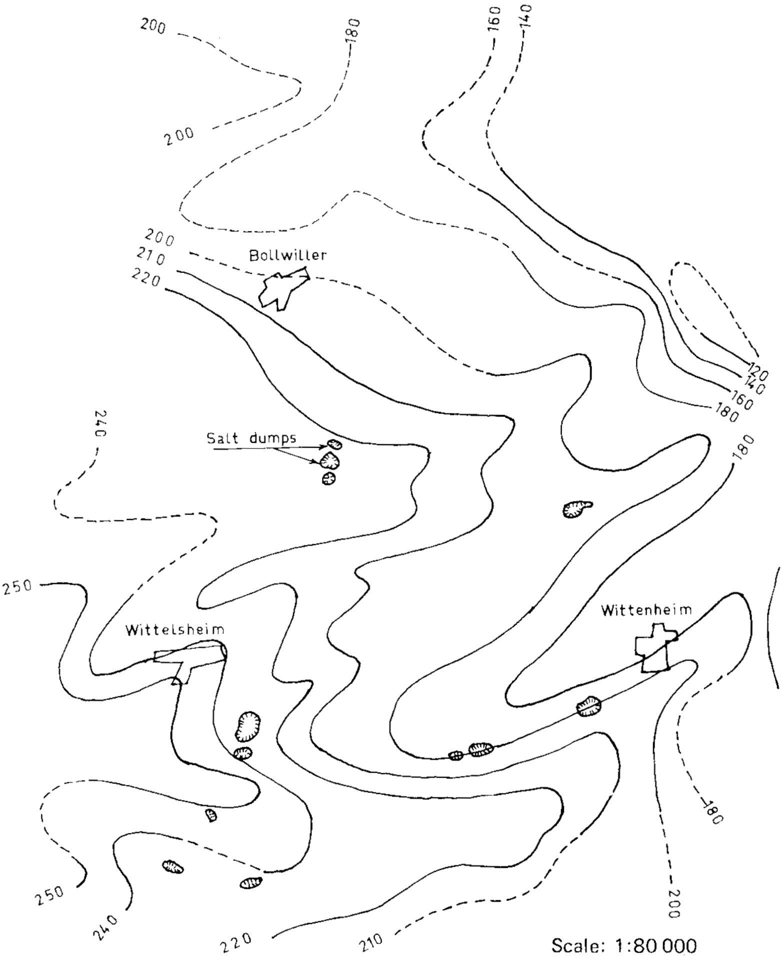

Fig. 6.1.4. Map of the bedrock contour lines.

The measurement and control of pollution

The main measurement and control devices are deep and shallow piezometers and surface stations (limnigraphs and salinographs). Fig. 6.1.7 shows some results obtained with these devices: the horizontal extent of salinity in zone 2, near the dumps. Fig. 6.1.7 should be compared to the geophysical document in Fig. 6.1.6. The original aspects of the experimental devices are given in the following note.

Note on the measurement and control devices (Fried et al., 1971a and b)

(1) Levels of the aquifer. In order to detect the exchanges between a stream and the aquifer, a line of piezometers 25 m deep and screened on the last 5 m

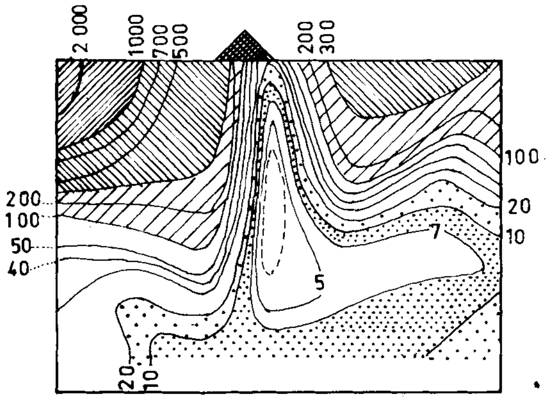

Fig. 6.1.5. Vertical resistivity distribution (distorted scales) — geoelectrical method.

has been set. The captors are probes with a capacitor effect using the dielectrical rigidity contrast between air and water, any raising of the water level yielding a change in capacity of these probes. They have been calibrated directly on the piezometers to take into account the influences of the tubes and of the soil. The characteristics of such a captor are summarized in Fig. 6.1.8.

(2) Levels of the streams. For the analogue recording, two types of device have been used: a mechanical limnigraph with counterweight and float and a pneumatic limnigraph with air line and pressure transmission to a mercury tank where level measurements are performed by float and counterweight. The analogue digital conversion is performed mechanically, the levels being perforated every 15 minutes on tape; the analysis and treatment of these tapes are done by computer. Calibration curves between heights and flowrates have been established for these stations by gauging with a current meter.

(3) Control of the salt concentrations in the streams. This has been done by point sampling with time and by recordings of the resistivity of the water. Fig. 6.1.9 describes the device schematically.

A scanning device consisting of several probes (a small sequential that can be programmed) can be used. Temperature compensation and correction to obtain the measured resistivity at 20°C is ensured by a second electrode, identical to the measurement electrode, immersed in a calibration solution having the same ionic profile as the tested water and the resistivity of which at 20°C is known and called ρ'. The compensation is satisfactory if the two probes are in thermal equilibrium, a condition that is almost always realized in rivers.

Fig. 6.1.10 shows a pollution-measurement station in the zone of light contamination.

(4) Control of pressures and salt concentrations downstream the dumps.

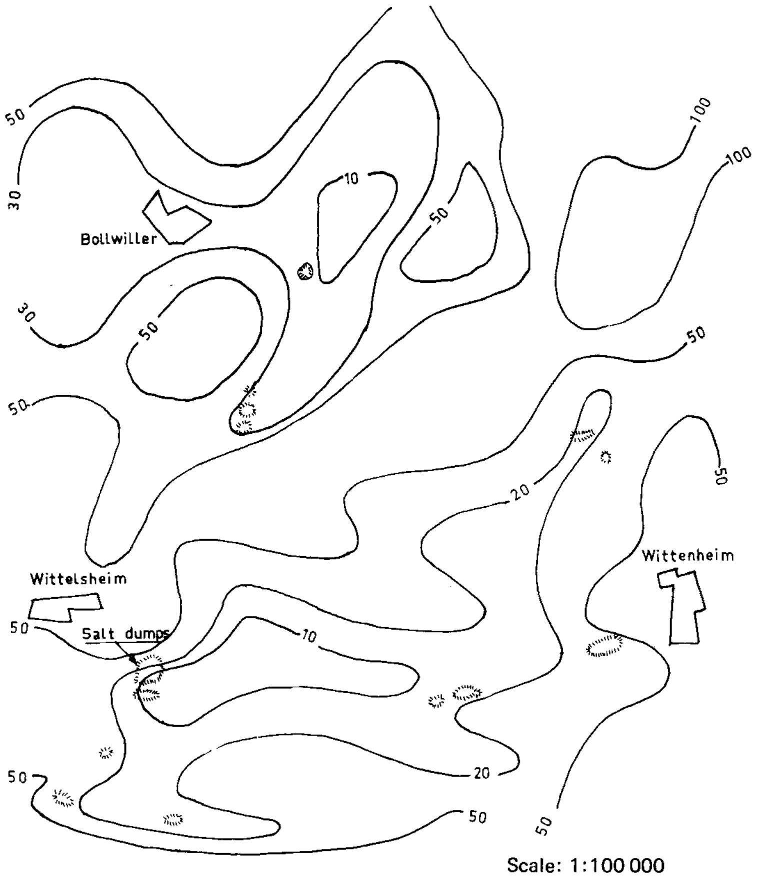

Fig. 6.1.6. Horizontal resistivity distribution — geoelectrical method.

Two types of observation wells have been drilled downstream from the dumps: fully penetrating piezometers screened over the whole depth of the aquifer to measure fresh-water equivalent heads (Lusczynski, 1961) and sets of three wells (Fig. 6.1.11) to measure the concentration and pressure evolutions at various depths.

6.1.3. The models

As displayed on the flow chart (Fig. 6.1.3) two types of mathematical models are used to describe and forecast the evolution of salinity: (1) at a hectometric scale, a dispersion model; and (2) at a kilometric scale, a mechanical convective model.

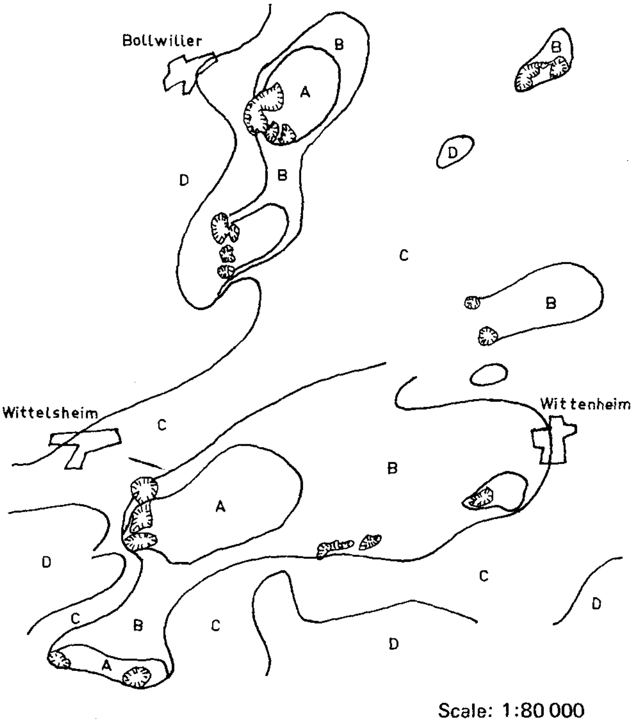

Fig. 6.1.7. Extent of salinity, measured with wells. $A > 10$ g/l, $B > 1$ g/l, $C > 100$ mg/l, $D < 100$ mg/l.

The dispersion model

It uses the dispersion scheme (Chapter 3), simplified thanks to the following assumptions.

(1) At the hectometric scale, the medium is homogeneous.

(2) The salt dump is in contact with the aquifer, which means that the influence of the unsaturated zone is neglected (this is a very conservative assumption).

(3) Viscosity μ is constant and density ρ depends linearly on the concentrations as $\rho = ac + b$, a and b being constants determined by type curves.

(4) From Fig. 6.1.5, it has been assumed that the salt reaches the bottom of the aquifer and that, at the right-hand side under the dump, salt concentration is constant and maximum along the whole depth of the aquifer. This is also a very conservative assumption.

(5) At each dump in Fig. 6.1.6, there is a corresponding model. The velocity direction is constant (Fig. 6.1.6) and horizontal.

These assumptions lead to a horizontal, bidimensional model, which describes the horizontal spread of salt. The axes are the velocity direction and

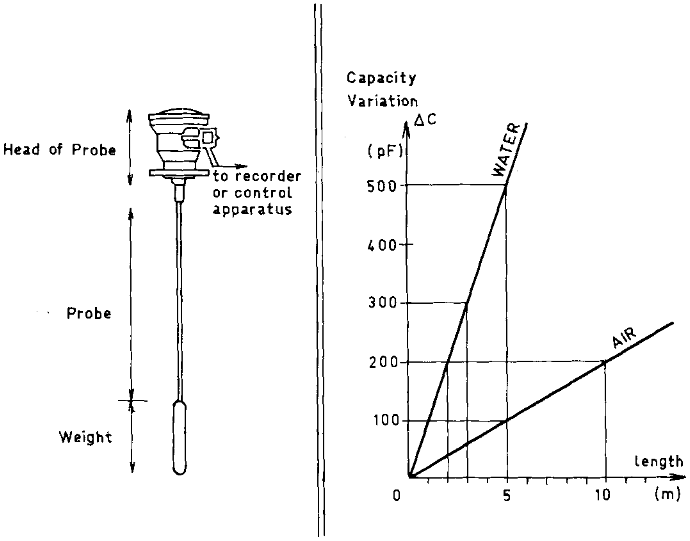

Fig. 6.1.8. Probe with a capacitor effect.

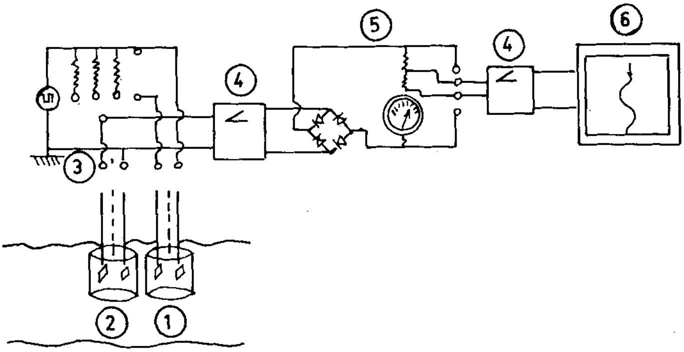

Fig. 6.1.9. Principle of the resistivity meter with heat compensation. 1 = reference electrode (reference resistivity ρ'), 2 = measuring electrode (unknown resistivity ρ), 3 = source, 4 = amplifier, 5 = measurement device, 6 = recorder.

its perpendicular and the dispersion tensor is diagonal. The dispersion scheme reduces to:

$$\frac{\partial}{\partial x}\,[K_L\,\rho\partial(c/\rho)/\partial x] + \frac{\partial}{\partial y}\,[\,K_T\,\rho\partial(c/\rho)/\partial y] - \partial(uc)/\partial x = \partial c/\partial t$$

$$u_x = -\frac{k}{\phi\mu}\,(\partial p/\partial x)$$

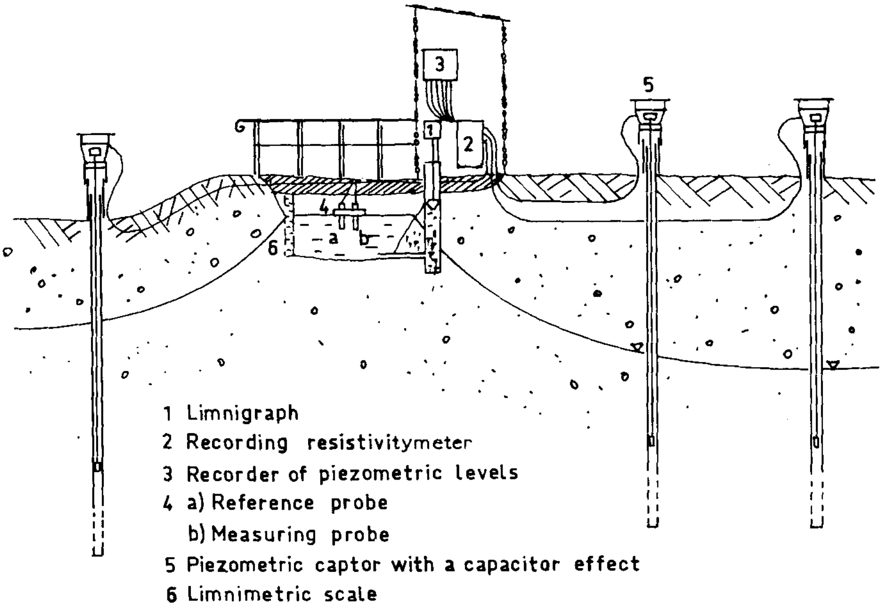

Fig. 6.1.10. Head measuring station.

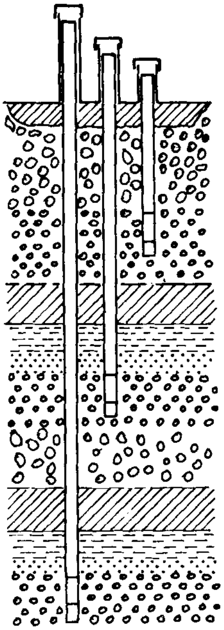

Fig. 6.1.11. Cluster of wells to measure pressure and concentration at various depths.

$$u_y = 0$$

$$\partial(\rho u_x)/\partial x = -\partial\rho/\partial t$$

$$\rho = ac + b$$

where K_L and K_T are, respectively, the longitudinal and transverse components of dispersion. All other notations have been defined in Chapter 3.

An estimate of the mean-flow pore velocity, from pumping tests, of the mean grain-size distribution and of the molecular diffusion coefficient of NaCl allows a computation of the dispersion Peclet number and shows that mechanical dispersion is predominant (§2.4.2). Thus K_L and K_T are written:

$$K_L = \alpha\,|U| \quad \text{and} \quad K_T = \alpha'\,|U|$$

The boundary conditions are defined in Fig. 6.1.12.

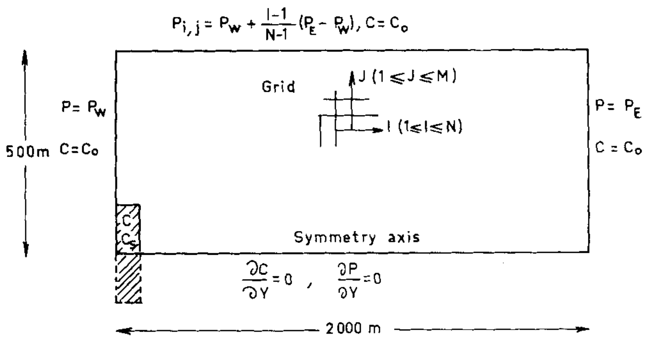

Fig. 6.1.12. Domain of the mathematical model — Boundary conditions.

The computation approximation is the Alternate Direction Implicit Procedure (§9.4.4) and the dispersion scheme is the general case, detailed in Chapter 3, which consists of the following iterative method: at time t, ρ, c and U are known; ρ is assumed constant and U is computed from the continuity and Darcy's equations at time $t + \mathrm{d}t$; c is then given by the dispersion equation at time $t + \mathrm{d}t$ and ρ by the equation of state. Of course, there are several iterations during the same time-step until convergence is obtained.

Calibration of the model is performed by comparison with the map in Fig. 6.1.7 and calibration curves are given in Fig. 4.2.31.

The hydro-convective model

It is assumed that the differences in viscosities and densities between the two fluids (salt water infiltrated from the streams or from the salt dump, and fresh water from the aquifer) are negligible. This assumption is well founded, considering the kilometric scale of the model (which is the scale of the watershed) and the relatively small contrast of concentrations in the case of hydraulic exchanges between stream and aquifer (1 g/l in the stream and 100 mg/l in the aquifer).

The model is convective, which means that the dispersion term of the general dispersion equation is neglected. The classical dispersion scheme (Chapter 3) reduces to a hydraulic model, which yields the velocities, and a mass-conservation equation which is purely convective. Concentrations in a mesh are computed by weighting the saline charges at the entrance and the exit of the mesh.

The flow is bidimensional and unconfined and it verifies Dupuit assumptions, i.e., the equipotential surfaces are vertical and the flow essentially horizontal; the pressure distribution is hydrostatic. The flow is governed by Boussinesq's equation:

$$\frac{\partial}{\partial x} K_{xx}(h-\eta)\frac{\partial h}{\partial x} + \frac{\partial}{\partial y} K_{yy}(h-\eta)\frac{\partial h}{\partial y} = S_y \frac{\partial h}{\partial t} + Q$$

where $h(x, y, t)$ and $\eta(x, y, t)$ denote the elevation of the free surface and of the bottom of the aquifer, respectively, above some datum level. S_y is the specific yield and Q is transfer water (see §9.5).

The evolution of the concentrations is governed by the convection equation:

$$\operatorname{div}(Uc) = -\frac{\partial c}{\partial t}$$

The movement equation is solved first, the term Q of the second member comprising all the punctual flow rates of pumping or of injection. The salt dumps are assimilated to injection wells, taking pluviometry into account; the stream—aquifer exchanges are assimilated to a line of wells, feeding or draining wells according to the exchange mode. Then the convection equation is solved. The computations of new piezometries and concentration distributions are performed by line overrelaxation.

Before being used to forecast the possible evolution of the groundwater salinity, the model is calibrated on an annual cycle of observations. The grid and some results are given in Figs. 6.1.13, 6.1.14 and 6.1.15.

These results show a significant spread of the pollution which has been linked to the progressive disappearance of industrial wells used to collect a major part of the effluents. This is an interesting *paradox*: the progressive disappearance of an industry increases the pollution.

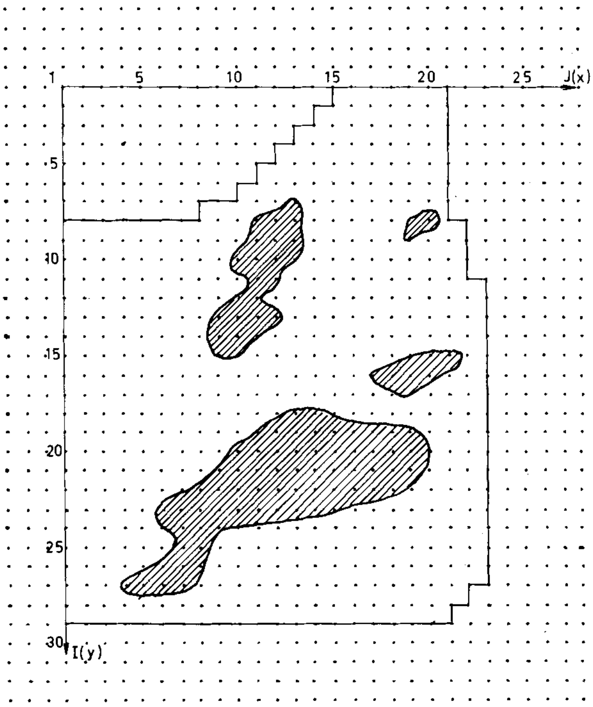

Fig. 6.1.13. Observed salt intrusion during 1970.

A mechanical convective model

In the zone of light contamination, a mechanical model has been set up to represent bidimensional flow in a vertical aquifer section of unit width, perpendicular to the stream, and contamination to and from the streams. It is a conductive-paper-type model adapted to the study of a transient phenomenon with an iterative procedure. Results are shown in Fig. 6.1.16.

6.1.4. Conclusions

This case displays the basic steps of the methodology presented in Chapter 3: the collection of preliminary data, the decision criteria and fundamental assumptions, the models and the collection of pollution parameters. The last step was performed by using the preliminary data for velocity parameters and by calibrating a model on the existing pollution for dispersion coefficients, as the pollution is on a regional scale.

For the case studied itself, the results were the setting up of predictive models on two scales, on the scale of a dump and on the scale of the whole region of the mines, and, more generally, a whole set of observation means of the aquifer and the streams, allowing accurate knowledge of the present pollution and a check on the predictions of the models.

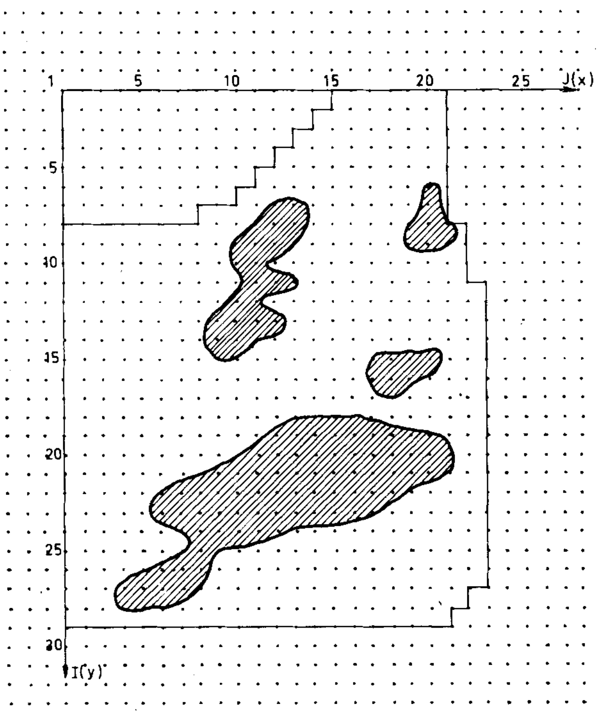

Fig. 6.1.14. Computed salt intrusion during 1970.

6.2. *THE PROTECTION OF AN AQUIFER AGAINST POSSIBLE POLLUTION*

An urban community plans to protect its drinking-water wells against normal urban pollution and against accidents. As an example, here is the study conducted near the town of Lyons in central France, to derive mathematical models aiming at, on the one hand, describing the unavoidable urban pollution and helping in establishing protection rules, and, on the other hand, estimating the usefulness and delay of an intervention in the event of an accident near a well. This study has been performed strictly according to the methodology of Chapter 3 (Fried, 1972a; Fried and Ungemach, 1973a).

6.2.1 Preliminary study of existing data

The reservoir is alluvial, with sands and gravels, slightly stratified with clay lenses; it is locally multilayered but globally monolayered, as pumping tests and non-equilibrium methods display a mean permeability in the zone of influence of the wells. But permeabilities derived from grain-size distributions

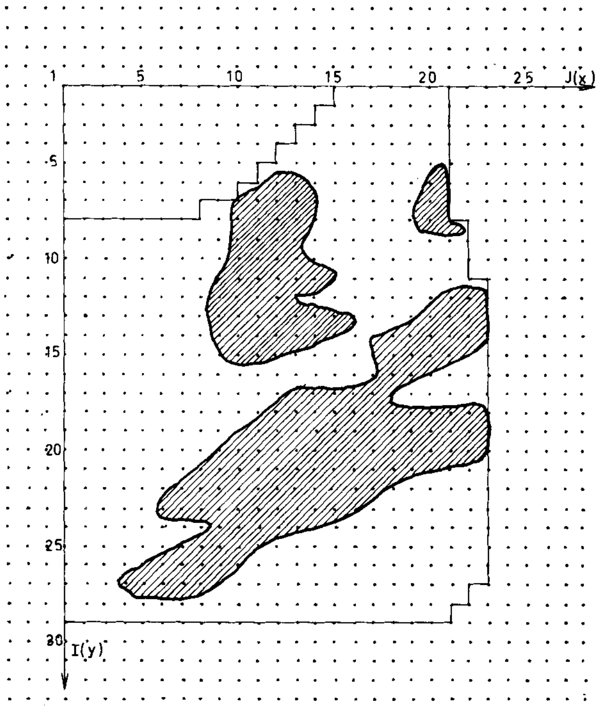

Fig. 6.1.15. Computed salt intrusion for 1975.

on soil samples have different values along a vertical. An estimate of the mean global pore velocity (5 m/day) can be derived from these pumping tests. Also, there exists a mean grain-size, d_{50}, equal to 1.5 cm. The aquifer is 20 m thick, and the water table is at —4 to —5 m.

The unavoidable main pollutions are due to hydrocarbons (in small proportions, less than 0.4 mg/l), sulfates and nitrates. Besides these, it appears that the greatest pollution hazard comes from trucks carrying chemicals miscible with water and also from light hydrocarbons, such as domestic fuels, which, after reaching the water table, could be washed downstream.

Thus, only miscible pollutions have to be taken into account and hydro-convective or hydrodispersive models will be set.

6.2.2. *The working assumption*

The demand being for a protective area around pumping wells, the corresponding scale is 20 to 100 m, i.e. global scale 2, and a dispersion model has been chosen accordingly, which is a multistrata model to account for the permeability variations along a vertical and which represents the locally multilayered aquifer, but where concentrations are averaged over the aquifer

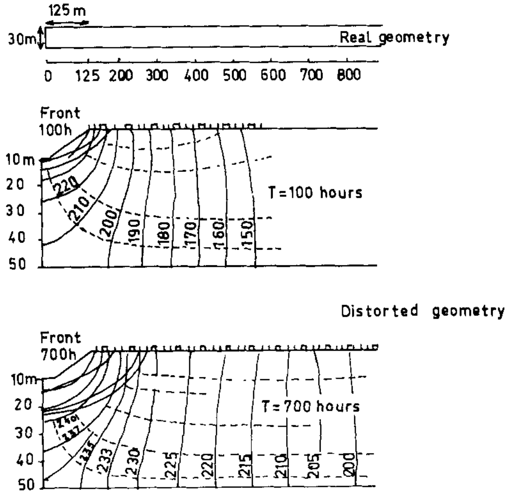

Fig. 6.1.16. Conductive-paper model — contamination of the aquifer by a stream.

depth to simulate the global monolayered aquifer. The layers are horizontal and a horizontal, multilayered, hydrodispersive model has been conceived, where the dispersion tensor is diagonal, because at the scale of the study, the streamlines are almost parallel and straight. The Peclet number, computed from a mean diffusion coefficient, is:

$$Pe = (5 \cdot 10^{-3} \times 1.5)/10^{-5} = 750$$

Thus, the possible pollutions will be governed by a dynamic dispersion regime and the dispersion coefficients are given by $K = \alpha u$. The parameters that have to be collected are the global velocities u and the intrinsic dispersion coefficients α.

6.2.3. The determination of the dispersion parameters

In order to refine the knowledge of the stratification and also to assemble the dispersion coefficients that could be used to model a pollution by light hydrocarbons remaining in the upper part of the aquifer, a local experiment has been performed by the single-well pulse method with radioactive tracers (§4.2.1). It has yielded the vertical distribution of longitudinal-dispersion coefficients at one site (Fig. 6.2.1).

The dispersion parameters at the global scale 2 have been collected at five experimental sites, in order to draw a map of dispersion coefficients covering an area of 35 km^2 (Fig. 6.2.2). These experimental sites were chosen as the most representative, according to the geology and lithology of the region.

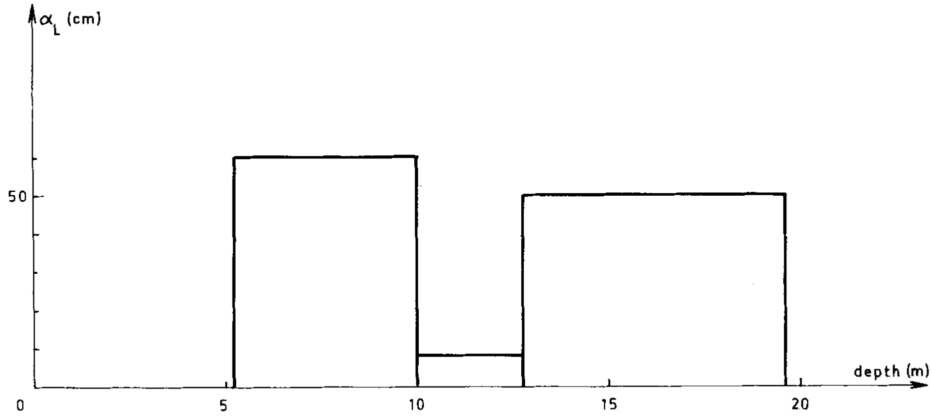

Fig. 6.2.1. Vertical distribution of longitudinal dispersion coefficient.

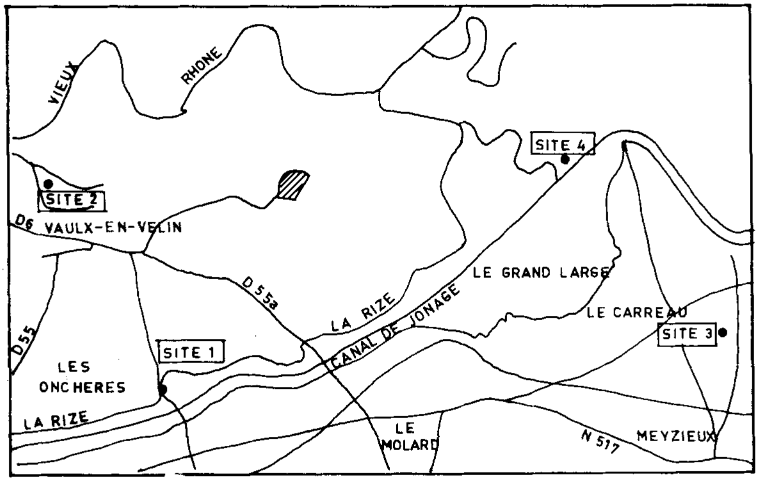

SCALE: 1:100 000

Fig. 6.2.2. Location of the experimental sites.

One of these experimental sites is a sanitary landfill, that yields dispersion coefficients valid at the scale of 600—1000 m using environmental tracer methods. On the four other sites, the experimental device used was the single-well method in geophysics, i.e. the injection of salt water and its detection by resistivity measurements performed at the ground surface. Although this method is thoroughly described in §4.2.3, some details of the operations are given here for information purposes:

(1) The time spent on one site was 15 days, including conveyance of equipment, injection, control measurements, geophysical measurements, drilling

TABLE II

Characteristics of the sites

Site No.	Depth of of borehole (m)	Depth of the water table (m)	Width of the aquifer (m)	Transmissivity (m^2/sec)	Horizontal permeability (m/sec)	Storage coefficient (S.D.%)	Resistivity before injection (Ω cm)	Equivalent NaCl 18°C (mg/l)	Number of piezometers
1	20	3.3	16.7	$5.5 \cdot 10^{-2}$	$3.3 \cdot 10^{-3}$				5
2	23.5	4.5	19	$1.4 \cdot 10^{-1}$	$7.0 \cdot 10^{-3}$		1658	350	2
3	35	16.5	18.5	$5.0 \cdot 10^{-2}$	$2.8 \cdot 10^{-3}$		2180	250	
4	19.6	2.06	17.5	10^{-1}	$5.5 \cdot 10^{-3}$	13	3375	160	2
5	18.3	2.40	15.90	$3.0 \cdot 10^{-2}$	$2.0 \cdot 10^{-3}$				22

TABLE III

Adopted stratification on each site and results

Site No.	Strata No.	Width (m)	Permeability (m/sec)	Porosity	Mean velocity (m/day)	Velocity per stratum (m/day)	Intrinsic longitudinal dispersion coefficient (m)	Intrinsic lateral dispersion coefficient (m)	Transmissivity (m^2/sec)
1	1	5.5	0.0040	0.2	7.2	7.9	12.00	7.000	0.055
	2	7.5	0.0020	0.2		3.9		14.000	
	3	2.0	0.0090	0.2		17.7		3.110	
2	1	4.0	0.0005	0.2	9.6	0.7	8.00	1.000	0.140
	2	7.0	0.0010	0.2		1.3		0.500	
	3	6.0	0.0110	0.2		14.3		0.045	
	4	2.0	0.0325	0.2		42.3		0.015	
3	1	5.8	0.0050	0.2	13.00	24.6	5.00	0.290	0.050
	2	10.2	0.0001	0.2		0.5		14.500	
	3	2.0	0.0050	0.2		24.6		0.290	
	4	1.0	0.0100	0.2		49.2		0.145	
4	1	8.5	0.0005	0.2	9.00	0.8	7.00	1.000	0.100
	2	2.8	0.0020	0.2		3.1		0.250	
	3	3.0	0.0010	0.2		1.5		0.500	
	4	2.0	0.0160	0.2		24.8		0.031	
	5	1.0	0.0551	0.2		85.2		0.009	

of an observation well, and withdrawal of the equipment. An average of 200 kg/h of salt (NaCl) was injected for 160—225 h depending on the site, over the whole depth of the aquifer from a completely screened well.

(2) The preliminary data actually used in the modelling of the geophysical experiment are summarized in Table II, and the results of the model calibration are given in Table III. Results of the calibration on site 5 are given in §4.2.4.

6.2.4. The models

The model defined in §4.2.4, which is calibrated on salt-water intrusion, is used as a predictive model for the whole area spanned by the five sites at the scale of 100 m and the model defined in §4.2.5 (bidimensional, horizontal-monolayered) is used for pollutions at the scale of 500 m.

6.3. SALT-WATER INTRUSION INTO A COASTAL AQUIFER

Coastal aquifers represent an important water resource, especially in semi-arid zones bordering the sea (southern Italy or Tunisia, for instance). Pumping programmes must, however, be very carefully established to prevent pollution by salt which can act in two ways (Fig. 6.3.1): (1) salt water coming into the pumping well, which pollutes the extracted water; and (2) global intrusion of sea water, which can destroy the surface agriculture: vineyards in the Medoc region, in southwestern France, for instance, are endangered by such pollution.

When water is badly needed, it may be advantageous to pump at the utmost limit and then to relax and allow a recharge of the aquifer, and to iterate the process. The possible occurrence of a transition zone, the evolution of its width and its forward and backward movements under the pulsation of the pumping programme and also under the effect of tidal conditions become very important factors. In order to try to understand the mechanisms of this particular type of pollution, a methodological study, based on the elements presented in Chapter 3, has been initiated. The objectives of this study are: (1) to define experiments, models and rules necessary for the derivation of a pumping programme in a coastal zone; and (2) to define the setting of control and observation points.

This experimental study has been performed on the Malika aquifer in Senegal.

6.3.1. Preliminary studies

The aquifer is located about 20 km from Dakar. It is a fresh-water lens at most 50 m deep, lying everywhere on salt water (Fig. 6.3.3). This lens is about

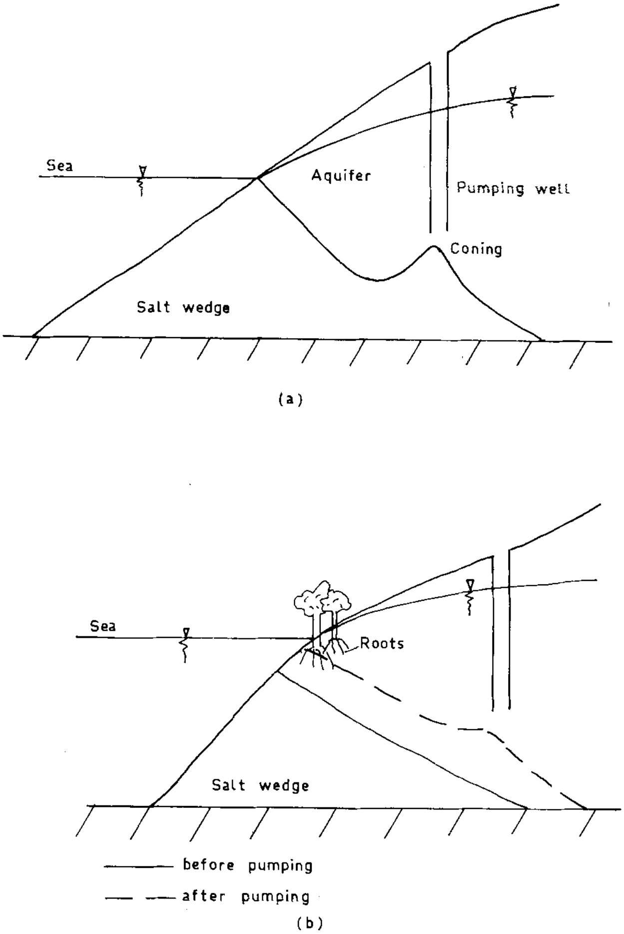

Fig. 6.3.1. Salt-water intrusion in a coastal aquifer.

1 km wide and is bounded on the north by the ocean and to the south by salt waters (at the ground surface the salt waters appear as lakes, which are parallel to the coastline and their salinity varies from 14 to 53 g/l) (Fig. 6.3.2) (Debuisson, 1970).

The aquifer is made up of sands with clay lenses and some gravels and is relatively homogeneous; the water table is between 3 and 6 m deep. The aquifer flows to the sea and also to the southern lake, the water-divide fluctuating with the seasons. The boreholes are permanently equipped for resistivity measurement which have approximately defined the geometric characteristics of the transition zone (Fig. 6.3.3).

The transition zone, which is due to tides and seasonal variations since no systematic pumping takes place, is 2—12 m wide. Considering its mean

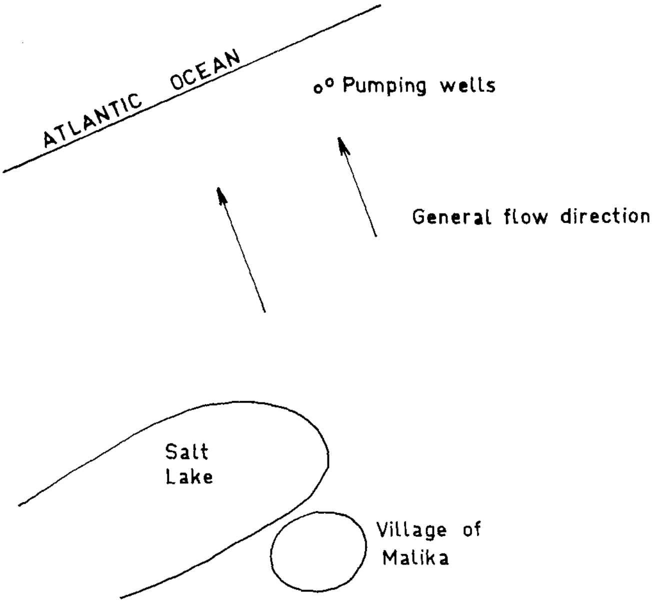

Fig. 6.3.2. Location of the aquifer (Debuisson, 1970).

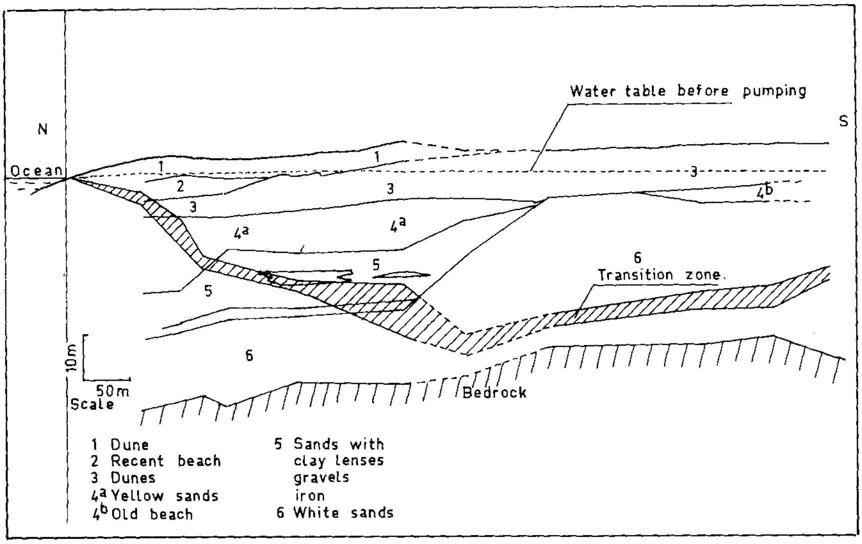

Fig. 6.3.3. Vertical section of the aquifer showing the transition zone and the heterogeneities (after Debuisson, 1970).

position as an interface between fresh and salt waters, it can be observed that the ratio between fresh-water heights above and below sea level varies between 1/5 and 1/75, which is very different from the Ghyben-Herzberg value of 1/40.

Also, it has been observed that after heavy rains recharging the aquifer, the limits of the transition zone are displaced downwards and its width varies. Pumping has been performed during three months, with two wells at a global flow rate of 26 m^3/hour. The amount of water pumped out was 63,400 m^3 and observation wells were drilled around the pumping well to define the depression cone. A mean transmissivity of $6 \cdot 10^{-3}$ m^2/sec and a storage coefficient of 0.17 were computed.

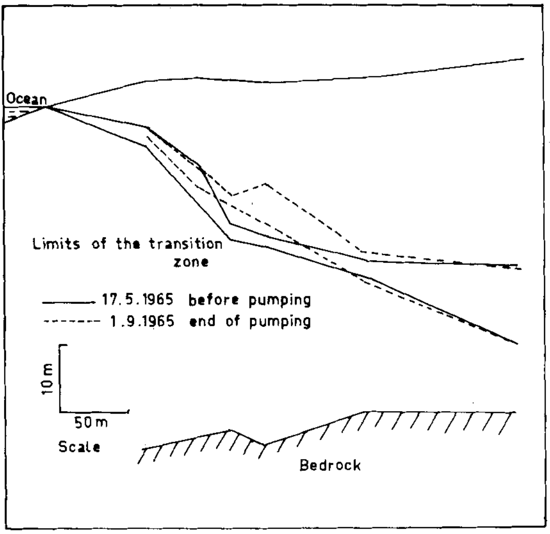

Fig. 6.3.4. Evolution of the transition zone with pumping (after Debuisson, 1970).

Pumping has influenced the transition zone within a radius of 200 m (Fig. 6.3.4). Measurements by electrical soundings have also been performed, which record the variations of superficial equiresistivity curves with the pumping. The results are plotted on maps, an example of which is given in Fig. 6.3.5, showing the inward movement of salt water.

Among the usable data, it should be noticed that tidal waves have been recorded in the aquifer: pressure variations at various levels have been noticed, corresponding to tidal variations more or less damped according to the geology of the layer. These results have been interpreted as displaying the horizontal stratification of the aquifer and linked to the effective porosity of the various layers.

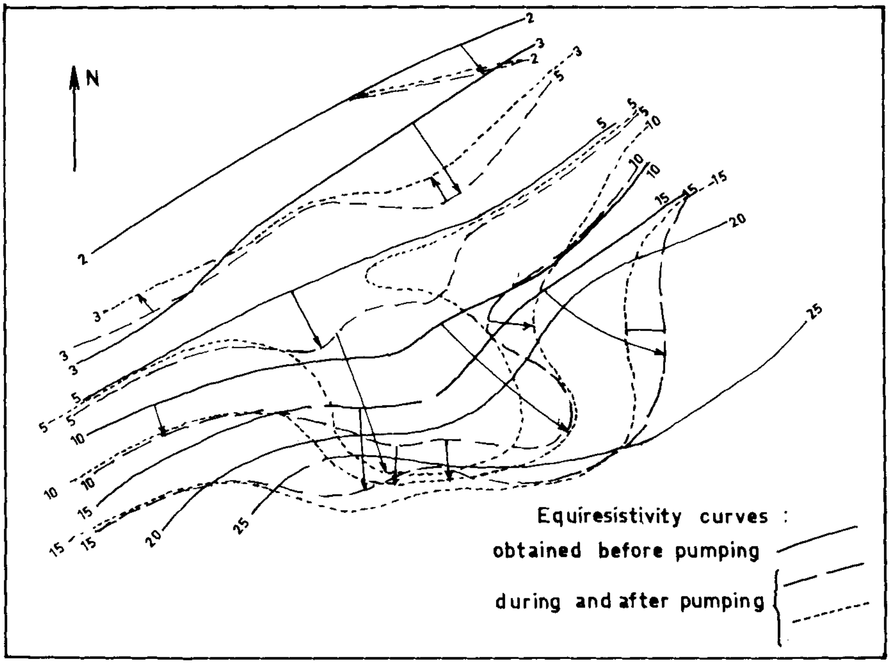

Fig. 6.3.5. Evolution of the equiresistivity curves with pumping (after Debuisson, 1970).

6.3.2. *The working assumption*

The preliminary data show that we have a medium-scale pollution by a pollutant miscible to water. The extent of the source (the sea), the recorded dimensions of the transition zone and its importance relative to the studied domain imply the use of a hydrodispersive model and the setting of a dispersion scheme.

6.3.3. *Use of the dispersion scheme*

Prior to introducing the equation itself, hydraulic models have been derived to refine the knowledge of the multilayered aquifer in terms of strata geometry (extension and thickness) and hydrodynamic characteristics (horizontal and vertical permeabilities, storage coefficients) and fresh-water flow rates to the sea.

Immiscibility assumptions are introduced as a first approximation and vertical hydraulic models are adjusted on the mean transition zone in the permanent regime and on piezometric oscillations due to tidal waves in the transient regime.

Then a stratified, horizontal hydraulic model is used, with vertical transfer of water between the strata. It is coupled with the horizontal dispersion model, also stratified and with vertical mass transport between layers. The hydrodispersive model is adjusted on curves analogous to the resistivity lines of Fig. 6.3.5, simulating the mean encroachment variation. A finite-element method has been proposed for this model and is being tested at the time of writing.

6.3.4. Difficulties of the study

As pointed out by Bear (1972), the main difficulty in salt-water modelling is the fact that not only is the dispersion scheme non-linear, but also the domain is not known, because some of its boundaries are free surfaces. The first results of the present study have been to define the difficulties which we now detail.

The mechanisms of movements and dispersion are not well known, but some experimental facts provide a theory: it has been noticed that near seas which have no tide (such as the Mediterranean), the transition zone is usually very narrow and sometimes non-existent; near seas with tides (the Atlantic Ocean, as presented here), the transition zone may be rather considerable (Fig. 6.3.3).

The theory is then the following. Without tides and without pumping, and neglecting seasonal recharges due to rains (an especially valid assumption in semi-arid climates), the mean salt—freshwater interface does not move. The only movement is fresh water flowing to the sea on the salt water (Fig. 6.3.6) which generates a probably small transverse dispersion, as it is linked to the vertical permeability. Also, salt water dispersing in the aquifer will be carried away by the fresh water.

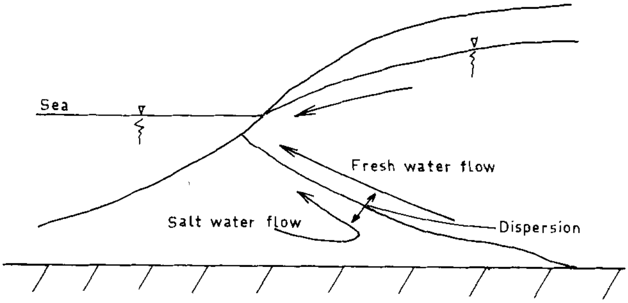

Fig. 6.3.6. Transverse dispersion from fresh-water movement to the sea.

When there is a tide, the horizontal component of the salt-wedge velocity is larger than the vertical component and, especially if the aquifer is horizontally stratified, it will create a large longitudinal dispersion. This dispersion is the origin of the rather significant transition zones that are observed. Of course, tides and seasonal recharges are oscillatory phenomena and a back-and-forth movement of the wedge is expected; the oscillatory movement raises a question: will the transition zone widen with time or will it reach an equilibrium? According to known data, it seems that in practical cases an equilibrium is reached, probably due to the washing-out phenomenon already mentioned: part of the dispersing salt water is washed out to the sea by the aquifer discharging naturally. Another explanation (which does not contradict the previous one) is that dispersion is in some respects reversible and that part of the transition zone created by an inward movement will be erased by the outward movement.

We have mentioned here the evolution of the dispersion zone under natural conditions (tides, rains). The main problem is to check the validity of this theory under pumping conditions and to see whether the washing-out of the salt water by the aquifer compensates the possible dispersion effects. This is the purpose of the study mentioned here and which is under way. If pumping does not influence the width of the dispersion zone, then immiscible models of the fresh—salt-water interface will be used and it will not be necessary to compute dispersion coefficients from field experiments which are always very difficult to carry out at convenient large scales.

The dispersion theory of salt-water intrusion is important in determining pumping policies in semi-arid zones; in that case, each drop of fresh water is necessary and it is sometimes planned to over-operate the aquifer, i.e. to inverse its gradient, which creates heavy intrusion; this intrusion is then pushed back to the sea by the natural recharge during the rain period and it must be determined whether some pollution still remains: the oscillatory theory of dispersion with rinsing and reversibility should provide an answer.

6.4. A RADIOACTIVE POLLUTION BY LIQUID WASTES

Radioactive pollution hazards are likely to increase in the next few years with the continuing development of atomic-energy sources. Both psychologically and physically, the radioactive pollution is a danger and should be treated adequately. As a case-history illustrating the methodology presented in Chapter 3 the case presented briefly here does not differ very much from the industrial-salt pollution of §6.1. We shall see that overall scales are certainly different, but the basic modelling and techniques are equivalent. We prefer to present it separately, however, because we wish to stress the importance of miscible pollution techniques applied to this very special type of pollution. Thus the emphasis is not put on the methodology but on the types of data and on the scale aspects.

The facts presented here concern the disposal of liquid wastes at the National Reactor Testing Station, on the Eastern Snake River plain in southern Idaho (U.S.A.) studied by the United States Geological Survey (Robertson et al., 1974).

6.4.1. Preliminary studies

Geological setting

The eastern Snake River Plain is a large downwarped basin 31,000 km^2 in area. It has been filled to its present level with perhaps 1500 m of thin basaltic lava flows and interbedded sediments. The Snake River Plain aquifer flows to the southwest (Fig. 6.4.1) at high velocities (1.5—8 m/day) and its transmissivity ranges from 10^4 to 10^6 m^2/day. Its storage coefficient range from 0.001 to 0.2 and from 0.01 to 0.06 at the waste-disposal site. Most of the aquifer flow occurs along the upper and lower contacts of successive basaltic flows which have fractures and fissures.

The National Reactor Testing Station occupies 2320 km^2 of this plain. Fig. 6.4.2 shows the NRTS boundaries and the contours of the water table, which are used to compute the main flow velocity of the aquifer.

The wastes

There are two main waste-discharge facilities, namely the Test Reactor Area (TRA) and the Idaho Chemical Processing Plant (ICPP), which discharge 80% of the total chemical wastes and over 90% of the total radioactive waste. Depth to the water table at these locations is about 140 m.

The pollutants, i.e. the wastes that affect water quality, are non-radioactive, such as sodium chloride, chromium and heat, and radioactive, such as tritium, strontium 90 and cesium 137.

Chloride has been a continuous waste product at both sites. Natural chloride concentration in the aquifer water ranges from 10 to 20 mg/l and a value of 15 mg/l was used as a lower limit to indicate waste contamination. The average effluent concentration, from 1962 to 1972, was 245 mg/l at the ICPP.

Sodium is discharged with chloride as sodium chloride; it behaves as chloride, but its movement is retarded by sorption (ion exchange): for instance, at observation wells where the chloride concentration is 60 mg/l the sodium concentration is only 14 mg/l, although the injected sodium mass is 2/3 of the chloride mass.

Chromium: the contamination level was fixed at 0.01 mg/l and the highest recorded level is 0.5 mg/l.

Heat: the natural water temperature is 12°C and the temperature of the effluent discharge at the ICPP is about 21°C. Heat transport has created a detectable plume of warmer water about 3 km^2 in area.

Tritium is the most abundant waste radioisotope, occurring as tritiated water. The natural tritium concentration in the aquifer water is less than 0.2 pCi/ml (pico curie per millilitre) and the normal detection limit in NRTS tritium analyses is 2 pCi/ml used at the lower mapping limit. The average

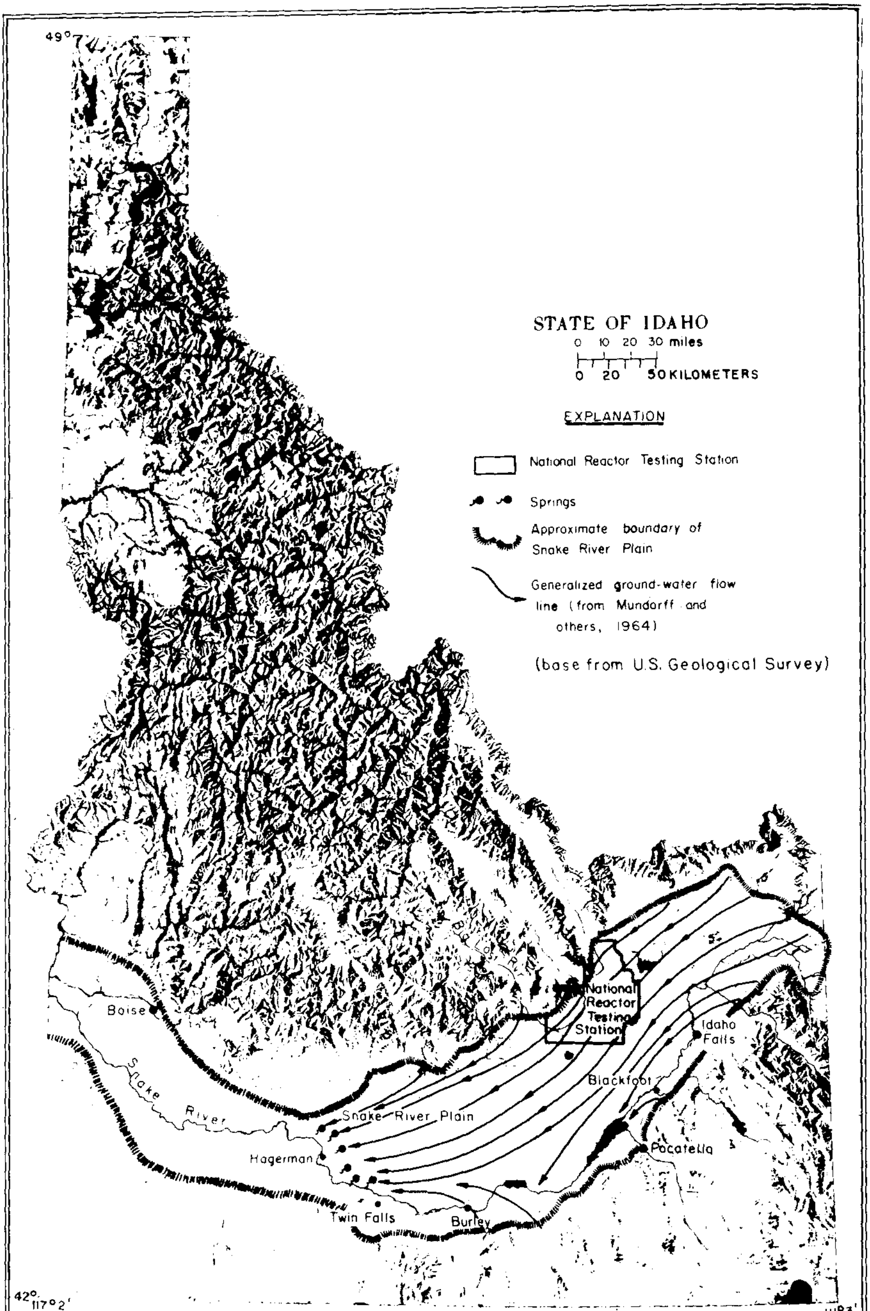

Fig. 6.4.1. Map showing location of NRTS, Snake River Plain and inferred groundwater flow lines of Snake River Plain aquifer (Robertson and Barraclough, 1973).

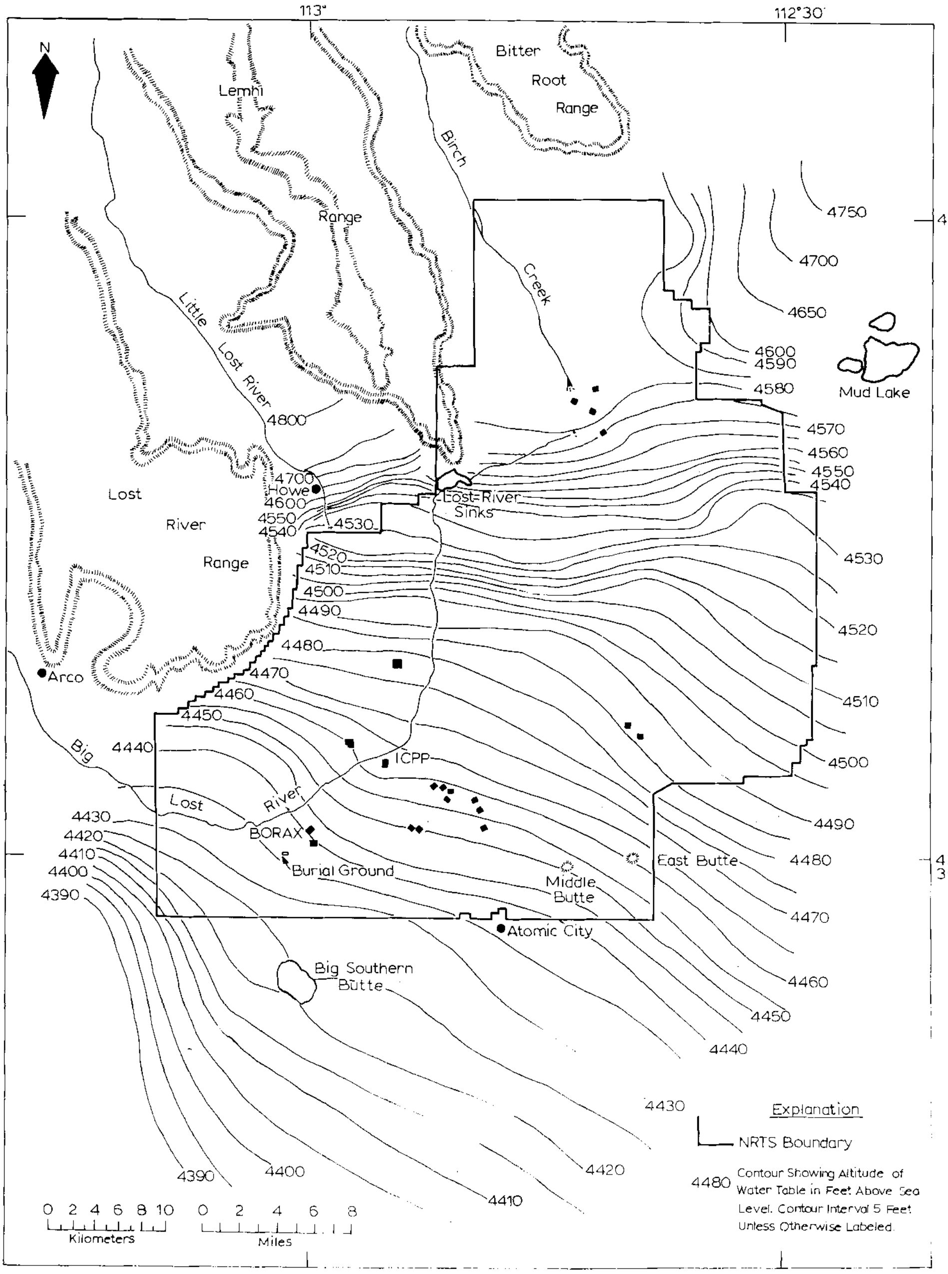

Fig. 6.4.2. Map of the NRTS and the vicinity showing contours on the regional water table (after Robertson, 1974).

concentrations of tritium discharged at TRA and ICPP, respectively, are 615 pCi/ml and 430 pCi/ml (from 1962 to 1972).

Strontium 90 and cesium 137: the maximum ^{90}Sr concentration was 0.15 pCi/ml at the ICPP and the lower detection limit was set at 0.005 pCi/ml. Sorption is important, it retards the movement and strengthens the influence of radioactive decay on concentration reduction. ^{137}Cs has been discharged in the same quantities as ^{90}Sr, but due to heavy sorption, was never detected.

Waste discharge facilities

The TRA generates several different types of liquid waste and uses four types of disposal systems.

(1) Low-level radioactive wastes are discharged to three interconnected seepage ponds and percolate to the water table.

(2) Corrosive, but non-radioactive chemical wastes are discharged to a separate seepage pond.

(3) Non-radioactive cooling-tower blow-down wastes are discharged directly into the aquifer through a disposal well, 395 m deep, which generally contains 1200 mg/l of naturally occurring dissolved solids (five times as much as groundwater).

(4) Sanitary wastes are discharged to a separate seepage pond.

The ICPP discharges all its low-level effluents directly to the aquifer through a 180 m deep well. Nearly all radioactivity is removed from the effluent by distillation and ion exchange before discharge, except for tritium and small amount of strontium 90 and cesium 137.

6.4.2. Decision criteria

Obviously, we are facing a pollution miscible with the aquifer water. The problem is to determine the scale of the study.

Of course, the amounts of the various discharged pollutants are known, but more interesting are the recorded maps of pollution concentrations in space and time, which really fix the scales. Fig. 6.4.3 shows such maps in the case of chloride pollution. For other pollutants the maps are alike.

From these maps, it appears that the pollution takes place at a regional scale, that the waste-disposal facilities are equivalent to a point source, but that the intensity of that source is such that dispersion effects must be taken into account; the very aspect of the waste plumes shows that both longitudinal and lateral dispersion are large. Modelling is thus based upon the working assumption that the pollutions are governed by the dispersion scheme.

6.4.3. The dispersion scheme

It is based upon a generalized form of the usual dispersion equation to include sink effects, radioactive decay, sorption effects and medium compressibility:

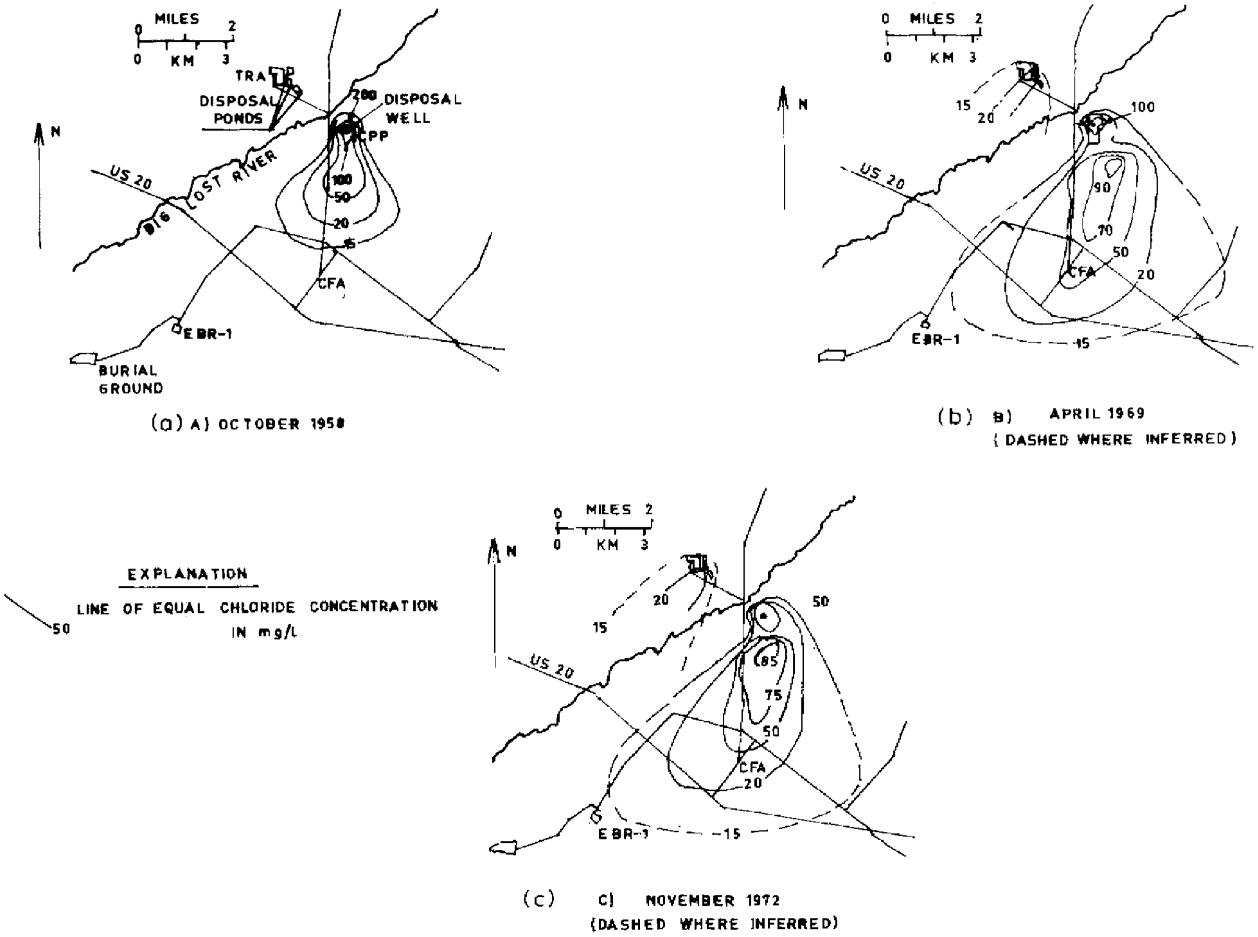

(a) A) OCTOBER 1958

(b) B) APRIL 1969
(DASHED WHERE INFERRED)

(c) C) NOVEMBER 1972
(DASHED WHERE INFERRED)

Fig. 6.4.3. Map of ICPP-TRA vicinity showing distribution of waste chloride in Snake River Plain aquifer water in 1958 (a); 1969 (b); 1972 (c) (Robertson and Barraclough, 1973).

$$\frac{\partial c}{\partial t} = \operatorname{div}(K \operatorname{grad} C) - \operatorname{div}(UC) - C\alpha\frac{\partial p}{\partial t} - QC_s - \lambda C - \frac{\partial}{\partial t}[(1-\phi)N] \qquad [6.4.1]$$

where C_s is the solute concentration in a source or a sink, α the compressibility of the medium, λ the radioactive decay constant of the solute and N the concentration of sorbed solute on solid phase. All other terms have been defined in Chapter 3.

Ion exchange can also be modelled by introducing a distribution coefficient A which is the ratio of the nuclide concentration in the solid phase to its concentration in the liquid phase (pCi/cm^3), assuming instantaneous equilibrium, reversible, linear adsorption isotherm, and multiplying the left-hand side of [6.4.1] by $\phi/[\phi + A(1-\phi)]$.

Pollution takes place in the tracer case, and in the dynamic dispersion regime, with dispersion coefficients proportional to velocity. The aquifer is horizontally stratified and it has been observed that most of the pollution flows horizontally. The dispersion model is then bidimensional. The aquifer flow is governed by the usual hydrologic equation for confined aquifers (see Appendix I):

$$\operatorname{div}(T \operatorname{grad} H) = S\frac{\partial h}{\partial t} + q$$

The dispersion scheme has been discretized on the grid of Fig. 6.4.4.

The flow equation has been solved by ADIP and the dispersion equation by the method of characteristics (§9.4.6). An example of the result is sketched in Fig. 6.4.5.

6.4.4. The determination of the dispersion coefficients

We know that to operate the dispersion scheme, field values of the dispersion coefficients must be obtained. The present study is performed at a very large regional scale and the dispersion coefficients have been derived by using the pollutions as environmental tracers.

A good environmental tracer must be free from chemical reactions, such as ion exchanges and precipitations for instance, and must not react with the medium. The initial and boundary conditions must be known (essentially by injected amounts and their history). Chloride was then chosen as the simplest and most accurate dispersion tracer. Tritium could be used also, but its behaviour is more complex than that of chloride, because of its very variable discharge rates and its radioactive decay.

Chromium too, could be used, but certainly not sodium because of its

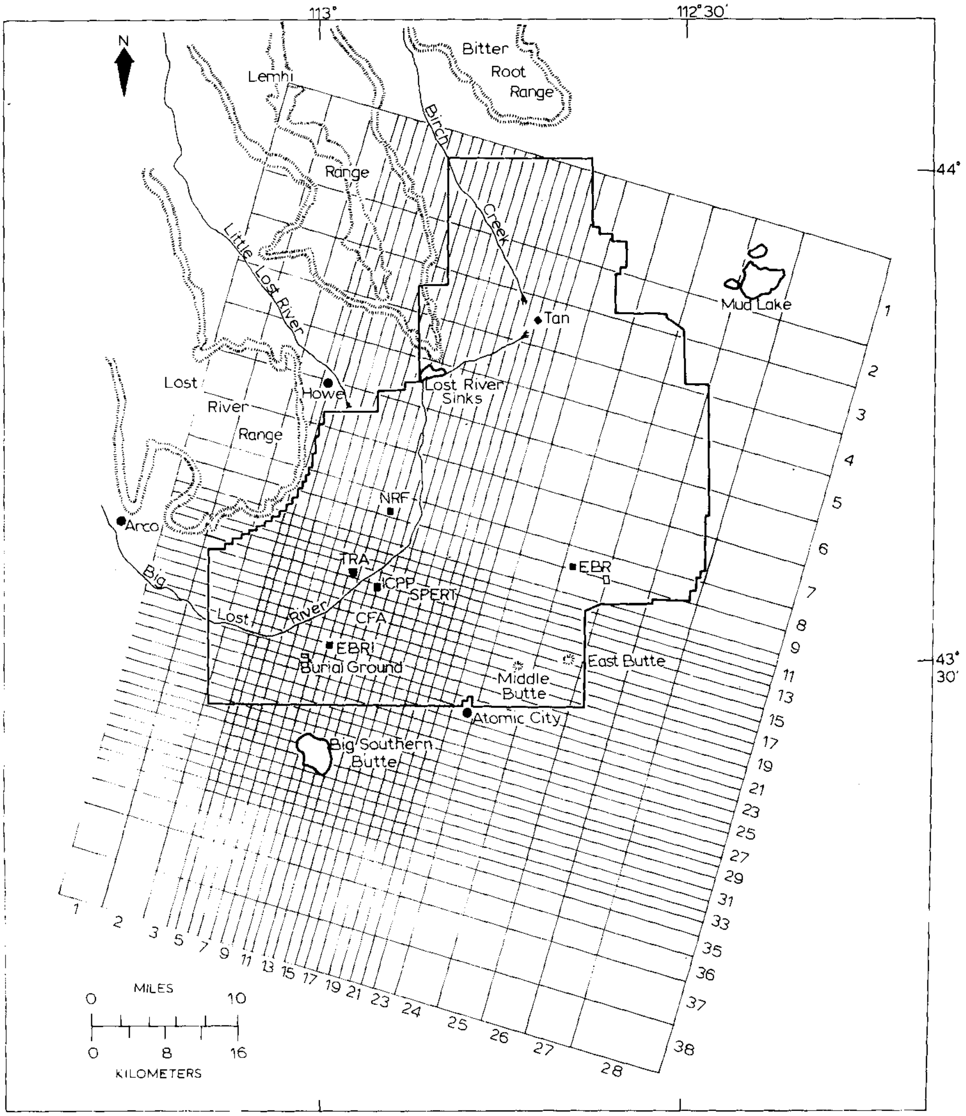

Fig. 6.4.4. Finite-difference grid. Shaded area is used for the forecasting of waste immigration (Robertson, 1974).

adsorption. The dispersion was then adjusted on chloride-concentration curves and the values obtained for α_L and α_T were:

$$\alpha_L = 91 \text{ m} \quad \text{and} \quad \alpha_T = 137 \text{ m}$$

These values were used to adjust a tritium model on the experimental tritium concentration curves accounting for radioactive decay (Fig. 6.4.5) and a

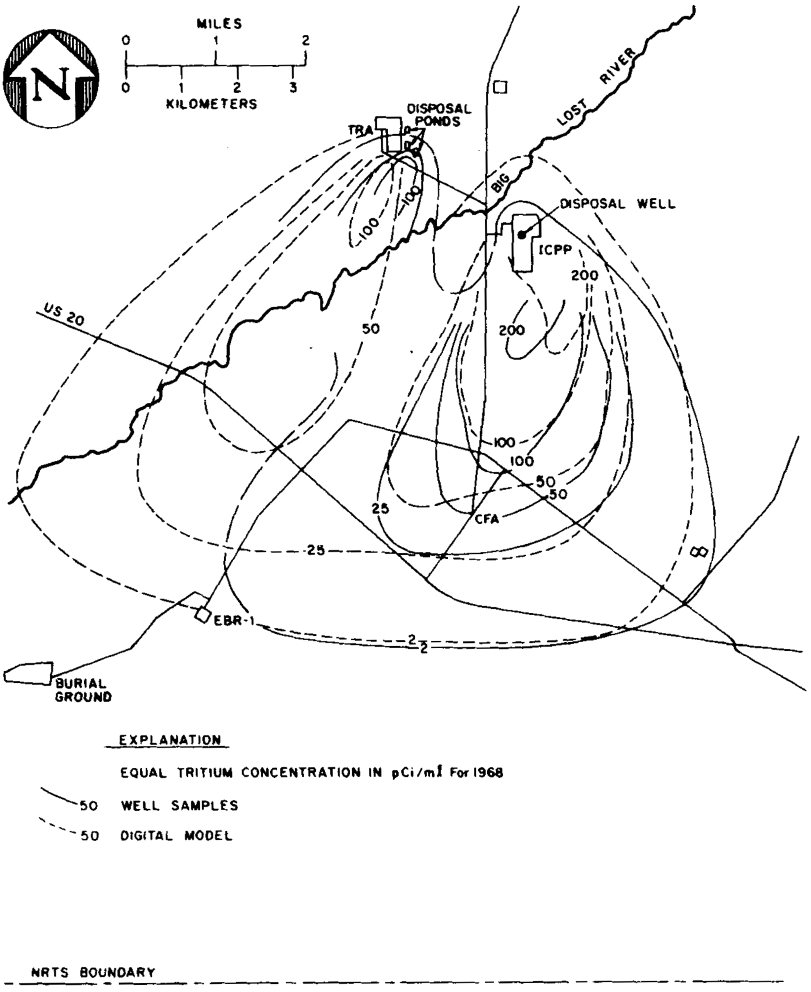

Fig. 6.4.5. Comparison of computed and measured concentration curves for tritium (Robertson, 1974).

strontium model for a uniform sorption-distribution coefficient. The large value of the lateral dispersion coefficient is probably due to the very large scale of the model and to the fissured nature of the aquifer.

6.4.5. *A forecasting model of pollution*

The dispersion scheme can be used as a forecasting model for various hydrologic and disposal conditions.

CHAPTER 7

POLLUTION AND THE MANAGEMENT OF WATER RESOURCES — A GENERAL METHODOLOGY

The economic importance of water is obvious and with growing needs all the water resources become important and especially groundwater which is water stocked in natural reservoirs. Water is used in two principal ways, for consumption (human, agricultural, industrial) and for transportation; by this last word we mean the carrying away of wastes, both human and industrial. Of course this transportation of wastes implies a cumulative degradation of water quality, sometimes tempered by self-purification processes and usually governed by dispersion models; this phenomenon is pollution.

Imagine two users of the water of an aquifer: the creation of the pollution by the upstream user may yield economic stresses on the downstream user, if pollution has not been reduced to an acceptable level during transportation. For instance an industry needs a water with certain quality specifications, which it may not find in an already polluted water; it will invest in purification devices or it will bring water from far away; its economy will be influenced by pollution acting on the quality of the water and also on its quantity.

In general, we can say that pollution is a constant degradation factor of water, which influences both its quality and quantity: for instance, a qualitative property of water may be used (such as its refrigeration property) and not an amount of water; but the quality of the water depends on the rate of pollution, which is a function of both the carried quantity of pollution and the carrying amount of water.

Thus the quality and quantity of water are interdependent notions and the economic study of a pollution, i.e. of the quality of water, is tightly linked to the economic study of water itself; pollution studies are part of the management of water resources.

Groundwater pollution is a factor of groundwater management, itself part of water management; thus groundwater pollution must not be treated separately from other economic aspects of water.

In the previous chapters, we have seen that pollution problems have technical solutions, with fairly good approximations; now when speaking economically, must we consider pollution as *the* problem?

Is it so expensive to treat pollution that financial difficulties cannot be overcome? To answer, we quote an example due to Emsellem (1972b) made for river waters, but of course even more valid for groundwater. It is possible to estimate the cost of suppressing all arrivals of pollution to rivers in France, and surprisingly this cost is rather low. A citizen and his economic activity are represented by an equivalent inhabitant, worth three inhabitants, which means that France has a population of 150 million equivalent-inhabitants. The mean investment for one equivalent-inhabitant is $30; maintenance costs of purification stations represent 6% per year of the investment. The investment is thus $150{,}000{,}000 \times 30 = \$4500$ million.

To simplify, this program is financed on a long term; this sum is thus doubled to take into account the interest rate and will be paid in ten years. This yields $9000/10 + 0,06 \times 4500 \approx \$120$ million.

This amount should be compared to the budget of the country, which amounts to $4000 million. The treatment of pollution, or its storage, are not as expensive as thought!

Thus the problem is not "pollution is the tragedy of the century", because its solutions exist both technologically and financially. The problem is "facing the development problems of our society, do we give priority to pollution problems?" If the answer is yes, which is a good approximation, do we have the right tools, financial, fiscal, administrative and technical to reach the objective without neglecting other priority objectives?

The real difficulty of the problem is not pollution by itself, but the political definition of the national objectives: the pollution programs must be included in sets of priority objectives, discussed at the political level.

In this chapter, we give an outline of an integrated study of water-resources management, both technically and economically, presenting a methodology used to prepare the technical files, which are the kernel of the study, and a practical economic approach already successfully used for water-resources problems. The methodology is a generalization of that presented in Chapter 3, which was specific to groundwater pollution and uses some mathematical tools which we briefly describe. In the economic approach, we do not detail specific economic models — this is not the aim of this book, and should be left to the economists — but we provide the engineer, hydrologist, and physicist with practical and simple rules to help him understand and direct an integrated water-resources study including pollution factors.

7.1. TECHNICAL METHODOLOGY

The management of water resources has an ecologic and economic component, water quality. Water quality can be quantified, by introducing pollution contents, diffusion, dispersion, convection and integrated in simulation models. Calibrated simulation models are generally used to forecast and they are mainly mathematical models. These "quantity—quality" models take place between field operations and economical and political decisions; they are used to identify and treat field parameters, and to forecast their evolutions under various working assumptions, their results forming the starting points of economic models.

The various necessary operations to go from the field to the forecasting models and their results, are strictly defined within a methodology, the aim of which is to optimize the collection and treatment of the useful field data.

The methodology is summarized in the flow chart of Fig. 7.1.1 which shows the logical sequence of operations (Emsellem et al., 1973).

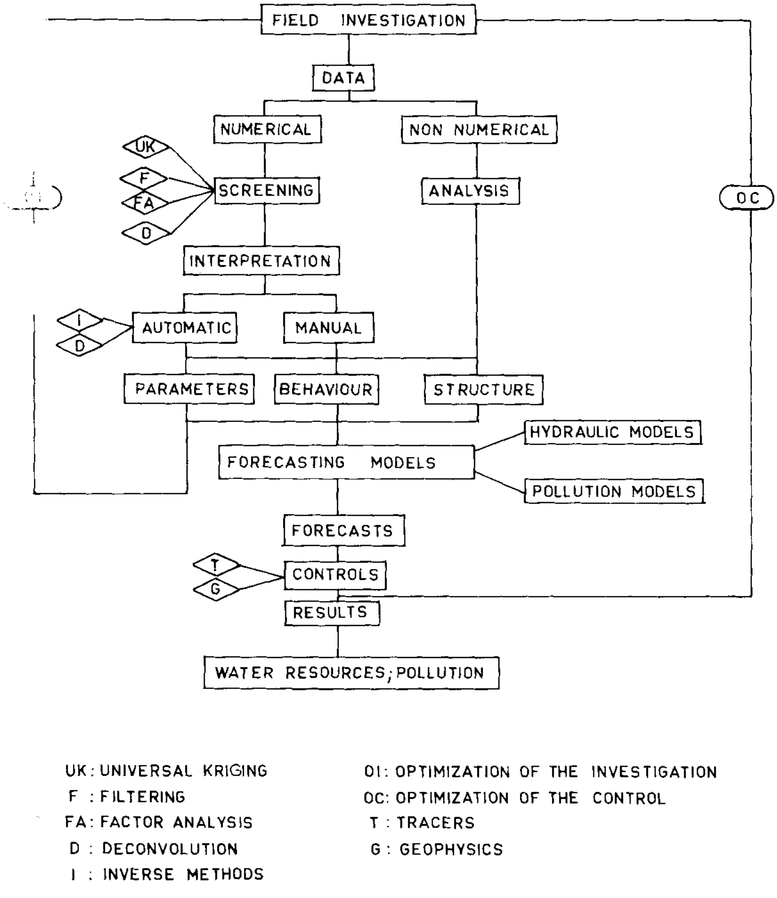

Fig. 7.1.1. General methodology flow chart.

The operations start in the field, with the investigations. These give two sets of information, numerical and non-numerical data. The numerical data are hydrometeorological, geophysical, hydraulic and chemical information; the non-numerical data are information about the geology, the lithology and the structure.

These data are screened and then used to identify the system. The system is defined by its structure, the parameters of its elementary blocks and its behaviour under perturbations. It should be noticed that the knowledge of structure and parameters yields the behaviour; and also, that the knowledge of structure and behaviour yields the parameters; this is very useful as information on these three characteristics is always available: it allows the derivation and calibration of models by using the necessary consistence between model and information.

Once the model has been built, it may be necessary to go back to the field because of lack of information and the optimization of the field investigations can be automatically directed with the help of a computer.

Once the model is calibrated, it is used to forecast the behaviour of the hydraulic system under new operations or new developments. Of course, the forecasting has to be checked and means of control have to be set and optimized by computer.

The methodology appears to be divided up into two parts: (1) preparation and treatment of the information; and (2) derivation and use of the models.

The distinction between these two aspects is fundamental, as the derivation and the use of a model must comprise a set of controls to localize the errors in the available data and also in the adopted interpretation structure which it simulates. § 7.2 examines the various tools used to prepare and treat the information, while § 7.3 describes the adopted models.

7.2. PREPARATION AND TREATMENT OF THE INFORMATION

The flow chart comprises four blocks which are absolutely necessary for the derivation and use of the models: (1) system identification; (2) screening of numerical informations; (3) structuration of non-numerical informations; and (4) optimization of the investigation and control sets. Here is some information about the various tools that have to be used within these blocks.

7.2.1. System identification

The behaviour of a system under perturbations is determined in two possible ways.

(1) The system is internally investigated to determine its structure and to measure the values of its characteristic parameters. Relationships between these parameters are then determined by observing the system's behaviour and considering the physical laws governing the phenomena which take place in the system. A model is derived, which represents reality as closely as possible.

(2) The investigator does not try to understand the physics of the system. He considers the system as a black box and measures the response of the

system to a given external perturbation. It is the method of increasing covering, an application of which is the impulse-response analysis method or deconvolution. It consists in estimating the value of the unknown variable which best satisfies a partial differential equation in the whole domain; then the partition of the domain into subdomains is considered, and on each subdomain the mean values, satisfying the partial differential equation the best, are computed. The process is iterated by partitioning the subdomains. The basic idea of such a method is that data are given with errors not uniformly distributed in space or time; any local modification of the parameter estimate implies the same modification of the values of the parameters everywhere else, which erases sharp local errors and assures numerical stability. This method has been applied to inverse problems, such as the determination of the transmissivities from piezometric data (Emsellem and De Marsily, 1971) and to deconvolution problems such as the determination of unit hydrographs (Emsellem et al., 1971).

The behaviour of a system can be quantified by type-curves, from impulse response data. This method is detailed in §5.3.

7.2.2. Screening of numerical information

Once the information has been structured, it is screened and various techniques can be used.

Universal kriging

Kriging is an estimation method introduced by Matheron (1965, 1969, 1971) for mining applications; it finds the best possible linear estimator of the grade of a panel, taking into account all the available information, i.e. the assay values of the various collected samples either inside or outside the given panel. Kriging assigns a weight to the assay of each sample, these weights being computed in order to minimize the resultant estimation variance according to the geometrical characteristics of the problem (shapes, dimensions, relative setting of the panel and the samples). Intuitively a low weight will be assigned to distant samples and conversely, except when complex phenomena appear.

The effective computation of the proper optimal weights of the samples is based upon certain assumptions about the structural characteristics of the studied orebody by means of the *variogram* of the *random function*, a realization of which is the set of punctual assays.

Such a random function has been called by Matheron, a "regionalized random variable", and is a function of space, the values of which vary from one point to another, with some continuity and the variation of which cannot be represented by an extrapolable mathematical law; for instance, the set of depths of the bottom of the sea, as recorded by sounding from a ship, is the realization of such a regionalized variable.

An extreme case of regionalized variable appears when its values, taken from any two different points, are independent; all intermediate, structural cases are possible until a complete organization of the space.

A variogram is a most important tool to describe these various structural cases. Take x and $x + h$, two points of space (one, two or three dimensions) and set $f(x)$, $f(x + h)$, the values of the regionalized variable f, at these points. The variogram, or more correctly, the semi-variogram, is a function $\gamma(h)$ defined by:

$$\gamma(h) = \frac{1}{2} E\,[f(x + h) - f(x)]^2$$

where $E(x)$ is the mathematical expectation of the random variable x.

Assuming the intrinsic hypothesis, i.e. for any vector h, the increment $f(x_0 + h) - f(x_0)$ has an expectation and a variance which are independent of the support point x_0', we see that γ is not linked to any particular position of x but to the increment between two moving points, x, $x + h$. It helps to grab quantitatively whether what happens at one point looks like what happens in the average at a distance h. It quantifies the notion of the influence zone of a sample and the structure of a body, essentially through its behaviour near the origin and at infinity.

(1) The continuity and the regularity, in space of f are expressed by the behaviour of $\gamma(h)$ near the origin. There are roughly four cases (Fig. 7.2.1):

(a) parabolic trend: $\gamma(h)$ is twice differentiable at $h = 0$, $f(x)$ is then differentiable and highly regular (in the mean square*);

(b) linear behaviour: $\gamma(h)$ is continuous but not differentiable at $h = 0$, f is continuous (in the mean square*) but not differentiable and much less regular;

(c) nugget effect: $\gamma(h)$ does not tend to 0 when h tends to 0, f is not even continuous in the mean square;

(d) $f(x)$ and $f(x + h)$ are independent for any two distinct points; it is the "white noise" of the physicists.

(2) The behaviour of γ at infinity displays the connections between the blocks of the studied system: if the variogram ends by a horizontal part, starting at a range a (Fig. 7.2.2a), $f(x)$ and $f(x + h)$ are without correlation for $h > a$; if the variogram ends by an ascending part there is a regional drift (Fig. 7.2.2b).

---

*The random function $y(x)$ is said to be continuous in the mean square if we have $E[\{Y(x + h) - Y(x)\}^2] \to 0$ when $h \to 0$.

In a one-dimensional space, we define the random function $Y'(x)$ as the derivative in the mean-square sense of the random function $Y(x)$ if $E[\{[Y(x + h) - Y(x)]/h - Y'(x)\}^2] \to 0$ when $h \to 0$.

There are similar definitions for n-dimensional spaces with $n > 1$.

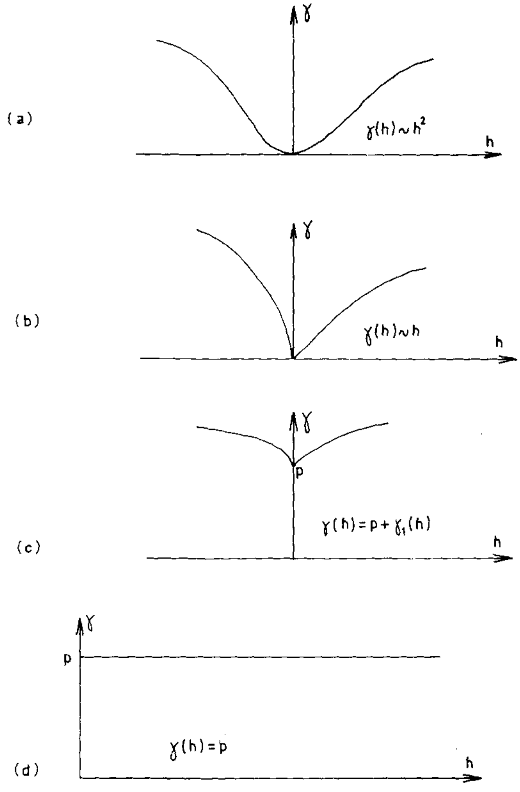

Fig. 7.2.1.

Of course, the range will depend on the direction of vector *h*, which may reveal preferential directions of the variable in the field. In general, different behaviours of the variogram in different directions of space reveal anisotropies.

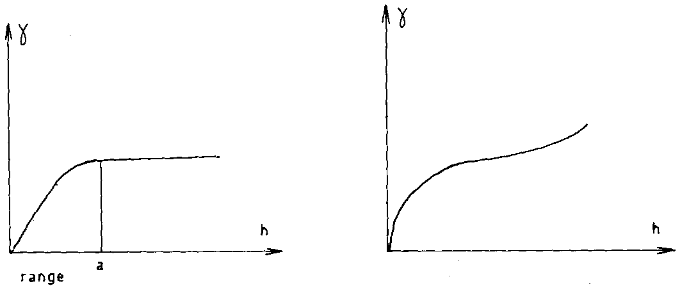

(a) (b)

Fig. 7.2.2.

Matheron has generalized kriging into universal kriging to estimate drifts (sometimes also called trends) of regionalized variables, the drift of $f(x)$ being its a priori expectation $E\ [f(x)]$.

Applied to hydrology and pollution, kriging first yields maps of the quantity measured on a discrete set of points: for instance, the concentrations of a pollutant being measured in a set of points at a given time t, kriging yields the continuous distribution of concentrations in space at t. But it is much more than a simple interpolation method, it yields the structure of the phenomenon in space, an estimate of the white noise, and the estimation variance; i.e., it tells how reliable the estimation is in the whole space. Further on in the paragraph, we shall see how important it is for the optimization of measurement grids and for the optimal determination of missing data.

Filtering

Experimental errors are always introduced in the measurements of real data which yield an information and a noise. Experimental data should be filtered by using the available information on the signal (regularity, frequency, energy) and on the noise (zero means or estimation of the noise standard deviation).

Kriging and standard statistical methods can be used. The data being generally used in models, an analysis of the model's sensitivity to errors should be performed, a theoretical example of which is presented in § 8.

Factor-analysis of correspondences

The measurements of a given phenomenon lead to defining several individuals (measured objects), which take a set of characters (measurements): for instance, a set of level measurements at given dates (characters) for a set of piezometers (individuals), or a set of chemical analyses (characters) for a set of water samples (individuals).

The correspondence analysis represents individuals and characters by points, and the group of points, associated in clouds, shows the system organization. The clouds and their dispersion give the necessary parameters and the roughness of the interpretation structure for a given treatment (Benzecri et al., 1973).

For pollution problems, a form of this correspondence analysis, called the factor analysis of stabilities and evolutions, is generally used to include the time variable (Monget et al., 1974). It describes the principal features of the evolution of a pollution process without a priori assumptions as to the space—time relationships; furthermore, it allows comparisons between theoretical and observed global evolutions of the process with accidental local fluctuations.

The factor analysis of correspondence can be used in three ways.

(1) Descriptive analysis of causes and effects, by determining the principal

inertia axes of the clouds and the minimal number of variables representing the system with a sufficient variance; this is a filtering which erases the noise. Individuals with similar profiles are grouped, which structures the set of individuals and the set of characters.

(2) Structuring analysis by ellipses: a character being fixed for a set of individuals, their clouds present inertia axes which are projected on the factorial plane and are represented by ellipses. These ellipses can be classified to refine the structuration of the data.

(3) Structuring analysis by a factor analysis of the correspondences of variograms: when several variables are simultaneously measured, it may be interesting to determine comparable zones and to observe which measured factor yields possible differences. In each zone a local variogram is computed. The local variograms are then classified by correspondence analysis which yields the zones with similar structures. Of course, such a process must be used very carefully, although it is now automatic.

Deconvolution

The measurement of some quantity is done by experimental devices. If such a device does not measure point values, but detects and integrates all values around the investigated point, it is necessary to treat the results to obtain the real value at that point. For instance (Fried et al., 1972), during the investigation of radioactivity in an aquifer, the probe does not give point values but integrates the radioactivity in the ground around it. Usually it can be assumed that the operation is linear and is a convolution; the space properties of the measurement device being described by some functions $f(x)$, the real values being the function $E(x)$ and the observed values, through the probe, being $s(x)$, f, E and s satisfy the relationship:

$$s(x) = \int_S f(x-t)e(t)\mathrm{d}t$$

S being the space where the measurements are performed.

The problem is then: knowing f and s, to determine e, the space distribution of real values; of course, the first problem will be to determine f, the function of the measurement device, also called the impulse response of the system (s is equal to f if e is a Dirac δ function). The problem is solved by the deconvolution method, briefly described in § 7.2.1.

7.2.3. Structuration of non-numerical information

Most of the time the information is both numerical and non-numerical: for instance, during a pollution experiment we need the hydraulic parameters of the aquifer, but because their measurements are expensive, we have to use the geological and lithological descriptions of the ground obtained from direct field investigation.

A quantification of these data is not possible, but these non-numerical data do give upper and lower limits to the model parameters. For instance, it is possible to establish classes of soils defined by the ranges of the various hydraulic and pollution parameters and even, with good experience, to localize a given soil within its class and reduce the estimation range of its parameters. Such an analysis has been introduced in Chapter 3 to extend the results obtained in a given area to other areas by geological analogies.

7.2.4. Optimization of the investigation and control nets

Optimization of the investigation

Field data are used to derive simulation and forecasting models, and at each stage of the investigation, the problem is to determine whether the acquired information is accurate and dense enough, i.e. whether there are enough accurate measurements to derive a significant model.

For instance, consider piezometric measurements in an aquifer; the optimization of the investigation of the characteristics of an aquifer (piezometric levels) consists in estimating the minimal number of measurement points (boreholes) to obtain a given knowledge of the characteristics.

Optimization is first obtained by kriging, basically as follows: the initial grid of measurement points is kriged and the map of the estimation variances is drawn; in the areas where the estimation variance is larger than the expected experimental errors, the grid will be completed by new measurement points and the kriging process is iterated. Thus kriging automatically localizes the points which improve the overall knowledge the best, which of course reduces the number of measurement points.

If the state of knowledge is already rather good, inverse methods and kriging can be used together: for instance, piezometric levels are used to identify the transmissivities of the aquifer by solving an inverse problem with the increasing-covering method (§ 7.2.1); during identification, interpretation-error residues appear in the subdomains and these residues may decrease or stabilize during the iteration process; if they stabilize, it means that the available information cannot tell more and that:

— the data are erroneous
— the data are not in sufficient quantity
— the structure of interpretation is not correct.

The superposition of the maps of identification residues and of estimation variances shows, in the areas with high residue values, that: (1) the density of piezometric measurements is not sufficient and indicates whether it has to be increased by new drillings (high variance); (2) the piezometric measurements are erroneous (high variance and high density); or (3) that the hydrogeologic knowledge of the structure is not correct (low variance).

If both the residue and the variance are low, then optimal conditions are reached and the work is finished.

Optimization of the control

Forecasting models should be controlled while working: some parameters must be constantly measured to make sure that forecasts are good; but measurements are costly and it is desirable to reduce their number without loosing too much information, whilst keeping an optimal set of measurements in order to be able to determine the information that is not measured.

Factor analysis provides an automatic classification of comparable measurement groups and in each group, only one measurement has to be chosen to determine the others. The reduction of the number of measurement points depends on the required accuracy for the missing data.

7.3. THE MODELS

All through this book, we have seen that the handling of pollution models (or quality models as they are often called) requires knowledge of the mechanics of the groundwater flow; and especially the velocities. Sometimes the velocities are measured directly (in the case of local pollution studies), but most of the time and especially for the management of pollution in large areas, they will be computed by models. This is the reason why we briefly present here the various possible hydraulic models; further, as they can be "solved" without any quality consideration, we present them separately from the pollution models.

7.3.1. The hydraulic models

The hydraulic models are divided up into three categories: groundwater flow, surface flow and non-saturated flow. For groundwater pollution hydraulic models of groundwater flow are the most important; we have detailed their use in Chapter 9 and given their basic physical characteristics in Appendix II. But surface and non-saturated flows determine the boundary conditions of the groundwater hydraulic and pollution models and deserve to be mentioned in this paragraph.

Groundwater models

Consider a cube of aquifer. A horizontal flux of water travels through its vertical faces from or to the neighbouring cubes, these fluxes are positive or negative, according to the flow direction. Also a vertical flux of water travels through its horizontal faces from upper and lower cubes and this is called drainage flow.

The algebraic sum of these fluxes is called the transport flux. In addition, feeding from independent sources, such as rainwater, rivers or pumping wells, yields a flux of water called transit flux and this is taken as positive if water is brought to the block and as negative if water is taken out from the block.

During some time period, the block either gains or looses some water: this algebraic quantity is called stocked-water flux. The basic relationship of groundwater modelling is then:

$$\text{stocked flux} = \text{transit flux} + \text{transport flux} \qquad [7.3.1]$$

The transport flux is expressed by means of the transmissivities and piezometries of the block and its neighbours, the transit flux is expressed by means of pumpings or injections, evaporation and infiltration; the stocked-water variations are related to the pressure variations of the reservoir through the storage coefficient and the stocked flux is characterized by the variations of the piezometric levels with time. For an infinitesimal block, [7.3.1] yields the classical hydrologic equation:

$$\operatorname{div}(T \operatorname{grad} h) = S\frac{\partial h}{\partial t} + Q \qquad [7.3.2]$$

where h is the head (piezometry), S the storage coefficient, T the transmissivity and Q the transfer water (see §9.5.1).

The domain of application of the model is taken as large as possible in order to minimize the influence of boundary-condition errors on the investigated areas.

Of course, [7.3.2] is a model of quantity, as shown by the use of the transmissivity concept. It is a regional model and the velocities which can be derived are mean regional velocities. To model local flow conditions it has to be refined and permeability concepts have to be directly introduced, by Darcy's law and the continuity equation; anyway, locally, it is always better, if possible, to measure the velocities experimentally.

Surface-water models

For water-resources management, two types of problem have to be modelled.

(1) The forecasting of floods, which is a problem of safety; there are several well-known techniques, which are usually based on impulse-response methods and convolutions: the pluviometry is convoluted with some watershed transfer function to yield the amount of water reaching the rivers.

(2) The relationships between groundwaters and surface waters. Groundwater pollution widely depends on these relationships: for instance, pollution from a sanitary landfill will depend on the pluviometry, the infiltration rate and also the surface run-off which may dilute the pollutants but also extend the superficial polluted zone, thus changing the boundary conditions for groundwater pollution flow. Hydraulic models integrating groundwater and surface-water flows have been introduced: the classical hydrologic model (defined for instance by [7.3.2]) is used and the superficial-water system is a boundary condition of the groundwater model.

The inputs of the superficial system are the meteorological phenomena, which are convoluted with the transfer functions of the superficial system to yield the input of the groundwater model, transferred to the underground blocks by classical connections between the various blocks of the model.

Non-saturated flow

With regards to pollution, the non-saturated zone is very important, because most of the chemical reactions, such as biodegradation and self-purification, occur while surface water is moving through it. But the movement of pollution and especially its dispersion are not yet known; laboratory studies have started on the subject, based on physical models, but no satisfactory mathematical model exists. What is usually done, is to make a very conservative assumption, saying that the non-saturated zone does not influence pollution concentrations and only delays pollution flow, the delay being computed by Darcy's law and gravity flow with vertical-permeability coefficients and without dispersion.

With regards to water resources, Emsellem (1971), has noticed two phenomena linked to the behaviour of the non-saturated zone: deep-pumped aquifers drain shallow aquifers and the non-saturated zone; the water content of this zone decreases because of the decrease of the superficial aquifer levels, which means that the permeability decreases; infiltration is then much more difficult and feeding also decreases, which accelerates the decrease of the superficial levels. Deep pumping may then erase marshes or streams, and, for instance, the feeding of a river from the aquifer to prevent too much lowering of the river, may dry the upstream part of this river. Another phenomenon is that agriculture becomes more and more difficult, as plant roots do not reach the water, and the paradox is that part of this pumped groundwater has to be reinjected by irrigation.

7.3.2. The pollution models

Two types of pollution models are used in water-resources management: groundwater-pollution models and surface-water pollution models. The groundwater-pollution models are the object of this book and are detailed in the other chapters; within the context of management, let us emphasize one result: these models are derived from laboratory studies on the dispersion mechanisms but they have determined the field investigational procedures.

Due to the interconnections between streams and aquifers, stream pollution may influence aquifer pollution and conversely.

A stream is a boundary condition in piezometric head for the hydraulic model and in pollution concentration and flux for the groundwater-pollution model. These concentration conditions are the outputs of stream-pollution models which can be dispersion, self-purification and impulse-response models.

(1) Dispersion models have the same characteristics as their groundwater counterparts; dispersion coefficients result from turbulence considerations. They are valid for conservative pollution only; but oxydoreduction, biological and physico-chemical phenomena reduce pollution in streams, which leads to self-purification models.

(2) A classical self-purification model, used in many studies, is based on Streeter-Phelps equations. Set b the biologic oxygen demand (in mg/l) and d the dissolved oxygen deficit (in mg/l), assume:

$$\frac{db}{dt} = -K_1 b \quad \text{and} \quad \frac{dd}{dt} = K_1 b - K_2 d \qquad [7.3.3]$$

where K_1 is the rate of desoxygenation per day and K_2 the rate of oxygenation per day and t is time in days. The integration of [7.3.3] yields the following expression of d and b as functions of time:

$$b = b_0 C_1 \quad \text{and} \quad d = K b_0 (C_1 - C_2) + d_0 C_2 \qquad [7.3.4]$$

where b_0 and d_0 are respectively the values of b and d for $t = 0$, $C_1 = \exp(-K_1 t)$, $C_2 = \exp(-K_2 t)$, and $K = K_1/(K_2 - K_1)$.

Equation [7.3.4] describes self-purification in a stream. If the water velocity is constant, time t is proportional to a travelled distance and [7.3.4] can be written with a new variable, the curvilinear abscissa of a point in the stream. Water velocity depends on the flow rate, such as K_2; moreover K_1 and K_2 are functions of the temperature of the stream, which leads various authors to divide the streams into sections where flow rate and temperature are constant and with a length of the order of a few kilometers.

(3) As dispersion models loose their meaning over rather long distances, an impulse-response technique has been introduced (Guizerix et al., 1970): a pollution wave is observed by a control station; the origin of the pollution can be localized if there exists a map of the amounts of pollution emitted by the known sources along the stream. The preliminary experimental determination of the transfer function of the river allows a deconvolution of the recorded pollution wave and a comparison to the map of possible amounts of pollution, localizes the pollution sources.

7.4. MANAGEMENT CONCEPTS

Extensive work on these problems has been performed by Emsellem (1972a, b; 1974a, b) who has given new orientations around simple concepts.

7.4.1. Place of groundwater-pollution management

At the beginning, pollution was treated separately from other economic aspects of water and the basic idea was: the polluter will pay for pollution and the user of water will pay for the water he uses. The amount of the taxes, defined according to these aims, will be devoted to developing resources and to fight pollution. These taxes are voted, thus negotiated and established at some market level.

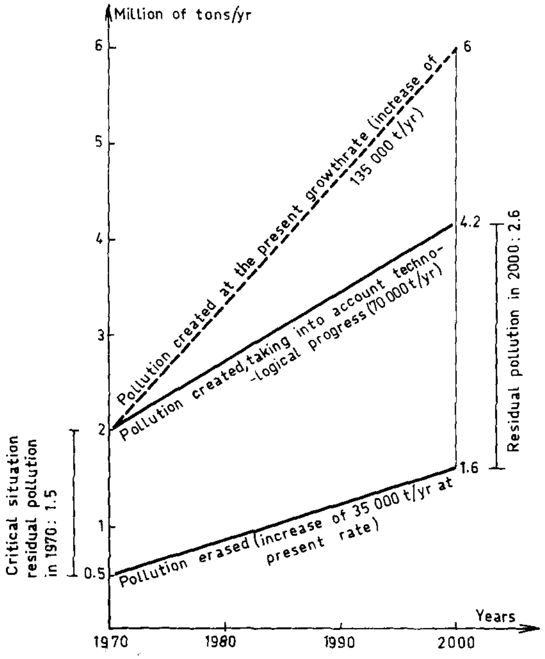

Fig. 7.4.1. Comparison between created pollution and erased pollution, according to present planning.

Since 1964 France has been divided up into six financial watershed agencies which provide water to their areas and fight against pollution. An agency council gathers together people from the state, from urban communities and from economic sectors. Fig. 7.4.1 shows that in 1970 the amount of taxes in a French watershed agency represents a quarter of the amount needed to erase the existing pollution. If the rate of increase of the finances available does not change, this difference will greatly increase in absolute value. Thus, the agency had to modify its initial tax policy to progressively reduce the difference (Fig. 7.4.2.).

The underlying problem of Figs. 7.4.1 and 7.4.2 is that within the political and financial context of the time, in both the agency and in the country as a

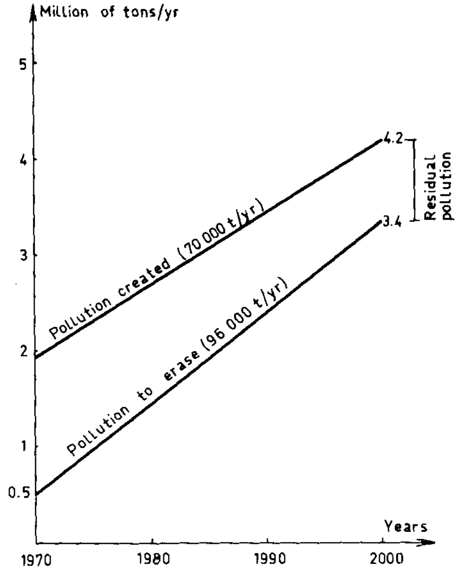

Fig. 7.4.2. Proposal to erase 80% of the pollution created in the watershed in 2000.

whole, the fight against pollution was not a top-priority objective: when the pollution taxes were set, the financial availabilities of groups and activities using or polluting water were at such levels that the first financial income from the taxes was not sufficient to seriously reduce pollution levels; other economic sectors had already used some of the financial availabilities of the groups and activities. This means that political realities have defined pollution as being one problem among others, and not as a single problem, that could be treated separately. Of course at the beginning, the various implications of a pollution project and its relationships with other objectives, were not known. Actually, many effects in the economics of water are not always very obviously interrelated. To illustrate this fact, consider a dam which provides electricity: as all electric distribution networks are interconnected, obviously this dam has a national interest, at the scale of the country; now consider a dam which prevents flooding or which irrigates an agricultural area: its effects are local, but it would be wrong to invest in its building by taking into account the local effects only. In the economy of the country, an increase of public safety or an increase of agricultural production may have long range, although not obvious, financial implications.

Thus, groundwater-pollution management should be considered within the wider scope of water-resources management, which itself cannot be separated from other political development objectives. Results and methodology of water-resources management should contain all possible information on pollution management.

7.4.2. Elements of water-resources management

Outline of the methodology

The management of water resources is first a problem of choices.

(1) Choice of priorities. There is not enough water and a classification of priorities has to be made between groups and activities. It should be stressed that the occurrence of water by itself does not develop an activity: water is a limiting factor in development but not a structuring factor, at least not in industrialized countries.

(2) Choice of payers. It has been said at the beginning of this chapter that the cost of erasing pollution was well within the financial possibilities of a country. But the problem is to decide who is going to pay.

The problem can be schematized by considering the country as a black box containing activities and groups, and submitted to a political program of development with a classification of objectives.

For example group A gives 5, group B gives 9, group C gives 2 and group D gives 13; after some time by the natural mechanism of economics A, B, C and D respectively receive 6, 11, 4, 10. C has been favoured, A and B are at the same level and D has been wronged. This means that the country by its general management, has emphasized the development of C, probably because this development corresponds to the general aims of the country. It is a problem of transfers which represent a political trend implying a development of C and a recession of D, and which leads to asking whether the transfer system and the increased rate of activities and groups is compatible with such a policy. If the answer is no, it will be necessary to choose which economical, legal and financial tools have to be modified. If the answer is yes, it will be necessary to forecast the coming difficulties, as for instance, the handling of D.

Thus, the outlines of a methodology of water management appear: several political programs exist, based upon the fulfillment of objectives by consistent options depending on various possible investments. It should be investigated whether these options can be realized, whether the available tools allow of realizing these options within the financial, sociological, technical and legal context, and whether these options have to be corrected. Then the analysis of consequences and means characterizing each set of options yields a set of synthetic files which, compared to each other, will help the men who decide, the men who develop and the men who bear responsibilities to make a clear choice.

At this stage, it should be stressed, that the first question never is: an investment in a hydraulic development project has been decided, how can it be optimized? A well-posed problem always implies a choice between realizations: a watershed is not developed for the sake of best using its water but, for a given development assumption, water has to be used the best.

Elements of planning analysis

The country should be divided up into hydraulically homogeneous sets (watersheds for instance). Of course, these sets should not be too small. One set will be modelled at the regional scale, thus first divided up into blocks, hydraulically, economically and administratively homogeneous. Hydraulic and pollution models will connect these blocks, for a given development option. These models propagate quality and quantity fluxes and establish relationships between upstream and downstream consumers. On this oriented grid, the economic activity will be projected at various times (1980, 2000, for example).

Then needs in water will be estimated. They result from the economical activity at the chosen times and depend on the consumer. Thus, a typology of consumers expressed in quality and quantity needs, will be derived from the real data collected in the chosen geographical set. This description of the consumers, linked to forecasts of activity levels per group, yields an estimate of the needs in water for a group and for a block of the grid. A circulation model of quality and quantity fluxes is derived, as a forecasting model.

Then needs and resources should be compared. Thus, the typology of the existing, planned or possible hydraulic works will be derived to determine their influence on the hydraulic functions of the forecasting model. They will be included in a simulation model of the hydraulic system.

At last the project must be financed. First, of course, one must make sure that it can be realized globally. Then existing legal procedures should be investigated, which distribute the costs between those who pay. By comparing transfers and objectives of the option, it is possible to determine whether changes should take place. This procedure is summarized in Emsellem's flow chart (Fig. 7.4.3).

Three types of blocks appear:

(1) Alternate political parameters. These depend on the politician whose function it is to have a global view of the area and its future, with objectives and means. These parameters consist of socio-economical development assumptions, a development policy and financial possibilities. The politician must assume the consistency between these parameters and a given set of these three political parameters determines a solution. Of course, there are many possible solutions.

(2) Treatment tools. These are models or typologies. For instance, a model of employment (the development assumption is expressed in terms of employment per group), a forecasting model (the development assumption is expressed in terms of hydraulic functions, based upon the needs in water), a simulation model (the development assumption is verified in terms of hydraulic works satisfying the known needs) and a cost-distribution model (development costs are distributed among the consumers). Also two typologies have been defined, a typology of consumers and a typology of hydraulic works.

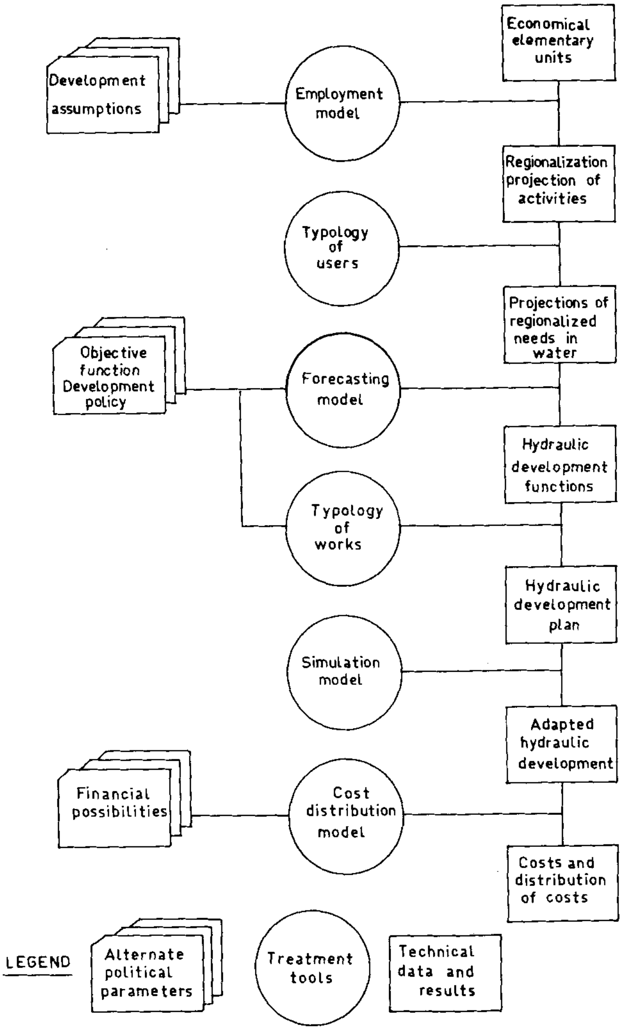

Fig. 7.4.3. Logical sequence of operation blocks for water management.

(3) Technical data and results. These are the hydraulic solution of the set of political parameters.

Of course, this approach may yield an infinity of possible solutions by varying the size of the hydraulic works for instance. Then a series of technical criteria should be used to optimize the hydraulic development project, within a given political option, which clarifies the choice between options.

7.4.3. Basic principles of an approach to water-resources management

As a conclusion to this chapter, we propose the basic principles of

Emsellem's alternative-options approach to the management of water resources as a base of thought for the water economist, the engineer and the student. Of course, this is not the only possible approach, but it has yielded results that can be applied directly as such to groundwater-pollution management and represents a very good working tool.

Refusal of the cost—benefit analysis (C.B.A.)

The C.B.A. is interesting as it introduces a global objective function that can be analyzed by computers, but the C.B.A. has the following weaknesses:

(1) It is difficult to define and model some results which are then neglected: for example a tax on industry will raise its prices, influence its exports and the level of its activities.

(2) Some aspects of a problem may be neglected to reduce its complexity: for instance, pollution alone will be studied and we have seen that this is a mistake.

(3) Time is a very important factor, as it greatly influences the price of money, hence the advantages of the investment loans.

(4) A stress and a variable are not considered equally in the objective function: a stress may be satisfied when a production variable is not maximum.

It is possible to overcome these difficulties, but, fundamentally, the C.B.A. introduces a unit which is the monetary value of various elements and takes into account market parameters only. Of course, it could be possible to give a value to ideas or to non-numerical parameters such as politics, environment or life, but it is not an easy task.

Furthermore, the aim will be the optimal use of water and water will be considered as the only structuring factor of growth. This is fine for arid zones, but often wrong for industrialized nations, because in most cases, for an individual consumer water is only a marginal factor of production and for a group of consumers water can be reused or replaced. Finally, an objective function should represent the preference of collectivities which is valid for well-identified collectivities with one decision factor. When, however, the number of decision-takers increases and when individual interests diverge, then the derivation of only one optimal objective function is very hard and does not represent reality. There exist many optimal, but quite unfeasible, solutions.

The principles

There is not one objective and one decision-maker and the method will not try to optimize well-being, profit or any other criterion of only one group or one activity. What should be attempted, is to reach a balanced development of groups and activities with decision centers determined by institutions, economic mechanisms and traditions.

Although the water is divided between consumers, it should be considered as indivisible collective goods: the consumers are interdependent and modelling should take place in a geographical unit taking into account this interdependence. For instance, a watershed can be considered as a good geographical unit for large-scale studies.

Water is characterized by a set of non-ordered data such as geographical, mechanical or physico-chemical variables. A model must take into account the various laws that govern these variables, which are quality as well as quantity variables. Actually no distinction between quality and quantity should be made, as most of the needs depend on both these factors together.

The economical role of water depends on the climate: in arid zones, for instance a development program can be based on the optimal valorization of water resources, at the national level; in temperate countries, future needs of water depend on regional development programs.

But industrialized countries have become aware of ecological problems and water can become a limiting factor of development: the fight against pollution usually replaces one pollution problem by another, but the economical growth is responsible for this pollution and growth criteria should be completed by ecological criteria.

As a consequence of pollution, many industrialized nations have declared that water is scarce, even if they have huge amounts of it, of course polluted. This particular type of scarcity must be especially accounted for, to prevent great mistakes being committed.

An objective of development could well be the optimization of natural resource and not only the optimization of economic growth.

Numerous hydraulic planning solutions correspond to a given socio-economical development theory of watersheds. The method consists in helping the political choice of solutions by comparing synthetic files: each file is built upon only one political option of development of the set of activities and groups of the geographical units. This defines the needs in water; these needs are satisfied by a set of hydraulic works which put the development objectives in hydraulic terms. These hydraulic works are then financed and their costs distributed among the payers according to transfer laws.

Then the file is complete. It consists of a comparison between needs and resources, including pollution stresses, a distribution of cost charges and the global costs; it defines the expected non-numerical advantages such as the socio-economical development, the environmental priorities, and the general safety. It can be compared to the other files on the basis of objectives, necessary means and consequences. Nothing is optimized as a unique decision factor. The economists and the engineers do not replace the politician, who has the final choice with the help of alternative option files which he can compare.

This Page Intentionally Left Blank

CHAPTER 8

AN INVERSE DISPERSION PROBLEM: THE POINT-DILUTION THEORY

The present theory is part of the attempted solutions to the basic problem of groundwater-pollution studies and modelling, the determination of the dispersion coefficients. It stems from considerations of single-well techniques and the quest for local coefficients, when reduction is sought of the number of measurement points. It shows that it is quite possible to compute the diffusion-operator coefficients from a series of experiments performed at only one point in the medium and provides explicit formulas for these coefficients.

It is based upon the following principles: we impose an initial condition in concentration localized in the neighbourhood of the measurement point and we observe the evolution of concentration with time at that point. On this concentration, we perform some weighted averaging (at some sense, given in the chapter) and start the experiment again with an initial condition even more localized in the neighbourhood of the measurement point. The limit of the weighted averages for increasingly localized initial conditions, yields the dispersion coefficients.

Three cases are successively studied: the isotropic dispersion operator, with constant coefficients; the isotropic dispersion operator with varying coefficients; and eventually the anisotropic dispersion operator with varying coefficients.

Of course, we mean varying coefficients in space but not with time. This chapter is completed by a study of the stability of the solutions of a dispersion problem with respect to the dispersion coefficients, i.e. the behaviour of the difference of the real solution and the theoretical solution computed with the dispersion coefficient obtained by point-dilution.

8.1. PRELIMINARY DEFINITIONS

These definitions are taken from Unterberger and Unterberger (1970, 1971). Consider a vector space X on R of dimension n and Ξ its dual, $|x|^2$ and $\mathrm{d}x$ are a quadratic form and a Lebesgue measure on x, $|\xi|^2$ and $\mathrm{d}\xi$ the corresponding form and measure on Ξ. In this chapter, we only consider $X = R^n$ and $\Xi = R^n$. R^n has its canonical structure of Hilbert space.

Definition 1. Let s be a real number; $H^s(X)$ is the space of distributions

$T \in \mathcal{S}'(X)$ whose Fourier transform $\hat{T}$ is a function satisfying:

$$\int_{\Xi} (1 + |\xi|^2)^s |\hat{T}(\xi)|^2 d\xi < +\infty$$

This space is given the topology defined by the norm:

$$\|T\|_s = \|(1 + |\xi|^2)^{s/2} \hat{T}(\xi)\|_{L^2(\Xi)}$$

and is called Sobolev space of order s.

Definition 2. Let m be a real number; $(Xx\Xi, m)$ is the space of functions a on $Xx\Xi$ with complex values and C^∞ such that:

$$\forall p, q \in \mathbb{N}^n, \quad \forall M \in \mathbb{N}, \quad \exists C > 0:$$

$$(1 + |x|^2)^M \, |D_x^p \partial_\xi^q a(x, \xi)| \leqslant C(1 + |\xi|^2)^{(m - |q|)/2}$$

with $p = (p_1, ..., p_n)$, $q = (q_1, ..., q_n)$, $D_x^p = \left(\dfrac{1}{2i\pi} \dfrac{\partial}{\partial x_1}\right)^{p_1} \cdots \left(\dfrac{1}{2i\pi} \dfrac{\partial}{\partial x_n}\right)^{p_n}$

and: $\partial_\xi^q = \left(\dfrac{\partial}{\partial \xi^1}\right)^{q_1} \cdots \left(\dfrac{\partial}{\partial \xi^n}\right)^{q_n}$, $|q| = q_1 + ... + q_n$

Definition 3. If $a \in (Xx\Xi, m)$, $\operatorname{Op}(a)$ is the operator defined on $\mathcal{S}(X)$ by formula:

$$[\operatorname{Op}(a)(u)](x) = \int_{\Xi} a(x, \xi) \hat{u}(\xi) e^{2i\pi x \xi} d\xi$$

Definition 4. (1) $\epsilon(\Xi, m)$ is the space of functions b, C^∞ on Ξ with complex values such that:

$$\forall q \in \mathbb{N}^n \; \exists C > 0: |\partial_\xi^q b(\xi)| \leqslant C(1 + |\xi|^2)^{(m - |q|)/2}$$

(2) S^m is the direct sum of $\mathcal{S}(Xx\Xi, m)$ and $\epsilon(\Xi, m)$ identified to a functional space on $Xx\Xi$.

Definition 5. We call operator of order $\leqslant m$ any linear operator $A: \mathcal{S}(X) \to \mathcal{S}'(X)$ that can be extended for all s as a continuous operator of $H^s(x)$ into $H^{s-m}(x)$; an operator of order $\leqslant m$ for all real m is called an operator of order $-\infty$.

8.2. THE DETERMINATION OF THE DIFFUSION COEFFICIENT OF AN ISOTROPIC DIFFUSION OPERATOR WITH CONSTANT COEFFICIENTS

The general theory, presented later, of course applies to an operator with constant coefficients. But the results of the general theory are obtained here in the case of the operator with constant coefficients by a direct method only using the classical tools of physical mathematics, as they are taught in most graduate courses for physicists.

The isotropic dispersion equation with constant coefficient is:

$$K\Delta C - \sum_{i=1}^{n} \beta_i \frac{\partial C}{\partial x^i} + \gamma C = \frac{\partial C}{\partial t}$$

where n is the space dimension, and β_i the components of the mean flow velocity. Coefficient γ has various physical interpretations, for instance $-\gamma$ is the reciprocal of a radioactive tracer mean life time.

Lemma. Let c_τ be the x-tempered solution of Cauchy's problem:

$$K\Delta C = \frac{\partial C}{\partial t}, \quad c_\tau(x, 0) = \exp[-\pi\tau(x - x_0)^2] \qquad [8.2.1]$$

where t and K are real and strictly positive, where x_0 belong to R^n. Let s be a real number, strictly comprised between $-n/2$ and 0. The following relationship is verified for all τ:

$$\tau^{-s} \int_0^\infty t^{-s-1} C_\tau(x_0, t) \mathrm{d}t = 2^{2s}\pi^s \frac{\Gamma(-s)\,\Gamma(s + n/2)}{\Gamma(n/2)} K^s \qquad [8.2.2]$$

Proof. To simplify the notations, take $x_0 = 0$, the general case is immediately given by the translation x_0.

Set $a^2 = \sum_{i=1}^{n} a_i^2$

Apply Fourier transform in x to the system [8.2.1]:

$$-4\pi^2 \xi^2 K\hat{c} = \frac{\mathrm{d}\hat{c}}{\mathrm{d}t}, \qquad \hat{c}_\tau(\xi, 0) = \tau^{-n/2} \exp(-\pi\xi^2/\tau)$$

which yields:

$$\hat{c}_\tau(\xi, t) = \tau^{-n/2} \exp\left[-\pi\left(4\pi K t + \frac{1}{\tau}\right)\xi^2\right]$$

and by inverse Fourier transform:

$$c_\tau(0,t) = (4\pi K t\tau + 1)^{-n/2}$$

Taking the value back into the integral [8.2.2] and doing the successive changes of variables $\sigma = 4\pi K t\tau$ and $v = 1/(\sigma+1)$, we obtain:

$$\begin{aligned}
\tau^{-s}\int_0^\infty t^{-s-1}c_\tau(0,t)\mathrm{d}t &= \tau^{-s}\int_0^\infty t^{-s-1}(4\pi K t\tau + 1)^{-n/2}\mathrm{d}t\\
&= \int_0^\infty 2^{2s}\pi^s K^s \sigma^{-s-1}(\sigma+1)^{-n/2}\mathrm{d}\sigma\\
&= 2^{2s}\pi^s K^s\int_0^1 (1-v)^{-s-1}v^{s+n/2-1}\mathrm{d}v\\
&= 2^{2s}\pi^s K^s B(-s, s+n/2)\\
&= 2^{2s}\pi^s\,\frac{\Gamma(-s)\Gamma(s+n/2)}{\Gamma(n/2)}K^s
\end{aligned}$$

q.e.d.

Theorem. Let c_τ be the x-tempered solution to Cauchy's problem:

$$K\Delta C - \sum \beta_i\partial_i C + \gamma C = \frac{\partial c}{\partial t}, \qquad c_\tau(x,0) = \exp[-\pi\tau(x-x_0)^2] \qquad [8.2.3]$$

where τ, K, β, γ are real, τ and K strictly positive, x_0 belongs to R^n. Let s be real, strictly comprised between $-n/2$ and 0. For all $\lambda \leqslant -\gamma$, the following relationship is verified:

$$\lim_{\tau\to\infty}\tau^{-s}\int_0^\infty t^{-s-1}e^{\lambda t}C_\tau(x_0,t)\mathrm{d}t = 2^{2s}\pi^s\,\frac{\Gamma(-s)\Gamma(s+n/2)}{\Gamma(n/2)}K^s \qquad [8.2.4]$$

Proof. (Fried, 1971c, p. 47). Take $x_0 = 0$.

Set $a^2 = \sum_{i=1}^n a_i^2, \quad ab = \sum_{i=1}^n a_i b_i, \quad \mathrm{d}x = \mathrm{d}x^1\mathrm{d}x^2\ldots\mathrm{d}x^n$

Apply the Fourier transform in x to the system [8.2.3]:

$$-4\pi^2\xi^2 K\hat{c} - 2i\pi\beta\xi\hat{c} + \gamma\hat{c} = \frac{\mathrm{d}\hat{c}}{\mathrm{d}t}, \quad \hat{c}_\tau(\xi,0) = \tau^{-n/2}\exp(-\pi\xi^2/\tau)$$

which yields:

$$\hat{c}_\tau(\xi, t) = \tau^{-n/2} \exp\left(-\pi \frac{\xi^2}{\tau}\right) \exp[(-4\pi^2 \xi^2 K - 2i\pi\beta\xi)t]\, e^{\gamma t}$$

Apply the inverse Fourier transform:

$$c_\tau(x, t) = (4\pi K t)^{-n/2} e^{\gamma t} \int_{R^n} \exp[-\pi\tau(x-\eta)^2] \exp\left[-\frac{1}{4Kt}(\eta - \beta t)^2\right] d\eta$$

$$c_\tau(0, t) = (4\pi K t)^{-n/2} e^{\gamma t} \int_{R^n} \exp(-\pi\tau\eta^2) \exp\left[-\frac{1}{4Kt}(\eta - \beta t)^2\right] d\eta$$

and set:

$$\zeta = \eta - \frac{\beta}{4K\left(\pi\tau + \dfrac{1}{4Kt}\right)}$$

$$c_\tau(0, t) = (4\pi K t)^{-n/2} e^{\gamma t} \exp\left(-\frac{\beta^2 t}{4K}\right) \exp\left[\frac{\beta^2}{16K^2\left(\pi\tau + \dfrac{1}{4Kt}\right)}\right]$$

$$\times \int \exp\left[\left(-\pi\tau + \frac{1}{4Kt}\right)\zeta^2\right] d\zeta$$

or:

$$c_\tau(0, t) = (4\pi K t_\tau + 1)^{-n/2} e^{\gamma t} \exp\left(-\frac{\beta^2 t}{4K}\right) \exp\left(\frac{\beta^2 t}{16K^2\pi t\tau + 4K}\right)$$

Replacing $c_\tau(0, t)$ by its value in the integral [8.2.4] and setting $\theta = t\tau$, we obtain:

$$\int_0^\infty \theta^{-s-1}(4\pi K\theta + 1)^{-n/2} \exp\left[(\lambda + \gamma)\frac{\theta}{\tau}\right] \exp\left(-\frac{\beta^2\theta}{4K\tau}\right)$$

$$\exp\left[\frac{\beta^2\theta}{(16K^2\pi\theta + 4K)}\right] d\theta$$

Set $f(\theta, \tau)$ as the function in the integral and take τ greater than 1. $f(\theta, \tau)$ is bounded independently of τ, by the integrable function $\theta^{-s-1}(4\pi K\theta + 1)^{-n/2}$ $\exp(\beta^2/16K^2)$; also, when τ tends to infinity, $f(\theta, \tau)$ tends to

$\theta^{-s-1}(4\pi K\theta + 1)^{-n/2}$. According to Lebesgue's dominated-convergence theorem and the preceding lemma:

$$\int_0^\infty f(\theta, \tau)\mathrm{d}\theta \to 2^{2s}\pi^s\Gamma(-s)\Gamma(s + n/2)K^s/\Gamma(n/2) \qquad \text{q.e.d.}$$

The initial condition $c_\tau(x, 0) = \exp[-\pi\tau(x - x_0)^2]$ has been used to express the integral [8.2.4] simply. The results can be generalized to functions of R^n into R, indefinitely continuously differentiable and rapidly decreasing, by the following calculations:

$$c_\tau(x, 0) = c_1(x\sqrt{\tau}), \quad \hat{c}_\tau(\xi, 0) = \tau^{-n/2}\hat{c}_1\left(\frac{\xi}{\sqrt{\tau}}\right) \qquad [8.2.5]$$

The solution of the system [8.2.3] with the conditions [8.2.5] is:

$$c_\tau(x, t) = (4\pi Kt)^{-n/2}\mathrm{e}^{\gamma t}\int_{R^n} c_1(n\sqrt{\tau}) \exp\left[-\frac{1}{4Kt}(x - \eta - \beta t)^2\right]\mathrm{d}\eta$$

$$c_\tau(0, t) = (4\pi Kt)^{-n/2}\mathrm{e}^{\gamma t}\int_{R^n} c_1(\eta\sqrt{\tau}) \exp\left[-\frac{1}{4Kt}(-\eta - \beta t)^2\right]\mathrm{d}\eta$$

which yields, by carrying $c_\tau(0, t)$ in the integral [8.2.4]:

$$I = \tau^{-s}\int_0^\infty t^{-s-1}(4\pi Kt)^{-n/2}\mathrm{e}^{(\gamma+\lambda)t}$$
$$\left[\int_{R^n} c_1(\eta\sqrt{\tau}) \exp\left\{-\frac{1}{4Kt}(\eta + \beta t)^2\right\}\mathrm{d}\eta\right]\mathrm{d}t$$

and setting $t\tau = \theta$ and $\eta\sqrt{\tau} = z$:

$$I = \int_0^\infty \theta^{-s-1}(4\pi K\theta)^{-n/2}\exp\left[(\gamma + \lambda)\frac{\theta}{\tau}\right]$$
$$\left[\int_{\mathbb{R}^n} c_1(z) \exp\left\{-\frac{\left(z + \beta\frac{\theta}{\sqrt{\tau}}\right)}{4K\theta}\mathrm{d}z\right\}\right]\mathrm{d}\theta$$

τ tends to infinity, by applying the Lebesgue dominated-convergence theorem twice, we obtain (with $\theta + \lambda < 0$):

$$\lim_{\tau\to\infty} I = \int_0^\infty \theta^{-s-1}(4\pi K\theta)^{-n/2}\left[\int_{R^n} c_1(z)\exp\left(-\frac{z^2}{4K\theta}\right)\mathrm{d}z\right]\mathrm{d}\theta$$

and setting $\sigma = 4\pi K\theta$ and $z = y\sqrt{\sigma}$:

$$\lim_{\tau\to\infty} I = 2^{2s}\pi^s K^s \int_0^\infty \sigma^{-s-1} \left[\int_{R^n} c_1(y\sqrt{\sigma}) \exp(-\pi y^2) dy \right] d\sigma$$

$$\lim_{\tau\to\infty} \tau^{-s} \int_0 t^{-s-1} e^{\lambda t} c_\tau(x_0, t) dt = 2^{2s}\pi^s K^s \int_0^\infty \sigma^{-s-1}$$

$$\left[\int_{R^n} c_1(y\sqrt{\sigma}) \exp(-\pi y^2) dy \right] d\sigma$$

Links with the physical experience

The existence of the coefficient $\exp(\lambda t)$ which assures the convergence of the integral does not modify the limit [8.2.4]. This means that this integral is very concentrated at the origin of times: it will not be necessary to perform long experiments and a good precision will be reached by computing this integral on a rather short time interval.

The type of initial condition introduced here is what can usually be realized experimentally: an experimental step-input function looks like some $\exp(-\pi\tau x^2)$ near the origin.

8.3. THE DETERMINATION OF THE COEFFICIENTS OF THE DIFFUSION OPERATOR WITH VARYING COEFFICIENTS

8.3.1. The isotropic diffusion operator

Consider the diffusion operator:

$$A = K_{(x)}\Delta + \sum_{j=1}^n \beta_j(x) \frac{\partial}{\partial x} + \gamma(x)$$

Assume that the coefficients K, β_j, γ are C^∞, that K is bounded as all its derivatives to the second order, that β_j are bounded as all their derivatives to the first order, that γ is bounded. Also assume that K has a strictly positive lower bound. The operator A is then said to be strictly elliptic.

According to Yosida (1968), there are two real numbers λ and μ satisfying $\mu > \lambda$, such that for all $\alpha > \mu$ the operator $A - \lambda I$ is inversible and the following inequality holds:

$$\|(A - \alpha I)^{-1}\| \leqslant \frac{1}{\alpha - \lambda}$$

where $\| \ \|$ is the canonical norm in L^2.

Choose $\nu > \mu$ and set $c = -A + \nu I$ and $c' = -A + \mu I$; $(c' - \alpha I)^{-1}$ exists for $\alpha < 0$ and:

$$\|(c' - \alpha I)^{-1}\| = \|\{A - (\mu - \alpha)I\}^{-1}\| \leqslant \frac{1}{\mu - \alpha - \lambda} \leqslant \frac{1}{-\alpha}$$

According to the Hille—Yosida theorem, $-c'$ is the infinitesimal generator of a contractive semi-group, i.e.:

$$\|e^{-tc'}\| \leqslant 1$$

hence the inequality:

$$e^{tA} \leqslant e^{\mu}$$

Lemma 1. The integral $f(s, c) = (\int_0^\infty t^{-s-1} e^{-tc} dt)/\Gamma(-s)$ converges for $\operatorname{Re} s < 0$.

The condition $\operatorname{Re} s < 0$ assures the integrability at the origin. Noticing that $\|e^{-tc}\| = e^{(\mu-\nu)t}\|e^{-tc'}\| \leqslant e^{(\mu-\nu)t}$ with $\mu - \nu < 0$ we see that $f(s, c)$ is integrable at infinity.

According to Seeley (1967), for $\operatorname{Re} s < 0$ and with the previous conditions on A, the operator c^s can be defined as:

$$c^s = (-A + \nu I)^s = \frac{1}{2i\pi} \int_\Gamma z^s[-A + (\nu - z)I]^{-1} dz$$

where Γ is the contour coming from $-\infty$ on the real axis, around the origin as a circle of radius ϵ and returning to $-\infty$ above the real axis (Fig. 8.3.1).

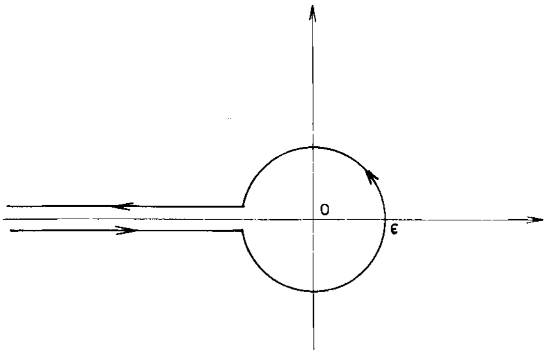

Fig. 8.3.1.

According to the previous assumptions, the origin belongs to the regularity set of c (c is inversible). Thus, there exists $\epsilon' > 0$ such that $(c - \epsilon I)^{-1}$ exists for $0 < \epsilon < \epsilon'$. The usual determination of $\ln z$ in the plane without the negative half axis is chosen. The comparison between the complex power of the operator c, as defined by Seeley, and the operator $f(s, c)$ yields the proof of the following proposition.

Proposition: The operator $f(s, C)$ coincides with the operator C^s

With the given conditions, $f(s, C)$ and C^s are holomorphic functions of s for $\operatorname{Re} s < 0$; thus it is enough to prove the equality for $\operatorname{Re} s < -1$.

The resolvent of the semi-group e^{-tC} is:

$$(C - zI)^{-1} = \int_0^{\infty} e^{-tC} e^{zt} dt$$

$$\text{Hence: } C^s = \frac{1}{2i\pi} \int_{\Gamma} z^s \left(\int_0^{\infty} e^{-tC} e^{zt} dt \right) dz$$

In order for these two integrals to commute, it is enough that the integral:

$$\int_0^{\infty} \int_{\Gamma} |z^s| \, \|e^{-tC}\| \, e^{(\operatorname{Re} z)t} dt \, d\sigma(z)$$

converges. ($d\sigma(z)$ is the element of curvilinear abscissa along Γ). Arg z is bounded, hence $|z^s| < b|z|^{\operatorname{Re} s}$ where b is a constant. As $\operatorname{Re} s < -1$, $\int |z|^{\operatorname{Re} s} e^{(\operatorname{Re} z)t} d\sigma(z)$ is bounded independently of t at infinity. Besides, $\|e^{-tC}\| \leqslant e^{(\lambda - \nu)t}$ with $\lambda - \nu < 0$.

Thus, $\int_0^{\infty} \int_{\Gamma} |z^s| \, \|e^{-tC}\| e^{(\operatorname{Re} z)t} dt \, d\sigma(z)$ converges. Fubini's theorem holds and the partial integrals may be commuted. Hence:

$$C^s = \frac{1}{2i\pi} \int_0^{\infty} e^{-tC} dt \int_{\Gamma} z^s e^{zt} dz$$

Hankel's formula yields:

$$\frac{1}{2i\pi} \int_{\Gamma} z^s e^{zt} dz = \frac{t^{s-1}}{\Gamma(-s)}$$

Hence the identity between C^s and $f(s, C)$.

If $\phi \epsilon L^2(R^n)$ and $\tau > 0$, ϕ_τ is defined as $\phi_\tau(x) = \tau^{n/2} \phi(\tau x)$ such that:

$$\|\phi_\tau\| = \|\phi\| \quad \text{and} \quad \hat{\phi}_\tau(\xi) = \tau^{-n/2} \phi\left(\frac{\xi}{\tau}\right)$$

Lemma 2. If k is a real number and R an operator of $\mathcal{S}$ into $\mathcal{S}'$, such that, for every real M, R may be extended as a continuous operator from $H^M(R^n)$ into $H^{M-k}_{\text{loc}}(R^n)$, then, if $-n/2 < M < 0$ and if $\alpha \in \mathbb{D}$, there exists C_1 such that $\forall \phi \in \mathcal{S}$.

$$\|\alpha R\phi_\tau\|_{M-k} < C_1\tau^M(\|\phi\|_{L^1} + \|\phi\|_{L^2})$$

Moreover, if $k < -n$, for every compact K of R^n, there exists C_2 such that:

$$\forall \phi \in \mathcal{S},\ \sup_K |R\phi_\tau(x)| < C_2\tau^M(\|\phi\|_{L^1} + \|\phi\|_{L^2})$$

Proof. For all $\phi \in \mathcal{S}$, for $M < 0$, we have:

$$\|\phi_\tau\|_M^2 = \tau^{-n}\int_{R^n} (1 + |\xi|^2)^M \left|\hat{\phi}\left(\frac{\xi}{\tau}\right)\right|^2 \mathrm{d}\xi = \int_{R^n} (1 + \tau^2|\eta|^2)^M |\hat{\phi}(\eta)|^2 \mathrm{d}\eta$$

$$< \tau^{2M} \int_{R^n} |\eta|^{2M} |\hat{\phi}(\eta)|^2 \mathrm{d}\eta$$

$$< \tau^{2M}\left[\int_{|\eta|<1} |\eta|^{2M}|\hat{\phi}(\eta)|^2\mathrm{d}\eta + \int |\hat{\phi}(\eta)|^2\mathrm{d}\eta\right]$$

If $M > -n/2$, $|\eta|^{2M}$ is integrable. Besides, we have:

$$\|\hat{\phi}_\tau\|_{L^\infty} \leqslant \|\phi\|_{L^1}$$

Hence the inequalities:

$$\|\phi_\tau\|_M^2 < \tau^{2M}\left(\|\hat{\phi}\|_{L^\infty}^2 \int_{|\eta|<1} |\eta|^{2M}\mathrm{d}\eta + \|\hat{\phi}\|_{L^2}^2\right)$$

$$< C_0\tau^{2M}(\|\hat{\phi}\|_{L^\infty}^2 + \|\hat{\phi}\|_{L^2}^2)$$

with $C_0 = \sup(1, \int_{|\eta|<1}|\eta|^{2M}\mathrm{d}\eta)$.
As R is a continuous operator from H^M into H^{M-k}_{loc}, αR is a continuous operator from H^M into H^{M-k}. Hence:

$$\|\alpha R\phi_\tau\|_{M-k} < C\|\phi_\tau\|_M < C_1\tau^M(\|\phi\|_{L^1} + \|\phi\|_{L^2})$$

Moreover, we assume $k \leqslant -n$; then $M - k > \frac{1}{2}n$. For $s > \frac{1}{2}n$, H^s is included in the space of bounded continuous functions with continuous injection. Hence:

$$\|\alpha R\phi_\tau\|_{L^\infty} < C_3\tau^M(\|\phi\|_{L^1} + \|\phi\|_{L^2})$$

and the second part of the lemma:

$$\sup_K |R\phi_\tau(x)| < C_2 \tau^M (\|\phi\|_{L^1} + \|\phi\|_{L^2})$$

choosing α equal to 1 in a neighbourhood of the support K.

Remark. We have used a result, proved by Unterberger and Unterberger (1970 and 1971): give $u \epsilon H^s$, with $s > n/2$; then $(1 + |\xi|^2)^{-s/2}$ and $(1 + |\xi|^2)^{s/2}\hat{u}(\xi)$ belong to $L^2(R^n)$. By Schwarz's inequality, we have:

$$\begin{aligned} \int_{R^n} |\hat{u}(\xi)| \mathrm{d}\xi &= \int_{R^n} (1 + |\xi|^2)^{-s/2}(1 + |\xi|^2)^{s/2} |\hat{u}(\xi)| \mathrm{d}\xi \\ &\leqslant C \|\delta\|_{-s} \|u\|_s \end{aligned}$$

hence: $\|u\|_{L^\infty} < \|\hat{u}\|_{L^1} \leqslant C'\|u\|_s$

Lemma 3. If B is an operator of the form:

$$B = \sum_{j=0}^{m} \mathrm{Op}(\tilde{a}_j) + R$$

where, for every j, $\tilde{a}_j \epsilon S^{2s-\alpha_j}$, with $0 = \alpha_0 < \alpha_1 < \ldots \alpha_n$, where $\tilde{a}_j\,(x, \xi)$ is homogeneous of order $2s - \alpha_j$ for $|\xi| > 1$ and where R is an operator (pseudo-differential or not) or order $< -n$*. Suppose $-n/2 < s < 0$. Let k be the largest integer $\leqslant m$ such that $2s - \alpha_j > -n$ for $j \leqslant k$ and B_j the operator defined by:

$$(B_j u)(x) = \int a_j(x, \xi) \hat{u}(\xi) \mathrm{e}^{2i\pi x \xi} \mathrm{d}\xi,\ u \epsilon \mathcal{S}$$

where a_j coincides with $\tilde{a}_j$ for $|\xi| \geqslant 1$ and is homogeneous of degree $2s - \alpha_j$ for $|\xi| \neq 0$. We use the functions $\phi_\tau(x) = \tau^{n/2}\phi[\tau(x - x_0)]$. Then, for every $M > -n/2$, for every $x_0 \epsilon R^n$, there exists a constant $C > 0$ such that, for every distribution of $H^r(R^n) \cap L^1$ with $r \geqslant 0$ and $r > n/2 + 2s$ and every number $\tau > 1$, we have:

$$B\phi_\tau(x_0) = \sum_{j=0}^{k} \tau^{n/2 + 2s - \alpha_j} B_j(\phi)(x_0) + R_\tau(\phi)(x_0)$$

with: $|R_\tau(\phi)(x_0)| \leqslant C\tau^M (\|\phi\|_{L^1} + \|\phi\|_{L^2})$

Proof. We give the proof at $x_0 = 0$ and it is valid at any point x_0 by translation of ϕ. First, a few remarks:

---

* I.e., acting from $H^t(R^n)$ into $H^{t+n}_{\mathrm{loc}}(R^n)$ for every real t.

(1) If ϕ (thus ϕ_T) ϵH^r with $r > n/2 + 2s$, $B\phi_T(0)$ is defined. B is an operator of order $2s$: for every $\alpha \epsilon \mathfrak{D}(R^n)$, there exists $C > 0$ such that for every $u \epsilon \mathcal{S}(R^n)$:

$$\|\alpha Bu\|_{r-2s} < C\|u\|_r$$

Furthermore, as $r - 2s > n/2$:

$$\|\alpha Bu\|_{L^\infty} < C\|\alpha Bu\|_{r-2s}$$

and Bu is a continuous function.
B may be extended to a continuous operator from H^r into the space of continuous functions.

(2) If $j \leqslant k$, $2s - \alpha_j > -n$ and thus $a_j(x, \xi)$ is integrable with respect to dξ in a neighbourhood of $\xi = 0$; this allows to define the operator B_j though its symbol has a singularity at the origin. Furthermore, $\tilde{B}_j - B_j$ acts from $H^{-\infty}$ into C^∞ as its kernel.

$$K(x, y) = \int |\tilde{a}(x, \xi) - a(x, \xi)\, a(x, \xi)|\, \mathrm{e}^{2i\pi(x-y)\xi} \mathrm{d}\xi$$

is everywhere C^∞.

Remark (1) shows that $B_j\phi_T(0)$ is also well defined when $\phi \epsilon H^r$ with $r > n/2 + 2s$.

(3) $B_j\phi(0)$ is always given by formula:

$$B_j\phi(0) = \int a_j(0, \xi)\hat{\phi}(\xi)\mathrm{d}\xi$$

when ϕ is a distribution of $H^r(R^n) \cap L^1$, with $r > n/2 + 2s - \alpha_j$. By definition this formula holds when ϕ belongs to $\mathcal{S}$ and both sides of this equality depend continuously on ϕ for the norm of $H^r \cap L^1$. For the left side, it results from Remarks (1) and (2). For the right side, noticing that $a_j(0, \xi)$ is C^∞ for $|\xi| \neq 0$ and that $\hat{\phi}$ is measurable, we write:

$$\int a_j(0, \xi)\hat{\phi}(\xi)\mathrm{d}\xi = \int_{|\xi|<1} a_j(0, \xi)\hat{\phi}(\xi)\mathrm{d}\xi + \int_{|\xi|>1} a_j(0, \xi)\hat{\phi}(\xi)\mathrm{d}\xi$$

$$\left| \int_{|\xi|<1} a_j(0, \xi)\hat{\phi}(\xi)\mathrm{d}\xi \right| \leqslant \|\phi\|_{L^1} \int_{|\xi|<1} |a_j(0, \xi)|\mathrm{d}\xi$$

and the integral $\int_{|\xi|<1} |a_j(0, \xi)|\mathrm{d}\xi$ converges.

$$\left| \int_{|\xi|>1} a_j(0, \xi)\hat{\phi}(\xi)\mathrm{d}\xi \right| \leqslant C \int (1 + |\xi|^2)^{s-\alpha_j/2} |\hat{\phi}(\xi)|\mathrm{d}\xi$$

$$\leqslant C \int (1 + |\xi|^2)^{s-\alpha_j/2}(1 + |\xi|^2)^{-N/2}(1 + |\xi|^2)^{N/2} |\hat{\phi}(\xi)|\mathrm{d}\xi$$

By Schwarz's inequality, we obtain:

$$\left| \int_{|\xi|>1} a_j(0,\xi)\hat{\phi}(\xi)\mathrm{d}\xi \right| < C \left| \int (1+|\xi|^2)^{2s-\alpha_j-N}\mathrm{d}\xi \right|^{1/2} \left| \int (1+|\xi|^2)^N |\hat{\phi}(\xi)|^2\mathrm{d}\xi \right|^{1/2} < C\|(1+|\xi|^2)^{s-\alpha_j/2-N/2}\|_{L^2}\|\phi\|_N$$

Choosing N such that $n+2s-\alpha_j < N < r$ so that:

$(1+|\xi|^2)^{s-\alpha_j/2-N/2} \epsilon L^2$ and $\|\phi\|_N \leqslant \|\phi\|_r$

Hence, the inequality:

$$\left| \int a_j(0,\xi)\hat{\phi}(\xi)\mathrm{d}\xi \right| \leqslant C \left| \|\phi\|_r + \|\phi\|_{L^1} \right|$$

Let us now prove Lemma 3.
$B - \sum_{j\leqslant k} B_j$ verifies the conditions of Lemma 1:

$$\begin{aligned} B - \sum_{j\leqslant k} B_j &= \sum_{j\leqslant k} B_j + \sum_{j=k+1}^{m} \tilde{B}_j + R - \sum_{j\leqslant k} B_j \\ &= \sum_{j\leqslant k} (\tilde{B}_j - B_j) + \sum_{j=k+1}^{m} \tilde{B}_j + R \end{aligned}$$

According to Remark (2), $\sum_{j\leqslant k}(\tilde{B}_j - B_j)$ operates from $H^{-\infty}$ into C^{∞} *, $\sum_{j=k+1}^{m} \tilde{B}_j$ is an operator of order $\leqslant -n$ by definition of k, R is assumed to be an operator of order $\leqslant -n$.
Thus, according to Lemma 2, we have:

$$\left| B\phi_\tau(0) - \sum_{j\leqslant k} B_j\phi_\tau(0) \right| \leqslant C_2\tau^M(\|\phi\|_{L^1} + \|\phi\|_{L^2})$$

$B_j\phi_\tau(0)$ has to be computed:

$$\begin{aligned} B_j\phi_\tau(0) &= \int a_j(0,\xi)\hat{\phi}_\tau(\xi)\mathrm{d}\xi = \int a_j(0,\xi)\tau^{-n/2}\hat{\phi}\left(\frac{\xi}{\tau}\right)\mathrm{d}\xi \\ &= \tau^{n/2}\int a_j(0,\tau\eta)\hat{\phi}(\eta)\mathrm{d}\eta = \tau^{n/2+2s-\alpha_j}\int a_j(0,\eta)\hat{\phi}(\eta)\mathrm{d}\eta \\ &= \tau^{n/2+2s-\alpha_j}B_j\phi(0) \end{aligned}$$

which ends the proof of Lemma 3.

---

* We briefly recall: $H^{\infty}_{\mathrm{loc}} = \cap H^{s}_{\mathrm{loc}} = C^{\infty}$
(1) $H^{\infty}_{\mathrm{loc}} \subset C^{\infty}$: $f \subset H^{\infty}_{\mathrm{loc}}$, $\forall \alpha \epsilon \mathfrak{D}$, $\alpha f \epsilon C^{\infty} \Rightarrow f \epsilon C^{\infty}$ (take $\alpha = 1$ locally)
(2) $C^{\infty} \subset H^{\infty}_{\mathrm{loc}}$: take $f \epsilon C^{\infty}$, $\forall \alpha \epsilon \mathfrak{D}$, $\alpha f \epsilon \mathfrak{D} \subset \mathcal{S} \subset H^{\infty} \Rightarrow f \epsilon H^{\infty}_{\mathrm{loc}}$

At this stage, the following remark is very important as a link with experimental dispersion: only local estimations are made on $R\phi_\tau$ (and even point estimations); thus it is always possible to replace R by αR with $\alpha \epsilon \mathfrak{D}$ and equal to 1 in a neighbourhood of x_0. It is not necessary to assume any decrease in x in the symbols. If only initial data ϕ_τ with compact support (for $\tau > 1$) are considered, the rest $R\phi_\tau(x_0)$ is majored by:

$$|R\phi_\tau(x_0) \leqslant C\tau^M \, \|\phi\|_{L^2}$$

as H^r_{comp} CL^2_{comp} CL^1_{comp}: for any compact set K, there exists a constant C such that for any function u of L^2 and with its support in K we have:

$$\|u\|_{L^1} \leqslant C \|u\|_{L^2}$$

from Schwarz's inequality:

$$\int_{R^n} u\mathrm{d}x = \int_K u\mathrm{d}x \leqslant \left(\int_K \mathrm{d}x\right)^{1/2} \left(\int_K u^2\mathrm{d}x\right)^{1/2} \leqslant C\|u\|_{L^2}$$

with this remark, it is possible to take into account initial step functions having a physical meaning.

Now, we shall apply Lemma 3 to the operator $B = (-A + \nu I)^s$ with $-n/2 < s < 0$, using the following results due to Seeley (1967).

There exists a real sequence $(\alpha_j)_{j \geqslant 0}$ increasing to $+\infty$ such that $\forall_j$, $a_j(x, \xi)$ is a C^∞ function of x and ξ, homogeneous of order $2s - \alpha_j$ for $|\xi| \geqslant 1$ and verifying the following properties:

(1) For all N, there exists n such that the operator $B - \sum_{j=0}^{m} O_p(a_j)$ operates for every real t from $H^t(R^n)$ into $H^{t-N}_{\text{loc}}(R^n)$.

(2) For $|\xi| \geqslant 1$, $\quad a_0(x, \xi) = [K(x)]^s(4\pi^2|\xi|^2)^s$.

The various preceding results yield the following theorem, which, for the sake of simplicity, we give in the case of an isotropic operator, i.e. with $a^{ij}(x) = k(x)\delta_{ij}$.

Theorem. Let the diffusion operator be given as:

$$A = K(x)\Delta + \sum_{j=1}^{n} \beta_j(x)\frac{\partial}{\partial x^j} + \gamma(x)$$

We assume that the coefficients K, β_j, γ are C^∞, that K and its derivatives of order $\leqslant 2$ are bounded, that β_j and its first derivative are bounded, that γ is bounded. We assume that K is bounded by a strictly positive number.

λ is a real number such that, for every $\alpha > \mu$, $(A - \alpha I)$ is inversible and the inequality:

$$\|(A-\alpha I)^{-1}\| \leqslant (\alpha-\lambda)^{-1}$$

holds, where $\|\ \|$ is the canonical norm in L^2. We choose $\nu > \mu$, and s real such that $-n/2 < s < 0$.

There exist an integer $k \geqslant 0$, an increasing sequence $(\alpha_j)_{1 \leqslant j \leqslant k}$ of positive numbers and a sequence $(B_j)_{1 \leqslant j \leqslant k}$ such that:

(1) for every $r > n/2 + 2s$, B_j is a linear, continuous (pseudo-differential) operator on $H^r(R^n)$ taking its values in the space of continuous functions;

(2) for every M such that $-n/2 < M < 0$, for every $x_0 \in R^n$ and for every compact K there exists a constant $C > 0$ such that for every distribution ϕ with its support contained in K, belonging to H^r with $r \geqslant 0$ and $r > n/2 + 2s$, and for every real $\tau > 1$, we have (taking $\phi_\tau(x) = \tau^{n/2}\phi[\tau(x-x_0)]$):

$$\frac{1}{\Gamma(-s)}\int_0^\infty t^{-s-1}e^{-\nu t}(e^{tA}\phi_\tau)(x_0)\,dt = \tau^{n/2+2s}\int_{R^n}[K(x_0)]^s(4\pi^2|\xi|^2)^s$$

$$\hat{\phi}(\xi)\,d\xi + \sum_{j=1}^{k}\tau^{n/2+2s-\alpha_j}B_j(\phi)(x_0) + R_\tau(\phi)(x_0)$$

with $|R_\tau(\phi)(x_0)| \leqslant C\tau^M \|\phi\|_{L^2}$

This result yields the formula:

$$\lim_{\tau\to\infty}\frac{\tau^{-n/2-2s}}{\Gamma(-s)}\int_0^\infty t^{-s-1}e^{-\nu t}(e^{tA}\phi_\tau)(x_0)\,dt$$

$$= [K(x_0)]^s\int_{R^n}(4\pi^2|\xi|^2)^s\hat{\phi}(\xi)\,d\xi$$

which is useful to determine the highest-order coefficient.

The conditions of Lemma 3, of course, can be applied to the equation with constant coefficients. As an example, an explicit formula of K at the origin is derived from the initial condition $\phi_\tau(x, 0) = \exp(-\pi\tau|x|^2)$:

$$\lim_{\tau\to\infty}\frac{\tau^{-s}}{\Gamma(-s)}\int_0^\infty t^{-s-1}e^{-\nu t}(e^{tA}\phi_\tau)(0)\,dt = [K(0)]^s(4\pi^2)^s\int|\xi|^{2s}\exp(-\pi|\xi|^2)\,d\xi$$

$$= [K(0)]^s(4\pi^2)^s\int_0^\infty \omega_n\exp(-\pi r^2)r^{2s+n-1}\,dr$$

where $\omega_n = 2\pi^{n/2}/\Gamma(n/2)$ is the R^n sphere surface

$$= [K(0)]^s(4\pi^2)^s\frac{\pi^{-s}}{\Gamma(n/2)}\Gamma(s+n/2)$$

by successively setting $r^2 = R$ and $\pi R = y$. Hence the relationship:

$$\lim_{\tau \to \infty} \tau^{-s} \int_0^\infty t^{-s-1} e^{-\nu t} (e^{tA} \phi_\tau)(0)\,dt = [K(0)]^s 2^{2s} \pi^s \frac{\Gamma(-s)\Gamma(s+n/2)}{\Gamma(n/2)}$$

which is the formula derived in § 8.2.

8.3.2. The anisotropic diffusion operator

Consider the operator:

$$A = \sum_{i,j} K^{ij}(x) \frac{\partial^2}{\partial x^i \partial x^j} + \sum_{i=1}^{n} \beta_i(x) \frac{\partial}{\partial x^i} + \gamma(x)$$

The preceding results and theorems hold in this case for the following assumptions:

We assume that the $K^{ij}(x)$ are real, C^∞, bounded and that their derivatives to the second order are bounded, that the $\beta_j(x)$ are C^∞ and bounded and their derivatives to the first order are bounded, that $\gamma(x)$ is C^∞ and bounded.

The assumption of strict ellipticity is verified by the $a^{ij}(x)$, i.e., there exist two positive constants λ_0 and μ_0 such that for all $x \in R^n$ and for all $\xi = (\xi_1, ..., \xi_n)$

$$\mu_0 \sum_{j=1}^{n} \xi_j^2 > a^{ij}(x)\xi_i\xi_j > \lambda_0 \sum_{j=1}^{n} \xi_j^2$$

Furthermore, physical considerations like Onsager's reciprocity relationships tell that (K^{ij}) is symmetrical, hence it can be diagonalized.

(1) Assume that the principal directions of the dispersion-diffusion tensor are not known. Yosida and Seeley's results can be directly applied with the given assumptions and yield the same lemmas and theorems as in the isotropic cases. Initial test function ϕ_τ must be chosen to account for the anisotropy:

$$\phi_\tau(x) = (\det a)^{1/2} \tau^{n/2} \phi(\tau a x)$$

where a is a regular matrix (a_{ij}) with fixed coefficients; here ϕ_τ will be concentrated at the origin.by modifying one parameter only, τ.

Preceding majoration lemmas are found by noticing that the Fourier transform of $\phi_\tau(x)$ is:

$$\frac{\tau^{-n/2}}{(\det a)^{1/2}} \hat{\phi}\left(\frac{a^{-1}\xi}{\tau}\right)$$

the symbol of the highest-degree term is:

$$a_0(x, \xi) = (4\pi^2)^s [K(x)\xi, \xi]^s$$

$$\text{with: } [K(x)\xi, \xi] = \sum_{i,j} K^{ij}(x)\xi^i\xi^j$$

and $B_0\phi_\tau(0)$ can be computed as previously.

$$B_0\phi_\tau(0) = \int (4\pi^2)^s [K(0)\xi, \xi] \frac{\tau^{-n/2}}{(\det a)^{-1/2}} \hat{\phi}\left(\frac{a^{-1}\xi}{\tau}\right) \mathrm{d}\xi$$

$$= (4\pi^2)^s (\det a)^{1/2} \tau^{n/2+2s} \int [K(0)a\eta, a\eta]^s \hat{\phi}(\eta)\mathrm{d}\eta$$

with $[K(0)a\eta, a\eta] = K^{ij}_{(0)}a_{i,k}\eta^k a_{j1}\eta^1$ and Einstein's summation convention.

To determine the $n(n + 1)/2K^{ij}$ coefficients, the integral has to be computed for $n(n + 1)/2$ matrices a. There is no explicit formulation of the coefficients. The method yields the values of the dispersion coefficients and the principal directions of the dispersion tensor.

(2) The principal directions of the dispersion tensor are known (by physical considerations for instance).

Preceding results can be applied for initial conditions:

$$\phi_\tau(x) = \left(\prod_{i=1}^{n} a_i\right)^{1/2} \tau^{n/2}\phi(\tau a x)$$

where $a = (a_i)$ is a regular matrix diagonalized in the eigensystem of the dispersion tensor. Formulas are the same as in the general case, but the computations are easier if ϕ_τ is concentrated with τ in the principal direction corresponding to the computed coefficient: matrices a will have a dominant component in that direction.

8.4. THE MATHEMATICAL MODEL AND THE EXPERIENCE

8.4.1. Consistency between the model and the experience

The dispersion coefficients are estimated from experiments with a mathematical model, which represents the experiments, and a theory derived under the modelling conditions. A basic assumption is made, that experimental results are model results.

Assume that the initial condition ϕ_τ is given experimentally with a complete accuracy. It corresponds to an experimental concentration distribution $\tilde{c}_\tau(x, t)$ and usually $\tilde{c}_\tau(x, t)$ is not a solution of a diffusion equation, i.e., we do not have:

$$\frac{\mathrm{d}\tilde{c}_\tau}{\mathrm{d}t} = A\tilde{c}_\tau$$

The problem is then how to estimate the dispersion coefficients K as a function of the experimental concentrations $\tilde{c}_\tau$ which do not verify the dispersion equation. This estimation is then partly *arbitrary* but as it is the only way to reach $\tilde{K}_\tau$, we must give some conditions to restrict the arbitrary character of the estimation as much as possible. This estimation yields $\tilde{K}$ which is an approximate value of K if the following conditions hold:

(1) If functions $\tilde{c}_\tau(x, t)$ are exact solutions (i.e., if $A\tilde{c}_\tau = \mathrm{d}\tilde{c}_\tau/\mathrm{d}t$ with:

$$A = \sum_{ij} K^{ij} \frac{\partial^2}{\partial x^i \partial x^j} + \sum_j \beta_j \frac{\partial}{\partial x^j} + \gamma), \text{ then } \tilde{K}^{ij} = K^{ij}.$$

Remark. The estimation procedure necessarily comprises a truncation and this equality holds but for a truncation error.

(2) $\tilde{K}$ verifies a stability property. Take any initial function and set $\tilde{c}$ the theoretical solution corresponding to $\tilde{K}$ and c the true solution; if the mathematical model is consistent, the difference between $\bar{c}$ and c defined in an appropriate norm, must be compatible with the experimental errors.

The estimation of K^{ij} by the point-dilution theory verifies condition (1) Hereinafter, we analyse a computation of errors on the dispersion coefficient. These elements are applied to the formulas derived by the point-dilution theory but, of course, the analysis could be applied to any explicit formulation of K by other theories; then condition (2) is studied.

8.4.2. Elements for an error calculus on the dispersion coefficients

The error on K is due to measurement errors, to truncation errors of the time-integral and to truncation errors on τ in the limit operations. Proofs are given for the isotropic operator with constant coefficients, with the initial condition $\phi_\tau = \exp(-\pi\tau x^2)$, but could be easily generalized to the other operators. If we set:

$$\gamma(s) = 2^{2s}\pi^s \frac{\Gamma(-s)\Gamma(s+n/2)}{\Gamma(n/2)}$$

then K is given by the formula [8.2.4]:

$$K^s = |\gamma(s)|^{-1} \lim_{\tau\to\infty} \tau^{-s} \int_0^\infty t^{-s-1} c_\tau(0, t)\mathrm{d}t$$

How does an experiment take place? A value of τ is chosen, concentration $\tilde{c}(0, t)$ are recorded (by either continuous or discrete methods) during a time period $(0, t_0)$ necessarily finite. A finite number of such experiments is performed for increasing τ, necessarily bounded by some τ_0.
The effective dispersion coefficient $\tilde{K}$ satisfies:

$$\tilde{K}^s = |\gamma(s)|^{-1}\tau_0^{-s}\int_0^{t_0} t^{-s-1}\tilde{c}(0, t)\mathrm{d}t$$

The error on K comes from:

(1) measurement errors on $\tilde{c}(0, t)$ or δ_c;

(2) the approximation error on τ, i.e. the error made by replacing the infinite t-limit by the value:

$$\gamma(s)\tau_0^{-s}\int_0^{\infty} t^{-s-1}\tilde{c}(0, t)\mathrm{d}t$$

It is called the τ-error, δ_τ;

(3) the truncation error on the finite bound t_0. It is called the t-error;

(4) the numerical integration errors, which we do not consider here.

Notice that $c(x, t)$ quickly decreases to 0 when t tends to infinity; t_0 should not be too large as, after a short time, c is less than the measurement errors. An optimal t_0 is computed here.

Measurement errors are independent of the model. The τ-errors and the t-errors are estimated and minimized.

Set δ the error on K^s:

$$\gamma(s)\delta = \delta_\tau + \delta_t + \delta_c$$

δ_τ and δ_t are studied and δ_c is neglected, using the analytical solution:

$$\gamma(s)\delta = \left| \tau_0^{-s}\int_0^{\infty} t^{-s-1}c(0, t) - \lim_{\tau \to \infty} \tau^{-s}\int_0^{\infty} t^{-s-1}c(0, t)\mathrm{d}t \right|$$

and setting $\tau t = \theta$ and $\tau_0 t_0 = \theta_0$:

$$\gamma(s)\delta = \left| \int_0^{\infty} \theta^{-s-1}(1 + 4\pi K\theta)^{-n/2} \exp\left(-\frac{\beta^2\theta}{4K\tau}\right) \exp\left[\frac{\beta^2\theta}{\tau(4K + 16\pi K^2\theta)}\right] \mathrm{d}\theta \right.$$

$$\left. - \int_0^{\infty} \theta^{-s-1}(1 + 4\pi K\theta)^{-n/2} \mathrm{d}\theta \right|$$

$$= \left| \int_0^{\theta_0} \theta^{-s-1}(1 + 4\pi K\theta)^{-n/2} \left[\exp\left\{-\frac{\beta^2\theta}{4K\tau_0} + \frac{\beta^2\theta}{\tau_0(4K + 16\pi K^2\theta)}\right\} - 1\right] \mathrm{d}\theta \right.$$

$$+ \int_{\theta_0}^{\infty} \theta^{-s-1}(1 + 4\pi K\theta)^{-n/2} \exp\left(-\frac{\beta^2\theta}{4K\tau_0}\right) \exp\left[\frac{\beta^2\theta}{\tau_0(4K + 16\pi K^2\theta)}\right] \mathrm{d}\theta$$

$$\left. - \int_{\theta_0}^{\infty} \theta^{-s-1}(1 + 4\pi K\theta)^{-n/2} \mathrm{d}\theta \right|$$

$$\leqslant \left| \int_0^{\theta_0} \theta^{-s-1}(1 + 4\pi K\theta)^{-n/2} \right.$$

$$\left. \left[\exp\left(-\frac{\beta^2\theta}{4K\tau_0}\right) \exp\left\{\frac{\beta^2\theta}{\tau_0(4K + 16\pi K^2\theta)}\right\} - 1\right] \mathrm{d}\theta \right|$$

$$+ \left| \int_{\theta_0}^{\infty} \theta^{-s-1}(1 + 4\pi K\theta)^{-n/2} \exp\left(-\frac{\beta^2\theta}{4K\tau_0}\right) \right.$$

$$\left. \exp\left[\frac{\beta^2\theta}{\tau_0(4K + 16\pi K^2\theta)}\right] \mathrm{d}\theta \right|$$

$$+ \left| \int_{\theta_0}^{\infty} \theta^{-s-1}(1 + 4\pi K\theta)^{-n/2} \mathrm{d}\theta \right|$$

which is written:

$$\gamma(s)\delta \leqslant R_1 + R_2 + R_3$$

where R_2 and R_3 account for the t-errors.
By formula $|\mathrm{e}^{-a}\mathrm{e}^{b} - 1| \leqslant |b - a|\,\mathrm{e}^{b} \leqslant (a + b)\mathrm{e}^{b}$:

$$R_1 \leqslant \int_0^{\theta_0} \theta^{-s-1}(1 + 4\pi K\theta)^{-n/2} \left(\frac{\beta^2\theta_0}{4K\tau_0} + \frac{\beta^2}{16\pi K^2\tau_0}\right) \exp\left(\frac{\beta^2}{16\pi K^2\tau_0}\right) \mathrm{d}\theta$$

$$\leqslant \gamma(s) K^{s} \left(\frac{\beta^2\theta_0}{4K\tau_0} + \frac{\beta^2}{16\pi K^2\tau_0}\right) \exp\left(\frac{\beta^2}{16\pi K^2\tau_0}\right)$$

$$R_2 \leqslant \int_{\theta_0}^{\infty} (4\pi K)^{-n/2}\theta^{-s-1-n/2}\exp\left(-\frac{\beta^2\theta}{4K\tau_0}\right)\exp\left(\frac{\beta^2}{16\pi K^2\tau_0}\right)\mathrm{d}\theta$$

$$\leqslant (4\pi K)^{-n/2}\exp\left(\frac{\beta^2}{16\pi K^2\tau_0}\right)\frac{\theta_0^{-s-n/2}}{s+n/2}$$

$$R_3 \leqslant \int_{\theta_0}^{\infty} (4\pi K)^{-n/2}\theta^{-s-1-n/2}\mathrm{d}\theta \leqslant (4\pi K)^{-n/2}\frac{\theta_0^{-s-n/2}}{s+n/2}$$

and eventually:

$$\gamma(s)\delta \leqslant \gamma(s)K^s\left(\frac{\beta^2\theta_0}{4K\tau_0}+\frac{\beta^2}{16\pi K^2\tau_0}\right)\exp\left(\frac{\beta^2}{16\pi K^2\tau_0}\right) + (4\pi K)^{-n/2}\frac{\theta_0^{-s-n/2}}{s+n/2}$$
$$\times\left[1+\exp\left(\frac{\beta^2}{16\pi K^2\tau_0}\right)\right]$$

Now examine the influence of measurement errors on $\tilde{c}(0, t)$, δ_c, which are independent of the mathematical procedures and constant:

$$\gamma(s)\delta \leqslant \tau_0^{-s}\int_0^{t_0} t^{-s-1}(\delta_c)\mathrm{d}t = \frac{\theta_0^{-s}}{-s}\,\delta_c$$

The error δ due to the measurement of $c(0, t)$ increases when θ_0 increases. Usually τ_0 is given by experimental conditions and t_0 is varied. The optimal error is obtained when:

$$R(\theta_0) = \gamma(s)K^{s-1}\frac{\beta^2}{4}\frac{\theta_0}{\tau_0} + 2(4\pi K)^{-n/2}\frac{\theta_0^{-s-n/2}}{s+n/2} + \frac{\theta_0^{-s}}{-s}(\delta_c)$$

is minimum, assuming τ_0 large enough to neglect $\beta^2/(16K^2\pi\tau_0)$. The minimum is obtained for:

$$R'(\theta_{\mathrm{opt}}) = \gamma(s)K^{s-1}\frac{\beta^2}{4\tau_0} - 2(4\pi K)^{-n/2}\theta_0^{-s-n/2-1} + \theta_0^{-s-1}(\delta_c) = 0$$

equation which can be solved by a graph, setting $T = \theta_0^{-s-1}$ and computing the intersection T_0 of the curves:

$$Y = \gamma(s)K^{s-1}\frac{\beta^2}{4\tau_0} + T\delta_c$$

$$Y = 2(4\pi K)^{-n/2}T^{-n/2}$$

$\theta_{\text{opt}} = T_0^{-1/(s+1)}$ and:

$$R \leqslant \gamma(s)K^{s-1}\frac{\beta^2}{4}\frac{\theta_{\text{opt}}}{\tau_0} + 2(4\pi K)^{-n/2}\frac{\theta_{\text{opt}}^{-s-n/2}}{s+n/2} + \frac{\theta_{\text{opt}}^{-s}}{-s}\delta_c$$

Remark. Assuming that the measurement error is zero, some elements on the τ-convergence can be derived from the preceding computations. The error on K^s is then for a large enough τ_0:

$$\gamma(s)\delta \leqslant \gamma(s)K^{s-1}\frac{\beta^2}{4}\frac{\theta_0}{\tau_0} + 2(4\pi K)^{-n/2}\frac{\theta_0^{-s-n/2}}{s+n/2}$$

Set $\theta_0^{-n/2-s} = c\dfrac{\theta_0}{\tau_0}$; then $\theta_0 = c_1\tau^{1/(s+n/2+1)}$ and:

$$\gamma(s)\delta \leqslant \tau_0^{-(s+n/2)/(s+1+n/2)}\left[\gamma(s)K^{s-1}\frac{\beta^2}{4}c_1 + 2(4\pi K)^{-n/2}\frac{c_1^{-s-n/2}}{s+n/2}\right]$$

The two terms in the brackets vary contrariwise and their sum will be minimal when they are equal, which yields c_1:

$$c_1 = \left[\frac{2(4\pi K)^{-n/2}}{s+n/2}\times\frac{4K^{-s+1}}{\gamma(s)\beta^2}\right]^{\frac{1}{s+n/2+1}}$$

and:

$$\gamma(s)\delta \leqslant \tau_0^{-\frac{s+n/2}{s+1+n/2}}\left[\gamma(s)K^{s-1}\frac{\beta^2}{4}\left\{2\frac{(4\pi K)^{n/2}}{s+n/2}\times\frac{4K^{-s+1}}{\gamma(s)\beta^2}\right\}^{\frac{1}{s+n/2+1}} + \frac{2(4\pi K)^{-n/2}}{s+n/2}\left\{\frac{2(4\pi K)^{-n/2}}{s+n/2}\times\frac{4K^{-s+1}}{\gamma(s)\beta^2}\right\}^{\frac{-s-n/2}{s+n/2+1}}\right]$$

From this expression, it is possible to compute τ_0 such that for all $\tau < \tau_0$ $(\delta/K^s) \leqslant \epsilon$ for a given positive ϵ.

The τ-convergence is very slow: taking $n = 1$, $K = 1$, $\beta = 10^{-4}$, $s = -0.1$, it can be found for $\epsilon = 10^{-2}$, $\tau_0 = 10$ and for $\epsilon = 10^{-3}\tau_0 = 20\,000$.

8.4.3. Stability of the point-dilution theory

Consider the dispersion coefficient $\tilde{K}$ obtained from experiments interpreted by the point-dilution theory. $\tilde{K}$ is introduced into the dispersion equation, which is then solved for any initial condition. Set $\tilde{c}(0, t)$ the computed solution and $c(0, t)$ the true solution, i.e. the dispersion equation solution for a totally accurate K. Of course, this is a very strong assumption, namely that if there is no error on field phenomena they verify a dispersion equation rigorously.

We say that the point-dilution theory is stable if the difference between $c(0, t)$ and $\bar{c}(0, t)$ is of the order of the experimental error. The most reasonable norm is the uniform convergence norm:

$$\|c\| = \sup_t |c(x, t)|$$

Introducing the Fourier transform $\hat{c}(\xi, t)$ of c with respect to x, we get:

$$|c(x, t)| \leqslant \int |\hat{c}(\xi, t)| \mathrm{d}\xi$$

and: $\|c\| \leqslant \sup_t \int |\hat{c}(\xi, t)| \mathrm{d}\xi$ [8.4.1]

The problem is defined by the system:

$$K \Delta c - \sum_{j=1}^{n} \beta_j \frac{\partial c}{\partial x^j} = \frac{\partial c}{\partial t}$$

$$c(x, 0) = c_0(x)$$

$c_0(x)$ belongs to $\mathcal{S}\ (R^n)$.

The Fourier transform of the solution is written:

$$\hat{c}(\xi, t) = \hat{c}_0(\xi) \exp[-(4\pi^2 K \xi^2 + 2i\pi\beta\xi)t]$$

We set Er $c = c - \bar{c}$ and obtain from [8.4.1]:

$$\|\mathrm{Er}\ c\| \leqslant \sup_t \int |\mathrm{Er}\ \hat{c}(\xi, t)| \mathrm{d}\xi$$

δ being the error on K, given in § 8.4.2, we have:

$$|\mathrm{Er}\ \hat{c}| = 4\pi^2 \xi^2 t\, |\delta|\, |\hat{c}_0(\xi)| \exp[-(4\pi^2 K \xi^2 + 2i\pi\beta\xi)t]$$

or:

$$\|\mathrm{Er}\ c\| \leqslant \sup_t \int 4\pi^2 \xi^2 t\, |\delta|\, |\hat{c}_0(\xi)| \exp[-(4\pi^2 K \xi^2 + 2i\pi\beta\xi)t]\, \mathrm{d}\xi$$

$$\leqslant 4\pi^2 |\delta| \sup_t A$$

setting:

$$A = \int \xi^2 t\, |\hat{c}_0(\xi)| \exp[-(4\pi^2 K\xi^2 + 2i\pi\beta\xi)t]\, \mathrm{d}\xi$$

Stability depends on the behaviour of A at t:

$$A \leqslant \int \xi^2 t\, |\hat{c}_0(\xi)| \exp[-4\pi^2 K\xi^2 t]\, \mathrm{d}\xi$$

hence, by Schwarz's inequality:

$$A \leqslant 4\pi^2 \left[\int \xi^{2\alpha} |\hat{c}_0(\xi)|^2 \mathrm{d}\xi \right]^{1/2} \left[\int t^2 \xi^{4-2\alpha} \exp(-8\pi^2 K\xi^2 t)\mathrm{d}\xi \right]^{1/2}$$

and setting $\zeta = \eta/\tau^{1/2}$:

$$\int t^2 \xi^{4-2\alpha} \exp(-8\pi^2 K\xi^2 t)\mathrm{d}\xi = t^{\alpha-n/2} \int \exp(-8\pi^2 K\eta^2)\eta^{4-2\alpha}\mathrm{d}\eta$$

which is finite if $\alpha = n/2$. For $\alpha = n/2$, we obtain:

$$\|\mathrm{Er}\, c\| < 4\pi^2\, |\delta|\, \|C_0\|_{n/2}$$

which means that stability is obtained and the error on the model solution for an experimental K is of the order of the error on K if the initial function C_0 and its derivatives to the order $n/2$ are square integrable (C_0 belongs to the Sobolev space $H^{n/2}$).

CHAPTER 9

NUMERICAL ANALYSIS OF GROUNDWATER POLLUTION PROBLEMS

The purpose of this chapter is to provide the student with the basic approximations, methods and theorems enabling him to treat groundwater pollution problems numerically.

The emphasis is put on the very close relationships between the physics of the phenomena and the numerical analysis of the problem: the discretization processes must keep the physical laws and physical considerations as the basis of any improvement of the numerical analysis of a problem. Let us take an example.

We have seen that the convective part of the dispersion equation is written —div (uc), uc being a flux of matter due to the velocity of the aquifer. A discretization process consists in dividing up the domain into blocks of centers (I) and writing the flux variations between two blocks as:

$$(uc)(I) - (uc)(J)/IJ$$

IJ being the distance between the centers I and J (Fig. 9.0.1).

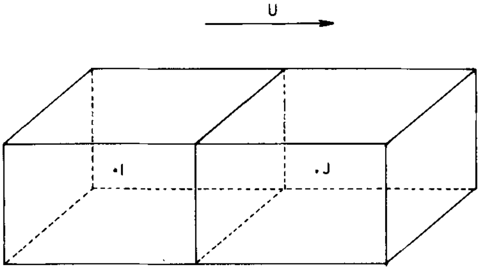

Fig. 9.0.1.

The discretization respects the physical meaning of uc, the mass transport of pollutant per unit area per unit of time.

Now let us imagine a mathematician, who has absolutely no knowledge of the physical meaning of the model, who nevertheless intends to treat the problem. For him, div (uc) can also be written u grad $c + c$ div u and he will discretize div uc as, for instance:

$$u(I)[c(J) - c(I)]/IJ + c(J)[u(J) - u(I)]/IJ$$

which does not respect the physical meaning; although, mathematically, both representations are equivalent, numerically and physically they are different and will yield different answers.

On the other hand, when physics is respected, all mathematical tools help the physicist solve his problem. We show both aspects of modelling in two paragraphs: §9.4 treats the theory of approximation of the diffusion-dispersion equation (valid as such, of course, for the hydrogeological basic equation) by mathematical considerations; it shows how mathematical tools can be used; §9.5 treats the hydrogeological basic equation by the balance of flux theory, showing how physical considerations lead to discretization techniques. §9.1 and 9.2 gather the useful mathematical tools (iterative methods and theorems).

We hope that no mathematician will feel insulted when we say that a physicist, with a good experimental and physical intuition and only a basic mathematical knowledge, will be a much better "mathematical modeller" than a good mathematician without a knowledge of physics. The best, of course, is a good physicist with a good mathematical background.

9.1. ITERATIVE PROCEDURES: PRINCIPLES AND THEOREMS

This paragraph is divided into two parts: from §9.1.1 to 9.1.3 we present the general principles of iterative procedures, based on simple geometrical examples. From §9.1.4 onward we develop iterative procedures for linear systems of equations and present the basic and useful theorems used in the mathematical models of groundwater pollution.

9.1.1. Principle

Consider a straight line (L) and a curve (C), which cuts L at point H in the plane xoy, represented in Fig. 9.1.1. The coordinates of H are (x_L, y_L). A point $H_0(x_0, y_0)$ on C being given, we intend to travel from H_0 to H, assuming that we know the equations of C and L. Fig. 9.1.1 shows a simple iterative process allowing to go from H_0 to H by horizontal and vertical jumps in a sequence of simple operations.

These jumps are chosen for the following reason: $H_0(x_0, y_0)$ being known, it is easy to determine the abscissa x_1 of point H_1 which is the abscissa of point K_1 on the line L. The equations of C and L being respectively:

$$y = f(x) \quad \text{and} \quad y = ax + b$$

the abscissa x_1 of K_1 and the ordinate y_1 of H_1 respectively are:

$$x_1 = \frac{y_0 - b}{a} \quad \text{and} \quad y_1 = f(x_1)$$

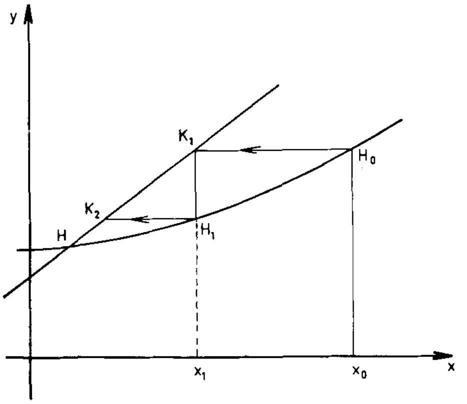

Fig. 9.1.1. Principle of an iterative procedure.

The process is then iterated.

At this point, we shall say that if we intend to solve an equation $F(x) = 0$* by an iterative process, we must *generate* a curve C (or a surface) and a straight line L so that the intersection H of L and C be the solution of $F(x) = 0$ (i.e. the coordinates x_L of H verify $F(x_L) = 0$).

Mathematically speaking, it is a problem of *construction* of the adequate and helpful curves. Of course, we shall try to simplify this construction as much as possible and usually the straight line $y = x$ may be chosen. The iterative process then becomes (Fig. 9.1.2):

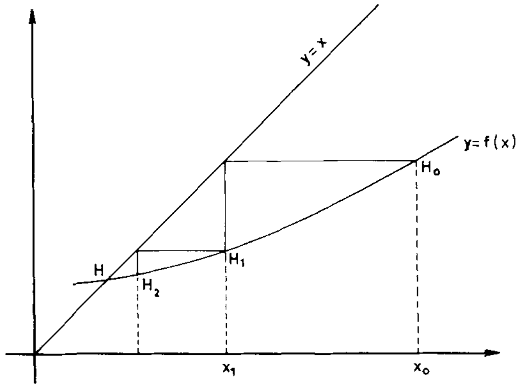

Fig. 9.1.2. Refined iterative procedure.

---

* Of course, x represents the coordinates of a vector $(x_1, x_2, \ldots x_n)$ in a n-dimensional space. In our simple example (Fig. 9.1.1) we have $x = (x_L, y_L)$.

$$y_0 = f(x_0)$$
$$x_1 = y_0$$
$$y_1 = f(x_1)$$
$$x_2 = y_1$$

which is written as:

$$x_1 = f(x_0)$$
$$x_2 = f(x_1)$$
$$x_n = f(x_{n-1}) \qquad [9.1.1]$$

This process *may* converge towards x_L when $n \to \infty$. Furthermore if f is a continuous function, we have:

$$x_L = f(x_L)$$

which shows that x_L is a solution of equation $x = f(x)$, defining the intersection of C and L.

9.1.2. *Convergence*

Convergence does not always exist and in Fig. 9.1.3, we show two possible cases. These two sketches help us to understand under which conditions convergence may be expected.

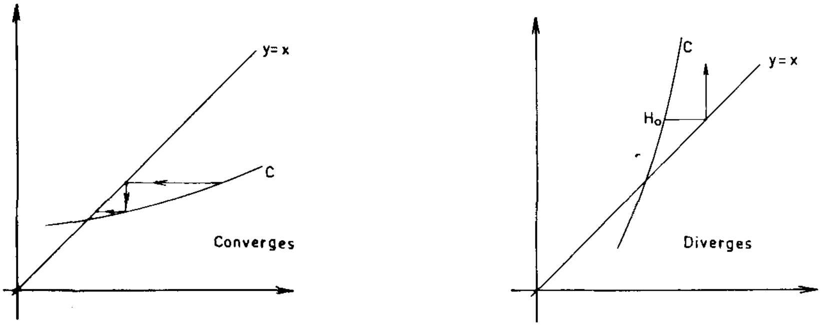

Fig. 9.1.3. Convergence and divergence of an iterative procedure.

Let us write [9.1.1] as follows:

$$\begin{aligned} x_1 &= f(x_0) \\ x_2 - x_1 &= f(x_1) - f(x_0) \\ x_3 - x_2 &= f(x_2) - f(x_1) \\ x_{n+1} - x_n &= f(x_n) - f(x_{n-1}) \end{aligned} \tag{9.1.2}$$

Besides x_{n+1} verifies the following equation:

$$x_{n+1} = (x_{n+1} - x_n) + (x_n - x_{n-1}) + \ldots + (x_2 - x_1) + (x_1 - x_0) + x_0 \tag{9.1.3}$$

If f is sufficiently regular, in a neighbourhood of the intersection point $H(x_L)$ we have (by a classical theorem):

$$\begin{aligned} x_2 - x_1 &= f(x_1) - f(x_0) = (x_1 - x_0)f'(\theta_1) \simeq (x_1 - x_0)f'(x_L) \\ x_3 - x_2 &= f(x_2) - f(x_1) = (x_2 - x_1)f'(\theta_2) \simeq (x_2 - x_1)f'(x_L) \\ &\simeq (x_1 - x_0)f'^2(x_L) \end{aligned} \tag{9.1.4}$$

$$\begin{aligned} x_{n+1} - x_n &= f(x_n) - f(x_{n-1}) = (x_n - x_{n-1})f'(\theta_n) \simeq (x_n - x_{n-1})f'(x_L) \\ &\simeq (x_1 - x_0)f'^n(x_L) \end{aligned}$$

where θ_i is a real number in the interval (x_{i-1}, x_i).

Equations [9.1.3] and [9.1.4] combined yield:

$$x_{n+1} = x_0 + [f(x_0) - x_0][1 + f'(x_L) + f'^2(x_L) + \ldots + f'^n(x_L)]$$

The convergence of x_{n+1} to x_L when $n \to \infty$ depends on the convergence of the geometric series $[f'^n(x_L)]$ and we know that such a series converges if $|f'(x_L)| < 1$ and diverges if $|f'(x_L)| \geqslant 1$.

This is a general result: the convergence of an iterative process is equivalent to the convergence of a geometric series; the convergence criteria will be the same and convergence will be obtained when some quantities, acting as $f'(x_L)$ of the previous example, will be less than 1 in absolute value.

Remark. We shall see that later in our case, these quantities are eigenvalues of some matrices called "iteration matrices".

Convergence may be increased and the various iterative methods which are studied in this book are different improvements, in terms of convergence velocity, of one basic method. For example, the previous iterative method may be improved. If the approximation:

$$f(x_{n+1}) - f(x_n) \simeq (x_{n+1} - x_n)f'(x_n)$$

is fairly good, we write:

$$
\begin{aligned}
x_L &= x_n + (x_{n+1} - x_n) + (x_{n+2} - x_{n+1}) + \ldots + (x_{n+m+1} - x_{n+m}) + \ldots \\
x_L^* &= x_n + (x_{n+1} - x_n)[1 + f'(x_n) + f'^2(x_n) + \ldots . + f'^m(x_n) + \ldots] \\
&= x_n + (x_{n+1} - x_n)[1/(1 - f'(x_n)]
\end{aligned}
$$

x_L^* is a better approximation of x_L than x_{n+1} and the process is iterated from x_L^* instead of x_{n+1}.

9.1.3. *Construction of an iterative process*

The given problem is to solve the equation:

$$f(x) = 0 \qquad [9.1.5]$$

and it is assumed that the solution is unique for $a < x < b$. To use an iterative method, we have to give a curve C and a straight line L, their intersection being the solution of [9.5].

Equation [9.1.5] is equivalent to:

$$f(x) + x = x \qquad [9.1.6]$$

and setting $f(x) + x = g(x)$, our problem is then equivalent to solving:

$$g(x) = x$$

i.e. to look for the intersection of the curve C and the straight line L, with respective equations:

$$y = g(x) \quad \text{and} \quad y = x$$

The process will be convergent if:

$$-1 < g'(x) < 1 \text{ (with } a < x < b)$$

or:

$$-2 < f'(x) < 0$$

Of course there are other ways of generating an iterative process, which we shall investigate, applied to linear systems of equations.

9.1.4. Application to linear systems of equations

The given problem is to solve the system:

$$\mathsf{AX} = \mathsf{B}$$

where X is the column matrix of unknowns, A the system square matrix and B a column matrix.

$$\mathsf{X} = \begin{bmatrix} x_1 \\ x_2 \\ \cdot \\ \cdot \\ \cdot \\ x_n \end{bmatrix} \qquad \begin{aligned} \mathsf{A} &= (aij) \\ i &= 1, \ldots, n \\ j &= 1, \ldots, n \end{aligned} \qquad \mathsf{B} = \begin{bmatrix} b_1 \\ b_2 \\ \cdot \\ \cdot \\ \cdot \\ b_n \end{bmatrix}$$

We assume that A^{-1} exists, i.e. the system has one and only one solution, given by

$$\mathsf{X} = \mathsf{A}^{-1}\mathsf{B}$$

We propose to find this solution by an iterative process. Using [9.1.6] we obtain:

$$\begin{aligned} \mathsf{AX} + \mathsf{X} &= \mathsf{B} + \mathsf{X} \\ \mathsf{X} &= (\mathsf{I} - \mathsf{A})\mathsf{X} + \mathsf{B} \end{aligned}$$

I being the unitary square matrix:

$$\mathsf{I} = \begin{bmatrix} 1 & 0 & . & . & . & 0 \\ 0 & 1 & . & . & . & 0 \\ \cdot & \cdot & & & & \cdot \\ \cdot & \cdot & & & & \cdot \\ \cdot & \cdot & & & & \cdot \\ 0 & 0 & & & & 1 \end{bmatrix}$$

The solution is the intersection of the curves:

$$\begin{aligned} Y &= (\mathsf{I} - \mathsf{A})\mathsf{X} + \mathsf{B} \quad && (C) \\ Y &= \mathsf{X} && (L) \end{aligned}$$

and we generate the following iterative process:

$$X_n = (I - \mathbf{A})X_{n-1} + \mathbf{B} \qquad [9.1.7]$$

If this process [9.1.7] converges, it will converge to the intersection of C and L for obvious continuity conditions of the equations.

A simple example will illustrate this construction. Consider the system:

$$\left.\begin{cases} -x - 1.5y = 2 \\ -1.5x - y = 0 \end{cases}\right\} \text{or } \mathbf{AX} = \mathbf{B}$$

$$\text{where } \mathbf{A} = \begin{bmatrix} -1 & -1.5 \\ -1.5 & -1 \end{bmatrix} \quad \mathbf{B} = \begin{bmatrix} 2 \\ 0 \end{bmatrix} \quad \mathbf{X} = \begin{bmatrix} x \\ y \end{bmatrix}$$

$$\begin{bmatrix} -1 & -1.5 \\ -1.5 & -1 \end{bmatrix}\begin{bmatrix} x \\ y \end{bmatrix} + \begin{bmatrix} x \\ y \end{bmatrix} = \begin{bmatrix} 2 \\ 0 \end{bmatrix} + \begin{bmatrix} x \\ y \end{bmatrix}$$

$$\text{or: } \begin{bmatrix} x \\ y \end{bmatrix} = \begin{bmatrix} 2 & 1.5 \\ 1.5 & 2 \end{bmatrix}\begin{bmatrix} x \\ y \end{bmatrix} + \begin{bmatrix} 2 \\ 0 \end{bmatrix}$$

$$\text{with } \mathbf{I} - \mathbf{A} = \begin{bmatrix} 2 & 1.5 \\ 1.5 & 2 \end{bmatrix}$$

Equation [9.1.7] is then:

$$\begin{bmatrix} x_n \\ y_n \end{bmatrix} = \begin{bmatrix} 2 & 1.5 \\ 1.5 & 2 \end{bmatrix}\begin{bmatrix} x_{n-1} \\ y_{n-1} \end{bmatrix} + \begin{bmatrix} 2 \\ 0 \end{bmatrix}$$

$$\text{or: } \begin{cases} x_n = 2x_{n-1} + 1.5y_{n-1} + 2 \\ y_n = 1.5x_{n-1} + 2y_{n-1} \end{cases}$$

We choose the initial vector $x_0 = 0.6$, $y_0 = -1.4$.

No. of iteration	1	2	3	4	5	6
x	1.10	1.35	1.475	1.538	1.569	1.585
y	-1.9	-2.15	-2.275	-2.338	-2.369	-2.385

We observe a convergence of the iterative process towards $x = 1.6$ and $y = -2.4$. Of course the number of iterations should be greater to increase the accuracy of the method. The exact solution can be computed by a direct inversion of A, treated in §9.3. Often direct inversions are not practical and iterative methods should be used.

9.1.5. Linear systems: basic theorems

The previous paragraph shows how to generate the curves C and L of an iterative process. We also have to choose the initial vector. In order to make this choice as easy as possible, we shall use the following theorem:

Theorem 1. An iterative process $X_m = \mathsf{M}X_{m-1} + \mathsf{B}$ converges for any initial vector X_0 if and only if all the eigenvalues of the matrix M are strictly less than 1 in absolute value.

We only give a proof in the case of a matrix M that can be diagonalized. The theorem holds for other matrices and a detailed proof is given by Forsythe and Wasow (1960, p. 215), who also show that Theorem 1 can be generalized to cases when some eigenvalues are equal to 1 in absolute value. We do not discuss these cases.

Proof. M may be diagonalized. There exists a base of eigenvectors $V_1, \ldots, V_n$, of the n-dimensional space of the vectors X_m. With our notations, M is the matrix $(\mathsf{I} - \mathsf{A})$ of the previous paragraph. We call X the solution of the equation $\mathsf{A}X = \mathsf{B}$. X is the limit of the sequence X_m, if there is a limit. Necessary condition: the limit X exists.

$$X_1 = \mathsf{M}X_0 + \mathsf{B}$$

$$X_2 = \mathsf{M}X_1 + \mathsf{B}$$

$$X_{m+1} = \mathsf{M}X_m + \mathsf{B}$$

$$X = \mathsf{M}X + \mathsf{B}$$

$$X - X_{m+1} = \mathsf{M}(X - X_m) = \mathsf{M}^2(X - X_{m-1}) = \mathsf{M}^{m+1}(X - X_0)$$

Let $\lambda_1, \ldots, \lambda_p$, $p \leqslant n$, be the eigenvalues of M. We assume that there exists k such that:

$$|\lambda_k| \geqslant 1$$

The choice of X_0 is such that $X - X_0$ belongs to the eigensubspace corresponding to λ_k:

$$X - X_0 = x^i V_i i \epsilon K$$

K is the set of indices of the eigenvectors corresponding to the eigenvalue λ_k. According to Einstein's convention we sum up on i:

$$X - X_{m+1} = \mathsf{M}^{m+1} x^i V_i = \lambda_k^{m+1} x^i V_i$$

x^i are fixed given numbers. Thus:

$$|\lambda_k|^{m+1} |x^i| \to \infty \quad m \to \infty$$

The sequence does not converge to X; X_0 cannot be chosen at random.

Sufficient condition: knowing that X exists and verifies $\mathsf{A}X = \mathsf{B}$ or $X = \mathsf{M}X + \mathsf{B}$, does the sequence (X_m) converge, when all eigenvalues are less than 1 in absolute value?

$$X - X_{m+1} = \mathsf{M}^{m+1}(X - X_0) = \lambda_i^{m+1} x_i^{\alpha i} V_{\alpha i}$$

with $i = 1, \ldots, p$ and α_i being the indices of the eigenvectors corresponding to the eigenvalue λ_i. The sum is on i and α_i. Introducing the norm, defined in Appendix 3, we have:

$$||X - X_{m+1}|| \leqslant |\lambda_i|^{m+1} |x^{\alpha i}| \, ||V_{\alpha i}||$$

This finite sum tends to zero when $m \to \infty$, if $|\lambda_i| < 1$, and the sequence (X_m) converges to X.

Interest of theorem 1

The interest of this theorem lies in the fact that X_0 may be chosen at random. Theoretically, convergence may be obtained by choosing $X - X_0$ in the eigensubspace corresponding to eigenvalues less than 1 in absolute value. Practically such a choice is impossible for two reasons:

(1) Usually nothing is known about X, the solution we are looking for

(2) In machine computation, round-off errors almost always introduce small components of all eigenvectors and the sequence will fail to converge.

Remark. In the example of §9.1.4, an easy computation yields the eigenvalues of $\mathsf{I} - \mathsf{A}$, $\lambda_1 = 0.5$ and $\lambda_2 = 3.5$. The initial vector X_0 was chosen such that $X_0 - X$ belonged to the subspace corresponding to $\lambda_1 = 0.5$ (X being the solution vector $x = 1.6$ and $y = -2.4$). The reader can easily verify that the process diverges if $X_0 - X$ has components in the eigensubspace corresponding to $\lambda_2 = 3.5$. (Take for instance $x_0 = 0$, $y_0 = 0$).

The main difficulty of an iterative process will be to estimate the eigenvalues, which usually cannot be computed directly. The following theorems allow of computing the bounds of the eigenvalues.

Definition: a matrix $\mathsf{M} = (a^j_i)$ is diagonally dominant if:

$$|a^i_i| \geqslant \sum_{j \neq i} |a^i_j| \qquad [9.1.8]$$

with strict inequality occurring for at least one i (i is the row index).

Definition: a matrix M is reducible if there exist a permutation of the rows and a permutation of the columns (usually different) so that the resulting arrangement of M takes the form:

$$\begin{pmatrix} \mathsf{A} & 0 \\ \mathsf{B} & \mathsf{C} \end{pmatrix}$$

where A, B, C are square submatrices and 0 is a zero matrix. Otherwise M is *irreducible.*

Theorem 2. A diagonally dominant, irreducible matrix M is regular. We give a short proof in the case when M is strictly diagonally dominant, i.e.:

$$|a^i_i| > \sum_{j \neq i} |a^i_j| \; \forall i \qquad [9.1.9]$$

Then it is not necessary to assume the irreductibility of M. For a general proof see Forsythe and Wasow (1960).

Proof. We assume that M is not regular. Its column vectors are not independent:

$$a^i_1 x^1 + a^i_2 x^2 + \ldots + a^i_n x^n = 0 \quad \text{for all } i$$

We set:

$$x^k = \sup |x^i|$$

The number of (x^i) is finite, thus x^k is one of the (x^i). From:

$$a^k_1 x^1 + \ldots + a^k_k x^k + \ldots + a^k_n x^n = 0$$

we get: $|a^k_k x^k| \leqslant \sum_{i \neq k} |a^k_i| \, |x^k|$ and $|a^k_k| \leqslant \sum_{i \neq k} |a^k_i|$

which contradicts the [9.1.9]. M is then regular, q.e.d.

Theorem 3 (*of Gerschgorin*). The eigenvalues of a matrix $\mathsf{M} = (a^j_i)$ are in the domain **D** defined as the union of all circles of centres a_i^i and of respective radii $\sum_{j \neq i} |a_j^i|$. This theorem is a direct consequence of Theorem 2: $\mathbf{M} - \lambda \mathbf{I}$ is a singular matrix when λ is an eigenvalue of **M**. Thus:

$$\exists\, i\colon\ |a_i^i - \lambda| \leqslant \sum_{j \neq i} |a_j^i|$$

Example (see Fig. 9.1.4):

$$\mathbf{M} = \begin{pmatrix} 2 & 1 & 0 \\ 1 & -3 & 1 \\ 0 & 1 & -1 \end{pmatrix}$$

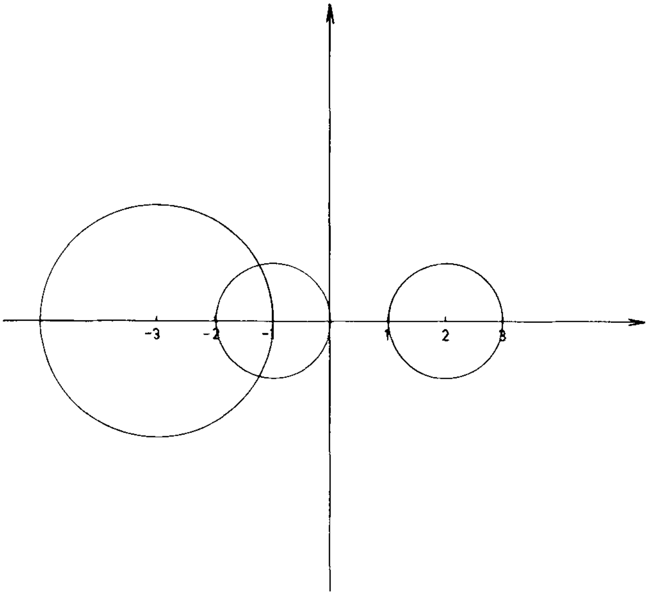

Fig. 9.1.4. Application of Gerschgorin's theorem.

To complete this survey of the basic theorems, we present here an *estimation of the largest eigenvalue* of a matrix **M**. Although we prove it for a Hermitian matrix only, it is valid for any matrix with one and only one real dominant eigenvalue (Remson et al., 1971, p. 187) and can be easily programmed for a computer.

M is Hermitian. It provides an orthonormal base of eigenvectors (V_1, V_2, . . . V_n) corresponding to the real eigenvalues λ_1, . . . λ_n which may be distinct or equal. Any vector X_0 may be written:

$$
\begin{aligned}
X_0 &= x^1 V_1 + x^2 V_2 + \ldots + x^n V_n \\
\mathsf{M} X_0 &= x^1 \lambda_1 V_1 + x^2 \lambda_2 V_2 + \ldots + x^n \lambda_n V_n
\end{aligned}
$$

We consider the iteration process, starting at X_0:

$$
\begin{aligned}
X_m &= \mathsf{M} X_{m-1} \\
X_m &= \mathsf{M}^m X_0 = x^1 \lambda_1^m V_1 + x^2 \lambda_2^m V_2 + \ldots + x^n \lambda_n^m V_n
\end{aligned}
$$

Assuming that λ_1 is the largest eigenvalue, we write:

$$
X_m = \lambda_1^m \left[x^1 V_1 + x^2 \left(\frac{\lambda_2}{\lambda_1}\right)^m V_2 + \ldots + x^n \left(\frac{\lambda_n}{\lambda_1}\right)^m V_n \right]
$$

When $m \to \infty$, we see that X_m tends to become parallel to the dominant eigenvector V_1, and λ_1 may be obtained by computing the limit of the ratio of the scalar products (X_{m+1}, X_m) and (X_m, X_m)

$$
\frac{(X_{m+1}, X_m)}{(X_m, X_m)} = \lambda_1 \frac{(x^1)^2 + (x^2)^2 \left(\frac{\lambda_2}{\lambda_1}\right)^{2m+1} + \ldots + (x^n)^2 \left(\frac{\lambda_n}{\lambda_1}\right)^{2m+1}}{(x^1)^2 + (x^2)^2 \left(\frac{\lambda_2}{\lambda_1}\right)^{2m} + \ldots + (x^n)^2 \left(\frac{\lambda_n}{\lambda_1}\right)^{2m}} \xrightarrow[m \to \infty]{} \lambda_1
$$

q.e.d.

9.2. ITERATIVE PROCEDURES FOR LINEAR SYSTEMS: METHODS

The most frequent iterative methods are described here, first for a very simple example and then for a general linear system.

9.2.1. Jacobi's method on a simple example

We consider permanent bidimensional flow in a porous medium with a homogeneous transmissivity $T = 1$. This flow is described (§9.5) by the equation:

$$
\frac{\partial^2 H}{\partial x^2} + \frac{\partial^2 H}{\partial y^2} = 0 \qquad [9.2.1]
$$

Discretizing [9.2.1] in a square grid (Fig. 9.2.1) and writing H_{ij} the value of the head at node i, j, we obtain the classical five-point scheme:

$$-4H_{i,j}+H_{i-1,j}+H_{i,j-1}+H_{i+1,j}+H_{i,j+1} = 0 \qquad [9.2.2]$$

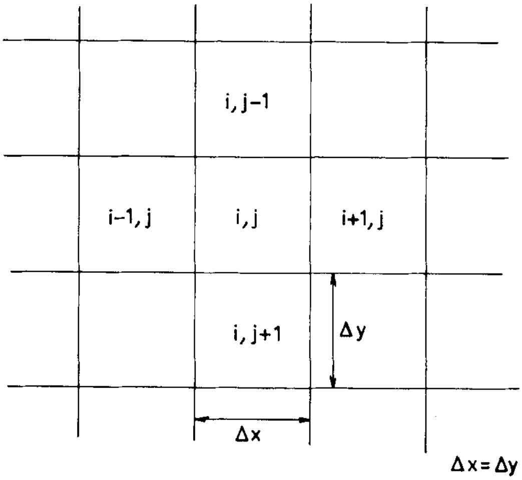

Fig. 9.2.1. Finite-difference bidimensional grid

Solving [9.2.2] for $H_{i,j}$, we obtain:

$$H_{i,j} = \frac{H_{i-1,j}+H_{i,j-1}+H_{i+1,j}+H_{i,j+1}}{4} \qquad [9.2.3]$$

Equation [9.2.3] generates a natural iterative process called Jacobi's method:

$$H_{i,j}^{(m+1)} = \frac{H_{i-1,j}^{(m)}+H_{i,j-1}^{(m)}+H_{i+1,j}^{(m)}+H_{i,j+1}^{(m)}}{4} \qquad [9.2.4]$$

The process starts with given arbitrary values of H at each node.

9.2.2. Gauss-Seidel method on a simple example

Formula [9.2.4] shows that H must be computed at every node during one step. In order to increase the convergence velocity, it is interesting to use new values of H immediately. As space sweeping is done for increasing i and j, when computation of $H_{i,j}^{(m+1)}$ takes place, $H_{i-1,j}^{(m+1)}$ and $H_{i,j-1}^{(m+1)}$ are already known. This remark has led to an improved iterative method, the Gauss-Seidel method defined by the following formula:

$$H_{i,j}^{(m+1)} = \frac{H_{i-1,j}^{(m+1)}+H_{i,j-1}^{(m+1)}+H_{i+1,j}^{(m)}+H_{i,j+1}^{(m)}}{4} \qquad [9.2.5]$$

9.2.3. Successive overrelaxation method on a simple example

A greater improvement of the convergence velocity may still be obtained. Let us come back to the basic principle of iterative methods.

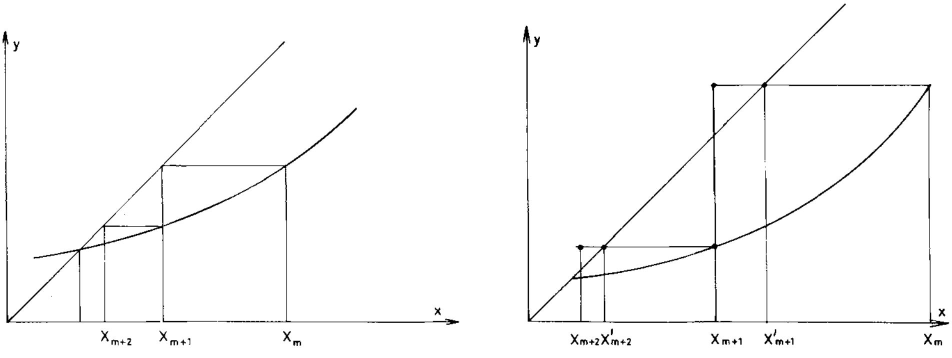

(a) (b)

Fig. 9.2.2. Successive overrelaxation.

By one of the previous methods, we obtain X'_{m+1}. In order to get nearer to the intersection, we multiply the vector $X'_{m+1} - X_m$ by an appropriate coefficient ω, which yields X_{m+1}. We iterate the process, that can be written:

$$X'_{m+1} = f(X_m)$$

$$X_{m+1} = X_m + \omega(X'_{m+1} - X_m)$$

Coming back to our simple example, we find that:

(1) the intermediate value $H'^{(m+1)}_{i,j}$ is computed by, say, the Gauss-Seidel formula:

$$H'^{(m+1)}_{i,j} = \frac{H^{(m+1)}_{i-1,j} + H^{(m+1)}_{i,j-1} + H^{(m)}_{i+1,j} + H^{(m)}_{i,j+1}}{4}$$

(2) $H^{(m+1)}_{i,j}$ is then given by:

$$H^{(m+1)}_{i,j} = H^{(m)}_{i,j} + \omega[H'^{(m+1)}_{i,j} - H^{(m)}_{i,j}] \qquad [9.2.6]$$

The obvious difficulty of course is how to choose an ω large enough to yield a good convergence velocity and small enough not to pass the intersection. In §9.2.5 we give some practical results concerning ω.

9.2.4. General formulas

Consider the system $\mathsf{AX} = \mathsf{B}$. To generate an iterative process, the matrix A is usually decomposed into the sum of diagonal matrix D, a strictly lower-triangular matrix L and a strictly upper-triangular matrix U. For example:

$$\begin{array}{ccccccc}\begin{bmatrix}1 & 2 & 3\\ 4 & 5 & 6\\ 7 & 8 & 9\end{bmatrix} & = & \begin{bmatrix}0 & 0 & 0\\ 4 & 0 & 0\\ 7 & 8 & 0\end{bmatrix} & + & \begin{bmatrix}1 & 0 & 0\\ 0 & 5 & 0\\ 0 & 0 & 9\end{bmatrix} & + & \begin{bmatrix}0 & 2 & 3\\ 0 & 0 & 6\\ 0 & 0 & 0\end{bmatrix}\\ \mathsf{A} & = & \mathsf{L} & + & \mathsf{D} & + & \mathsf{U}\end{array}$$

$$\text{or: } (\mathsf{L} + \mathsf{D} + \mathsf{U})\mathsf{X} = \mathsf{B} \qquad [9.2.7]$$

Equation [9.2.7] yields the various iterative formulas:
Jacobi:

$$\mathsf{X}^{(m+1)} = -\mathsf{D}^{-1}[(\mathsf{L} + \mathsf{U})\mathsf{X}^{(m)} - \mathsf{B}] \qquad [9.2.8]$$

Gauss-Seidel:

$$\mathsf{X}^{(m+1)} = -(\mathsf{D} + \mathsf{L})^{-1}\mathsf{U}\mathsf{X}^{(m)} + (\mathsf{D} + \mathsf{L})^{-1}\mathsf{B} \qquad [9.2.9]$$

Successive overrelaxation:

$$\begin{aligned} \mathsf{D}\mathsf{X}'_{m+1} &= -\mathsf{L}\mathsf{X}_{m+1} - \mathsf{U}\mathsf{X}_m + \mathsf{B}\\ \mathsf{X}_{m+1} &= \mathsf{X}_m + \omega(-\mathsf{D}^{-1}\mathsf{L}\mathsf{X}_{m+1} - \mathsf{D}^{-1}\mathsf{U}\mathsf{X}_m + \mathsf{D}^{-1}\mathsf{B} - \mathsf{X}_m) \qquad [9.2.10]\\ \mathsf{X}_{m+1} &= (\omega\mathsf{D}^{-1}\mathsf{L} + \mathsf{I})^{-1}(\mathsf{I} - \omega\mathsf{I} - \omega\mathsf{D}^{-1}\mathsf{U})\mathsf{X}_m + (\omega\mathsf{D}^{-1}\mathsf{L} + \mathsf{I})^{-1}\omega\mathsf{D}^{-1}\mathsf{B}. \end{aligned}$$

These formulas have to be expressed in terms of the various components of the matrices, to be usable on a computer; the system $\mathsf{AX} = \mathsf{B}$ is then written:

$$\sum_j a_{ij}x_j = b_i \quad i = 1, \ldots, n$$

and [9.2.7] yields:

$$\sum_{j=1}^{i-1} a_{ij}x_j + a_{ii}x_i + \sum_{j=i+1}^{n} a_{ij}x_j = b_i \quad i = 1, \ldots, n$$

Jacobi:

$$x_i^{(m+1)} = -\frac{1}{a_{ii}}\left[\sum_{j=1}^{i-1} a_{ij}x_j^{(m)} + \sum_{j=i+1}^{n} a_{ij}x_j^{(m)} - b_i\right] \qquad [9.2.11]$$

Gauss-Seidel:

$$x_i^{(m+1)} = -\frac{1}{a_{ii}}\left[\sum_{j=1}^{i-1} a_{ij}x_j^{(m+1)} + \sum_{j=i+1}^{n} a_{ij}x_j^{(m)} - b_i\right] \qquad [9.2.12]$$

Successive overrelaxation:

$$x_i^{(m+1)} = x_i^{(m)} + \omega\left[-\frac{1}{a_{ii}}\left\{\sum_{j=1}^{i-1} a_{ij}x_j^{(m+1)} + \sum_{j=i+1}^{n} a_{ij}x_j^{(m)} - b_i\right\} - x_i^{(m)}\right] \qquad [9.2.13]$$

9.2.5. Convergence of the methods

General discussion of convergence is to be found in Forsythe and Wasow (1960) and Remson et al. (1971). Here without proof, we give some practical results that are used in modelling groundwater pollution.

(1) A being the matrix of the system $\mathsf{AX} = \mathsf{B}$, if A is diagonally dominant and irreducible, then the Jacobi and Gauss-Seidel methods converge.

Remark. Of course, if A is strictly diagonally dominant, the irreductibility condition is not necessary.

The following definitions are taken from (Remson et al., 1971, p. 195).

(2) A square matrix A of order n is said to have property (A) if there exists a permutation matrix P such that $\mathsf{PA\tilde{P}}$ is diagonally block tridiagonal (Fig. 9.2.3) i.e. each D is diagonal.

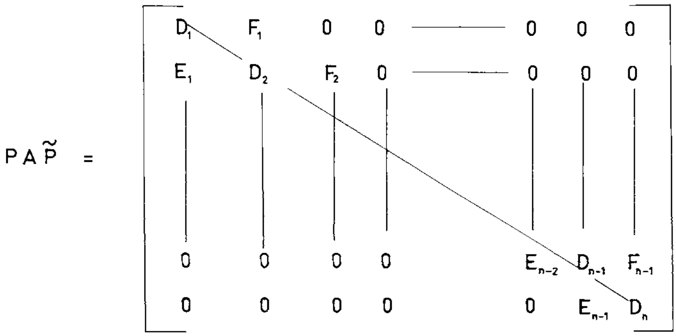

Fig. 9.2.3.

(3) In a system of linear equations $\mathsf{AX} = \mathsf{B}$, the components x_i and x_j are said to be coupled if either $a_{ij} \neq 0$ or $a_{ji} \neq 0$.

(4) The order of solving the equations $\mathsf{AX} = \mathsf{B}$ is consistent with this tridiagonal representation if, considering a grid, numbered by using the index

(i), the following permutation holds: the first node remains unchanged; the other mesh points are numbered by using an index $g(i)$ such that:

$$g(p) = g(i) + 1 \quad \text{for } p > i$$

$$g(p) = g(i) - 1 \quad \text{for } p < i$$

for each point p and all points i to which p is coupled. For example see Fig. 9.2.4.

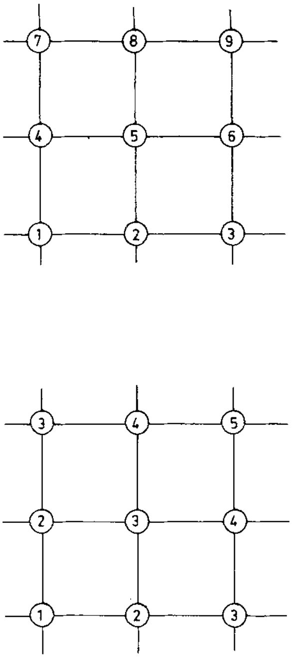

Fig. 9.2.4. Consistent ordering (Remson et al., 1971).

A very useful theorem is then:

Theorem. The matrix A of the system $\mathsf{AX} = \mathsf{B}$ being diagonally dominant, consistently ordered and having property (A), the successive overrelaxation method converges for $0 < \omega \leqslant 2$ and the eigenvalues λ of the iteration matrix $(\omega\mathsf{D}^{-1}\mathsf{L} + \mathsf{I})^{-1}(\mathsf{I} - \omega\mathsf{I} - \omega\mathsf{D}^{-1}\mathsf{U})$ are related to ω and μ by:

$$(\lambda + \omega - 1)^2 = \omega^2\mu^2\lambda$$

where μ is an eigenvalue of the Jacobi iteration matrix $-\mathsf{D}^{-1}(\mathsf{L} + \mathsf{U})$.

The best overrelaxation coefficient is:

$$\omega_{\text{opt}} = \frac{2}{1+\sqrt{1-\mu_{\max}^2}}$$

where $\mu_{\max}$ is the spectral radius of the Jacobi matrix. For this coefficient the number of iterations is minimum. The problem is then to determine ω_{opt}. Several approaches are discussed in (Remson et al., 1971, p. 199), such as Carré's method, that can be easily programmed.

We also recommend the direct computation of the largest eigenvalue by the ratio of scalar products as defined in §9.1.5. Another result may also be very useful: in the case of a rectangular grid of n internal columns and m internal rows, the largest eigenvalue of the Jacobi matrix corresponding to the discretization of $\partial^2 H/\partial x^2 + \partial^2 H/\partial y^2$ is exactly:

$$\tfrac{1}{2}\left[\cos\left(\frac{1}{n+1}\pi\right)+\cos\left(\frac{1}{m+1}\pi\right)\right]$$

This case corresponds to a homogeneous bidimensional aquifer. It can be empirically extended to a quasi-rectangular domain (Fig. 9.2.5), by taking an average value of the number of rows and columns.

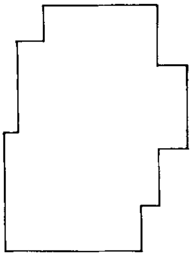

Fig. 9.2.5. A quasi-rectangular domain.

9.2.6. *Block iterative methods*

We shall just give a few basic principles of these methods, especially in view of applications to alternate direction procedures which will be developed in the case of time dependent equations in §9.6.

The principle of block iterative methods is to solve the system $\mathbf{AX} = \mathbf{B}$ by solving a sequence of tridiagonal systems. At each iteration step, a Gaussian elimination method (see §9.3) is used and the convergence velocity is increased.

This method will be best understood on a simple example, a homogeneous aquifer, of transmissivities 1, discretized as represented in Fig. 9.2.6; blocks 1 to 6 are at a constant potential; eastern and western boundaries of the aquifer are impervious. The regime is permanent and pumping and infiltration are represented by singularities Q_7 to Q_{15} in each block.

1	2	3
7	8	9
10	11	12
13	14	15
4	5	6

Fig. 9.2.6.

Using the method described in §9.5, we obtain the following system of equations:

$$\left[\begin{array}{ccc|ccc|ccc} -3 & 1 & 0 & 1 & 0 & 0 & 0 & 0 & 0 \\ 1 & -4 & 1 & 0 & 1 & 0 & 0 & 0 & 0 \\ 0 & 1 & -3 & 0 & 0 & 1 & 0 & 0 & 0 \\ \hline 1 & 0 & 0 & -3 & 1 & 0 & 1 & 0 & 0 \\ 0 & 1 & 0 & 1 & -4 & 1 & 0 & 1 & 0 \\ 0 & 0 & 1 & 0 & 1 & -3 & 0 & 0 & 1 \\ \hline 0 & 0 & 0 & 1 & 0 & 0 & -3 & 1 & 0 \\ 0 & 0 & 0 & 0 & 1 & 0 & 1 & -4 & 1 \\ 0 & 0 & 0 & 0 & 0 & 1 & 0 & 1 & -3 \end{array}\right] \begin{bmatrix} H_7 \\ H_8 \\ H_9 \\ H_{10} \\ H_{11} \\ H_{12} \\ H_{13} \\ H_{14} \\ H_{15} \end{bmatrix} = \begin{bmatrix} Q_7 - H_1 \\ Q_8 - H_2 \\ Q_9 - H_3 \\ Q_{10} \\ Q_{11} \\ Q_{12} \\ Q_{13} - H_4 \\ Q_{14} - H_5 \\ Q_{15} - H_6 \end{bmatrix} \tag{9.2.14}$$

There are three blocks $\mathsf{X} = (H_7 H_8 H_9)$, $\mathsf{Y} = (H_{10} H_{11} H_{12})$ and $\mathsf{Z} = (H_{13} H_{14} H_{15})$. Setting:

$$\mathsf{A} = \begin{bmatrix} -3 & 1 & 0 \\ 1 & -4 & 1 \\ 0 & 1 & -3 \end{bmatrix} \quad \mathsf{I} = \begin{bmatrix} 1 & 0 & 0 \\ 0 & 1 & 0 \\ 0 & 0 & 1 \end{bmatrix} \quad \mathsf{O} = \begin{bmatrix} 0 & 0 & 0 \\ 0 & 0 & 0 \\ 0 & 0 & 0 \end{bmatrix}$$

$$\mathsf{Q}_X = \begin{bmatrix} Q_7 - H_1 \\ Q_8 - H_2 \\ Q_9 - H_3 \end{bmatrix} \qquad \mathsf{Q}_Y = \begin{bmatrix} Q_{10} \\ Q_{11} \\ Q_{12} \end{bmatrix} \qquad \mathsf{Q}_Z = \begin{bmatrix} Q_{13} - H_4 \\ Q_{14} - H_5 \\ Q_{15} - H_6 \end{bmatrix}$$

and [9.2.14] is then written:

$$\begin{bmatrix} \mathsf{A} & \mathsf{I} & 0 \\ \mathsf{I} & \mathsf{A} & \mathsf{I} \\ 0 & \mathsf{I} & \mathsf{A} \end{bmatrix} \begin{bmatrix} \mathsf{X} \\ \mathsf{Y} \\ \mathsf{Z} \end{bmatrix} = \begin{bmatrix} \mathsf{Q}_X \\ \mathsf{Q}_Y \\ \mathsf{Q}_Z \end{bmatrix}$$

The resolution method becomes now equivalent to a point resolution method, coefficients being matrices. For instance Jacobi's block method is:

$$\begin{aligned} \mathsf{AX}_{m+1} &= \mathsf{Q}_X - \mathsf{IX}_m \\ \mathsf{AY}_{m+1} &= \mathsf{Q}_Y - \mathsf{IX}_m - \mathsf{IZ}_m \\ \mathsf{AZ}_{m+1} &= \mathsf{Q}_Z - \mathsf{IY}_m \end{aligned}$$

In the same way, block Gauss-Seidel and overrelaxation methods may be defined. The inversion of A is easily obtained by Gaussian elimination (§9.3).

Remark. Other blocks could be defined of course. In the example, we have given the natural block decomposition in columns and rows, the decomposition that is used in alternate direction procedures.

9.3. DIRECT PROCEDURES

We present the general direct method of Gauss elimination and its simplified form for tridiagonal matrices.

9.3.1. General Gauss elimination method

Consider the linear system of equations:

$$\begin{aligned} a_{11}x_1 + a_{12}x_2 + \ldots + a_{1n}x_n &= b_1 \\ a_{21}x_1 + a_{22}x_2 + \ldots + a_{2n}x_n &= b_2 \\ \\ a_{n1}x_1 + a_{n2}x_2 + \ldots + a_{nn}x_n &= b_n \end{aligned}$$

We divide the first line by a_{11}, multiply it then by a_{21} and subtract it from the second line:

$$\left(a_{21}-\frac{a_{21}}{a_{11}}a_{11}\right)x_1+\left(a_{22}-\frac{a_{21}}{a_{11}}a_{12}\right)x_2+\ldots+\left(a_{2n}-\frac{a_{21}}{a_{11}}a_{1n}\right)x_n = b_2-\frac{a_{21}}{a_{11}}b_1$$

the coefficient of x disappears; we iterate the operation, multiplying the first line by a_{k1}. We obtain the new system:

$$\begin{aligned}
&x_1+a_{12}/a_{11}x_2+\ldots+a_{1n}/a_{11}x_n = b_1/a_{11}\\
&0 \quad b_{22}x_2+\ldots+b_{2n}x_n = b_2-(a_{21}/a_{11})\,b_1\\
&0 \quad b_{n2}x_2+\ldots+b_{nn}x_n = b_n-(a_{n1}/a_{11})\,b_1
\end{aligned}$$

with $b_{pk} = a_{pk}-(a_{1k}/a_{11})\,a_{p1}$.

Performing these operations starting from the second new line and iterating the process, we obtain the system:

$$\begin{aligned}
x_1+c_{12}x_2+\ldots+c_{1n}x_n &= d_1\\
x_2+\ldots+c_{2n}x_n &= d_2\\
x_n &= d_n
\end{aligned}$$

The last equation yields x_n, put into the preceding equation to yield x_{n-1} and so on.

9.3.2. Tridiagonal Gauss elimination method

Consider the tridiagonal system:

$$\begin{aligned}
&b_1X_1+c_1X_2 = d_1\\
&a_iX_{i-1}+b_iX_i+c_iX_{i+1} = d_i \quad (i = 2,\ldots n-1)\\
&a_nX_{n-1}+b_nX_n = d_n
\end{aligned} \qquad [9.3.1]$$

or:

$$\begin{pmatrix} b_1 & c_1 & 0\ldots 0 & 0\\ a_2 & b_2 & c_2\ldots 0 & 0\\ 0 & 0 & 0\ldots a_n & b_n\end{pmatrix}\begin{pmatrix}X_1\\X_2\\X_n\end{pmatrix}=\begin{pmatrix}d_1\\d_2\\d_n\end{pmatrix}$$

Writing:

$$X_i = \alpha_i - \beta_i X_{i+1} \quad (i = 1, \ldots, n-1)$$
$$X_n = \alpha_n \qquad [9.3.2]$$

and eliminating X_{i-1}, X_i and X_{i+1} between the three equations:

$$X_{i-1} = \alpha_{i-1} - \beta_{i-1} X_i$$
$$a_i X_{i-1} + b_i X_i + c_i X_{i+1} = d_i \quad (i = 2, \ldots, n-1)$$
$$X_i = \alpha_i - \beta_i X_{i+1}$$

We obtain:

$$\left.\begin{aligned} a_i\alpha_{i-1} - a_i\beta_{i-1}\alpha_i + \alpha_i b_i &= d_i \\ a_i\beta_{i-1}\beta_i - b_i\beta_i + c_i &= 0 \end{aligned}\right. \quad (i = 2, \ldots, n-1)$$

and:

$$\left.\begin{aligned} \alpha_i &= \frac{d_i - a_i\alpha_{i-1}}{b_i - a_i\beta_{i-1}} \\ \beta_i &= \frac{c_i}{b_i - a_i\beta_{i-1}} \end{aligned}\right. \quad (i = 2, \ldots, n-1)$$

for $i = 1$:

$$\begin{aligned} b_1 X_1 + c_1 X_2 &= d_1 \\ X_1 &= \alpha_1 - \beta_1 X_2 \end{aligned} \quad \text{yields} \quad \begin{aligned} \alpha_1 &= \frac{d_1}{b_1} \\ \beta_1 &= \frac{c_1}{b_1} \end{aligned}$$

for $i = n$:

$$a_n X_{n-1} + b_n X_n = d_n$$
$$X_{n-1} = \alpha_{n-1} - \beta_{n-1} X_n \quad \text{yields} \quad \alpha_n = \frac{d_n - a_n\alpha_{n-1}}{b_n - a_n\beta_{n-1}}$$
$$X_n = \alpha_n$$

The solution of the tridiagonal system [9.3.1] is thus found by computing

α_i and β_i from $i = 1$ to $i = n$ then replacing α_i and β_i by their values in [9.3.2]. This method is quite easily programmed.

9.4. *THE THEORY OF APPROXIMATION OF THE DISPERSION EQUATION*

9.4.1. *Approximation of derivatives*

Under some regularity conditions (for our problems, it will be enough to consider that C has continuous derivatives up to the order 4), the function C can be expanded in a Taylor series in a neighbourhood of x; y, z, t are constant:

$$c(x + h, y, z, t) = c(x, y, z, t) + h \frac{\partial c}{\partial x}(x, y, z, t) + \frac{h^2}{2} \frac{\partial^2 c}{\partial x^2}(x, y, z, t) + \frac{h^3}{3!} \frac{\partial^3 c}{\partial x^3}(x, y, z, t) + \ldots + \frac{h^n}{n!} \frac{\partial^n c}{\partial x^n}(x, y, z, t) + 0(h^n) \qquad [9.4.1]$$

The remaining terms of the series are equal to $0(h^n)$: we say that a function f is equal to $0(h^n)$ if there exists a positive constant k such that $|f| \leqslant k\,|h^n|$. Thus as $|h^n| \to 0$, $|f| \to 0$ at least as rapidly.

Taking $h = \Delta x$ and $h = -\Delta x$, we find, respectively:

$$c(x + \Delta x, y, z, t) = c(x, y, z, t) + \Delta x \frac{\partial c}{\partial x}(x, y, z, t) + \frac{\Delta x^2}{2} \frac{\partial^2 c}{\partial x^2}(x, y, z, t) + 0(\Delta x^3) \qquad [9.4.2]$$

$$c(x - \Delta x, y, z, t) = c(x, y, z, t) - \Delta x \frac{\partial c}{\partial x}(x, y, z, t) + \frac{\Delta x^2}{2} \frac{\partial^2 c}{\partial x^2}(x, y, z, t) + 0(\Delta x^3) \qquad [9.4.3]$$

These equations can be solved for $\partial c/\partial x$ to give:

$$\frac{\partial c}{\partial x} = \frac{c(x + \Delta x, y, z, t) - c(x - \Delta x, y, z, t)}{2\Delta x} + 0(\Delta x^2)$$

which yields the *central-difference approximation* of the derivative:

$$\frac{\partial c}{\partial x} \simeq \frac{c(x + \Delta x, y, z, t) - c(x - \Delta x, y, z, t)}{2\Delta x}$$

We drop the remaining terms of the series called "truncation error", equal to $0(\Delta x^2)$. Stopping the Taylor's expansion at $n = 1$ (we put $n = 1$ into [9.4.1]), we obtain from [9.4.2] and [9.4.3]:

$$\frac{\partial c}{\partial x} = \frac{c(x + \Delta x, y, z, t) - c(x, y, z, t)}{\Delta x} + 0(\Delta x)$$

$$\frac{\partial c}{\partial x} = \frac{c(x, y, z, t) - c(x - \Delta x, y, z, t)}{\Delta x} + 0(\Delta x)$$

This yields the *forward-difference approximation* of the derivative:

$$\frac{\partial c}{\partial x}(x, y, z, t) \simeq \frac{c(x + \Delta x, y, z, t) - c(x, y, z, t)}{\Delta x}$$

and the *backward-difference approximation* of the derivative:

$$\frac{\partial c}{\partial x}(x, y, z, t) \simeq \frac{c(x, y, z, t) - c(x - \Delta x, y, z, t)}{\Delta x}$$

Both approximations have a truncation error of order Δx. To obtain an approximation of the second-order derivative, we combine [9.4.2] and [9.4.3] expanded at $n = 4$:

$$\frac{\partial^2 c}{\partial x^2}(x, y, z, t) \simeq \frac{c(x + \Delta x, y, z, t) - 2c(x, y, z, t) + c(x - \Delta x, y, z, t)}{(\Delta x)^2}$$

which has a truncation error of order $(\Delta x)^2$.

In the same way, we obtain approximations of $\partial c/\partial y$, $\partial c/\partial z$, $\partial^2 c/\partial y^2$, $\partial^2 c/\partial z^2$. The forward-difference approximation of $\partial c/\partial t$ is used in dispersion problems.

9.4.2. Approximation of the equation

For the sake of simplicity, we restrict ourselves to the study of the monodimensional dispersion equation with constant coefficients. The methods we develop on this simple example are general and will easily be extended by the student to other dispersion equations. We have to approximate:

$$\frac{\partial c}{\partial t} = -u\frac{\partial c}{\partial x} + K\frac{\partial^2 c}{\partial x^2} \qquad [9.4.4]$$

We choose an approximation of $\partial c/\partial x$ (backward, forward or central) and we approximate $\partial^2 c/\partial x^2$. The approximation of $-u\,(\partial c/\partial x) + K\,(\partial^2 c/\partial x^2)$ at point x and time t is written $\Gamma(x, t)$ and we have:

$$\frac{\partial c}{\partial t}(x, t) = \Gamma(x, t) \qquad [9.4.5]$$

as a first approximation of the dispersion equation. The discretization of $\partial c/\partial t$ is based on the fact that we know $c(x, t_1)$ and we are looking for $c(x, t_2)$ with $t_2 > t_1$, which gives:

$$\frac{\partial c}{\partial t} = \frac{c(x, t_2) - c(x, t_1)}{t_2 - t_1}$$

We can choose now $\Gamma(x, t)$ at time t_1, time t_2 or in-between. This will yield the three approximations of the dispersion equation.

(1) *The explicit approximation.* We take Γ at time t_1:

$$\frac{c(x, t_2) - c(x, t_1)}{t_2 - t_1} = \Gamma(x, t_1) \qquad [9.4.6]$$

Equation [9.4.5] provides a geometrical interpretation of [9.4.6] : $\Gamma(x, t_1)$ is the slope of the tangent to the curve of equation $t \to C(x, t)$ at point t_1. If $C(x, t_2)$ is the computed value and $\gamma(x, t_2)$ the exact value, we have Fig. 9.4.1.

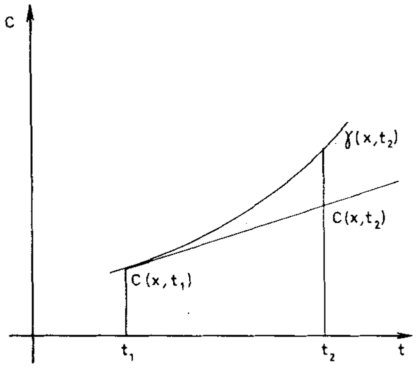

Fig. 9.4.1. The explicit approximation.

(2) *The implicit approximation.* We take Γ at time t_2:

$$\frac{c(x, t_2) - c(x, t_1)}{t_2 - t_1} = \Gamma(x, t_2) \qquad [9.4.7]$$

The geometrical interpretation is represented in Fig. 9.4.2. $\Gamma(x, t_2)$ is the slope of the tangent at point t_2 and the straight line $c(xt_2)\,c(xt_1)$ is parallel to this tangent.

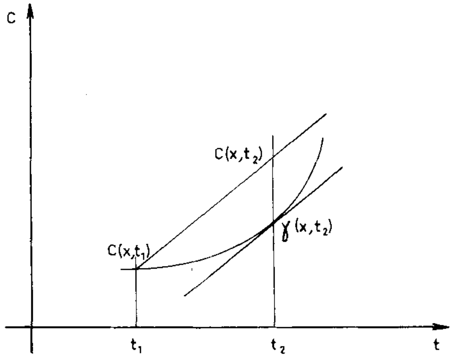

Fig. 9.4.2. The implicit approximation.

(3) *The Crank-Nicolson approximation.* We assume that $\Gamma(x, t)$ is linear on the interval (t_1, t_2) and we write:

$$\frac{c(x, t_2) - c(x, t_1)}{t_2 - t_1} = \lambda\Gamma(x, t_1) + (1 - \lambda)\,\Gamma(x, t_2) \qquad [9.4.8]$$

The name "Crank-Nicolson" is given when $\lambda = 0.5$, which corresponds to Fig. 9.4.3.

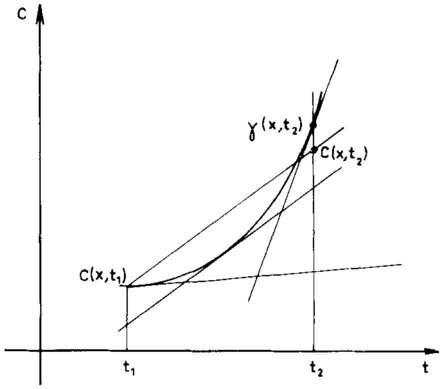

Fig. 9.4.3. The Crank-Nicolson approximation.

9.4.3. Stability and convergence of the approximations

The object of the approximations is to provide an estimate of the concentration at time t_2 knowing the concentration at time t_1. To be valid this estimate should be close, in some sense*, to the exact solution of the dispersion equation ([9.4.4] for instance), which requires two conditions for the use of the approximations: stability and convergence. As previously we call $c(x, t)$ the computed solution and $\gamma(x, t)$ the exact solution of the dispersion equation. We set $t_2 - t_1 = \Delta t$.

Definition of convergence. A finite-difference approximation is *convergent* if the difference between $\gamma(x, t)$ and $c(x, t)$ tends to zero when Δx and Δt tend to zero, at given x and t.

Definition of stability. When time varies, we compute $e(x, t + \Delta t)$ from $c(x, t)$. This is an iterative process, which is valid if the difference between $\gamma(x, t)$ and $c(x, t)$ is bounded in some sense, when $t \to \infty$, for given Δx and Δt. If such a condition is verified, the approximation is stable.

We admit that the approximations just presented are convergent and we investigate their stabilities. It should be noticed that stability and convergence are related and that it can be proved that under good conditions they are equivalent.

Results on stability are given with short rough proofs, the purpose of which is mainly to teach how to use the basic theorems of §9.1 in real problems.

(1) *The explicit approximation.* Equation [9.4.6] is written between time t_n and time t_{n+1}, taking a square grid of space $(\Delta x, 2\Delta x, \ldots, i\Delta x, \ldots, I\Delta x)$ and backward difference of the convective term:

$$\frac{c(i, t_{n+1}) - c(i, t_n)}{t_{n+1} - t_n} =$$

$$-U\,\frac{c(i, t_n) - c(i-1, t_n)}{\Delta x} + K\,\frac{c(i+1, t_n) - 2c(i, t_n) + c(i-1, t_n)}{\Delta x^2}$$

or:

$$c(i, t_{n+1}) = c(i-1, t_n)\left(\frac{K\Delta t}{\Delta x^2} + \frac{U\Delta t}{\Delta x}\right) + c(i, t_n)\left(1 - \frac{U\Delta t}{\Delta x} - 2\,\frac{K\Delta t}{\Delta x^2}\right)$$

$$+ c(i+1, t_n)\,\frac{K\Delta t}{\Delta x^2} \qquad [9.4.9]$$

---

* The "closeness" of two functions depends on the type of norm adopted for the functional space they belong to. In this book we do not give details about this problem; let us only remember that the most usual norms in our case are $\| f \|_\infty = \sup | f(x) |$ $\| f \|_2 = [\int_R f^2(x)\,dx]^{1/2}$ or $\| f \|_1 = \int_R | f(x) |\,dx$. The closeness of f and g is then defined by the size of the real positive number $\| f - g \|$.

with $t_{n+1} - t_n = \Delta t$.

This system of equations may be written under the matrix form:

$$C(t_{n+1}) = \mathsf{M}\, C(t_n)$$

$$\mathsf{M} = \begin{bmatrix} \ddots & \ddots & & & 0 \\ & & & & \vert \\ 0 - a_1 & a_2 & a_3 & \text{---} & 0 \\ \vert & & \ddots & \ddots & \\ 0 & \text{---} & & & \end{bmatrix}$$

with:

$$a_1 = \frac{K\Delta t}{\Delta x^2} + \frac{U\Delta t}{\Delta x};\ a_2 = 1 - \frac{U\Delta t}{\Delta x} - 2\frac{K\Delta t}{\Delta x^2};\ a_3 = \frac{K\Delta t}{\Delta x^2}$$

$C(t_n)$ is a vector of components $c(i, t_n)$.

From Gerschgorin's theorem (§9.1), the eigenvalues of M lie in the interval $[1 - 2(U\Delta t/\Delta x) - 4(K\Delta t/\Delta x^2), 1]$. From the general convergence theorem (§9.1), the iterative process defined by [9.4.9] does not converge if the eigenvalues of the iteration matrix are greater than 1 in absolute value. Thus, the explicit approximation is stable if:

$$1 - 2\frac{U\Delta t}{\Delta x} - 4\frac{K\Delta t}{\Delta x^2} > -1$$

or:

$$\Delta t < \Delta t_c \qquad [9.4.10]$$

with:

$$\Delta t_c = \frac{\Delta x}{2\dfrac{K}{\Delta x} + U}$$

Δt_c is called the critical time step, and the *approximation is said to be stable, conditionally to [9.4.10]*.

Remark. With forward or central differences, Δt_c is different of course. Computation of Δt_c is obvious in all cases.

(2) *The implicit approximation*. Discretizing as previously, we obtain:

$$c(i-1, t_{n+1})\left(-\frac{K\Delta t}{\Delta x^2} - \frac{U\Delta t}{\Delta x}\right) + c(i, t_{n+1})\left(1 + \frac{U\Delta t}{\Delta x} + 2\frac{K\Delta t}{\Delta x^2}\right)$$
$$+ c(i+1, t_{n+1})\left(-K\frac{\Delta t}{\Delta x^2}\right) = c(i, t_n) \qquad [9.4.11]$$

or, under matrix form:

$$\mathsf{N}C(t_{n+1}) = C(t_n)$$

N being the triangular matrix:

$$\mathsf{N} = \begin{pmatrix} \ddots & \ddots & \ddots & 0 \\ & a_1 & a_2 & a_3 \\ 0 & & \ddots & \ddots \end{pmatrix}$$

with:

$$a_1 = -\frac{K\Delta t}{\Delta x^2} - \frac{U\Delta t}{\Delta x};\ a_2 = 1 + \frac{U\Delta t}{\Delta x} + 2\frac{K\Delta t}{\Delta x^2};\ a_3 = -\frac{K\Delta t}{\Delta x^2}$$

The iteration matrix is then N^{-1}.

From Gerschgorin's theorem (§9.1), the eigenvalues of N lie in the interval $[1, 1 + 2\ (U\Delta t/\Delta x) + 4\ (K\Delta t/\Delta x^2)]$ which implies that they are greater than 1. Thus the eigenvalues of N^{-1} have their absolute values smaller than 1. From the general convergence theorem (§9.1), the iterative process [9.4.11] converges.

We say that the implicit approximation is *unconditionally stable.*

(3) *The Crank-Nicolson approximation.* Using the same discretization as previously, we have:

$$\begin{aligned} & c(i-1, t_{n+1})\left[-\frac{1}{2}\left(\frac{K\Delta t}{\Delta x^2} + \frac{U\Delta t}{\Delta x}\right)\right] + c(i, t_{n+1})\left[1 + \frac{1}{2}\left(\frac{U\Delta t}{\Delta x} + 2\frac{K\Delta t}{\Delta x^2}\right)\right] \\ & \quad + c(i+1, t_{n+1})\left[-\frac{1}{2}\frac{K\Delta t}{\Delta x^2}\right] = c(i-1, t_n)\left[\frac{1}{2}\left(\frac{K\Delta t}{\Delta x^2} + \frac{U\Delta t}{\Delta x}\right)\right] + c(i, t_n) \\ & \quad \left[1 - \frac{1}{2}\left(\frac{U\Delta t}{\Delta x} + 2\frac{K\Delta t}{\Delta x^2}\right)\right] + c(i+1, t_n)\left[\frac{1}{2}\frac{K\Delta t}{\Delta x^2}\right] \end{aligned}$$

written under matrix form as:

$$\mathsf{M}C(t_{n+1}) = \mathsf{N}C(t_n)$$

where M and N are tridiagonal matrices, the coefficients on a line being the coefficients, respectively, of $c(i-1)$, $c(i)$, $c(i+1)$.

Calling P the tridiagonal matrix a line of which is made up of the coefficients:

$$\frac{K\Delta t}{\Delta x^2} + \frac{U\Delta t}{\Delta x}, -\frac{U\Delta t}{\Delta x} - 2\frac{K\Delta t}{\Delta x^2}, \frac{K\Delta t}{\Delta x^2}$$

we notice that P, $\mathsf{M} = \mathsf{I} - \frac{1}{2}\mathsf{P}$ and $\mathsf{N} = \mathsf{I} + \frac{1}{2}\mathsf{P}$ have the same eigenvectors, which implies that $(\mathsf{I} - \mathsf{P}/2)^{-1}$ and $\mathsf{M}^{-1}\mathsf{N}$ have the same eigenvectors as $\mathbf{P}$.

p being the corresponding eigenvalue of P, $1 - p/2$ and $1 + p/2$ are the corresponding eigenvalues, respectively, of M and N. Thus the corresponding eigenvalue a of the iteration matrix $\mathsf{M}^{-1}\mathsf{N}$ is:

$$a = \frac{1 + p/2}{1 - p/2}$$

According to Gerschgorin's theorem, the eigenvalues of P lie in the interval $[-2\{(U\Delta t/\Delta x) + 2(K\Delta t/\Delta x^2)\}, 0]$ and are negative, which shows that $|a|$ is smaller than 1.

The Crank-Nicolson approximation is unconditionally stable.

9.4.4. *Alternating Direction Implicit Procedure* (*ADIP*)

When the domain is bidimensional rectangular or at least very regular (convex for instance), fast resolution may be obtained by the ADIP introduced by Peaceman and Rachford. This method has a great advantage: instead of computing the inverse of a general matrix, one computes the inverses of two tridiagonal matrices. This is done by the simplified Gaussian elimination method (§9.3.2) and is very quick in terms of computer time. We discuss ADIP on a simple example.

Consider the dispersion equation:

$$K_L \frac{\partial^2 c}{\partial x^2} + K_T \frac{\partial^2 c}{\partial y^2} - u\frac{\partial c}{\partial x} = \frac{\partial c}{\partial t}$$

An approximation of this equation during one time-step consists in dividing up this time-step into two and expressing the derivatives with respect to x implicitly and the derivative with respect to y explicitly during the first half time-step. During the second half time-step the derivatives with respect to x are expressed explicitly and the derivative with respect to y implicitly:

$$(1)\ K_L \frac{c^+(i+1,j) - 2c^+(i,j) + c^+(i-1,j)}{\Delta x^2} - U\frac{c^+(i,j) - c^+(i-1,j)}{\Delta x} =$$
$$\frac{c^+(i,j) - c_1(i,j)}{\Delta t/2} - K_T \frac{c_1(i,j+1) - 2c_1(i,j) + c_1(i,j-1)}{\Delta y^2}$$

$$(2)\ K_T\,\frac{c_2(i,j+1)-2c_2(i,j)+c_2(i,j-1)}{\Delta y^2}=\frac{c_2(i,j)-c^+(i,j)}{\Delta t/2}-$$
$$K_L\,\frac{c^+(i,+1,j)-2c^+(i,j)+c^+(i-1,j)}{\Delta x^2}+u\,\frac{c^+(i,j)-c^+(i-1,j)}{\Delta x}$$

$c_1(i,j)$ and $c_2(i,j)$ are the concentrations at times t_1 and $t_2(t_2-t_1=\Delta t)$, at points (i,j) and $c^+(i,j)$ is an intermediate value which has no physical meaning. The solution progresses by computing c^+ for all lines i by tridiagonal Gaussian elimination, assuming c_1 is known, and then by computing c_2 for all columns j also by tridiagonal Gaussian elimination. It can be shown that the ADIP is convergent and unconditionally stable.

9.4.5. *Some difficulties of the finite-difference approximations*

Finite-difference methods are easy to handle, sometimes fast and usually fairly well known. But in the case of dispersion models, two difficulties arise, which are not completely solved up to now: overshoot and numerical diffusion.

(1) *Overshoot.* Consider the injection of a unit concentration step-input function in a one-dimensional flow governed by the dispersion equation:

$$K\frac{\partial^2 c}{\partial x^2}-u\frac{\partial c}{\partial x}=\frac{\partial c}{\partial t}$$

comparison of the analytical solution and the computed solution at time t is given in Fig. 9.4.4.

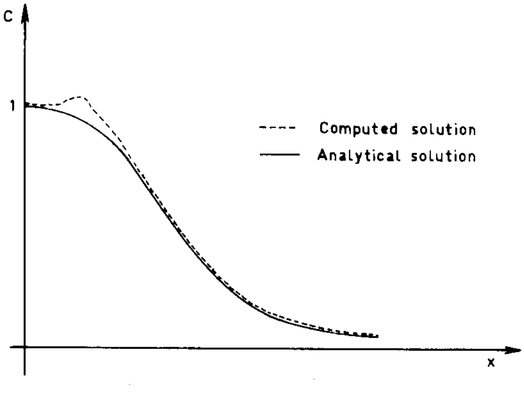

Fig. 9.4.4. Overshoot.

It very often appears that computed concentration exceeds one near the c-axis. This discrepancy is known as "overshoot". It may be explained as follows. Time-steps and spatial dimensions are not well adjusted and the aquifer cannot "absorb" numerically the injected mass of pollutant. The time-steps should be chosen carefully and adapted to the problem. Often the choice of the time increment as the general term of the geometrical series ($\Delta t_n = a\Delta t_{n-1}$, with $1 < a < 2$) is found to erase the overshoot. For instance, Shamir and Harleman (1967b) have used $a = 1.3$ in some of their problems.

We recommend testing any model with a unit-concentration step-input function to adjust time-steps and grid spacing before using it for general boundary conditions.

(2) *Numerical diffusion.* Consider the injection of a unit-concentration step-input function in a one-dimensional flow, governed by the dispersion equation:

$$K\frac{\partial^2 c}{\partial x^2} - u\frac{\partial c}{\partial x} = \frac{\partial c}{\partial t}$$

Take $K = 0$. Analytical and computed solutions at time t are given in Fig. 9.4.5.

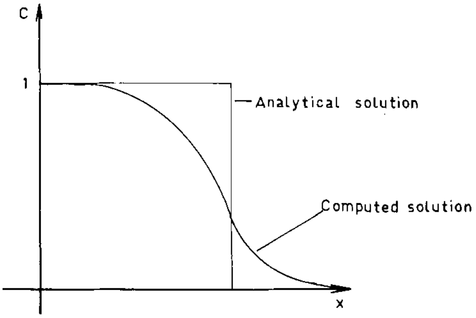

Fig. 9.4.5. Numerical diffusion.

The shape of the computed curve explains why the name "numerical diffusion" has been given to the phenomenon: it behaves as if the finite-difference approximation of the convection equation $-u\,(\partial c/\partial x) = \partial c/\partial t$ was some diffusion equation:

$$D\frac{\partial^2 c}{\partial x^2} - u\frac{\partial c}{\partial x} = \frac{\partial c}{\partial t}$$

the coefficient D having no physical meaning. Some explanations have been given by Lantz (1969, 1970): numerical diffusion is a truncation error; the finite-difference approximations to the first-order derivatives (both time and space) give rise to error terms proportional to second-order derivatives

(§9.4.1), the proportionality constants depending both on space and time increments.

Take our simple example, the space first derivative being approximated by a backward difference:

$$u \frac{\partial c}{\partial x} \simeq u \frac{c(x) - c(x - \Delta x)}{\Delta x} - u \frac{\Delta x}{2} \frac{\partial^2 c}{\partial x^2}$$

A numerical dispersion coefficient $- u\Delta x/2$ is thus introduced, which may be of the order of the physical-dispersion coefficient K. This artificial dispersion is a matter of concern in the domain of dynamic dispersion (when $K = \alpha u$) for values of the order of $\Delta x/2$. No real solution has yet been found for this anomaly, except by testing a mean longitudinal dispersion coefficient of the form $(\alpha u - u\Delta x/2)$ allowing some erasing of the numerical dispersion.

Of course for large-scale dispersion problems, numerical dispersion may be negligible for suitable mesh sizes.

9.4.6. The method of characteristics

In order to reduce or suppress the above-mentioned difficulties, Garder et al. (1964) have introduced a tentative improvement of the classical finite-difference resolution schemes which they call the method of characteristics. The problem is still approached by finite differences but physical considerations on the evolution of dispersion lead to establishing a first-order partial differential equation equivalent to the dispersion equation and to determining its characteristic lines.

The problem is defined by the dispersion equation:

$$K_L \frac{\partial^2 C}{\partial x^2} + K_T \frac{\partial^2 C}{\partial y^2} - U_x \frac{\partial C}{\partial x} - U_y \frac{\partial C}{\partial y} = \frac{\partial C}{\partial t}$$

where:

$$U_x = -\frac{k}{\phi\mu}\left(\frac{\partial p}{\partial x} + \rho g \frac{\partial h}{\partial x}\right), \qquad U_y = -\frac{k}{\phi\mu}\left(\frac{\partial p}{\partial y} + \rho g \frac{\partial h}{\partial y}\right) \qquad [9.4.12]$$

considering that dispersion may be neglected with respect to convection, they assimilate the equation to a first-order partial-differential equation and look for its characteristics, solving the usual system:

$$dx/dt = U_x, \qquad dy/dt = U_y \qquad [9.4.13a]$$

$$\frac{dC}{dt} = K_L \frac{\partial^2 C}{\partial x^2} + K_T \frac{\partial^2 C}{\partial y^2} \qquad [9.4.14a]$$

The characteristics (Garabedian, 1964) span the solution. A moving point (xp, yp) is associated with each characteristic p, which is given by its parametric equation $x_p(t)$, $y_p(t)$ where t is time.

The experimental domain, which is assumed to be rectangular, is divided by a conventional stationary grid into rectangles of dimensions Δx and Δy. Each point (i, j) is made the center of the rectangle Ri, j. Initially the moving points are distributed at random, two moving points per grid interval being sufficient (a greater number does not really improve the accuracy of the method), with initial coordinates $x_p(0)$ $y_p(0)$ and an initial concentration $Cp(0)$.

Ci, j, n being known at the grid points, the viscosity and density at each point are known, and the pressure is determined from the equation (ϕ is taken as constant):

$$\operatorname{div}\left[(k/\mu)(\operatorname{grad} p + \rho g \operatorname{grad} h)\right] = 0$$

using the Peaceman and Rachford method. From the set [9.4.12] the velocity components are determined at the centers of the grid intervals and everywhere by bilinear interpolation. The new positions of point (x_p, y_p) are obtained from [9.4.13a] as:

$$x_{p,n+1} = x_{p,n} + \Delta t_n\, U_x(x_{p,n}, y_{p,n}), \qquad y_{p,n+1} = y_{p,n} + \Delta t_n\, U_y(x_{p,n}, y_{p,n}) \qquad [9.4.13b]$$

All points are then examined to determine which rectangle Ri, j, they lie in. Each rectangle Ri, j is assigned a concentration C^+i, j, n equal to the average of the concentrations Cp, n of all the points in their new positions in Ri, j. The change in concentration due to dispersion in each rectangle is derived from equation [9.4.14a] as:

$$\Delta C^+_{i,j,n} = (\Delta t_n/\phi)\,(K_L \Delta_x^2 C^+_{i,j,n} + K_T \Delta_y^2 C^+_{i,j,n}) \qquad [9.4.14b]$$

where Δ_x^2 and Δ_y^2 are the approximations of $\partial^2 c/\partial x^2$ and $\partial^2 c/\partial y^2$.

Each moving point is then assigned a new concentration:

$$C_{p,n+1} = C_{p,n} + \Delta C^+_{i,j,n}$$

The change in concentration due to dispersion is the same for all moving points falling in the same rectangle.

The concentrations at the stationary grid points at the new time-step are then given by:

$$C_{i,j,n+1} = C^+_{i,j,n} + \Delta C^+_{i,j,n}$$

This procedure is then repeated for each subsequent time-step. This method prevents numerical dispersion: if dispersion is zero ($K_L = K_T = 0$) there is no change in concentrations Cp, n: thus any discontinuity in concentration is preserved and translated.

Although numerical dispersion does not appear, overshoot is not easily overcome (Reddell and Sunada, 1970). This method may be of interest for very particular problems (Robertson, 1974) but is hard to generalize, its uses being very tedious; computer-time requirements are high.

9.4.7. A finite-element approximation: Galerkin's method

The finite-difference schemes introduce a discretization of the domain in squares or rectangles or parallelepipeds. Such a representation is not convenient when the boundaries are complicated curves or when fluxes will not follow straight lines. Of course, finite-difference approximations are always possible but may introduce truncation errors greater than the ordinary experimental errors; a better representation of the domain is required and a finite-element approximation can provide it.

The basis of the finite-element approximation is the partition of the domain into subdomains or finite elements, usually of the same form. The unknown function c is approximated by a trial solution $\hat{c}$ of linear form:

$$\hat{c} = \sum_{i=1}^{n} a_i u_i$$

where the u_i are linearly independent selected functions, which exist over the domain and its boundaries and the a_i are unknown parameters to be determined subsequently. In the subdivided domain (Fig. 9.4.6) n nodes are chosen, usually at element vertices and at particular geometric locations. The trial solution is represented in a piecemeal fashion across the domain, element by element, in terms of the space variables and the nodal values of the solution and its derivatives.

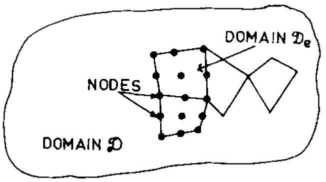

Fig. 9.4.6. Domain divided into finite-elements (Norrie and De Vries, 1973).

There are mainly two types of methods, namely residual and variational methods, using trial functions like $\hat{c}$.

(1) If c verifies some equation $L(c) = 0$, the trial solution $\hat{c}$ verifies some

equation $L(\hat{c}) = R$, where R is the residual. The problem is to minimize R in some way, usually by minimizing a weight function of R in a well-chosen vector space. The Galerkin method, detailed in this paragraph is a residual method. The minimization conditions yield a set of algebraic equations that can be solved by classical linear-system methods.

(2) In a variational method, the solution c gives an extremum value to some functional $F(c)$. The technique is then to substitute $\hat{c}$ in F and to minimize $F(\hat{c})$ which yields a set of algebraic equations and the solution of this set, by classical linear-system methods, yields the coefficient a_i (Norrie and De Vries, 1973).

A possible application of the residual method, called Galerkin's method, has been proposed by Pinder (1973) to solve the dispersion scheme and applied to a chromium pollution of an aquifer.

The dispersion scheme is defined by the equations:

$$L_c(c) = \operatorname{div}(K \operatorname{grad} c) - \operatorname{div}(uc) - \frac{\partial c}{\partial t} + Qc' = 0$$

$$L_h(h) = \operatorname{div}(T \operatorname{grad} h) - \frac{\partial h}{\partial t} + Q = 0$$

with our usual notations (Chapter 3). Q is a sink function incorporating well discharge and leakage into a confining layer and c' is the pollution concentration in the source fluid.

Trial solutions are:

$$\hat{c} = \sum_{i=1}^{n} C_i(t)\, U_i(x) \qquad \hat{h} = \sum_{i=1}^{n} H_i(t)\, w_i(x)$$

where x means $(x, y, z, \ldots)$.

U_i and $w_i (i = 1 \ldots, n)$ are basic functions satisfying the boundary conditions for each equation. These basic functions are linearly independent and represent first n functions of complete systems in the domain. The objective is to determine the coefficient functions $C_i(t)$ and $H_i(t)$ that minimize the linear forms $L_c(c)$ and $L_h(h)$.

The minimization of $L_c(c)$ is obtained by setting n integrals of the weighted residual $L_c(\hat{c})$ equal to zero:

$$\int_D L_c(\hat{c})\, U_i \mathrm{d}D = 0 \quad (i = 1, 2 \ldots n) \qquad [9.4.15]$$

The weighting functions are the basic functions U_i. In the same way we have:

$$\int_D L_h(\hat{h})\, w_i \, \mathrm{d}D = 0 \quad (i = 1, 2 \ldots, n) \qquad [9.4.16]$$

Remark. Geometrically, these relationships express the fact that if the projections of a vector on the three usual coordinate axes in R^3 are zero, then the vector is zero. This property is extended to more general functional spaces, spanned by complete bases: a set of functions U_i is said to be *complete* if any arbitrary function f, admissible for the problem considered, can be approximated by a linear combination:

$$\sum_{i=1}^{n} a_i U_i(x)$$

to any desired accuracy by choosing n large enough. When n tends to infinity

$$\sum_{i=1}^{n} a_i U_i(x)$$

converges (in some norm) to f. A complete base in a general functional space acts like a usual base for an n-dimensional vector space like R^3 for instance.

The suitability of the Galerkin technique for computer application depends upon the choice of basic functions and elements. Pinder uses the curved isoparametric quadrilateral (Fig. 9.4.7).

Linear, quadratic, cubic polynomial basis functions may be defined along the edges of the elements and different-order functions may be used along each side to accomodate the geometry of boundaries or the anticipated form of the unknown solution. To facilitate integration, a dimensionless and curvilinear local (ξ) coordinate system is introduced in which the elements appear as a square with the side nodes located at mid-points (quadratic side) or one-third point (cubic side) (Fig. 9.4.7; Norrie and De Vries, 1973, p. 86). The functions $Ui(x)$ and $wi(x)$ are written in terms of ξ and are selected such that they fulfill the basic requirements of a basis function and relate the global and local coordinate systems (Zienkiewicz, 1971).

From the dispersion scheme and [9.4.15] and [9.4.16] two sets of algebraic equations can be obtained:

$$[\mathsf{N}]\ \{C\} + [\mathsf{M}]\ \{\mathrm{d}C/\mathrm{d}t\} + \{F\} = 0 \qquad [9.4.17]$$

$$[\mathsf{P}]\ \{M\} + [\mathsf{R}]\ \{\mathrm{d}H/\mathrm{d}t\} + \{U\} = 0 \qquad [9.4.18]$$

where $\mathsf{N}, \mathsf{M}, \mathsf{P}, \mathsf{R}$ are $(n - m) \times (n - m)$ matrices (m being the number of passive nodes due to Dirichlet boundary conditions), and C, H, $\mathrm{d}C/\mathrm{d}t$ and $\mathrm{d}H/\mathrm{d}t$ are vectors containing the undetermined coefficients and their time derivatives. The coefficients of the coefficient matrices are expressed in terms of integrals over the domain of the basis functions and their derivatives. The computations of these integrals are performed in the local rather than the global coordinate system, with limits of integration of -1 and $+1$ and Gaussian quadrature is used. According to experience, exact solutions must be obtained from these integrals. The coefficients depend on the boundary conditions.

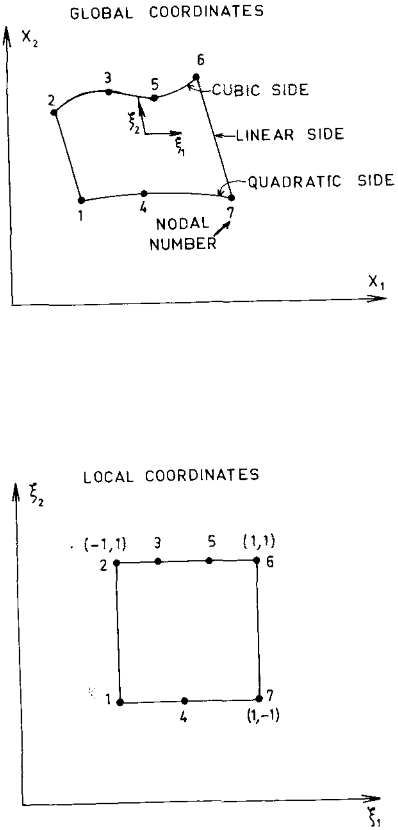

Fig. 9.4.7. Deformed mixed isoparametric quadrilateral elements on global x and ξ coordinates (Pinder, 1973).

Systems [9.4.17] and [9.4.18] are solved by approximating the time derivatives of concentration and hydraulic head by a finite-difference scheme with a backward difference in the dispersion equation:

$$[\mathrm{N}]\ \{C\}_{t+\Delta t} + [\mathrm{M}](\{C\}_{t+\Delta t} - \{C\}t)/\Delta t + \{F\} = 0$$

$$[\mathrm{P}]\ \{H\}_{t+\Delta t} + [\mathrm{R}](\{H\}_{t+\Delta t} - \{H\}_t)/\Delta t + \{U\} = 0$$

These equations are solved sequentially for each time-step, for given initial and boundary conditions.

9.5. THE BALANCE-OF-FLUXES THEORY OF THE HYDROLOGIC EQUATION

One of the main parameters of groundwater pollution is the velocity of the groundwater. We already have investigated field methods which provide this factor. Of course such methods cannot be used for predictive models and management models, when pumping and recharge vary, when projects of new wells and industries are studied, in general when the regime of the polluted aquifer varies with time. Thus mathematical modelling of groundwater movement has to be introduced.

The general hydrologic equation is:

$$\operatorname{div}(T \operatorname{grad} H) = S\frac{\partial H}{\partial t} + Q \qquad [9.5.1]$$

where $T = Ke$ transmissivity of the aquifer (see Appendix I), S = storage coefficient, H = heads, Q = field singularities (such as evaporation or wells, for instance).

This equation can be approximated, using the mathematical results of §9.4. But in this paragraph, we present a discretization method which is closer to the physics of the phenomenon, and illustrates the philosophy of modelling we have sketched in the Introduction. These methods complete each other and should be used together in any real problem.

For the sake of simplicity, we consider a bidimensional horizontal confined aquifer, the third dimension being included in the transmissivity term. Our results may very easily be extended to more general aquifers and we leave this to the reader.

9.5.1. Balance of elementary blocks

The basic principle is to isolate a block of ground by thought; water comes in through some faces and out through other faces; besides this some water is stocked in the pores. We apply the principle of mass conservation, with the following convention: when a block receives water, the received quantity is positive and when it loses water, the lost quantity is negative. The balance of mass is then written:

stocked water = received water — lost water

Now we analyze the various components of this balance. The elementary blocks of ground are cubes, of length Δx. The aquifer is discretized as shown in Fig. 9.5.1.

Remark. The theory is valid for any other discretization of the aquifer: the simple geometry of the example does not imply any simplification of the theory.

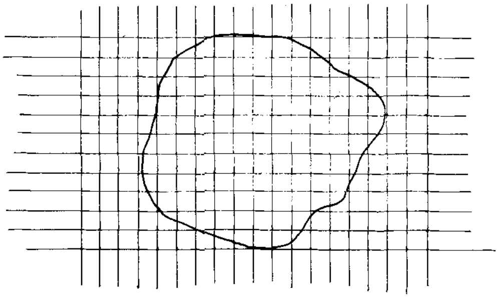

Fig. 9.5.1.

The center of an elementary block is C; N, S, E, W are respectively the centers of blocks north, south, east and west of C (Fig. 9.5.2).

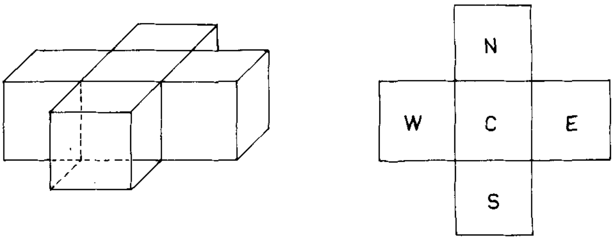

Fig. 9.5.2.

The distributions of head and hydraulic parameters are defined by allocating the mean value of the considered quantity in its block to the center of the block and computing the balance for block C between two times t_1 and t_2. The density of the water is assumed to be constant, thus we only consider a conservation-of-volume equation.

Stocked water

Between t_1 and t_2, the piezometric level varies from H_c to H_c^*. By definition of the storage coefficient, the stocked volume of water is, *algebraically*:

$$(\text{Stocked water between } t_1 \text{ and } t_2) = S_c(H_c^* - H_c)\,\Delta x^2$$

— if the level goes up, stocking is positive.
— if the level goes down, stocking is negative.

Water received or lost

It has two origins: (1) the water which flows through the block due to exchanges with the neighbouring blocks; this is called *transit water*; and (2) the water injected or pumped by boreholes, evaporation, infiltration; this is called *transfer water*.

(1) Transit water. The flow of water from block W to block C is:

$$Q_{wc} = T_{wc} \Delta x \frac{Hw - Hc}{\Delta x}$$

T_{wc} is the mean transmissivity on the contact face. A very common approximation (based on regularity properties of the aquifer) is:

$$T_{wc} = \tfrac{1}{2}(T_w + T_c)$$

with this approximation:

$$Q_{wc} = \tfrac{1}{2}(T_w + T_c)(H_w - H_c)$$

Estimating the fluxes from other blocks, we have the total flux Q_{tot}:

$$\begin{aligned} Q_{\text{tot}} = {} & \tfrac{1}{2}(T_N + T_C)(H_N - H_C) + \tfrac{1}{2}(T_S + T_C)(H_S - H_C) \\ & + \tfrac{1}{2}(T_E + T_C)(H_E - H_C) + \tfrac{1}{2}(T_W + T_C)(H_W - H_C) \end{aligned}$$

(2) Transfer water. The transfer water Q_c is:

Q_c = + (the sum of the injection wells' flow rates)—(the sum of the pumping wells' flow rates) + infiltration—evaporation

From t_1 to t_2, the amounts of transit and transfer water respectively are $Q_{\text{tot}}(t_2 - t_1)$ and $Q_c(t_2 - t_1)$. The balance of flux is then written:

$$S_c(H_c^* - H_c)\Delta x^2 = Q_{\text{tot}}(t_2 - t_1) + Q_c(t_2 - t_1)$$

and setting $\Delta t = t_2 - t_1$, we have the discretized form of the hydrologic equation:

$$\begin{aligned} S_c \frac{(H_c^* - H_c)}{\Delta t} = {} & \frac{1}{\Delta x^2}\Big[\tfrac{1}{2}(T_N + T_C)(H_N - H_C) + \tfrac{1}{2}(T_S + T_C)(H_S - H_C) \\ & + \tfrac{1}{2}(T_E + T_C)(H_E - H_C) + \tfrac{1}{2}(T_W + T_C)(H_W - H_C)\Big] + \frac{Qc}{\Delta x^2} \end{aligned} \qquad [9.5.2]$$

Remark 1. $(H_c^* - H_c)/\Delta t$ is the mean velocity of the piezometric level between t_1 and t_2.

Remark 2. $Q_c/\Delta x^2$ is homogeneous to a flow rate per unit surface area; this means that we homogenize the representation of the surface exchanges (infiltration and evaporation) and the representation of the punctual exchanges (wells).

Equation [9.5.2] is an approximation of [9.5.1] that is only based upon the fact that water mass is conservative; it displays the physical meaning of [9.5.1]. Actually some authors (Emsellem, 1970) derive [9.5.1] from [9.5.2] by taking the limits of the various terms when Δx and Δt decrease to zero.

9.5.2. *Boundary conditions*

An aquifer is bounded and the exchanges of water with the exterior are governed by boundary conditions, which are of two types:

(1) Boundary conditions external to the equation. These are the conditions that are usually referred to, in the literature, as boundary conditions. The most usual conditions are:

— constant potentials; these are due to ponds, lakes, streams, outcropping of the aquifer

— at zero flux; these are due to impervious boundaries

— at a potential varying with time, such as sea-water levels in coastal aquifers.

(2) Boundary conditions that can be internal to the equation. Consider a well; if its size is small with respect to the mesh size, its flow rate may be considered as a transfer flow rate of its block, thus included in the equation as some Q_c. In the same way, evaporation and infiltration may be considered either as variable flux conditions or as transfer flow rates also included in the equation. According to the problem, we have either boundary conditions or field singularities included in the equation as a term Q_c.

9.5.3. *A simple example*

We consider the aquifer discretized in Fig. 9.5.3. The values of transmissivities, the boundary conditions and the singularities are described in Fig. 9.5.3. The regime is permanent, i.e. time-independent.

N° of mesh

1	2	3
4	5	6
7	8	9

Transmissivity $m^2/sec \times 10^{-3}$

6	4	2
10	6	2
6	8	6

Fig. 9.5.3(a).

We will write the flux equations for each mesh:

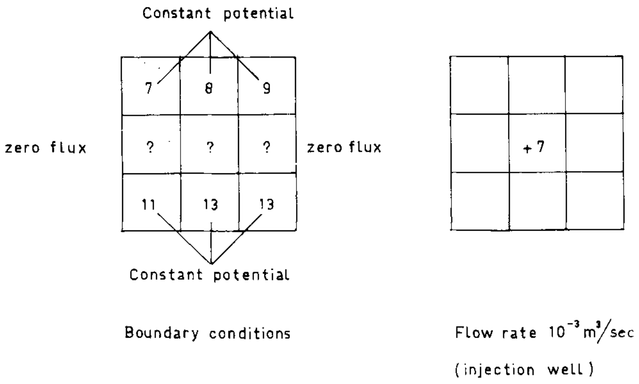

Boundary conditions

Flow rate $10^{-3}\,\mathrm{m^3/sec}$ (injection well)

Fig. 9.5.3(b).

Flux coming from / towards mesh N	N	S	E	W	Flow rate
4	$8(7-H_4)$	$+8(11-H_4)$	$+8(H_5-H_4)$	$+0$	$=\ 0$
5	$5(8-H_5)$	$+7(13-H_5)$	$+4(H_6-H_5)$	$+8(H_4-H_5)$	$=-7$
6	$2(9-H_6)$	$+4(13-H_6)$	$+0$	$+4(H_5-H_6)$	$=\ 0$

We arrange the coefficients of H_4, H_5, H_6 for each equation in a table:

Mesh / Coeff.	H_4	H_5	H_6
4	-24	8	0
5	8	-24	4
6	0	4	-10

$$\begin{bmatrix} H_4 \\ H_5 \\ H_6 \end{bmatrix} = \begin{bmatrix} -144 \\ -138 \\ -\ 70 \end{bmatrix}$$

which is usually written as:

$$\begin{bmatrix} -24 & 8 & 0 \\ 8 & -24 & 4 \\ 0 & 4 & -10 \end{bmatrix} \begin{bmatrix} H_4 \\ H_5 \\ H_6 \end{bmatrix} = \begin{bmatrix} -144 \\ -138 \\ -\ 70 \end{bmatrix}$$

The coefficient matrix of H_4, H_5, H_6 is called the hydraulics matrix or transmissivity matrix **T**.

9.5.4. Some properties of the transmissivity matrix

In the previous example, we observe that the transmissivity matrix is diagonally dominant and symmetric. These are general properties.

(1) Symmetry. i and j being the numbers of two neighbouring blocks, the flux from i to j is equal, in absolute value, to the flux from j to i. The coefficient of H_i is equal to the coefficient of H_j.

(2) Diagonal dominance. Consider the flux-balance equation at point c, in a permanent regime:

$$T_{NC}(H_N - H_C) + T_{SC}(H_S - H_C) + T_{WC}(H_W - H_C) + T_{EC}(H_E - H_C) = Q_C$$

arrange as:

$$T_{NC}H_N + T_{SC}H_S + T_{WC}H_W + T_{EC}H_E - (T_{NC} + T_{SC} + T_{WC} + T_{EC})H_C = Q_C$$

It appears then that the coefficient of H_C is on the principal diagonal and is greater than or equal to the sum of the other coefficients, which are positive.

Strict inequality may occur when a block, say N, is at a constant given potential on a boundary. H_N is known and the balance-of-flux equation is then written:

$$T_{SC}H_S + T_{WC}H_W + T_{EC}H_E - (T_{NC} + T_{SC} + T_{WC} + T_{EC})H_C = Q_C - T_{NC}H_N$$

keeping only unknown quantities on the left-hand side. The inequality is obvious.

Remark. Consider the previous example. We could have written the whole system of equations for all blocks:

Mesh No. / Equation	1	2	3	4	5	6	7	8	9		
1	H_1									=	7
2		H_2								=	8
3			H_3							=	9
4	$8H_1$			$-24H_4$	$+8H_5$		$+8H_7$			=	0
5		$5H_2$		$+8H_4$	$-24H_5$	$+4H_6$		$+7H_8$		=	-7
6			$2H_3$		$+4H_5$	$-10H_6$			$+4H_9$	=	0
7							H_7			=	11
8								H_8		=	12
9									H_9	=	13

This is not efficient because we have equations 1, 2, 3, 7, 8, 9 which are not useful. We write the matrix system:

$$\begin{bmatrix} 1 & 0 & 0 & 0 & 0 & 0 & 0 & 0 & 0 \\ 0 & 1 & 0 & 0 & 0 & 0 & 0 & 0 & 0 \\ 0 & 0 & 1 & 0 & 0 & 0 & 0 & 0 & 0 \\ 8 & 0 & 0 & -24 & 8 & 0 & 8 & 0 & 0 \\ 0 & 5 & 0 & 8 & -24 & 4 & 0 & 7 & 0 \\ 0 & 0 & 2 & 0 & 4 & -10 & 0 & 0 & 4 \\ 0 & 0 & 0 & 0 & 0 & 0 & 1 & 0 & 0 \\ 0 & 0 & 0 & 0 & 0 & 0 & 0 & 1 & 0 \\ 0 & 0 & 0 & 0 & 0 & 0 & 0 & 0 & 1 \end{bmatrix} \begin{bmatrix} H_1 \\ H_2 \\ H_3 \\ H_4 \\ H_5 \\ H_6 \\ H_7 \\ H_8 \\ H_9 \end{bmatrix} = \left[\begin{array}{r} 7 \\ 8 \\ 9 \\ 0 \\ -7 \\ 0 \\ 11 \\ 12 \\ 13 \end{array}\right] \begin{array}{l} \text{pressure} \\ \text{pressure} \\ \text{pressure} \\ \text{flux} \\ \text{flux} \\ \text{flux} \\ \text{pressure} \\ \text{pressure} \\ \text{pressure} \end{array}$$

This matrix is still diagonally dominant but it has lost its symmetry because it comprises pressure equations and flux equations at the same time. This is exactly what should not be done.

9.6. PRACTICAL USE OF MODELLING TECHNIQUES AND PROGRAMMING

We have seen two types of techniques:

(1) Approximations: explicit, implicit, Crank-Nicolson or ADIP techniques yield an estimate of $C(t + \Delta t)$ from $C(t)$.

(2) Procedures: point or block successive overrelaxation Gauss-Seidel or Jacobi techniques solve a linear system of equations by iterations. Gauss' elimination technique solves a linear system of equations by directly inverting the coefficient matrix of the system.

The complete-resolution technique consists then in choosing an approximation of the transient problem. If the approximation is explicit, $C(t + \Delta t)$ is directly computed by a simple addition of multiplications; if the approximation is implicit (or Crank-Nicolson), a procedure has to be chosen to solve the linear system of equations at each time-step. If the approximation is ADIP, the tridiagonal systems in rows and columns at each time-step are solved by the Gaussian elimination method. In the case of a steady-state problem, of course, only a procedure has to be used.

The choice of an approximation and a procedure will depend on the geometry of the domain; the ADIP will be reserved to very rectangular or convex domains, and point-successive overrelaxation will be used in the case of complex geometries. Block-successive overrelaxation can be used in the case of a geometry that is complex along one direction and simple along the other one.

When there is a need to refine the knowledge of a section of the domain, varying grids are introduced (Fig. 9.6.1) and point-successive overrelaxation is well adapted. This situation, for instance, occurs when pollution near a pumping well is studied.

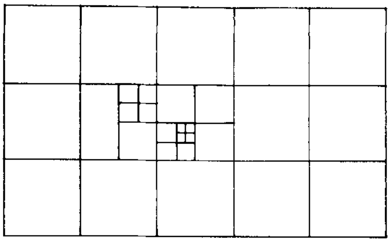

Fig. 9.6.1. A varying grid.

As an illustration, we give three basic programmes, namely two procedures and the tridiagonal Gauss elimination. Although they are not probably the optimal FORTRAN writings of the problems, they can be used as a control of exercises by the students.

The procedures are used to solve the following problems: a horizontal aquifer is represented by the discretized domain of Fig. 9.6.2; determine the potential knowing that the potential of the boundaries is 100 m, that transmissivities are constant and equal to 10^{-3} m^2/sec and that there is a central well pumping at the rate of 0.05 m^3/sec.

The regime is steady and the model is defined by [9.5.2] with $H_c^* = H_c$.

(1) Gauss-Seidel:

```
PROGRAM GAS(INPUT, OUTPUT)
                                   METHOD OF GAUSS SEIDEL

DIMENSION T(21, 11), Q(21, 11), H1(21, 11)
                             *DATA  INPUT*
    READ 100, IMIN, IMAX, JMIN, JMAX
 100 FORMAT(4I3)
    DO  1  I=IMIN, IMAX
    DO  1  J=JMIN, JMAX
    T(I, J)=0.001
    Q(I, J)=0.
  1 CONTINUE
    Q(11, 6)=0.05
                             *INITIAL CONDITIONS*
    DO  2  I=IMIN, IMAX
    DO  2  J=JMIN, JMAX
    H1(I, J)=0.
  2 CONTINUE
                             *BOUNDARY CONDITIONS*
```

```
      DO  3  I=IMIN, IMAX
      H1(I, JMIN)=100.
      H1(I, JMAX)=100.
    3 CONTINUE
      DO  4  J=JMIN, JMAX
      H1(IMIN, J)=100.
      H1(IMAX, J)=100.
    4 CONTINUE
      DO  5  L=1, 150
      U=0.
      IMI=IMIN+1
      IMA=IMAX-1
      JMI=JMIN+1
      JMA=JMAX-1
      DO  6  I=IMI, IMA
      DO  6  J=JMI, JMA
      TN=0.5*(T(I, J)+T(I-1, J))
      TS=0.5*(T(I, J)+T(I+1, J))
      TE=0.5*(T(I, J)+T(I, J+1))
      TW=0.5*(T(I, J)+T(I, J-1))
      TTOT=TN+TS+TW+TE
      Z=TN*H1(I-1, J)+TS*H1(I+1, J)+TE*H1(I, J+1)+TW*H1(I, J-1)
      Z=Z/TTOT
                              *COMPUTATION OF THE RESIDUE*
      U=U+(Z-H1(I, J))*(Z-H1(I, J))
      H1(I, J)=Z
    6 CONTINUE
      IF(U-0.001)8, 8, 7
    7 CONTINUE
      PRINT 1000, L, U
    5 CONTINUE
                              *RESULTS*
    8 PRINT 1001
      DO  10  I=IMIN, IMAX
      PRINT 1002, I, (H1(I, J), J=JMIN, JMAX)
   10 CONTINUE
 1000 FORMAT(5X, *ITERATION*, 13, *RESIDUE*, E15.8)
 1000 FORMAT(1H1, 5X, *POTENTIAL MAP*//)
 1002 FORMAT(1H, I2, 3X, 11(E10.3, 1X)//)
      STOP
      END
```

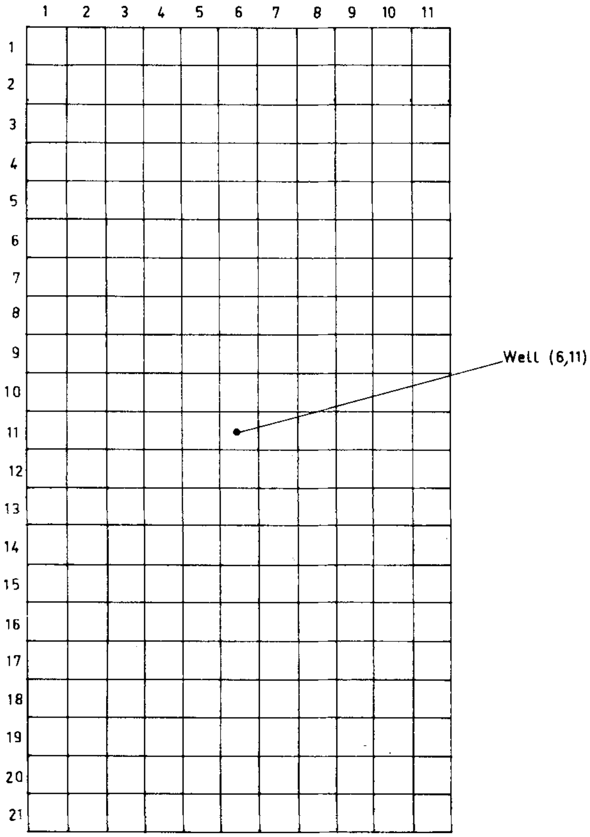

Fig. 9.6.2.

(2) Successive overrelaxation:

```
PROGRAM SOR(INPUT, OUTPUT)
                              METHOD OF FRANKEL-YOUNG

DIMENSION T(21, 11), Q(21, 11), H1(21, 11)
                              *DATA INPUT*
      R=1.9
      READ 100, IMIN, IMAX, JMIN, JMAX
  100 FORMAT(4I3)
      DO  1  I=IMIN, IMAX
      DO  1  J=JMIN, JMAX
      T(I, J)=0.001
      Q(I, J)=0.
    1 CONTINUE
      Q(11,6)=0.05
```

```
                              *INITIAL CONDITIONS*
  DO 2 I=IMIN, IMAX
  DO 2 J=JMIN, JMAX
  H1(I, J)=0.
2 CONTINUE
                           *BOUNDARY CONDITIONS*
  DO 3 I=IMIN, IMAX
  H1(I, JMIN)=100.
  H1(I, JMAX)=100.
3 CONTINUE
  DO 4 J=JMIN, JMAX
  H1(IMIN, J)=100.
  H1(IMAX, J)=100.
4 CONTINUE
  DO 5 L=1, 150
  U=0.
  IMI=IMIN+1
  IMA=IMAX-1
  JMI=JMIN+1
  JMA=JMAX-1
  DO 6 I=IMI, IMA
  DO 6 J=JMI, JMA
  TN=0.5*(T(I, J)+T(I-1, J))
  TS=0.5*(T(I, J)+T(I+1, J))
  TE=0.5*(T(I, J)+T(I, J+1))
  TW=0.5*(T(I, J)+T(I, J-1))
  TTOT=TN+TS+TW+TE
  Z=TN*H1(I-1, J)+TS*H1(I+1, J)+TE*H1(I, J+1)+TW*H1(I, J-1)
  Z=Z/TTOT
                           *COMPUTATION OF THE RESIDUE*
  V=Z-H1(I, J)
  U=U+V*V
  H1(I, J)=H1(I, J)+R*V
6 CONTINUE
  IF(U-0.001)8, 8, 7
7 CONTINUE
  PRINT 1000, L, U
5 CONTINUE
                           *RESULTS*
8 PRINT 1001
  DO 10 I=IMIN, IMAX
```

```
       PRINT 1002, I, (H1(I, J), J=JMIN, JMAX)
    10 CONTINUE
  1000 FORMAT(5X, *ITERATION*, 13, *RESIDUE*, E15.8)
  1001 FORMAT(1H1, 5X, *POTENTIAL MAP*//)
  1002 FORMAT(1H, I2, 3X, 11(E10.3, 1X)//)
       STOP
       END
```

(3) Tridiagonal Gauss elimination method:
The problem is to solve the system [9.3.1].

```
DIMENSION ALF(N), BETA(N), B(N), C(N), D(N), X(N),
      ALF(1)=D(1)/B(1)
      BETA(1)=C(1)/B(1)
      DØ1I=2, N
      ALF(I)=(D(I)-A(I)*ALF(I-1))/(B(I)-A(I)*BETA(I-1))
      BETA(I)=C(I)/(B(I)-A(I)*BETA(I-1))
1     CONTINUE
      X(N)=ALF(N)
      II=N-I
      DØ2III=1, II
      I=N-III
      X(I)=ALF(I)-BETA(I)*X(I+1)
2     CONTINUE
      STOP
      END
```

APPENDIX I

BASIC FACTS OF GROUNDWATER MOVEMENT

This Appendix intends to give the basic definitions only, linked to the practical aspects of water movement in the ground and of its measurements. For instance, we approach the concept of "head" only by associating it to the level of water in a well, which actually is the only practical way of measuring this head in an aquifer. If the reader intends to go deeper into the theory of groundwater movement, there are many excellent text books on this subject that we recommend, such as Jacob Bear (1972), David Todd (1959), De Wiest (1965), especially for the case of non-potential flow, which we do not present here, and the general aspects of Darcy's law.

A.1.1. Cause of groundwater movement

The driving phenomenon of waterflow in the ground is the hydraulic potential or head. This potential is represented by the level of water in boreholes: the difference in head between two points is equal to the difference of the water levels in two wells drilled at these points. Actually, the cause of the movement is the difference of potential:

— if the fluid is at the same head everywhere, there is no flow

— if there exists a difference of head in space, water flows in the direction of decreasing heads (Fig. A.1.1).

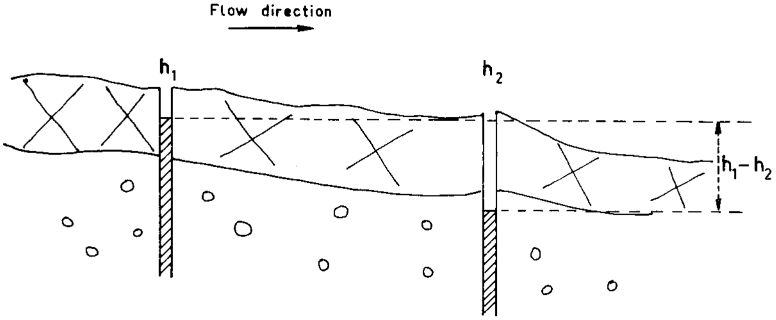

Fig. A.1.1

Hints for theory fans

Hydrostatics tells us that $p_1 = \rho g(h_1 - z_1)$

p being the pressure, ρ the density and g the gravity, h and z are defined in Fig. A.1.2.

$h_1 = p_1/\rho g + z_1$

h_1 is the head at point 1. Actually, the head is given by the relationship:

$$h = \frac{p_1}{\rho g} + \frac{v^2}{2g} + z$$

where v is the velocity of the water. In a porous medium, v^2 can be neglected. Along a streamline, we have, according to Bernoulli:

$$\frac{p_1}{\rho g} + z_1 = \frac{p_2}{\rho g} + z_2 + \Delta h$$

where Δh is the loss of head (drawdown) due to irreversible dissipation of heat by viscosity.

Thus the drawdown is equal to the difference between the water levels, $h_1 - h_2$.

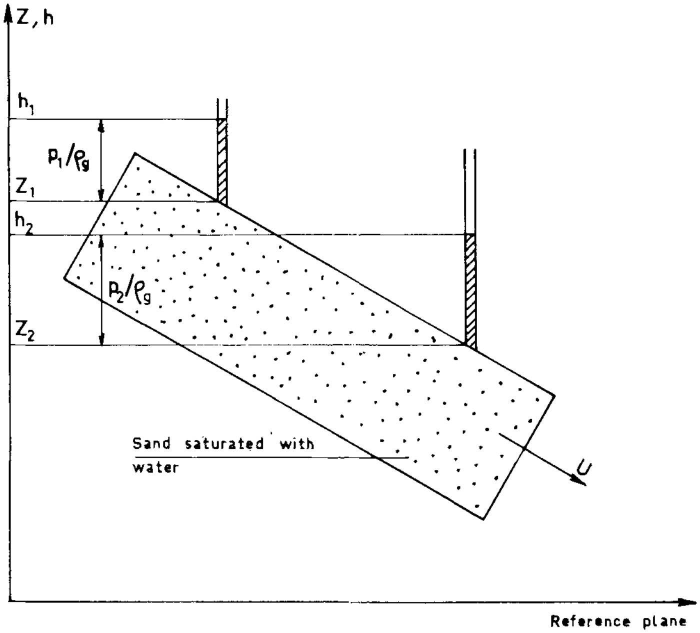

Fig. A.1.2. An illustration of the concept of head.

A.1.2. Confined and unconfined aquifers

A well is drilled into an aquifer; the drilling stops when water is reached for the first time:

— if the water level in the borehole is stabilized above the bottom of the hole, the aquifer is confined

— if the water level does not rise in the borehole, the aquifer is unconfined.

The same aquifer can be confined in some areas and unconfined in others. The fact of being confined or unconfined is a local property of the aquifer. It is a very simple application of the principle of communicating vases (Fig. A.1.3).

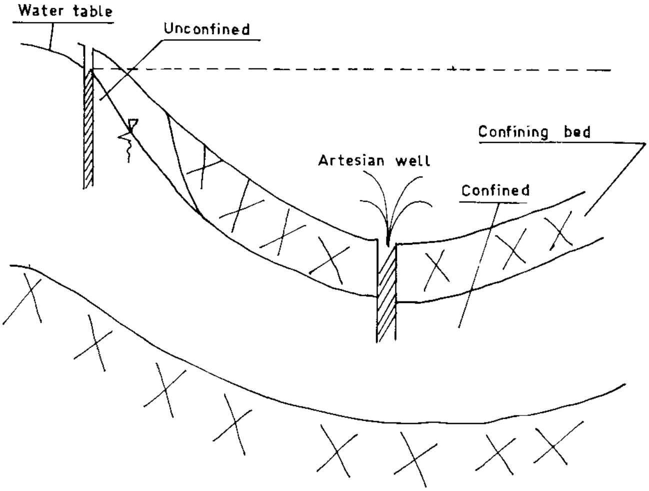

Fig. A.1.3. Confined and unconfined aquifer.

The water in a borehole is stabilized at a level called the piezometric level. The surface which joins all the water levels is the piezometric surface. If the piezometric surface is identical to the water table, it is a free surface and the aquifer is unconfined. Otherwise the piezometric surface is above the water table.

A.1.3. Hydraulic gradient and velocities

Hydraulic gradient

Along a horizontal streamline, we consider two points A and B and their corresponding heads (or piezometric levels) H_A and H_B. The distance between A and B along the streamline is L (Fig. A.1.4).

The hydraulic gradient in the direction A to B is:

$$i = \frac{H_B - H_A}{L}$$

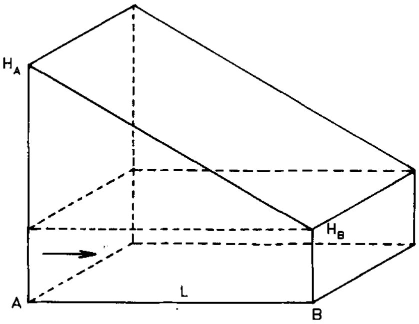

Fig. A.1.4.

It is an algebraic number: if the hydraulic gradient is taken in the direction of flow, it is negative because we have said that flow occurs in the direction of decreasing heads.

The quantity $H_A - H_B$ is called the drawdown between A and B

Velocities

Several velocities can be introduced: (1) the apparent velocity is the velocity of the general flow through a porous medium; (2) the real velocity is the velocity of a microscopic drop in the porous medium.

Let us consider an example (Fig. A.1.5).

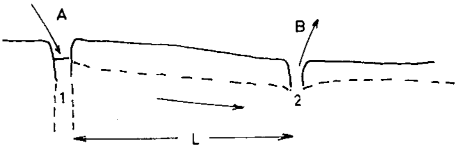

Fig. A.1.5.

AB being on a streamline, we inject a large amount of radioactive tracer into well No. 1. After some time period T, a probe in well No. 2 records the occurrence of radioactive water. The apparent velocity is:

$$V = L/T$$

L being the horizontal distance between the wells.

Actually, the molecules do not follow a rectilinear path in the porous medium, their velocities are higher than the apparent velocity because the length of the actual path is greater than L, due to the solid matrix (Fig. A.1.6).

The apparent velocity is called the macroscopic velocity V_M or mean pore velocity V_M. The real velocity is called the microscopic velocity V_m.

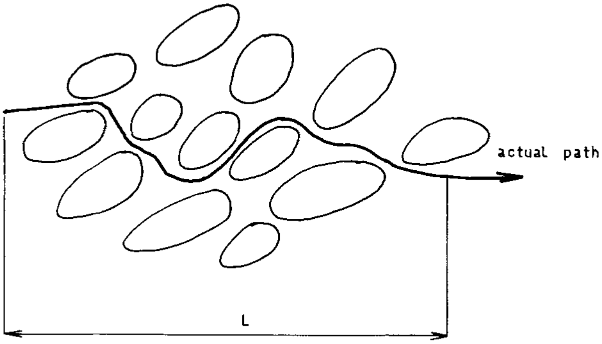

Fig. A.1.6. Actual and mean paths.

A.1.4. Darcy's law

Along a streamline we have:

$$V_M \doteq -K_M i$$

where K_M is a coefficient homogeneous to a velocity. The sign comes from the fact that the displacement occurs in the direction of decreasing heads.

Darcy's law states that the groundwater velocity is proportional to the hydraulic gradient.

A.1.5. Filtration rate of flow

We compute the flow rate through a ground section (Fig. A.1.7).

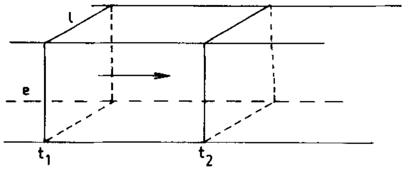

Fig. A.1.7. Elementary block of ground.

Consider the groundwater flow through a section of thickness e, of width l, perpendicular to the flowlines. Assume first a much simpler phenomenon, a continuous fluid without the porous matrix. Between times t_1 and t_2, a volume q of fluid flows through the section, which defines a length L by the relationship:

$$q = l.e.L$$

L can be interpreted as the virtual distance travelled by the section during time $t_2 - t_1$.
A mean velocity V_M between t_1 and t_2 is then defined by:

$$V_M = L/(t_2 - t_1)$$

and the flow rate Q through the section is expressed as:

$$Q = q/(t_2 - t_1) = V_M l.e$$

By analogy, the flow rate Q through a section of porous medium is expressed as:

$$Q = V_D l.e \qquad [A.1.1]$$

where V_D is the Darcy's velocity. From the way it has been introduced, it is obvious that Darcy's velocity is not a real velocity of some kind, but an abstract concept. Equation [A.1.1] defines V_D, from the measurable quantities Q, l and e.

A.1.6. Darcy's porosity

The flow rate Q can also be expressed in terms of the macroscopic velocity V_M by:

$$Q = V_M S$$

where S is the area of the pores in the section.
Darcy's porosity is defined by:

$$\phi_D = V_D / V_M$$

and setting $K_D = \phi_D K_M$, we find another form of Darcy's law:

$$V_D = -K_D i$$

and K_D is called the permeability.

It should be stressed that Darcy's porosity has a hydraulic meaning, as it represents the fraction of porous medium which really yields water by pressure flow. It is an effective porosity: the measurement of the percentage of voids in a porous medium yields a real porosity ϕ greater than ϕ_D; it is explained by the occurrence of dead-end pores, adsorbed water and more generally water linked to the solid matrix which does not take part in the flow.

A.1.7. Transmissivity

The real discharge of fluid is:

$$Q = -K_D eli$$

written as: $Q = -(K_D e)li = -Tli$

by setting: $T = K_D e$

T is the transmissivity, homogeneous to L^2T^{-1}

As an example, a transmissivity of 1 m²/sec for a width l of 1 m and a gradient i of -1, yields a flow rate of 1 m³/sec.

The transmissivity concept is generally used for confined aquifers, where e represents the thickness of the aquifer. It allows the treatment of tri-dimensional cases with bidimensional models, especially with regard to the estimate of water resources; these models are less adequate to determine a movement and the generalized Darcy's law is then required (§A.1.9).

A.1.8. The storage coefficient

Unconfined aquifers

The term "storage coefficient" is used wrongly in the case of unconfined aquifers, but anyhow, we give its usual definition in that case.

When pumping the aquifer, the piezometric level decreases from H_A to H_B (Fig. A.1.8). A volume V_W of water is extracted on section A. The volume V_P of porous medium swept by the water table is:

$$V_P = (H_A - H_B) \cdot A$$

where A is the section area.

$$V_W = \phi_D \cdot V_P = \phi_D (H_A - H_B) \cdot A$$

and as $\phi_D < 1$, we have $V_W < V_P$. The storage coefficient is the effective porosity.

Confined aquifers

The term storage coefficient actually applies only for confined aquifers. Although in both cases, the schemes are the same, the physical mechanisms are different.

V_W being the real volume of water extracted by sweeping a fictitious pressure "volume" V_P (Fig. A.1.9), we define the storage coefficient S by:

$$V_W = SV_P$$

S is dimensionless.

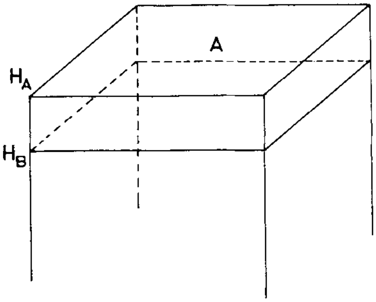

Fig. A.1.8.

The mechanism can be explained as follows. When the piezometric level decreases, water is less compressed, which yields a first fraction of water $V_1 \cdot \beta$ being the compressibility coefficient of water defined by:

$$\beta = -\frac{\Delta V}{V} \Big/ \Delta p$$

we have: $|\Delta V| = \beta |\Delta p| V\phi$

where ΔV is the volume of water contained in a ground volume $V = Ae$, where e is the thickness of the aquifer and A the surface area defined in Fig. A.1.8.

Thus: $V_1 = \beta |(H_B - H_A)\rho g| Ae\phi$

where ϕ is the porosity of the aquifer. $Ae\phi$ is the volume of pores. As pressure decreases, the solid matrix extends and pushes out another fraction of water V_2:

$$V_2 = \alpha[(H_B - H_A)\rho g] Ae(1 - \phi)$$

where α is the compressibility coefficient of the solid matrix. $Ae(1 - \phi)$ is the volume of the solid matrix. The total volume V of extracted water is then:

$$V = V_1 + V_2 = A |H_B - H_A| [\phi\beta\rho g + (1 - \phi)\alpha\rho g] e$$

The storage coefficient is then:

$$S = [\phi\beta\rho g + (1 - \phi)\alpha\rho g] e$$

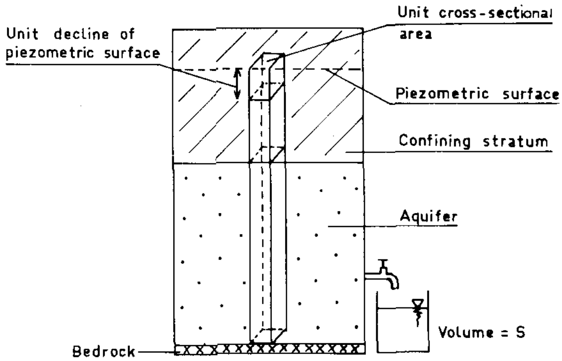

(a) Confined aquifer

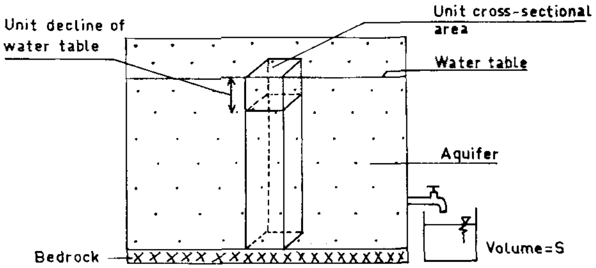

(b) Unconfined aquifer

Fig. A.1.9. Definition of the storage coefficient.

Another useful form of the definition of S is: the storage coefficient is the volume of water that an aquifer releases from or takes into storage per unit surface area of aquifer per unit change in the head normally to that surface.

A.1.9. Generalization of Darcy's law

The hydraulic gradient

Consider the piezometric level $h(x, y, z)$ at point (x, y, z) and a flowline going through the points A and B of respective coordinates, (a_1, a_2, a_3), (b_1, b_2, b_3) in some reference system. The hydraulic gradient between A and B is the vector defined by:

$$i_{AB} \begin{cases} [h(b_1, b_2, b_3) - h(a_1, a_2, a_3)]/(b_1 - a_1) \\ [h(b_1, b_2, b_3) - h(a_1, a_2, a_3)]/(b_2 - a_2) \\ [h(b_1, b_2, b_3) - h(a_1, a_2, a_3)]/(b_3 - a_3) \end{cases}$$

This definition is directly derived from § A.1.3.

If B tends towards A, i_{AB} tends towards the vector i_A.

$$i_A \begin{cases} \dfrac{\partial h}{\partial x}(a_1, a_2, a_3) \\[2ex] \dfrac{\partial h}{\partial y}(a_1, a_2, a_3) \\[2ex] \dfrac{\partial h}{\partial z}(a_1, a_2, a_3) \end{cases}$$

i_A will be called the hydraulic gradient at A, grad h.

Darcy's law

K_M being the coefficient of a macroscopic velocity and K_D being Darcy's coefficient, Darcy's law is generalized in a first step as:

$$V_M = -K_M \text{ grad } h$$

$$V_D = -K_D \text{ grad } h$$

and the components of vectors V_M and V_D are:

$$V_M \begin{cases} V_{Mx} = -K_M \dfrac{\partial h}{\partial x} \\[2ex] V_{My} = -K_M \dfrac{\partial h}{\partial y} \\[2ex] V_{Mz} = -K_M \dfrac{\partial h}{\partial z} \end{cases} \qquad V_D \begin{cases} V_{Dx} = -K_D \dfrac{\partial h}{\partial x} \\[2ex] V_{Dy} = -K_D \dfrac{\partial h}{\partial y} \\[2ex] V_{Dz} = -K_D \dfrac{\partial h}{\partial z} \end{cases}$$

If the medium is not isotropic and homogeneous, Darcy's law is further generalized as:

$$\begin{cases} V_{Dx} = -K_{xx} \dfrac{\partial h}{\partial x} - K_{xy} \dfrac{\partial h}{\partial y} - K_{xz} \dfrac{\partial h}{\partial z} \\[2ex] V_{Dy} = -K_{yx} \dfrac{\partial h}{\partial x} - K_{yy} \dfrac{\partial h}{\partial y} - K_{yz} \dfrac{\partial h}{\partial z} \\[2ex] V_{Dz} = -K_{zx} \dfrac{\partial h}{\partial x} - K_{zy} \dfrac{\partial h}{\partial y} - K_{zz} \dfrac{\partial h}{\partial z} \end{cases}$$

Remark. The most general form of Darcy's law as used until now, applies to non-potential flow and is written:

$$V_D = -\frac{k}{\mu}(\operatorname{grad} p + \rho g \operatorname{grad} z)$$

This form must be used when the density ρ is not constant, which occurs in some pollution problems (we have called this case the "general case" and have given an example with salt intrusion from salt dumps).

k is the intrinsic permeability coefficient, homogeneous to L^2, and μ the dynamic viscosity. If ρ is constant, the usual form of Darcy's law is found:

$$V_D = -\frac{k\rho g}{\mu}\operatorname{grad}\left(\frac{P}{\rho g}+z\right) = -K_D \operatorname{grad} h$$

with $K_D = \dfrac{k\rho g}{\mu}$ and $h = \dfrac{P}{\rho g} + z.$

Derivation of the hydrologic equation (Emsellem's method)

An equation describing the movement of groundwater is derived from the continuity equation and Darcy's law for confined and unconfined aquifers (De Wiest 1965; J. Bear, 1972). As an example, we give a derivation of the hydrologic equation for a confined aquifer due to Emsellem (1971).

Equation [9.5.2] is written:

$$S\frac{H_c^* - H_c}{\Delta t} = \frac{1}{\Delta x^2}1/2\,[(T_N + T_C)(H_N - H_C) + (T_S + T_C)(H_S - H_C)$$
$$+ (T_E + T_C)(H_E - H_C) + (T_W + T_C)(H_W - H_C)] + Q/\Delta x^2$$

Δt and Δx tend to 0; then:

$$\frac{H_c^* - H_c}{\Delta t} \to \frac{\partial h}{\partial t}(c)$$

$$\frac{H_N - H_c}{\Delta x} \to \frac{\partial h}{\partial x}(c)$$

$$\frac{\frac{1}{2}(T_N + T_C)\frac{H_N - H_c}{\Delta x} - \frac{1}{2}(T_S + T_C)\frac{H_c - H_S}{\Delta x}}{\Delta x} \to \frac{\partial}{\partial x}\left[T\frac{\partial h}{\partial x}(c)\right]$$

$\dfrac{Q}{\Delta x^2} \to q$, local flux.

Equation [9.5.2] becomes:

$$S\frac{\partial h}{\partial t} = \frac{\partial}{\partial x}\left(T\frac{\partial h}{\partial x}\right) + \frac{\partial}{\partial y}\left(T\frac{\partial h}{\partial y}\right) + q$$

or: $S\dfrac{\partial h}{\partial t} = \operatorname{div}(T \operatorname{grad} h) + q$

A.1.10. Some considerations about the flow regimes

Consider a closed aquifer, i.e. an aquifer that does not receive any water from anywhere, submitted to pumping at constant flow rates and follow the level variations with time.

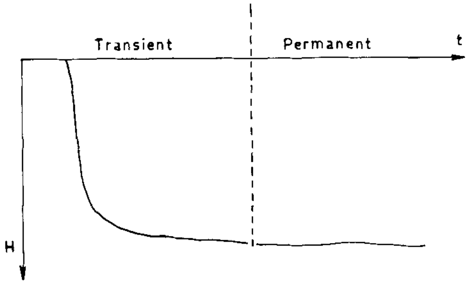

Fig. A.1.10. Transient and permanent regimes.

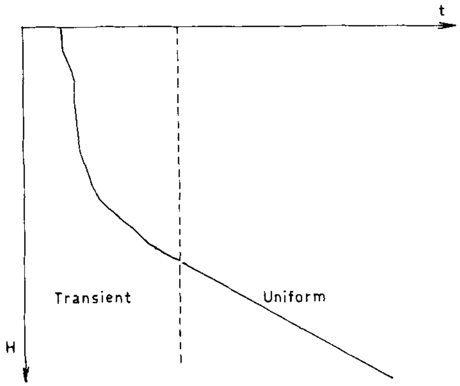

Fig. A.1.11. Transient and uniform regimes.

First, the level goes down according to the characteristic shape of the transient regime, which is a propagation regime. After some time, it can be observed that the shape of the piezometric surface no longer changes: the aquifer goes down uniformly; its evolution at one point is coupled with its evolution at all other points and the draw-down velocity is uniform. The regime is called uniform.

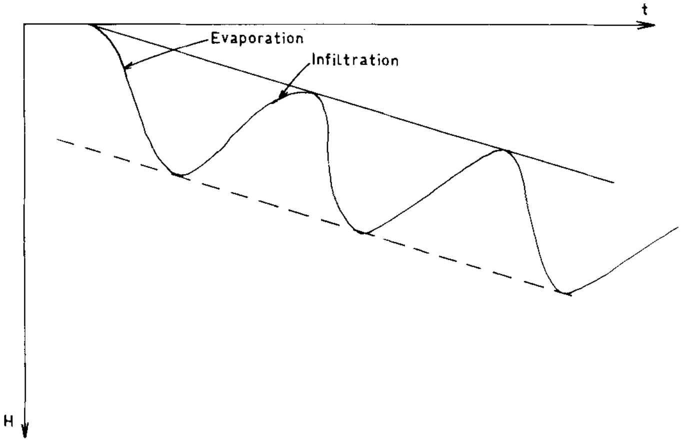

Fig. A.1.12. Cyclic regime with deficit.

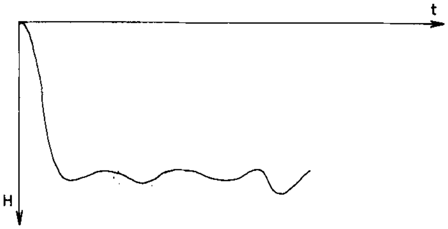

Fig. A.1.13. Cyclic regime with feeding.

Assume now that rain brings a fixed quantity of water to the aquifer, according to an annual cycle, and that this quantity of water is less than the total output. The uniform drawdown, due to pumping, will be modulated by the evaporation—infiltration flow rates but, as water due to rain does not cover the output, we have a cyclic regime with deficit; otherwise we have a cyclic regime with feeding.

The various regimes are presented in Figs. A.1.10—13.

APPENDIX II

ELEMENTS OF GEOPHYSICS : SURFACE ELECTRICAL METHODS

Electrical-sounding techniques are widely used to determine the geometry of aquifers, especially alluvial aquifers which offer electrically well contrasted layers. Described in several books (Kunetz, 1966; Todd, 1959), they are very well summarized by Ungemach (Thesis, 1975), whom we largely quote here.

The idea of prospecting the natural electrical fields from the surface is rather old (19th century) and was called spontaneous potential or self potential (SP). Later, Schlumberger (1920) injected a continuous current into the soil and obtained data on the nature and the structure of the subsoil from discrepancies observed with the ideal scheme of a homogeneous and isotropic soil. We shall now examine the various techniques, recalling that for a semi-infinite homogeneous medium of resistivity ρ, the electrical potential due to a point source is:

$$U(r) = \rho I/2\pi$$

where r is the distance to the source and I the intensity. The anisotropy coefficient λ is:

$$\lambda = \sqrt{\rho_t/\rho_l}$$

where ρ_t is the transverse (or lateral) resistivity and ρ_l the longitudinal (or normal) resistivity.

A.2.1. Potential method (P.M.)

At point M ($AM = MB = a$, Fig. A.2.1), the electric field is approximately constant and, parallel to AB, can be expressed as:

$$E_x = \frac{\rho I}{\pi a^2}\Big/ (1 + z^2/a^2)^{3/2}$$

and at the ground surface $E_0 = \rho I/\pi a^2$.

The equipotential lines, obtained from potential measurements at various points, are circular for a homogeneous soil. An increase or a decrease of the resistivity will yield a change of the equipotential net. This change in the ideal cases of simple geometric structures (spheres, cylinders, circular plates) can be measured through an explicit analytical formula and type curves can be derived.

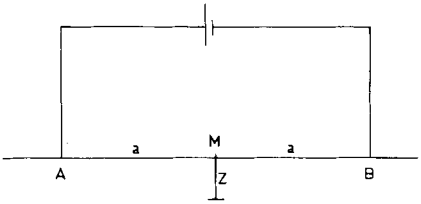

Fig. A.2.1. Potential method.

A possible application of this method in the case of groundwater pollution is the following: an electrode is put into the aquifer and sends the current, the other electrode being put at an infinite distance (i.e. a very large distance); the first electrode represents potential 100 and the other potential 0 (Fig. A.2.2).

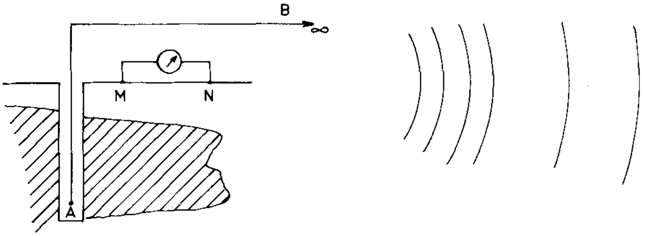

Fig. A.2.2. An application of the potential method with an electrode at infinity.

The potentials are expressed as fractions of the potential difference $U_A - U_B$ and can be measured in MN in two ways: (1) either a reference equipotential line is drawn by moving an electrode in the field to reach that value; or (2) the potential U_M is expressed with respect to a measured value on a standing electrode (N for instance), electrically stable (i.e. out of reach of the perturbation). This procedure has proved successful in checking the movement of an electrically well contrasted perturbation.

A.2.2. Resistivity measurements

Consider the device shown in Fig. A.2.3.

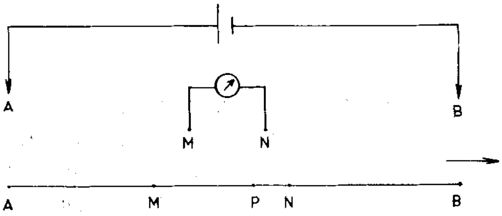

Fig. A.2.3. Resistivity measurements.

AB is the emission line and MN the measurement line. The apparent resistivity ρ_a, corresponding to an integrated response of the investigated layers for a given length AB, is:

$$\begin{aligned}\rho_a &= 2\pi \left[\left(\frac{1}{AM}-\frac{1}{AN}\right)-\left(\frac{1}{BM}-\frac{1}{BN}\right)\right]^{-1} \frac{\Delta U}{I} \\ &= K\Delta U/I\end{aligned}$$

where K appears as a geometrical characteristic constant of the device. Also, ρ_a could be expressed as a function of the potential ratios in a five-electrode device, with a moving B, as represented in Fig. A.2.3:

$$\begin{aligned}\rho_a &= KR \\ R &= \Delta U_{MP}/\Delta U_{PN} \\ K &= (AN-AP)/(AP-AM)\end{aligned}$$

Resistivity measurements are used for resistivity profiles and rectangle measurements.

A.2.3. Resistivity profiles

AB and MN are simultaneously moved along the profile, their lengths being kept constant: the investigation depth, which is proportional to AB, thus remains constant (Fig. A.2.4).

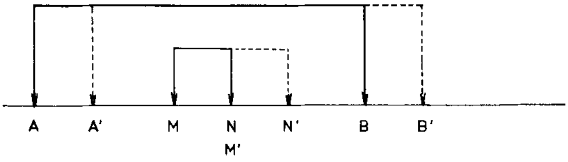

Fig. A.2.4. Determination of resistivity profiles.

A.2.4. Rectangle measurements

Apparent-resistivity measurements are performed, for a given AB, on a rectangular net of electrodes MN contained in a rectangle, the dimensions of which with respect to the emission line are such that the electrical field can be assumed constant with the exception of a few heterogeneities (Fig. A.2.5).

This type of measurement is well adapted to the study of a very local zone: it requires the derivation, by computation, of the coefficient K at each measurement point and the introduction of a correction factor to normalize the investigation depth, for a given *AB*, which is maximal at the center of the rectangle and minimal at its ends.

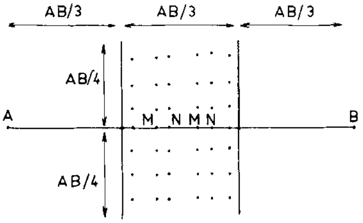

Fig. A.2.5. Rectangle measurements.

The displacement of the rectangle requires an overlapping of the measurements and a smoothing at the interfaces, which can be complicated by electrode effects.

A.2.5. Electrical soundings

Electrical sounding is a vertical exploration of the layers, with cumulative effects, by a progressive increase of *AB*, the distance between the measurement electrodes remaining small with respect to *AB* ($MN < AB/5$). In the Schlumberger quadripole device (Fig. A.2.6) the variations due to the contact of the electrodes with a heterogeneous soil are controlled by an overlapping of the measurements for a change of *AB* (Fig. A.2.7).

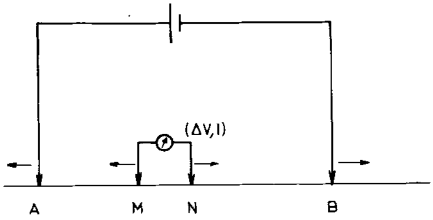

Fig. A.2.6. Electrical-sounding quadripole-injection-measurement.

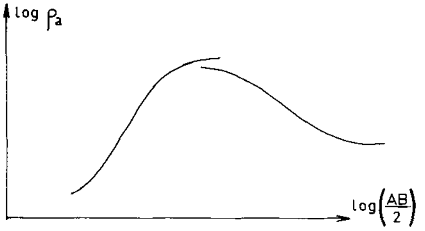

Fig. A.2.7. Electrical-sounding curve.

ΔU and I are measured with a potentiometer by an opposition method and the values of the apparent resistivity ρ_a are put on log-log paper as a function of $AB/2$. In this representation the multiplication of the values of the resistivities or of the layer widths is given by a translation of the curve parallel to the y-axis or the x-axis.

Electrical soundings thus yield a discrete sequence of apparent-resistivity values as a function of the distance between electrodes and sources. The interpretation of the measurements is a typical identification problem, which is to find a vertical distribution of resistivities $\rho(z)$ corresponding to the measured sequence $\rho_a(r)$. We give now a few hints about this interpretation.

We assume a semi-infinite medium with a horizontal homogeneous stratification. A layer i influences the measured response through its transverse resistance R_{ti} and its conductance C_{li} which are related to the electrical and geometrical characteristics of the layer by the formulas:

$$R_{ti} = \rho_{ti} e_i$$

$$C_{li} = e_i / \rho_{li}$$

where ρ_i and e_i, respectively, are the real resistivities (transverse and longitudinal) and the thickness of the layer i. To take into account the occurrence of water, another parameter is introduced, called the formation factor F and equal to the ratio of the real resistivity of the saturated layer (solid matrix and water) to the resistivity of the water alone ρ_w. F is a function of the porosity of the layer. A widely used representation of this function is Archie's relationship:

$$F = \rho_l / \rho_w = \phi^{-m}$$

where ϕ is the effective porosity and m a coefficient depending upon the degree of consolidation of the aquifer ($1 < m < 2$).

The electrical-sounding curve represents the global effect of the investigated layers and special numerical processes have to be introduced to obtain the spectrum of the various layers; type curves and a semi-automatic treatment are used according to the following principles.

In a stationary regime and under the previously mentioned stratification and isotropy ($\rho_t = \rho_l$) conditions, the potential verifies the partial-differential equation:

$$\frac{\partial^2 U}{\partial r^2} + \frac{1}{r}\frac{\partial U}{\partial r} + \frac{\partial^2 U}{\partial z^2} = 0 \qquad \text{[A.2.1]}$$

which has the solution:

$$U_i\,(r,z) = \int_0^{\infty} [A_i\,(\lambda)\,\mathrm{e}^{\lambda z} + B_i(\lambda)\,\mathrm{e}^{-\lambda z}]\, J_0(\lambda r)\,\mathrm{d}\lambda \qquad [\text{A.2.2}]$$

where i is the layer number ($1 < i < N$), r the distance to the source, z the vertical coordinate, taken positive downwards, λ an arbitrary integration constant, $J_0\,(\lambda r)$ the zero-order Bessel function of the first kind, A_i and B_i the constants computed from the boundary conditions.

The boundary conditions are:

— at the interface between layers, the continuity of the potential ($U_i = U_{i+1}$) and of the normal component of flow $\partial U_i/\partial n = \partial U_{i+1}/\partial n$

— at the ground surface, the nullity of the normal component of flow everywhere except at the source

— in the Nth layer, of infinite thickness, the nullity of the potential.

A_i and B_i are thus given by a linear system of $2N$ equations with $2N$ unknowns.

The function $A_i\,(\lambda)\mathrm{e}^{\lambda z} + B_i\,(\lambda)\mathrm{e}^{-\lambda z}$ is called Stefanesco's function, $S[\lambda, \rho(z)]$. The ground-surface potential can be written:

$$U\,(r,0) = C\left[\frac{1}{r} + \int_0^{\infty} S\,\{\lambda, \rho(z)\}\, J_0(\lambda r)\,\mathrm{d}\lambda\right] \qquad [\text{A.2.3}]$$

which yields the value of the reduced apparent resistivity, defined as the ratio of the electrical field measured at the ground surface to its theoretical value, proportional to:

$$-\,r^2\,\frac{\partial U}{\partial r}\,(r,0)$$

or: $$\rho'_a\,(r) = 1 + 2\,r^2 \int_0^{\infty} S\,[\lambda,\rho(z)]\;\lambda J_1(\lambda r)\,\mathrm{d}\lambda \qquad [\text{A.2.4}]$$

The function S gathers all the information about the stratification and allows the derivation for "N layers"-type curves; for instance, four-layers-type curves have been obtained by an expansion of [A.2.4] in a series of functions.

These type of curves can be used for identification purposes of real soils, taking into account some limitations of the method:

(1) Equivalence principle. If a conductive layer i lies between two resistive layers (or a resistive layer i between two conductive layers), the electrical-sounding curve is not modified by the multiplication of e_i and ρ_i by a factor K (or alternatively by the simultaneous multiplication of e_i and division of ρ_i by a factor K).

(2) Suppression principle. A resistive layer between a highly conductive layer and a highly resistive layer has almost no influence on the electrical sounding.

A spectral representation of an electrical sounding can be obtained by computing the cumulated resistances and conductances defined by numbering the layers downwards as:

$$R_t\,(p) = \sum_{i=1}^{p} \rho_i e_i \quad (p = 1,\ldots n)$$

$$C_1\,(p) = \sum_{i=1}^{p} e_i/\rho_i$$

and drawing the curve:

$$\sqrt{R_t(p)/C_1(p)} = f\,[\sqrt{R_t(p)C_1(p)}]$$

on log-log paper.

To determine e_i and ρ_i, supplementary data have to be used: reference borings with a geological log or parametric boring allowing the measurement of the real resistivity of a layer.

Two cases of interpretation may occur: (1) the field electrical-sounding curve corresponds to an existing type of curve; and (2) there is no total correspondence. A smoothing will then be introduced.

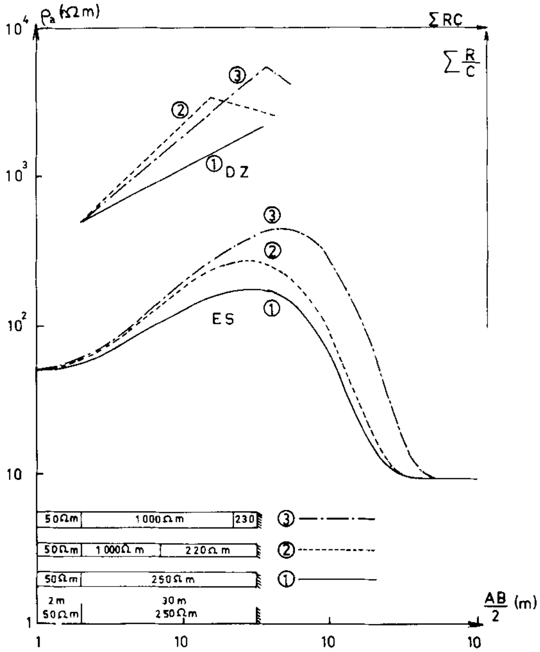

Fig. A.2.8. Electrical-sounding curve and cumulated resistance—conductance curve.

Fig. A.2.8 is an example of electrical-sounding curves (E.S.) and of cumulated resistance—conductance curves (D.Z.).

The interpretation of the experimental curves can now be improved by automatic treatments (Kunetz, 1966), but it should be stressed that to derive resistivities from the electrical field is a rather unstable problem. A small variation of ρ yields a small variation of the electrical field E, but the converse is not true and unless we have perfect electrical measurements (which is quite unreasonable), no unicity can be reached. A procedure has thus been derived which consists in:

(1) Computing a kernel function $\phi(\lambda,\rho)$ equivalent to S, by solving an integral equation with a second member made up of measurements. This kernel is the Fourier transform of the sequence of the electrical images of the source at the interfaces of elementary layers.

(2) Deriving the sequence of resistivities from ϕ, starting at the ground surface.

This procedure applied to a single electrical sounding has been extended to correlations between electrical soundings, under assumptions of regularity and continuity in the stratification.

APPENDIX III

SOME ELEMENTS OF MATRIX ALGEBRA

A.3.1. The vector space R^n

Consider the reference system $oxyz$ of rectangular axes (Fig. A.3.1). On each axis, give a vector of unit length e_1 on ox, e_2 on oy, and e_3 on oz. M being a point of the space, any vector OM can be written:

$$OM = a_1 e_1 + a_2 e_2 + a_3 e_3$$

where the set of real numbers (a_1, a_2, a_3) are the *components* of OM on the base (e_1, e_2, e_3).

By geometrical composition of the vectors $a_1 e_1$, $a_2 e_2$, $a_3 e_3$, we verify that

$$a_1 e_1 + a_2 e_2 + a_3 e_3 = 0 \quad \text{implies that} \quad a_1 = a_2 = a_3 = 0.$$

We say that e_1, e_2 and e_3 are independent. It can be easily checked that three vectors of origin O which do not belong to the same plane are independent.

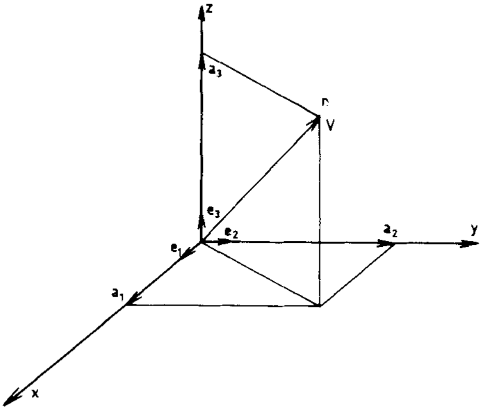

Fig. A.3.1. Usual reference system.

Consider two vectors **OV** and **OW** of respective components (a_1, a_2, a_3) and (b_1, b_2, b_3). The *scalar product* of OV and OW, written $\langle OV, OW \rangle$, is defined by:

$$\langle OV, OW \rangle = a_1 b_1 + a_2 b_2 + a_3 b_3$$

We say that OV and OW are *orthogonal* if $\langle OV, OW\rangle = 0$.

The length of vector OV is the number $L(OV)$ such that:

$$L(OV) \;=\; (a_1^2 + a_2^2 + a_3^2)^{1/2} \;=\; [\langle OV, OW\rangle]^{1/2}$$

It is also called the *norm* of OV and written $\|OV\|$.

The set of vectors OM for all M of the usual space makes up the vector space R^3 with the origin O.

All the preceding definitions can be extended to sets of vectors with the same origin but having n components, i.e. defined by a set of real numbers $(a_1, a_2, \dots a_n)$. They make up the vector space R^n, defined by the following operation:
sum of two vectors OM $(a_1, \dots a_n)$ and ON $(b_1, \dots b_n)$:

$$OM + ON \;=\; OP\,(a_1 + b_1, a_2 + b_2, \dots, a_n + b_n)$$

zero vector $00(0, \dots, 0)$
For all real λ and μ, we have:

$$\lambda OM \;=\; ON\,(\lambda a_1, \dots, \lambda a_n)$$

$$(\lambda + \mu)OM \;=\; \lambda OM + \mu ON$$

$$\lambda(OM + ON) \;=\; \lambda OM + \lambda ON$$

$$\lambda(\mu OM) \;=\; (\lambda\mu)OM$$

$$1 \cdot OM \;=\; OM$$

The vectors $e_1, \dots, e_n$ are independent if:

$$a_1 e_1 + \dots a_n e_n \;=\; 0 \longrightarrow a_1 \;=\; \dots \;=\; a_n \;=\; 0$$

A basis is a set of n independent vectors and any vector of R^n can be expressed as a unique linear combination of these vectors.

Scalar product: $\langle OV, OW\rangle \;=\; \sum_{i=1}^{n} a_i b_i$

Length of OV: $\langle OV, OV\rangle^{1/2} = \left(\sum_{i=1}^{m} a_i^2\right)^{1/2} = \|OV\|$

A.3.2. Matrices

Consider the linear system of equations:

$$\begin{aligned} a_1^1 x^1 + a_2^1 x^2 + \dots + a_n^1 x^n &= b^1 \\ a_1^2 x^1 + a_2^2 x^2 + \dots + a_n^2 x^n &= b^2 \\ a_1^P x^1 + a_2^P x^2 + \dots + a_n^P x^n &= b^P \end{aligned} \qquad [A.3.1]$$

A *matrix* is a table of n columns and p rows:

$$\mathsf{A} = \begin{bmatrix} a_1^1 & a_2^1 . & . & .a_n^1 \\ . & . & . & . \\ a_1^P & a_2^P . & . & .a_n^P \end{bmatrix}$$

Assuming that the real numbers $x^1, \dots x^n$ and $b^1, \dots. b^p$ are the components of vectors X and B of R^n and R^p, we say that the application of matrix A to X yields vector B and we write the system [A.3.1] as:

$$\mathsf{AX} = \mathsf{B}$$

defining AX by:

$$\mathsf{AX} = \begin{bmatrix} a_1^1 & . & . & . & a_n^1 \\ a_1^P & . & . & . & a_n^P \end{bmatrix} \begin{bmatrix} x^1 \\ x^n \end{bmatrix} = \begin{bmatrix} a_1^1 x^1 + & . & . & . & + a_n^1 x^n \\ a_1^P x^1 + & . & . & . & + a_n^P x^n \end{bmatrix}$$

A applies R^n into R^p.

In this book, we only consider square matrices, i.e. we state $n = p$. A square matrix of order n (i.e. with n columns and n rows) applies R^n into R^n: it transforms a vector with n components into a vector with n components.

We investigate now the meaning of the various columns of a matrix of order n. Consider the usual space and an orthogonal system $oxyz$ as given in Fig. A.3.1. We have defined a base of three orthonormal vectors (e_1, e_2, e_3) and in the reference system, the components of e_1, e_2 and e_3 respectively are (1, 0, 0), (0, 1, 0) and (0, 0, 1).

Consider a matrix of order n, A with coefficient a_i^j ($i = 1, 2, 3$ and $j = 1, 2, 3$). We apply A to e_1 and determine the resulting vector B

$$\mathsf{A}e_1 = B$$

According to [A.3.1], we have:

$$a_1^1 \times 1 + a_2^1 \times 0 + a_3^1 \times 0 = b^1$$

$$a_1^2 \times 1 + a_2^2 \times 0 + a_3^2 \times 0 = b^2$$

$$a_1^3 \times 1 + a_2^3 \times 0 + a_3^3 \times 0 = b^3$$

a system which yields $b^1 = a_1^1$, $b^2 = a_1^2$ and $b^3 = a_1^3$.

Thus the transform of the vector e_1 by the matrix A is the first column of A. The reader will easily check that the transforms of e_2 and e_3 are respectively the second and third columns of A.

These results can be easily extended to the vector space R^n: the columns of a matrix A, considered as vectors, are the transforms by A of the base $(e_1, ..., e_n)$ expressed in the same base i.e.:

$$\mathsf{A}e_i = a_i^1 e_1 + a_i^2 e_2 + ... + a_i^n e_n = \sum_{j=1}^{n} a_i^j e_j \qquad [A.3.2]$$

Application to a change of coordinate system

As an example, we wish to rotate the system oxy around the origin of an angle θ to obtain OXY. The basis vectors (unit vectors) are respectively (e_1, e_2) and (E_1, E_2). We express a vector $\boldsymbol{OM}$ in both systems, its components being respectively (x, y) and (X, Y). From Fig. A.3.2, we have:

$$OM = xe_1 + ye_2 = XE_1 + YE_2$$

$$E_1 = \cos\theta e_1 + \sin\theta e_2$$

$$E_2 = -\sin\theta e_1 + \cos\theta e_2 \qquad [A.3.3]$$

and $OM = (X\cos\theta - Y\sin\theta)e_1 + (X\sin\theta + Y\cos\theta)e_2$

which yields the system:

$$X\cos\theta - Y\sin\theta = x$$

$$X\sin\theta + Y\cos\theta = y$$

written under matricial form as:

$$\begin{bmatrix} \cos\theta & -\sin\theta \\ \sin\theta & \cos\theta \end{bmatrix} \begin{bmatrix} Y \\ Y \end{bmatrix} = \begin{bmatrix} x \\ y \end{bmatrix} \qquad [A.3.4]$$

Comparing to [A.3.3], we see that a change of coordinate system can be defined by a matricial system, like [A.3.4], and the columns of the matrix are the transforms of the vectors of the old basis (here E_1 and E_2) expressed in the same old basis (e_1, e_2). This result can be generalized to non-orthonormal base changes in R^n.

The usefulness of the matrix theory now begins to appear: it offers a systematic representation of a linear system of equations and provides rules and theorems that can be used to solve the system. We go deeper into the theory of square matrices, by introducing the sum, the product and the inverse of matrices.

In what follows, we use Einstein's convention: in a product of indexed quantities, when upper and lower indices are the same letter, summation of

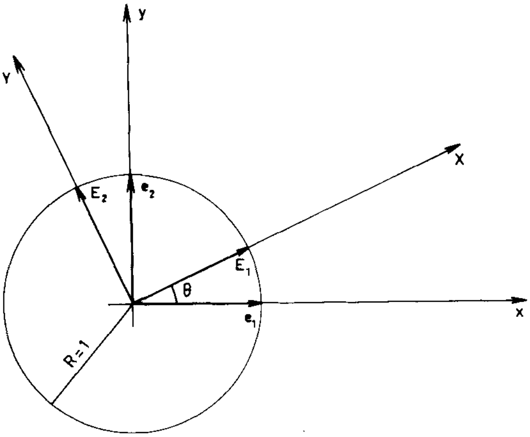

Fig. A.3.2. Rotation of an angle θ.

the corresponding products has to be done by varying the common index.

$$\sum_{i=1}^{n} a_i^j b_j = a_i^j b_j \qquad (j = 1, ..., n)$$

$$\sum_{j=1}^{n}\left(\sum_{i=1}^{p} x^i a_i^j\right) e_j = x^i a_i^j e_j \begin{pmatrix} i = 1, ..., p \\ j = 1, ..., n \end{pmatrix}$$

Consider the matrix A, of order n, given by its coefficients (a_i^j) and a scalar λ; we define the product λA as the matrix with coefficients (λa_i^j).

Example

$$2 \times \begin{bmatrix} 1 & 2 \\ 3 & 4 \end{bmatrix} = \begin{bmatrix} 2 \times 1 & 2 \times 2 \\ 2 \times 3 & 2 \times 4 \end{bmatrix} \equiv \begin{bmatrix} 2 & 4 \\ 6 & 8 \end{bmatrix}$$

Consider two matrices A and B, of order n, given by their coefficients (a_i^j) and (b_i^j), and a vector X of R^n, given by its components (x^i) on the basis $(e_1, ..., e_n)$. Apply A and B to X, which yields two vectors X_1 and X_2 of R^n and consider the geometrical sum Z of X_1 and X_2. The sum of A and B is the matrix C = A + B, of order n, defined by the relationships:

$$X_1 = \mathrm{A}X \qquad X_2 = \mathrm{B}X$$
$$Z = X_1 + X_2 = \mathrm{A}X + \mathrm{B}X = (\mathrm{A} + \mathrm{B})X = \mathrm{C}X$$

which yields the coefficients (c_i^j) of C, in the basis $(e_1, ..., e_n)$, using the definition of the product of a matrix by a scalar and equation [A.3.2]:

$$X = x^i e_i \quad X_1 = \mathsf{A} x^i e_i = x^i \mathsf{A} e_i = x^i a_i^j e_j \quad X_2 = x^i b^j e_j$$

$$Z = x^i a_i^j e_i + x^i b_i^j e_j = x^i (a_i^j + b_i^j) e_j = x^i c_i^j e_i$$

$$c_i^j = a_i^j + b_i^j$$

Example

$$\mathsf{A} = \begin{bmatrix} 1 & 2 \\ 3 & 4 \end{bmatrix} \quad \mathsf{B} = \begin{bmatrix} 5 & 6 \\ 7 & 8 \end{bmatrix} \quad \mathsf{C} = \mathsf{A} + \mathsf{B} = \begin{bmatrix} 1+5 & 2+6 \\ 3+7 & 4+8 \end{bmatrix} = \begin{bmatrix} 6 & 8 \\ 10 & 12 \end{bmatrix}$$

Consider now the previous matrices A and B, and the vector X; apply A to X, which yields X_1 and B to X_1, which yields Y. The product of B by A is a matrix $\mathsf{D} = \mathsf{BA}$, of order n, defined by the relationships

$$X_1 = \mathsf{A}X \qquad Y = \mathsf{B}X_1 = \mathsf{BA}X = \mathsf{D}X$$

which yields the coefficients (d_i^j) of D, in the basis $(e_1, \ldots, e_n)$

$$X = x^i e_i \qquad X_1 = x^i a_i^j e_j \qquad Y = x^i a_i^j \mathsf{B}(e_j) = x^i a_i^j b_j^k e_k$$

$$Y = x^i d_i^k e_k \text{ with } \quad d_i^k = b_j^k a_i^j$$

This coefficient d_i^k is the sum of the products of the elements of the line k of B by the elements of the column i of A.

Example:

$$\begin{bmatrix} 1 & 2 \\ 3 & 4 \end{bmatrix} \times \begin{bmatrix} 5 & 6 \\ 7 & 8 \end{bmatrix} = \begin{bmatrix} 1\times 5 + 2\times 7 & 1\times 6 + 2\times 8 \\ 3\times 5 + 4\times 7 & 3\times 6 + 4\times 8 \end{bmatrix} = \begin{bmatrix} 19 & 22 \\ 43 & 50 \end{bmatrix}$$

The sum of matrices is associative and commutative:

$$(\mathsf{A} + \mathsf{B}) + \mathsf{C} = \mathsf{A} + (\mathsf{B} + \mathsf{C}) = \mathsf{A} + \mathsf{B} + \mathsf{C}$$

$$\mathsf{A} + \mathsf{B} = \mathsf{B} + \mathsf{A}$$

The product of matrices is associative and non-commutative:

$$\mathsf{A}(\mathsf{BC}) = (\mathsf{AB})\mathsf{C} = \mathsf{ABC}$$

$$\mathsf{AB} \neq \mathsf{BA}$$

The matrix I of order n with 1 on the diagonal and 0 everywhere is a unitary matrix (or identity matrix):

$$\mathsf{I} = \begin{bmatrix} 1 & 0 & . & . & 0 \\ 0 & 1 & . & . & 0 \\ \vdots & \vdots & \ddots & \vdots & \vdots \\ 0 & 0 & . & . & 1 \end{bmatrix}$$

$\mathsf{I} \times \mathsf{A} = \mathsf{A} \times \mathsf{I} = \mathsf{A}$ for any A of order n.

If there exists a matrix B such that, for a given A:

$$\mathsf{BA} = \mathsf{AB} = \mathsf{I}$$

we say that B is the inverse of A and we write:

$$\mathsf{B} = \mathsf{A}^{-1}$$

Consider the linear system of equations:

$$\mathsf{AX} = \mathsf{B}$$

If there exists A^{-1}, we have:

$$\mathsf{A}^{-1}\mathsf{AX} = \mathsf{A}^{-1}\mathsf{B} = \mathsf{IX}$$

The system can be solved and its solution is $\mathsf{X} = \mathsf{A}^{-1}\mathsf{B}$. The methods presented in § 9.3 are numerical techniques to compute A^{-1}. In Chapter 9, all the results are based upon the theorem: if a linear system of n equations and n unknowns is such that its matrix has an inverse, it has one and only one solution, i.e. there exists one and only one set of numbers (x^i) such that $a_i^j x^i = b^j$ ($i = 1, ..., n$ and $j = 1, ..., n$).

We admit the result: a matrix is invertible if and only if its column vectors are independent. An invertible matrix is said to be "regular".

If a matrix is diagonal (i.e. all its coefficients are zero, except on the diagonal) its inverse is readily computed:

$$\mathsf{A} = \begin{bmatrix} a_1^1 & . & . & 0 \\ . & a_2^2 & . & . \\ . & . & . & . \\ 0 & . & . & a_n^n \end{bmatrix} \qquad \mathsf{A}^{-1} = \begin{bmatrix} \dfrac{1}{a_1^1} & . & . & 0 \\ . & \dfrac{1}{a_2^2} & . & . \\ . & . & . & . \\ 0 & 0 & . & \dfrac{1}{a_n^n} \end{bmatrix}$$

A matrix **A** is said to be symmetric if:

$$a_i^j = a_j^i$$

A matrix **A** is said to be antisymmetric if:

$$a_i^j = -a_j^i$$

This implies $a_i^i = 0$. The diagonal coefficients are zero. Symmetric matrices are a very important family, with interesting properties. They are frequently encountered in models of groundwater flow.

A.3.3. Determinants

Consider the system:

$$\begin{aligned} ax + by &= \alpha \\ cx + dy &= \beta \end{aligned} \qquad \text{or} \quad \begin{pmatrix} a & b \\ c & d \end{pmatrix}\begin{pmatrix} x \\ y \end{pmatrix} = \begin{pmatrix} \alpha \\ \beta \end{pmatrix}$$

We compute x by multiplying the first equation by d and the second equation by $-b$, and adding the resulting equations:

$$x = (\alpha d - \beta b)/(ad - bc)$$

In the same way:

$$y = (a\beta - \alpha c)/(ad - bc)$$

We notice that the denominator of x and y is the cross-product of the coefficients of the system matrix:

$$\left[\begin{tikzcd} a \arrow[dr, leftrightarrow] & b \\ c \arrow[ur, leftrightarrow] & a \end{tikzcd}\right]$$

It is called the determinant of the system.
If the determinant is zero, the system cannot be solved in that way:

$$ad - bc = 0 \quad \Rightarrow \quad \frac{a}{b} = \frac{c}{d}$$

If $a/b = c/d = \alpha/\beta$ the equations are proportional, the system reduces to one equation and there is an infinity of solutions given by:

$$x = (\alpha - by)/a \qquad \text{for any value of } y.$$

If $a/b = c/d \neq \alpha/\beta$ there is no possible solution. The system is impossible. It should be noticed that the determinant is zero if and only if the column vectors of the system matrix are proportional (i.e. if the matrix is not regular).

A determinant is written:

$$\begin{vmatrix} a & b \\ c & d \end{vmatrix}$$

As for matrices, algebraic operations on determinants can be defined.

If two column vectors are exchanged, the determinant takes the opposite sign:

$$\begin{vmatrix} a & b \\ c & d \end{vmatrix} = ad - bc = -(bc - ad) = -\begin{vmatrix} b & a \\ d & c \end{vmatrix}$$

this obviously implies:

$$\begin{vmatrix} a & a \\ c & c \end{vmatrix} = 0$$

If a column vector is the sum of two vectors, the determinant can be expanded into the sum of two determinants as follows:

$$\begin{vmatrix} a+e & b \\ c+f & d \end{vmatrix} = \begin{vmatrix} a & b \\ c & d \end{vmatrix} + \begin{vmatrix} e & b \\ f & d \end{vmatrix}$$

as is easily computed from the cross-product $(a + e)d - b(c + f)$.

A column vector may be added to another column vector without changing the determinant:

$$\begin{vmatrix} a+b & b \\ c+d & d \end{vmatrix} = \begin{vmatrix} a & b \\ c & d \end{vmatrix} + \begin{vmatrix} b & b \\ d & d \end{vmatrix} = \begin{vmatrix} a & b \\ c & d \end{vmatrix}$$

If a column is multiplied by a scalar λ, the determinant is multiplied by λ:

$$\begin{vmatrix} \lambda a & b \\ \lambda c & d \end{vmatrix} = \lambda(ad - bc) = \lambda\begin{vmatrix} a & b \\ c & d \end{vmatrix}$$

Determinants are generalized to linear systems for n equations with n

unknowns as follows: the determinant det (A), also written:

$$\det(A) = \begin{vmatrix} a_1^1 & \text{---} & a_n^1 \\ & \ddots & \\ a_1^n & \text{---} & a_n^n \end{vmatrix}$$

is the number obtained by:

(1) Doing all the possible products $a^1_{\alpha 1}\, a^2_{\alpha 2} \ldots a^n_{\alpha n}$ of n coefficients such that $\alpha_1\, \alpha_2 \ldots \alpha_n$ be a permutation of 1, 2, ..., n; no α_i is thus repeated.

(2) Counting the number of permutations of $\alpha_1 \ldots \alpha_n$, i.e. the number of exchanges of two indices α_i to obtain permutation 1, 2 ..., n. If this number is even, the product is preceded by +; if the number is odd, the product is preceded by −.

(3) Adding all the products with their signs.

Example

$$\begin{vmatrix} 1 & 2 & 3 \\ 4 & 5 & 6 \\ 7 & 8 & 9 \end{vmatrix} = 1 \times 5 \times 9 + 4 \times 3 \times 8 + 7 \times 2 \times 6 - 1 \times 8 \times 6 - 4 \times 2 \times 9 - 7 \times 3 \times 5$$

All the results obtained for determinants of order 2 are valid for determinants of order n. The most important result, for our problems, is that a matrix is regular if and only if its determinant is non-zero. Then we know that the corresponding linear system of equations has one and only one solution; otherwise, it may be impossible or have an infinity of solutions. The computation of the determinant may thus be required to check the possible existence of a solution. Another interesting feature of determinants is that they are needed to compute eigenvalues and eigenvectors of a matrix, as defined in § A.3.4.

Remark. In some very simple cases (two equations with two unknowns as seen) determinants can be used to compute the solution directly. This is almost never the case in our pollution problems.

A.3.4. Eigenvalues and eigenvectors of a matrix of order n

For any matrix M, there exist vectors V_i (different from the zero vector) and numbers λ_i such that:

$$\mathsf{M} V_i = \lambda_i V_i \qquad [\text{A.3.5}]$$

V_i is an eigenvector of M corresponding to the eigenvalue λ_i.

To any eigenvector V_i, there corresponds a unique value λ_i.

To any eigenvalues λ_i, there corresponds one or several eigenvectors which span a vector subspace of R^n, called the eigensubspace corresponding to λ_i.

A matrix of order n has at most n distinct eigenvalues. Equation [A.3.5] can be written:

$$(\mathsf{M} - \lambda_i \mathsf{I}) V_i = 0 \qquad [A.3.6]$$

The components of V_i being $(x^1, ..., x^n)$ and the column vectors of $\mathsf{M} - \lambda_i \mathsf{I}$ being $(A_1, ..., A_n)$, [A.3.6] yields:

$$x^1 A_1 + ... + x^n A_n = 0$$

which shows that $A_1, ..., A_n$ are dependent. Thus $\mathsf{M} - \lambda_i \mathsf{I}$ is not regular and has no inverse.

This implies that the determinant of $\mathsf{M} - \lambda_i \mathsf{I}$ is equal to zero; thus the eigenvalues of a matrix M are the roots of the polynomial equation in λ:

$$\det(\mathsf{M} - \lambda \mathsf{I}) = 0 \quad \text{or} \quad \begin{vmatrix} a_1^1 - \lambda & a_2^1 & . & a_n^1 \\ . & a_2^2 - \lambda & . & . \\ . & . & . & . \\ a_1^n & a_2^n & & a_n^n - \lambda \end{vmatrix} = 0$$

Example $M = \begin{bmatrix} 4 & 2 \\ 2 & 4 \end{bmatrix} \qquad \mathsf{M} - \lambda \mathsf{I} = \begin{bmatrix} 4 - \lambda & 2 \\ 2 & 4 - \lambda \end{bmatrix}$

$$\det(\mathsf{M} - \lambda \mathsf{I}) = (4 - \lambda)^2 - 4 = 0 = (6 - \lambda)(2 - \lambda)$$

The eigenvalues are 6 and 2. The components of the eigenvectors verify the systems:

$$\lambda = 6 \begin{cases} 4x + 2y = 6x \\ 2x + 4y = 6y \end{cases} \qquad \lambda = 2 \begin{cases} 4x + 2y = 2x \\ 2x + 4y = 2y \end{cases}$$

and the corresponding eigenvectors are all vectors proportional, respectively to $V_1 = \begin{bmatrix} 1 \\ 1 \end{bmatrix}$ for eigenvalue 6 and $V_2 = \begin{bmatrix} 1 \\ -1 \end{bmatrix}$ for eigenvalue 2. We verify that both systems have an infinity of solutions, because $\mathsf{M} - \lambda \mathsf{I}$ is not regular.

For our problem, the interests of the concept of eigenvalues and eigenvectors are: (1) the possibility of simplifying the linear system of equations; and (2) the introduction of convergence theorems for iterative procedures by establishing simple criteria for the convergence of sequences and series of matrices.

A linear system of equations is easily solved if its matrix is diagonal. In § A.3.2, we have seen that a column vector of a matrix is the transform of the vector of the basis expressed in the basis if, for instance, e_1 is also an eigenvector corresponding to the eigenvalue λ, then we have:

$$\mathsf{A}e_1 = \lambda e_1$$

and the components of $\mathsf{A}e_1$ in the basis $(e_1, e_2, \ldots, e_n)$ are $(\lambda, 0, \ldots 0)$.

From this consideration, we admit the theorem: a matrix A of R^n can be diagonalized if and only if there exists a basis of R^n made up of eigenvectors of A.

Of course, diagonalization is not always possible, but a matrix can always be put under triangular form, i.e. with either only zeros above the diagonal or only zeros under the diagonal, and eigenvalues on the diagonal. Under a triangular form, the system is very easily solved.

(1) if all eigenvalues of A are distinct, A can be diagonalized; and (2) a symmetric real matrix can always be diagonalized, even if its eigenvalues are not distinct. Furthermore its eigenvectors are orthogonal.

The convergence criteria are explained in the next paragraph.

A.3.5. Norms of vectors and matrices

In § A.3.1 we have introduced the norm of vector $V(x^1, \ldots, x^n)$ as $\|V\| = ({x^1}^2 + \ldots + {x^n}^2)^{1/2}$. Actually, this is the euclidean norm of V and the most natural, directly issued from the theorem of Pythagoras. Other norms can be introduced such as:

$$\|V\|_1 = \sum_{i=1}^{n} |x^i|$$

$$\|V\|_\infty = \sup_i |x^i|$$

All norms satisfy the relations:

$$\begin{aligned} &\|V\| \geqslant 0 \quad \text{and} \quad \|V\| = 0 \Leftrightarrow V = 0 \\ &\|\lambda V\| = |\lambda|\,\|V\| \quad \text{for all scalars } \lambda \\ &\|V + W\| \leqslant \|V\| + \|W\| \quad \text{(triangular inequality)} \end{aligned} \qquad [A.3.7]$$

In the same way, the norm of a matrix A is defined by the relations:

$$\begin{aligned} &\|\mathsf{A}\| > 0 \quad \text{and} \quad \|\mathsf{A}\| = 0 \Leftrightarrow \mathsf{A} = 0 \\ &\|\lambda \mathsf{A}\| = |\lambda|\,\|\mathsf{A}\| \quad \text{for all scalars } \lambda \\ &\|\mathsf{A} + \mathsf{B}\| \leqslant \|\mathsf{A}\| + \|\mathsf{B}\| \\ &\|\mathsf{AB}\| \leqslant \|\mathsf{A}\|\,\|\mathsf{B}\| \end{aligned} \qquad [A.3.8]$$

Now consider a matrix A of order n. We shall define two types of norms of A.

(1) We call the norm of A subordinate to the vector norm $\|V\|$, the positive number $\|\mathsf{A}\|$ defined by:

$$\|\mathsf{A}\| = \sup_{V \neq 0} \frac{\|\mathsf{A}V\|}{\|V\|}$$

$\|\mathsf{A}\|$ verifies the relations [A.3.8]. Obviously, we have:

$$\|\mathsf{A}V\| \leqslant \|\mathsf{A}\| \, \|V\| \qquad \text{(Schwarz's inequality)}$$

A matrix norm and a vector norm for which Schwarz's inequality holds are "compatible".

The matrix norm subordinate to the euclidean vector norm is called the "spectral" norm.

(2) Another norm of A, compatible with the euclidean norm of V is the euclidean norm of A defined by:

$$\|\mathsf{A}\|_{\mathrm{E}} = \left(\sum_{ij} |a_i^j|^2 \right)^{1/2}$$

which cannot be subordinate to any vector norm as:

$$\|\mathsf{I}\|_{\mathrm{E}} = n^{1/2} \neq \|\mathsf{I}\| = 1$$

The euclidean norm of A is practical as it can be very easily computed.

Remark 1. If V is an eigenvector of A, corresponding to the eigenvalue λ, from Schwarz's inequality, we have:

$$\|\mathsf{A}V\| = \|\lambda V\| \leqslant \|\mathsf{A}\| \, \|V\| \qquad |\lambda| \leqslant \|\mathsf{A}\|$$

The largest eigenvalue of A in absolute value (or spectral radius ρ) then satisfies $\rho \leqslant \|\mathsf{A}\|$.

Remark 2. If A is a real symmetric matrix, its spectral radius is equal to its spectral norm. In § A.3.4 we have said that the eigenvectors of A are an orthogonal basis of R^n. Then any vector V can be expressed in terms of eigenvectors E_i as:

$$V = x^i E_i$$

$$\mathsf{A}V = x^i \mathsf{A} E_i = \lambda_i x^i E_i$$

$$\|\mathsf{A}\| = \sup_V \left(\sum_i \lambda_i^2 x^{i^2} \right)^{1/2} \bigg/ \left(\sum_i x^{i^2} \right)^{1/2} \leqslant \rho$$

From Remark 1, we have: $\rho = \mathsf{A}$.

Now, we admit some criteria for convergence of sequences and series of matrices of order n:

— $\lim_{p \to \infty} \mathsf{A}^p = 0$ if $\|\mathsf{A}\| < 1$

— $\lim_{p \to \infty} \mathsf{A}^p = 0$ if and only if $\rho < 1$

— the series $\mathsf{I} + \mathsf{A} + \mathsf{A}^p + \ldots$ converges if and only if $\mathsf{A}^p \to 0$; it converges to $(\mathsf{I} - \mathsf{A})^{-1}$
— if any norm $\|\mathsf{A}\|$ is less than unity, $\mathsf{I} + \mathsf{A} + \mathsf{A}^2 + \ldots$ converges; this is not a necessary condition.

APPENDIX IV

WATER QUALITY: NORMS AND CRITERIA

International norms of water quality have been established for drinl water only (W.H.O., 1972); they represent the minimal norms that car reached by all countries. As countries can reach higher figures for econom and technical reasons, the World Health Organization has proposed Europ norms of higher standards (W.H.O., 1971). It should be stressed that tl norms are only recommendations and that it depends on each countr enforce them by law. The W.H.O. gives five classes of quality paramet biological pollutants, radioactive pollutants, toxic compounds, chemical c pounds which may be a health hazard and water-acceptability charact

(1) The bacteriological norms of biological pollution are based upon occurrence of microorganisms which are not pathogenic. These normal ge of fecal pollution are more numerous than pathogenic bacterias and they good pollution indicators, which can be detected quite easily. These ge are usually *Escherichia coli (E. coli)* and coliforms.

Any sample of 100 ml of chlorinated water entering the water distribu net should be free of these microorganisms. Any sample of 100 ml of r chlorinated water should be free of *E. coli* and, if this condition is reali could contain at most 3 coliforms. All samples taken in the distribution should be free of coliforms, which is not always possible. In individual w and springs, an upper limit of 10 coliforms will be observed to consider water as potable.

(2) Proposed levels of radioactive pollution are:

global alpha radioactivity	3 pCi/l
global beta radioactivity	30 pCi/l

These levels are applied to the average of all radioactivity measurement f time period of three months.

(3) Toxic compounds. Maximum concentrations are based upon the sumption of an average man of 70 kg consuming 2.5 liters of water per c Results are summarized in Table IV.

TABLE IV

Toxic Compounds (from W.H.O., 1972)

Compound, expressed as	Arsenic	Cadmium	Cyanides	Total mercury	Lead	Seleniu
Max. concentration (mg/l)	0.05	0.01	0.05	0.001	0.1	0.01

(4) Chemical compounds which may be a health hazard. Upper and lower concentration limits for fluorides depend upon temperature and vary between 0.6 and 0.9 mg/l for the lower limit and 0.8 and 1.7 mg/l for the upper limit. Nitrates (expressed as NO_3) should not exceed 45 mg/l. Polycyclic aromatic hydrocarbons are cancerogeneous and their concentration should not exceed 0.0002 mg/l. As for pesticides, no results have yet been proposed.

(5) Water acceptability characteristics have been derived from the usual physiochemical tests of water. They are summarized in Table V.

TABLE V

Water-acceptability Characteristics (from W.H.O., 1972)

Compound or property	Colour (platino-cobalt colour scale)	Odour	Turbidity	Total solids (mg/l)	*pH*	Total hardness (mg/l $CaCO_3$)
Max. concentration proposed	5 units	no limit	5 units	500	7—8.5	100
Max. concentration admissible	50 units	no limit	25 units	1500	65—9.2	500

Anionic detergents (mg/l)	Mineral oil (mg/l)	Phenols (mg/l)	Calcium (mg/l)	Chlorides (mg/l of Cl)	Copper (mg/l)	Iron (mg/l)
0.2	0.01	0.001	75	200	0.05	0.1
1.0	0.3	0.002	200	600	1.5	1.0

Magnesium (mg/l)	Manganese (mg/l)	Sulfates (mg/l of SO_4)	Zinc (mg/l)
< 30 if sulfate concentration > 250 otherwise < 150	0.05	200	5.0
150	0.5	400	15

REFERENCES

Agence Financière de Bassin Rhône-Méditerranée—Corse, 1971. Etude des risques d pollution de la nappe alluviale de la plaine de Lyon. Intern Rep.

Archie, G.E., 1942. The electrical resistivity log as an aid in determining some rese voir characteristics. Trans. A.I.M.E., 146: 54—61.

Aris, R., 1956. On the dispersion of a solute in a fluid flowing through a tube. Proc. Soc. London, Ser. A, 235: 67—77.

Aris, R. and Amundson, N.R., 1957. Some remarks on longitudinal mixing or diffusi in fixed beds. J. Am. Inst. Chem. Eng., 3: 280—282.

Arlab, 1974. Abaques de dispersion (Dispersion Type Curves by Y. Emsellem).

Arthur, K.B. and Metanomski, Z.G., 1965. Présentation de quelques procédés d'augme tation de la vitesse de convergence dans les solutions numériques des problèmes d diffusivité. C.R. 2ème Coll. Assoc. Rech. Tech. Forage et Production. Rue Malmaison, pp. 253—363.

Babot, Y. and Simler, L., 1970. Pollution des eaux souterraines. Etude bibliographi qu Service Géologique d'Alsace-Lorraine, 24.2.1970.

Bachmat, Y., 1967. On the similitude of dispersion phenomena in homogeneous an isotropic porous media. Water Resour. Res., 3: 1079—1083.

Bachmat, Y., 1969. Hydrodynamic dispersion in a saturated homogeneous porous m dium at low Peclet numbers and nonhomogeneous solution. Water Resour. Res., 139.

Bachmat, Y. and Bear, J., 1964. The general equations of hydrodynamic dispersio J. Geophys. Res., 69: 2561—2567.

Bachmat, Y. and Bear, J., 1972. Mathematical formulation of transport phenomena porous media. Int. Assoc. Hydr. Res.—Int. Soc. Soil Sci., Proc. 2nd Symp. Guelp pp. 174—193.

Bayer, M.B., 1972. A non-linear mathematical programming model for water qualit management. Int. Symp. on Modelling Techniques in Water Resour. Syst. E vironment Canada, Ottawa, p.p. 341—351.

Bear, J., 1960. The Transition Zone between Fresh and Salt Waters in Coastal Aquifer Thesis, Univ. of California, Berkeley, Calif.

Bear, J., 1961a. On the tensor form of dispersion. J. Geophys. Res., 66: 1185—119

Bear, J., 1961b. Some experiments on dispersion. J. Geophys. Res., 66: 2455—246

Bear, J., 1970. Two liquid flows in porous media. In: V.T. Chow (Editor), Advances i Hydroscience, 6. Academic Press, New York, pp. 142—252.

Bear, J., 1972. Dynamics of Fluids in Porous Media. American Elsevier, New Yor 764 pp.

Bear, J. and Bachmat, Y., 1967. A generalized theory on hydraulic hydrodynamic di persion in porous media. Int. Assoc. Sci. Hydr. Symp. Haifa, Publ., 72: 7—16.

Bear, J. and Dagan, G. The transition zone between fresh and salt waters in a coast aquifer. Hydraulic Lab. Technion Haifa Israël IASH; 1962a, Prog. Rep. 1, T steady interface between two immiscible fluids in a two-dimensional field of flo 1962, Prog. Rep. 2, A steady flow to an array of wells above the interface, approx mate solution for a moving interface; 1964a, Progr. Rep. 3, The interface below coastal collector; 1966, Progr. Rep. 4, Increasing the yield of a coastal collector means of special operation techniques; 1966a, Progr. Rep. 5, The transition zone at the rising interface below the collector.

Bear, J., Zaslavsky, D. and Irmay, S., 1968. Physical Principles of Water Percolation and Seepage, UNESCO, Paris.

Bellman, R., Kalaba, R.E. and Lockett, J.A., 1966. Numerical Inversion of the Laplace Transform. Elsevier, New York.

Ben Salah, M.D., 1965. Influence des contrastes de viscosité et de densité sur le déplacement en milieu poreux de deux fluides miscibles. Thèse Univ. de Toulouse.

Benzecri, J.P. et ses collaborateurs, 1973. Vol. I, La Taxinomie, Vol. 2, Analyse des correspondances. Dunod, Paris, 624 pp.

Bird, R.B., Stewart, W.E. and Lightfoot, E.N., 1960. Transport Phenomena. Wiley, New York.

Blackwell, R.J., 1959. Experiments on mixing by fluid flow in porous media. 52nd Ann. Meeting Soc. Pet. Eng., San Francisco, Preprint 29.

Blackwell, R.J., 1962. Laboratory studies of microscopic dispersion phenomena. Soc. Pet. Eng. J., 2: 1—8.

Blackwell, R.J., Rayne, J.R. and Terry, W.M., 1959. Factors influencing the efficiency of miscible displacement. Trans A.I.M.E., 217: 1—8.

Blanc, G., 1967. Contribution à l'étude des déplacements par fluides miscibles dans un milieu poreux; dispersion transversale. Thèse, Univ. Paris, Editions Technip.

Bochever, F.M. and Oradovskaya, A.Y., 1967. Convective salt diffusion in a radial subsurface stream in relation to the protection of subsurface water from contaminated discharges. Sov. Hydrol., Selected papers, 4.

Bolt, G.H. and Groenevelt, P.H., 1972. Coupling between transport processes in porous media. Int. Assoc. Hydr. Res.—Int. Soc. Soil Sci., Proc. 2nd Symp. Fundamentals of Transport Phenomena in Porous Media. Guelph, pp. 630—652.

Bredehoeft., J.D.,1969. Finite-difference approximations to the equations of groundwater flow. Wat. Resour. Res., 5-2: 531—534.

Bredehoeft, J.D., 1971. Comment on "Numerical Solution to the Convective Diffusion Equation" by C.A. Oster, J.C. Sonnichsen and R.T. Jaske. Water Res. Res., 7-3: 755—757.

Bredehoeft, J.D. and Pinder, G.F., 1972. Mass transport in flowing groundwater. Water Resour. Res., 9-1: 194—210.

Brenner, H., 1962. The diffusion model of longitudinal mixing in beds of finite length. Numerical values. Chem. Eng. Sci., 17: 229—243.

Brigham, W.E., Reed, P.W. and Dew, J.N., 1959. Experiments on mixing by fluid flow in porous media. A.I.Ch.E.—A.I.M.E. Symp. Oil Recovery Meth., San Francisco, Preprint 44.

Bruch, J.C. and Street, R.L., 1967. Two-dimensional dispersion. Proc. Am. Soc. Civ. Eng., 93: 17—39.

Bruch, J.C. Jr, 1970. Two-dimensional dispersion experiments in a porous medium Water Resour. Res., 6-3: 791—800.

Cagauan, B.G., Lau, L.S., Green, R.E. and Uehara, G., 1968. Solute dispersion in two Hawaian soils under saturated flow. Trans. 9th Int. Congr. Soil Sci., first paper, 20 pp.

Carslaw, H.S. and Jaeger, J.C., 1959. Conduction of Heat in Solids. Oxford Univ. Press, Oxford, 510 pp.

Castillo, E., Krizek, R.J. and Karadi, G.M., 1972. Comparaison of dispersion characteristics in fissured rock. Int. Assoc. Hydr. Res.—Int. Soc. Soil Sci. Proc. 2nd Symp. Fundamentals of Transport Phenomena in Porous Media, Guelph, pp. 778—797.

Chalengeas, J.L., 1970. Mesure des directions et vitesse d'écoulement d'une nappe d'eau souterraine par la méthode de déplacement des équipotentielles. Thèse, Univ. de Strasbourg.

Chow, V.T., 1952. On the determination of transmissibility and storage coefficients from pumping test date. Trans. Am. Geophys. Union, 33: 397—404.

Coats, K.H. and Smith, B.D., 1964. Dead end pore volume and dispersion in porous media. Soc. Pet. Eng., 4: 73—84.

Coe, J.J., 1970. Effects of solid waste disposal on groundwater quality. J. Am. Water Assoc., 12: 776—783.

Corompt, P., Gaillard, B., Guizerix, J., Margrita, R., Molinari, J., Corda, R., Crampon, N. and Olivier, D., 1974. Méthode pour la détermination de caractéristiques de transfert de substances polluantes dans les nappes aquifères. Int. Atomic Energy Agency. Symp. Isotope Techn. in Groundwater Hydr., Vienna. IAEA-SM, 182—41.

Crane, F.E. and Gardner, G.H.F., 1961. Measurements of transverse dispersion in granular media. J. Chem. Eng. Data, 6: 283.

Crank, J., 1967. The Mathematics of Diffusion. Oxford Univ. Press, Oxford, 347 pp.

Dagan, G., 1967. Hydrodynamic dispersion in a nonhomogeneous porous column. J. Geophys. Res., 72: 4075—4080.

Dagan, G., 1969. Some aspects of heat and mass transfer in porous media. IAHR Symp. Fundamentals of Transport Phenomena in Porous Media, Haifa.

Dagan, G., 1971. Perturbation solutions of the dispersion equation in porous mediums. Water Resour. Res., 7: 135—142.

Dagan, G. and Bear, J., 1968. Solving the problem of local interface upconing in a coastal aquifer by the method of small perturbations. J. I.A.H.R., 1, 6: 15—44.

Day, P.R., 1956. Dispersion of a moving salt-water boundary advancing through a saturated sand. Trans. Am. Geophys. Union, 37: 595—601.

Day, P.R. and Forsythe, W.M., 1957. Hydrodynamic dispersion of solutes in the soil moisture stream. Soil Sci. Soc. Am., Proc., 21: 477—480.

Deans, H.A., 1963. A mathematical model for dispersion in the direction of flow through porous media. J. Soc. Pet. Eng., 3: 49—52.

Debuisson, J., 1970. La nappe aquifère du cordon dunaire de Malika (Sénégal). Bull. Bur. Rech. Géol. Min., 3-3: 149—161.

Debuisson, J. and Moussu, H., 1967. Une étude expérimentale de l'intrusion des eaux marines dans une nappe cotière du Sénégal sous l'effet de l'exploitation. Int. Assoc. Sci. Hydr. Symp. of Haifa, Publ. 72: 334—349.

Defives, D., 1960. Transfert de matière. Rev. Inst. Fr. Pétrole, 15: 1141—1365.

Degot, B., Levêque, P.C., Courtois, G., Gasnier, M. and Godar, S., 1963. Deux utilisations du^{82}Br en hydrodynamique souterraine. Int. Atomic Energy Agency. Radioisotopes in hydrology, Tokyo.

Deininger, R.A., 1972. Minimum cost regional pollution control systems. Int. Symp. on Modelling Techniques in Water Resour. Syst. Environment Canada, Ottawa, pp. 352—361.

De Josselin de Jong, G., 1958. Longitudinal and transverse diffusion in granular deposits. EOS Trans. Am. Geophys. Union, 39: 67—74.

De Josselin de Jong, G., 1969. The tensor character of the dispersion coefficient in anisotropic porous media. I.A.H.R. Symp. on Fundamentals of Transport Phenomena in Porous Media, Haifa, pp. 259—267.

De Josselin de Jong, G., 1972. Dispersion of a point injection in an anisotropic porous medium. New Mexico Inst. Min. Techn. Socorro, 69 pp.

De Josselin de Jong, G. and Bossen, M.J., 1961. Discussion of paper by J. Bear, On the tensor form of dispersion. J. Geophys. Res., 10,66: 3623—3624.

De Josselin de Jong, G. and Shao Chih Way, 1972. Dispersion in fissured rock. New Mexico Inst. Min. Tech. Socorro, 30 pp.

De Wiest, R.J.M., 1965. Geohydrology. Wiley, New York, 366 pp.

De Wiest, R.J.M. (Editor), 1969. Flow through Porous Media. Academic Press, New York.

Ditkin, V.A. and Prudnikov, A.P., 1962. Operational Calculus in Two Variables. Int. Ser. Pure Appl. Math., Pergamon Press, London.

Douglas, J. Jr., Peaceman, D.W. and Rachford, H.H. Jr., 1959. A method for calculating multidimensional immiscible displacement. Trans. A.I.M.E., 216: 297—308.

Dracos, T. and Schiegg, H.O., 1971. Flow of immiscible fluids in unconfined aquifers. Mitt. Versuch. Wasserbau, Hydr. und Glaz. Eidg. Tech. Hochsch. Zurich, 2.

Drost, W. and Neumaier, F., 1974. The application of single-borehole methods in groundwater research. Int. Atomic Energy Agency, Symp. on Isotope Techniques in Groundwater Hydr., Vienna, IAEA-SM, 182—12.

Duprat, A., Simler, L. and Ungemach, P.O., 1970. Contribution de la prospection électrique à la recherche des caractéristiques hydrodynamiques d'un milieu aquifère. Terres et Eaux, V.XXIII-62: 23—31.

Dupuit, J., 1863. Etudes théoriques et pratiques sur le mouvement des eaux dans les canaux découverts et à travers les terrains perméables. Dunod, Paris, 304 pp.

Ebach, E.A. and White, R.R., 1958. Mixing of fluids flowing through beds of packed solids. J. Am. Inst. Chem. Eng., 2, 4: 161—164.

Elrick, D.E., 1969. Dispersion and reaction in unsaturated soils. Application to tracers. Bull. Int. Assoc. Hydr. Sci., 2: 49—60.

Elrick, D.E., Biggar, J.W. and Webber, L.R., 1966. Soil pollutants: their origin and behavior. J. Soil Wat. Conserv., pp. 7–11.

Emsellem, Y., 1971. Modèles mathématiques pour la gestion intégrée des ressources en eau. Ec. Nat. Sup. Mines Paris, LHM/R 71/6.

Emsellem, Y., 1972a. Modèles mathématiques de pollution pour la gestion intégrée des ressources en eau. Ec. Nat. Sup. Mines Paris, LHM/R72/13.

Emsellem, Y., 1972b. La gestion intégrée des ressources en eau. Ec. Nat. Sup. Mines Paris, LHM/R72/5.

Emsellem, Y., 1974a. Options de développement et gestion intégrée des ressources en eau. United Nations. Com. Ec. Europe. Comité Problèmes Eau. Coll. Utilis. Techn. Inf. Automation Syst. Ress. en eau, Washington.

Emsellem, Y., 1974b. Objectifs généraux de l'utilisation des techniques informatiques et de l'automation dans les systèmes de ressources en eau. United Nations. Com. Ec. Europe. Comité Problèmes Eau. Coll. Utilis. Techn. Inf. et automation Syst. Ress. en eau, Washington.

Emsellem, Y., De Marsily, G., Poitrinal, D. and Ratsimiebo, M., 1971. Déconvolution et identification automatique de paramètres en hydrologie. Int. Symp. Math. Mod. in Hydrology, Warsaw.

Emsellem, Y. and De Marsily, G., 1971. An automatic solution for the inverse problem. Water Resour. Res., 7-5: 1264—1283.

Emsellem, Y. and Fried, J.J., 1970. Schéma d'étude d'une pollution. Ec. Nat. Sup. Mines de Paris, LHM/N70/12.

Emsellem, Y., Fried, J.J. and Ungemach, P.O., 1973. Les modèles de pollution. 2ème Congrès sur la gestion intégrée de la pollution, Palerme, Preprint.

Emsellem, Y., Fried, J.J. and Ungemach, P.O., 1974. Modèles de prévision des pollutions souterraines et méthodologie de mesure. Colloque Intern. Informatique et Environnement. Fondation Universitaire Luxembourgeoise, Arlon.

Exler, H.J., 1972. Ausbreitung und Reichweite von Grundwasserverunreinigungen im Unterstrom einer Mülldeponie. Das Gas-und Wasserfach (GWF), Wasser Abwasser, 113: 101—112.

Farkasdi, G., Golwer, A., Knoll, K.H., Matthess, G. and Schneider, W., 1969. Mikrobiologische und hygienische Untersuchungen von Grundwasserverunreinigungen im Unterstrom von Abfallplätzen. Städtehygiene, 20: 25—31.

Farvolden, R.N. and Hughes, G.M., 1971. Hydrogeologic implications in solid waste disposal. Int. Union Geodet. Geophys.—Int. Assoc. Sci. Hydr., Symp. Moscow Proc.

Fatt, I., 1961. Deductions from the network model concerning diffusion and fluid flow through porous media. Interaction between fluids and particles. Instn. Chem. Eng., London, pp. 304—311.

Feller, R.W., 1966. An introduction to the theory of probabilities and its applications. Wiley, New York, Vol. 1: 509 pp.; Vol. 2: 626 pp.

Flint, L.F. and Eisenklam, P., 1970. Dispersion of matter in transitional flow through straight tubes. Proc. R. Soc. London, Ser. A, 315: 519—533.

Forsythe, G.E. and Wasow, W.R., 1960. Finite-difference methods for partial differential equations. Wiley, New York, 444 pp.

Freeze, R.A., 1972. Subsurface hydrology at waste disposal sites. I.B.M.J. Res. Develop., pp. 117—129.

Fried, J.J., 1968a. Les phénomènes de dispersion dans les milieux poreux. Etude Dir. Gén. Rech. Sci. Techn. Action concertée Eau. Secrétariat Permanent pour l'Etude des Problèmes de l'Eau, Paris.

Fried, J.J., 1968b. Application pratique des formules de dispersion. Etude Dir. Gén. Rech. Sci. Techn. Action concertée Eau. Secrétariat Permanent pour l'Etude des Problèmes de l'Eau, Paris.

Fried, J.J., 1968c. Changement d'échelle dans un milieu poreux appliqué à l'étude de la dispersion d'un traceur dans un fluide. Ann. Ponts Chaussées, V: 285—295.

Fried, J.J., 1969a. Intrusion d'eau de mer dans une nappe côtière: application de la théorie de la dispersion à l'étude de la zone de transition. Ec. Natl. Sup. Mines de Paris. Centre de Morphologie Math., 108.

Fried, J.J., 1969b. Détermination des caractéristiques physiques du terrain par la méthode du puits unique. Ec. Natl. Sup. Mines de Paris. Centre de Morphologie Math., 130.

Fried, J.J., 1971a. A mathematical model for the single-well pulse technique. Proc. Symp. Water Resour., Indian Inst. Sci., Bangalore.

Fried, J.J., 1971b. Quelques éléments pour l'étude des pollutions d'une nappe aquifère par invasion massive d'hydrocarbures. Ec. Natl. Sup. Mines de Paris, LHM/N71/14.

Fried, J.J., 1971c. Détermination ponctuelle du coefficient de dispersion de deux fluides miscibles dans un milieu poreux: une théorie de la dilution ponctuelle. C. Acad. Sci. Paris, 273-A: 47.

Fried, J.J., 1971d. Détermination ponctuelle du coefficient de diffusion—dispersion dans un milieu hétérogène mais isotrope: une théorie mathématique de la dilution. C. R. Acad. Sci., Paris, 273-A: 834.

Fried, J.J., 1972a. Etudes théoriques et méthodologiques de la dispersion en milieu poreux naturel. Thèse, Univ. de Bordeaux.

Fried, J.J., 1972b. Miscible pollutions of groundwater: a study in methodology. Proc. Int. Symp. on Modelling Techniques in Water Resources Syst. Environment Canada, Ottawa, pp. 362—371.

Fried, J.J., 1972c. Some recent applications of the theory of dispersion in porous media. Proc. Joint Symp. on Fundamentals of Transport Phenomena in Porous Media. Int. Assoc. Hydr. Res.—Int. Soc. Soil Sci., Guelph, Ontario, pp. 722—731.

Fried, J.J., 1973a. Groundwater pollution course. Univ. of Western Austraiia, Nedlands.

Fried, J.J., 1973b. Numerical Methods in hydrogeology. Univ. of Western Australia, Nedlands.

Fried, J.J., 1974. Moderne Trends in der Umweltschutzforschung. Koll. Ges. Strahlen und Umweltforschung, Munich.

Fried, J.J., 1975. Pollutions miscibles des nappes souterraines. Rap. Gén. Réunion Int. Comité Milieux Poreux—Int. Assoc. Hydr. Res., Zurich.

Fried, J.J. and Combarnous, M.A., 1971. Dispersion in porous media. In: V.T. Chow (Editor), Advances in Hydroscience, Academic Press, New York, pp. 169—282.

Fried, J.J. and Ungemach, P.O., 1971a. A dispersion model for a quantitative study of a groundwater pollution by salt. In: Water Research, 5. Pergamon Press, London, pp. 491—495.

Fried, J.J. and Ungemach, P.O., 1971b. Détermination in-situ du coefficient de dispersion longitudinale d'un milieu poreux naturel. C.R. Acad. Sci., Paris, 172-A, p. 1327.

Fried, J.J. and Ungemach, P.O., 1973a. Recherche des vitesses et des coefficients de dispersion. Mesures géophysiques et modèle hydrodispersif. Ec. Natl. Sup. Mines de Paris, LHM/R 73/15.

Fried, J.J. and Ungemach, P.O., 1973b. Cours de pollution des eaux souterraines. Ec. Natl. Sup. Mines de Paris.

Fried, J.J., Garnier, J.L. and Ungemach, P.O., 1971a. Etude quantitative d'une pollution de nappe d'eau souterraine: la salure de la nappe phréatique dans le département du Haut-Rhin. Bull. Bur. Rech. Géol. Min., Sect. III, 1: 105—115.

Fried, J.J., Garnier, J.L. and Ungemach, P.O., 1971b. Aspects méthodologiques d'une étude de pollution de nappe d'eau souterraine. Symp. I.U.G.G.—Int. Assoc. Sci. Hydr., Moscow, Préprint.

Fried, J.J., Levêque, P.C., Poitrinal, D. and Severac, J., 1972. Local studies of miscible pollutions of groundwater: the single-well pulse technique. Proc. Water Pollution, a working Conference. Water Res. Assoc., Reading.

Fried, J.J., Emsellem, Y., De Marsily, G., Ungemach, P.O., Combarnous, M.A., Vachaud, G. and Duprat, A., 1973. Modèles mathématiques et méthodologie pour la gestion intégrée de la pollution. 2ème Congrès sur la gestion intégrée des ressources en eau, Palerme, Préprint.

Fried, J.J., Ungemach, P.O., Emsellem, Y. and Duprat, A., 1974. Modèles de pollution des eaux souterraines. United Nations Com. Ec. Europe Comité Problems Eau. Coll. utilis. Tech. Inf. et automation Syst. Ress. en eau, Washington.

Garabedian, P.R., 1964. Partial Differential Equations. Wiley, New York, 672 pp.

Gardner, A.O. Jr., Peaceman, D.W. and Pozzi, A.L. Jr., 1964. Numerical calculation of multidimensional miscible displacement by the method of characteristics. Soc. Pet. Eng. J., 4: 26—36.

Gelhar, L.W. and Collins, M.A., 1971. General analysis of longitudinal dispersion in nonuniform flow. Water Resour. Res., 7: 1511—1521.

Golwer, A. and Matthess, G., 1967. Research on groundwater contaminated by deposits of solid waste. Int. Assoc. Sci. Hydr. Bern. Publ. 78: 129—133.

Golwer, A. and Matthess, G., 1969. Qualitative Beeinträchtigung des Grundwasserdargebotes durch Abfallstoffe. Dts. Gewässerk. Mitt. Sonderh. Dts. gewässerk. Tagung, Koblenz, 1968, pp. 51—55.

Golwer, A. and Matthess, G., 1972. Die Bedeutung des Gasaustausches in der Grundluft für die Selbstreinigungsvorgänge in verunreinigten Grundwässern. Z. Geol. Ges., 123: 29—38.

Golwer, A., Matthess, G. and Schneider, W., 1970. Selbstreinigungsvorgänge im Grundwasserbereich. Vom Wasser, Weinheim, pp. 64—92.

Golwer, A., Matthess, G. and Schneider, W., 1972a. Contamination de l'eau souterraine par des dèpôts de déchets et implications pour les méthodes d'évacuation des résidus. CEBEDEAU, 347: 428—433.

Golwer, A., Knoll, K.H., Matthess, G., Schneider, W. and Wallhäusser, K.H., 1972b. Mikroorganismen im Unterstrom eines Abfallplatzes. Gesundheits-Ingenieur, 93: 142—152.

Goodknight, R.C. and Fatt, I., 1963. Surface concentration build-up during diffusion in porous media with dead-end pore volume. J. Phys. Chem., 67: 949—950.

Goodknight, R.C., Klikoff, W.A. and Fatt, I., 1960. Non steady-state fluid flow and diffusion in porous media containing dead-end pore volume. J. Phys. Chem., 64: 1162—1168.

Government of India Atomic Energy Commission, 1971. A Bibliography on hydrological considerations in (1) Water resources for agriculture; (2) Ground disposal of radioactive wastes. Bhabha Atomic Research Centre, Desalination and Effluent Engineering Division, Bombay, 329 pp.

Greenkorn, R.A. and Kessler, D.K., 1969. Dispersion in heterogeneous non uniform anisotropic porous media. Flow through Porous Media Symp. Ind. Eng. Chem., 61-9: 14—32.

Groenevelt, P.H. and Bolt, G.M., 1972. Mixture of fluids and solid particles. Int. Assoc. Hydr. Res.—Int. Soc. Soil Sci., Proc. 2nd Symp. on Fundamentals of Transport Phenomena in Porous Media, Guelph, pp.653—666.

Guelfand, I.M. and Chilov, G.E., 1962. Les Distributions. Dunod, Paris, 376 pp.

Guizerix, J., Emsellem, Y., Corompt, P., Margrita, R. and De Marsily, G., 1970. Méthodes de traceur pour la détermination a priori de la propagation de substances polluantes dans le réseau hydrographique et a posteriori pour la localisation d'un point de réjet inconnu. Coll. Application des Tech. nucléaires à la mesure et au contrôle de la pollution du milieu.

Guizerix, J., Margrita, R., Gaillard, B., Corompt, P. and Alquier, M., 1974. Analyse des des informations fournies par les traceurs naturels ou artificiels dans l'étude des systèmes aquifères en hydrogéologie. Int. Atomic Energy Agency, Symp. on Isotope Techniques in Groundwater Hydr., Vienna. IAEA-SM 182/48.

Guymon, G.L., 1970. A finite-element solution of the one-dimensional diffusion—convection equation. Water Resour. Res., 6-1: 204—210.

Guymon, G.L., Scott, V.H. and Herrmann, L.R., 1970. A general solution of the two-dimensional diffusion convection equation by the finite-element method. Water Resour. Res., 6-6: 1611—1617.

Halevy, E. and Nir, A., 1962. The determination of aquifer parameters with the aid of radioactive tracers. J. Geophys. Res., 61: 2403.

Halevy, E., Moser, H., Zellhafer, O. and Zuber, A., 1966. Borehole dilution techniques: a critical review. Int. Atomic Energy Agency. Symp. on Isotope Techniques in Groundwater Hydr., Vienna, pp. 531—564.

Harleman, D.R.F. and Rumer, R.R., 1962. The dynamics of saltwater intrusion in porous media. M.I.T. Rep., 55.

Harleman, D.R.F. and Rumer, R.R., 1963. Longitudinal and lateral dispersion in an isotropic porous medium. J. Fluid Mech., 16-3: 385—394.

Harris, W.H., 1967. Stratification of fresh and saltwater on barrier Islands as a result of differences in sediment permeability. Water Resour. Res., 3-1: 89—97.

Heller, J.P., 1972. Observations of mixing and diffusion in porous media. Int. Assoc. Hydr. Res.—Int. Soc. Soil Sci., Proc. 2nd Symp. on Fundamentals of Transport Phenomena in Porous Media, Guelph, pp. 1—26.

Hiby, J.W., 1962. Longitudinal and transverse mixing during single-phase flow through granular beds. Symp. Interaction between fluids and particles, Inst. Chem. Eng., London, pp. 312—325.

Hoopes, J.A. and Harleman, D.R.F., 1967a. Dispersion in radial flow from a recharge well. J. Geophys. Res., 72-14: 3595—3607.

Hoopes, J.A. and Harleman, D.R.F., 1967b. Waste water recharge and dispersion in porous media. Proc. Am. Soc. Civ. Eng. (Hydraulics Div.), 93-5: 51—71.

Hörmander, L., 1969. Linear Partial Differential Operators. Springer, Berlin, 285 pp.

Int. Atomic Energy Agency—UNESCO, 1968. Int. Hydrol. Decade, Guidebook on Nuclear Techniques in Hydrology. Vienna, 298 pp.

Jacob, C.E., 1947. Flow of groundwater. In: H. Rouse (Editor), Engineering Hydraulics. Wiley, New York, pp. 321—386.

Jacquard, P., Lasvergeres, J.M. and Pottier, J., 1962. Résolution de l'équation de diffusivité du déplacement miscible en milieu radial circulaire. Inst. Fr. Pétrole. c 35/55059.

Jain, C., 1968. Etude numérique des déplacements miscibles en milieux hétérogènes. 3rd Coll. Assoc. Rech. Tech. Forage et Prod., Pau, pp. 491—506.

Javandel, I. and Witherspoon, P.A., 1968. Application of the finite-element method to transient flow in porous media. J. Soc. Pet. Eng., 8(3): 241–252.

Jeanson, B. and Dufort, J., 1969. Etude sur modèle physique des conditions de pollution des nappes côtières par l'eau salée lors de la production. Rapp. Inst. Fr. Pétrole, 17182.

Johnson, A.I., 1971. Gen. Rep. Symp. on Pollution of Groundwater. Session on pollution by waste deposits, waste water and miscellaneous sources. 15th Gen. Ass. IUGG, Moscow.

Kato, T., 1966. Perturbation Theory for Linear Operators. Springer, Berlin, 592 pp.

Kay, B.D. and Elrick, D.E., 1967. Adsorption and movement of lindane in soils. Soil Sci., 104-5: 314—322.

Klinkenberg, L.J., 1957. Pore-size distribution of porous media and displacement experiments with miscible liquids. J. Pet. Tech., 210: 366—369.

Klotz, D. and Moser, H., 1974. Hydrodynamic dispersion as aquifer characteristic. Model experiments by means of radioactive tracers. Int. Atomic Energy Agency Symp. on Isotope Techniques in Groundwater Hydr., Vienna, IAEA-SM-182/42.

Kohout, F.A. and Klein, H., 1967. Effect of pulse recharge on the zone of diffusion in the Biscayne aquifer. Int. Assoc. Sci. Hydr., Symp. of Haifa, Publ., 72: 252—270.

Krupp, H.K. and Elrick, D.E., 1968. Miscible displacement in an unsaturated glass bead medium. Water Resour. Res., 4-4: 809—815.

Kunetz, G., 1966. Principles of direct current resistivity prospecting. Geoexploration (Monograph Ser. 1, no. 1) Borntraeger, Berlin, 103 pp.

Landau, L.D. and Lifshitz, E.M., 1963. Fluid Mechanics. Pergamon Press, Oxford, 536 pp.

Lantz, R.B., 1969. Rigorous calculation of miscible displacement using immiscible reservoir simulators. Soc. Pet. Eng., Preprint 2594.

Lantz, R.B., 1970. Quantitative evaluation of numerical diffusion (truncation error). Soc. Pet. Eng., Preprint 2811.

Lau, L.S., Kaufmann, W.S. and Todd, D.K., 1959. Dispersion of a water tracer in radial laminar flow through homogeneous proous media. Progr. Rep. 5 Inst. Eng. Res., Ser. 93, Berkeley, Calif.

Lawson, D.W., 1971. Improvements in the finite-difference solution of two-dimensional dispersion problems. Water Resour. Res., 7-3: 721—725.

Lawson, D.W. and Elrick, D.E., 1972. A new method for determining and interpreting dispersion coefficients in porous media. Int. Assoc. Hydr. Res.—Int. Soc. Soil Sci., Proc. 2nd Symp., Guelph, pp. 753—777.

Legatski, M.W. and Katz, D.L., 1966. Dispersion coefficients for gases flowing in consolidated porous media. Soc. Pet. Eng., Preprint 1594.

Leipholz, H., 1974. Mechanics of Elastic Stability — Theory of Elasticity. Noordhoff, Leiden, 400 pp.

Lenda, A. and Zuber, A., 1970. Tracer dispersion in groundwater experiments. Isotope Hydrology. Int. Atomic Energy Agency, Vienna, pp. 619—641.

Levêque, P.C., 1969. Emploi des traceurs radioactifs naturels et artificiels en hydrologie souterraine. Houille Blanche, 8: 833.

Levêque, P.C., Giannotti, G.P., Grison, G., Mittempergher, M. and Fidoti, G., 1971. Critères hydrodynamiques de garantie de perennité pour le stockage géologique superficiel des déchets radioactifs. Assoc. Int. Hydr., 71 Conf. Tokyo, 197, III-71 S, p. 1248.

Levêque, P.C., Gros, J.C., Maurin, C., Severac, J. and Viguier, C., 1974. Utilisation des techniques isotopiques pour la résolution de problèmes hydrologiques en génie civil. Etude de trois cas précis. Int. Atomic Energy Agency. Symp. on Isotope Techniques in Groundwater Hydr., Vienna, IAEA-SM-182/43.

Li, W.H. and Canale, R.P., 1967. Dispersion from sources in nonuniform seepage flow. Proc. Am. Soc. Civ. Eng. (Hydraulics Div.), 93-3: 65—79.

Li, W.H. and Yeh, G.T., 1968. Dispersion at the interface of miscible liquids in a soil. Water Resour. Res., 4-2: 369—377.

Lichnerowicz, A., 1955. Algèbre et analyse linéaires. Masson, Paris, 316 pp.

Lieberstein, H.M., 1972. Theory of Partial Differential Equations. Academic Press, New York, 283 pp.

List, E.J. and Brooks, H.N., 1967. Lateral dispersion in saturated porous media. J. Geophys. Res., 72-10: 2531—2541.

Lusczynski, N.S., 1961. Head and flow of groundwater of variable density. J. Geophys. Res., 12-66: 4247—4256.

Marle, C., 1968. Les écoulements polyphasiques. Cours Ec. Natl. Sup. Pétroles et moteurs. Ed. Technip, Paris.

Marle, C. and Defrenne, P., 1960. La description mathématique de déplacement de fluides miscibles dans un milieu poreux. Rapp. Inst. Fr. Pétrole, 5433.

Marle, C. and Simandoux, P. , 1966. Diffusion avec convection dans un milieu stratifié. Coll. Centre Natl. Rech. Sci. 160.

Marle, C., Simandoux, P., Pacsirszky, J. and Gaulier, C., 1967. Etude du déplacement de fluides miscibles en milieu poreux stratifié. Rev. Inst. Fr. Pétrole, 22-2: 272—294.

Martin, J.M.,1969. Déplacement miscible en milieu naturel de grandes dimensions. Rapp. Inst. Fr. Pétrole, ARTFPA36/86.001.

Martin, J.M., 1971. Déplacements miscibles dans des milieux poreux naturels de grande extension. Rev. Inst. Fr. Pétrole, 26-11: 1065—1075.

Matheron, G., 1965. Les variables régionalisées et leur estimation: une application de la théorie des fonctions aléatoires aux sciences de la nature. Masson, Paris, 306 pp.

Matheron, G., 1967. Eléments pour une théorie des milieux poreux. Masson, Paris, 166 pp.

Matheron, G., 1969. Le Krigeage universel. Les Cahiers du Centre de Morphologie Mathématique. Ec. Natl. Sup. Mines de Paris, 83 pp.

Matheron, G., 1971. The theory of regionalized variables and its applications. Les Cahiers du Centre de Morphologie Mathématique. Ec. Natl. Sup. Mines de Paris, 211 pp.

Matthess, G., 1972. Hydrogeologic criteria for the selfpurification of polluted groundwater. 24th I.G.C., section II, pp. 296—304.

Matthess, G., 1973. Geologische und geohydrologische Probleme bei der Standortwahl von Deponien. Giessener Berichte zum Umweltschutz, Heft 3: 33—50.

Mercado, A., 1967. The spreading pattern of injected water in a permeability stratified aquifer. Int. Assoc. Sci. Hydr., Symp. Haifa, Publ. 72: 23—36.

Miller, M.C., 1966. Gravity effects in miscible displacement. Soc. Pet. Eng. Preprint 1531.

Monget, J.M., Berline, P., Bordet, J.P., Emsellem, Y., Fontaine, A., Lefoll, Y. and Albuisson, M., 1974. Traitement des séries spatio-temporelles sur ordinateur. United Nations. Comm. Econ. Europe. Coll. util, techn. Inform. et Automation Syst. Ress. en eau, Washington.

Moulu, J.C., 1968. Etude expérimentale du déplacement miscible dans un milieu hétérogène à nodule. 3rd Coll. Assoc. Rech. Tech. Forage Production. Pau, no. 30.

Mundorff, M.J., Crosthwaite, E.G., Chabot Kilburn, 1964. Groundwater for irrigation in the Snake River Basin in Idaho. U.S. Geol. Surv. Water Supply Pap., 1654: 224 pp.

Munera, H.A., 1974. Modelos matematicos simplificados para interpretacion de resultados de ensayos por el metodo de marcacion de toda la columna piezometrica. Int. Atomic Energy Agency. Symp. on Isotope Techniques in Groundwater Hydr., Vienna, IAEA-SM-182/44.

Neuman, S.P. and Witherspoon, P.A., 1970. Finite-element method of analyzing steady seepage with a free surface. Water Resour. Res., 3-6: 889—897.

Nöring, F., Farkasdi, G., Golwer, A., Knoll, K.H., Matthess, G. and Schneider, W., 1968. Über Abbauvorgänge von Grundwasserverunreinigungen im Unterstrom von Abfalldeponien. Gas-Wasserfach (GWF), Wasser Abwasser, 109, Heft 6: 137—142.

Norrie, D.H. and De Vries, G., 1973. The finite-element method. Academic Press, New York, 322 pp.

Nunge, R.J. and Gill, W.N., 1969. Mechanisms affecting dispersion and miscible displacement. Ind. Eng. Chem., 61-9: 33—49.

Ogata, A., 1961. Transverse diffusion in saturated isotropic granular media. U.S. Geol. Surv. Prof. Pap., 411-B.

Ogata, A. and Banks, R.B., 1961. A solution of the differential equation of longitudinal dispersion in porous media. U.S. Geol. Surv. Prof. Pap., 411-A.

Oroveanu, T., 1965. Quelques considérations sur le déplacement des fluides miscibles dans les milieux poreux. Rev. Roum. Sci. Tech., Ser. Mec. Appl. 10-6: 1365—1377.

Oroveanu, T. and Spulber, I., 1969. Sur le déplacement bidimensionnel des fluides miscibles dans les milieux poreux. Int. Assoc. Hydr. Res., 1st Symp. on Fundamentals of Transport Phenomena in Porous Media, Haifa, pp. 276—281.

Oster, C.A., Sonnichsen, J.C. and Jaske, R.T., 1970. Numerical solution to the convective diffusion equation. Water Resour. Res., 6-6: 1746—1752.

Patel, R.D. and Greenkorn, R.A., 1969. Prediction of recovery in miscible displacement in porous media using the dispersion equation. Soc. Pet. Eng., Preprint 2657.

Peaceman, D.W. and Rachford, H.H., 1955. The numerical solution of parabolic and elliptical differential equations. Soc. Indust. Appl. Math., 3-11: 28—41.

Peaceman, D.W. and Rachford, H.H., 1962. Numerical calculation of multidimensional miscible displacement. Soc. Pet. Eng. J., 2-4: 327—339.

Petrovski, I.G., 1966. Lectures on Partial Differential Equations. Wiley, New York, 245 pp.

Pfannkuch, H.O., 1963. Contribution à l'étude des déplacements de fluides miscibles dans un milieu poreux. Rev. Inst. Fr. Petrole, 18-2: 1—54.

Pfannkuch, H.O., 1969. On the correlation of electrical conductivity properties of porous systems with viscous flow transport coefficients. Int. Assoc. Hydr., Res. 1st Symp. on Fundamentals of Transport Phenomena in Porous Media, Haifa, pp. 42—54.

Pinder, G.F., 1973. A Galerkin finite-element simulation of groundwater contamination on Long Island, New York. Water Resour. Res., 9-6: 1657—1669.

Pinder, G.F. and Bredehoeft, J.D., 1971. Groundwater chemistry and the transport equations. Int. Assoc. Sci. Hydr. Int. Symp. Math. Mod. Hydr., Warsaw.

Pinder, G.F. and Cooper, H.H. Jr., 1970. A numerical technique for calculating the transient position of the saltwater front. Water Resour. Res., 6-3: 875—882.

Pinder, G.F. and Frind, E.O., 1972. Application of Galerkin's procedure to aquifer analysis. Water Resour. Res., 8-1: 108—120.

Pinder, G.F., Frind, E.O. and Papadopoulos, S.S., 1972. Functional coefficients in the analysis of groundwater flow using finite elements. Water Resour. Res., 9-1: 222—226.

Price, H.S., Cavendish, J.C. and Varga, R.S., 1968. Numerical methods of higher-order accuracy for diffusion—convection equations. Soc. Pet. Eng. J., 243: 293—303.

Raats, P.A.C., 1972. Jump conditions in the hydrodynamics of porous media. Int. Assoc. Hydr. Res.—Int. Soc. Soil Sci. Proc. 2nd Symp. on Fundamentals of Transport Phenomena in Porous Media, Guelph, pp. 155—173.

Raats, P.A.C. and Scotter, D.R., 1968. Dynamically similar motion of two miscible constituents in porous mediums. Water Resour. Res., 4-3: 561—568.

Raimondi, D., Gardner, G.H.F. and Petrick, C.B., 1959. Effect of pore structure and molecular diffusion on the mixing of miscible liquids flowing in porous media. AIChE. Soc. Pet. Eng., 52nd Ann. Meet., San Francisco, Preprint 43.

Reddell, D.L. and Sunada, D.K., 1970. Numerical simulation of dispersion in groundwater aquifers. Colo. State Univ., Fort Collins, Hydrol. Pap. 41: 79 pp.

Reid, G.W., 1972. Water quality modelling for forecastive and planning purposes. Int. Symp. on Modelling Techniques in Water Resour. Syst. Environment Canada, Ottawa, pp.383—390.

Remson, J., Hornberger, G.M. and Molz, F.V., 1971. Numerical Methods in Subsurface Hydrology. Wiley, New York, 389 pp.

Rifai, N.E., Kaufman, W.J. and Todd, D.K., 1956. Dispersion phenomena in laminar flow through porous media. Sanit. Eng. Rep. 3. Inst. Res. Ser. 90, Berkeley, Calif.

Roberts, K.V. and Weiss, N.O., 1966. Convective difference schemes. Math. Comput., 20-94: 272—297.

Robertson, J.B., 1974. Application of digital modelling to the prediction of radioisotope migration in groundwater. Int. Atomic Energy Agency. Symp. on Isotope Techniques in Groundwater Hydr., Vienna. IAEA-SM-182/50.

Robertson, J.B. and Barraclough, J.T., 1973. Radioactive and chemical waste transport in groundwater at National Reactor testing Station, Idaho: 20 year case history, and digital model. Underground waste manag. artif. rech. VI. Am. Assoc. Pet. Geol., U.S. Geol. Surv. Int. Assoc. Hydr. Sci., pp. 291—322.

Robertson, J.B., Schoen, R. and Barraclough, J.T., 1974. The influence of liquid waste disposal on the geochemistry of water at the National Reactor Testing Station, Idaho, 1952—1970. U.S. Geol. Surv. Open File Rep., IDO-22053: 231 pp.

Roebert, A.J., 1972. Fresh water winning and salt water encroachment in the Amsterdam dune water catchment area. Geol. Mijnbouw, 51-1: 35—44.

Rubin, H., 1973. Effect of solute dispersion on thermal convection in a porous medium layer. Water Resour. Res., 9-4: 968—974.

Rubin, J. and James. R.V., 1973. Dispersion-affected transport of reacting solutes in saturated porous media: Galerkin method, applied to equilibrium controlled exchange in unidirectional steady water flow. Water Resour. Res., 9-5: 1332.

Rumer, R.R. Jr., 1969. On the derivation of a convective dispersion equation by spatial averaging. Int. Assoc. Hydr. Res. 1st Symp. on Fundamentals of Transport Phenomena in Porous Media, Haifa, pp. 268—275.

Rumer, R.R. and Harleman, D.R.F., 1973. Intruded salt water wedge in porous media. Proc. Am. Soc. Civ. Eng. (Hydraulics Div.) 6-89: 193—220.

Rutledge, R.W., 1973. Geostatistics, review paper. Aust. N.Z. Assoc. Adv. Sci. Meet., Sect. 8, Perth, 34 pp.

Saffman, P.G., 1959. A theory of dispersion in a porous medium. J. Fluid Mech., 6: 321—349.

Saffman, P.G., 1960. Dispersion due to molecular diffusion and macroscopic mixing in flow through a network on capillaries. J. Fluid Mech., 7: 194—208.

Scheidegger, A.E., 1963. The Physics of Flow through Porous Media. Univ. of Toronto Press, Toronto.

Scheidegger, A.E., 1969. Stability conditions for displacement processes in porous media. Can. J. Phys., 47-2: 209—214.

Schlumberger, C., 1970. Etudes sur la prospection électirque du sous-sol. Gauthier Villars, Paris, 92 pp.

Schmorak, S., 1967. Salt water encroachment in the coastal plain of Israël. Int. Assoc. Sci. Hydr. Symp., Haifa, Publ. 72: 305:318.

Schwartz, L., 1973. Théorie des distributions. Hermann, Paris, 418 pp.

Secrétariat Permanent pour l'Etude des Problèmes de l'Eau — Service de la Carte Géologique d'Alsace-Lorraine, 1972. Etude bibliographique de la pollution des eaux souterraines par les dépôts d'ordures ménagères en milieu alluvial. Bur. Rech. Geol. Minières, 101 pp.

Seeley, R.T., 1967. The powers A^S of an elliptic operator A. Proc. Symp. Pure Math. 10, Singular integrals. Am. Math. Soc., pp. 288—307.

Shamir, U.Y. and Harleman, D.R.F., 1967a. Dispersion in layered porous media. Proc. Am. Soc. Civ. Eng. (Hydraulics Div.) 93-5: 237—260.

Shamir, U.Y. and Harleman, D.R.F., 1967b. Numerical solution for dispersion in porous mediums. Water Resour. Res., 3-2: 557—581.

Siemons, J., 1970. Numerical methods for the solution of diffusion advection equations. Delft Hydraulics Lab. Publ. 88.

Simpson, E.S., 1962. Transverse dispersion in liquid flow through porous media. U.S. Geol. Surv. Prof. Pap., 411-C.

Skogerboe, G.V., Walker, W.R. and Ayars, J.E., 1972. Modelling water quality from agricultural lands. Int. Symp. on Modelling Techniques Water Resour. Syst., Environment Canada, Ottawa, pp. 372—382.

Smith, I.M., Farraday, R.V. and O'Connor, B.A., 1972. Rayleigh-Ritz and Galerkin finite-elements for diffusion—convection problems. Simon Eng. Lab., Univ. of Manchester.

Spiegel, M.R., 1959. Vector and Tensor Analysis. Schaum's Outline Series. Schaum Publ., New York, 225 pp.

Stephen, H. and Stephen, T., 1964. Solubilities of Inorganic and Organic Compounds. Pergamon Press, London.

Stone, H.L. and Brian, P.L.T., 1963. Numerical solution of convective transport problems. A.I.Ch.E.J. 9-5: 681—688.

Tabti, M., 1968. Déplacement miscible, zone de transition, 3rd Coll. Assoc. Rech. Tech. Forrage Production, Pau, pp. 546—555.

Tahar, J., 1968. Déplacement miscible: étude expérimentale de l'influence du contraste de viscosité. Comm. 26, 3rd Coll. Assoc. Rech. Tech. Forage Prod., Pau.

Tahar, J., 1970. Contribution à l'étude des déplacements par fluides miscibles dans les milieux poreux. Dispersion longitudinale: influence du contraste de viscosité. Thèse, Inst. Fr. Pétrole, R 36/85406.

Task Committee on Saltwater Intrusion of the Committee on Ground-Water Hydrology of the Hydraulics Division, 1969. Saltwater intrusion in the United States. Proc. Am. Soc. Civ. Eng. (Hydraulics Div.) HY5: 1651—1669.

Taylor, G., 1953. Dispersion of soluble matter in solvent flowing slowly through a tube. Proc. R. Soc. London, Ser. A,219: 186—203.

Taylor, G., 1954. Conditions under which dispersion of a solute in a stream of solvent can be used to measure molecular diffusion. Proc. R. Soc. London, Ser. A, 225:473.

Theis, C.V., 1935. The relation between the lowering of the piezometric surface and the rate and duration of discharge of a well using groundwater storage. Trans. Am. Geophys. Union, 16: 519—524.

Thomas, G.H., Countryman, G.R. and Fatt, I., 1963. Miscible displacement in a multiphase system. Soc. Pet. Eng. J., 3: 189—196.

Todd, D.K., 1959. Ground Water Hydrology. Wiley, New York, 336 pp.

Triboix, A., Trinh Thieu, B. and Zilliox, L., 1975. Importance des conditions initiales dans l'étude de la pénétration d'un liquide miscible dans un écoulement de nappe à surface libre. Réunion Int. Comité Milieux Poreux. Int. Assoc. Hydr. Res., Zurich

Ungemach, P.O., 1975. Thèse, Univ. de Strasbourg.

Unterberger, A. and Unterberger, J., 1970. Operateurs pseudo-différentiels. Exposé 3. Séminaire Goulaouic-Schwarz, Ec. Polytech., Paris.

Unterberger, A. and Unterberger, J., 1971. Opérateurs pseudo-différentiels. Exposé. 4. Séminaire Goulaouic-Schwarz, Ec. Polytech., Paris.

Volker, R.E. and Cantatore, W.P., 1972. The numerical solution of the steady interface in a confined coastal aquifer. James Cook Univ. of N. Queensland, 26 pp.

Von Rosenberg, D.U., 1956. Mechanics of steady state single-phase fluid displacement from porous media. A.I.Ch.E.J. 2-1: 55—58.

Walton, W.C., 1962. Selected analytical methods for well and aquifer evaluation. Illinois State Water Surv. Bull. 49: 81 pp.

Webster, D.S., Proctor, J.F. and Marine, I.W., 1970. Two-well tracer test in fractured crystalline rock. U.S. Geol. Surv. Water Supply Paper, 1544-I.

Welsch, W.F., 1955. Groundwater pollution from industrial wastes. Sewage Ind. wastes, 27-9: 1065—1072.

Wenk, V.D., 1971. A Technology Assessment Methodology. Water Pollution: Domestic Wastes. The Mitre Corp.; Nat. Tech. Inf. Serv. U.S. Dept. of Commerce, 6: 293 pp.

Whitaker, S., 1967. Diffusion and dispersion in porous media. A.I.Ch.E.J. 13-3: 420—427.

Wooding, R.A., 1962. The stability of on interface between miscible fluids in a porous medium. Z. Angew. Math. Phys., 13-3: 255—265.

World Health Organization, 1971. Normes européennes applicables à l'eau de boisson. Geneva, 2nd ed.

World Health Organization, 1972. Normes internationales pour l'eau de boisson. Genève, 74 pp.

Yih, C.S., 1960. Flow of a non homogeneous fluid in a porous medium. J. Fluid Mech., 10: 133—140.

Yosida, K., 1968. Functional Analysis. Springer, Berlin, 465 pp.

Zienkiewicz, O.C., 1971. The Finite-Element Method in Engineering Science. McGraw Hill, New York, 521 pp.

Zilliox, L., 1974a. Mise en évidence sur modèles physiques de mécanismes hydrodynamiques intervenant dans le développement de pollutions des eaux souterraines. Symp. La Pollution des eaux souterraines. Gand. C.R.: CIPS 74/28.

Zilliox, L., 1974b. Mécanismes de pollutions d'une nappe d'eau souterraine libre: définition de la source et évolution de la zone contaminée. Séminaire sur contributions gestion qualité des eaux souterraines, Bruxelles.

Zilliox, L. and Muntzer, P., 1974. Influence de mécanismes hydrodynamiques sur le développement de la pollution des eaux souterraines: mise en évidence sur modèles physiques en milieux poreux saturé. Proc. 7th Int. Conf. Water Pollution Res., Paris. Pergamon Press, London.

Zuber, A., 1974. Theoretical possibilities of the two-well pulse method. Int. Atomic Energy Agency. Symp. Isotope Techniques in Groundwater hydr., Vienna. IAEA-5M 182/45.

This Page Intentionally Left Blank

INDEX